



UNIVERSITAT
POLITÈCNICA
DE VALÈNCIA



Secondary metabolites in plant defence mechanisms

Ph.D. Thesis in Biotechnology by

Celia Payá Montes

Advisors

Dr. M^a Purificación Lisón Párraga

Dr. M^a Pilar López Gresa

Valencia, March 2023

*“La vida no es ningún pasillo recto y fácil
que recorremos libres y sin obstáculos,
sino un laberinto de pasadizos, en el que
tenemos que buscar nuestro camino,
perdidos y confusos, detenidos, de vez en
cuando, por un callejón sin salida.*

*Pero, si tenemos fe, siempre se abre una
puerta ante nosotros; quizá no sea la que
imaginamos, pero sí será, finalmente, la
que demuestre ser buena para nosotros.”*

A.J. Cronin

Agradecimientos

Estas palabras de agradecimiento no se remontan únicamente a los 3 años en los que se ha realizado la presente tesis doctoral, sino a los 6 años que ha durado mi experiencia en el campo de la biotecnología vegetal y, sobre todo, formando parte del gran equipo que forma el “Laboratorio 2.02”.

Como en cualquier equipo del ámbito deportivo, cabe destacar el papel primordial que tienen los jugadores que salen a pelear al campo. Dentro de nuestro equipo de “pupilos” hemos contado con grandes fichajes, desde Miguel, pasando por Samuel, Kiko, Verónica, Alejandro, Lola, Patrick, Silvia, Malén, Laura, Lucía y Paula. De todos y cada uno de ellos me he llevado muchos momentos buenos, y sobre todo muchas enseñanzas. Ahora toca ir con el equipo titular, empezando por los nuevos fichajes, Gabriel, Eneritz y Marc. Aunque no hemos podido “jugar” en el campo mucho tiempo, solo quiero decir que aprovechéis cada momento de vuestra estancia en el laboratorio, que absorbáis los conocimientos y nuevos aprendizajes, y sobre todo que disfrutéis de todo el proceso. Seguimos con las jugadoras más nuevas, pero que ya son una parte muy importante del equipo, Samanta y Carmen. A pesar de que ahora vengan épocas de incertidumbre, podéis estar contentas y orgullosas de todo lo que habéis aportado a este equipo. Para mí ha sido un placer haberos echado una mano y disfrutar con la evolución que habéis hecho este último año. Por último, toca pasar a los jugadores más veteranos del equipo. Fran, muchas gracias por estos cuatro años en los que aparte de ser mi compañero de equipo más veterano, hemos disfrutado de almuerzos premium, conciertos, cotilleos e incluso mudanzas (discusiones científicas también, obviamente). Y Julia, solo puedo decirte que todo tu esfuerzo es, y va a ser recompensado, porque personas con tu inteligencia, perseverancia, resiliencia y alegría van a conseguir todo lo que se propongan y más.

También me gustaría dar gracias a aquellos componentes del equipo, que fueron jugadores en su momento, pero ahora ya se dedican a temas más técnicos. Muchas gracias, Borja y Paco por resolver cada una de las dudas, por muy tontas que fueran, y aconsejarme desde vuestra experiencia.

Ahora toca pasar a los altos directivos del equipo, encargados de la gestión y máximo exponente de conocimiento, Ismael y José María. Vuestra trayectoria profesional y sobre todo experiencia personal han sido toda una inspiración para mí.

Y, por último, las personas encargadas de dirigir y motivar al equipo, las entrenadoras. Muchas gracias Mapi por darle el punto de humor a todos los aspectos, tanto científicos como personales, de esta manera haces que la risa y el buen ambiente sean los protagonistas del laboratorio. Puri, solo puedo decirte que no he encontrado a una entrenadora que a la vez de dirigir la parte técnica del equipo sea capaz de entender, motivar y cuidar a cada uno de los jugadores, eres todo un ejemplo a seguir.

Como integrante del equipo solo quiero decir que formáis el binomio perfecto, y personalmente solo me queda agradeceros toda y cada una de las oportunidades que me habéis ofrecido, la confianza que habéis depositado en mí, y sobre todo por haberme entendido y apoyado en todos estos años de andanzas, en los que ha habido alguna sombra, pero sobre todo luces que han hecho el camino mucho más agradable.

Ya solo me queda dar gracias al pilar más importante, que es irrompible y va a permanecer siempre, mi familia. Mamá, papá y Maria, no tengo palabras para agradecer todo lo que habéis hecho, hacéis y haréis por mí. Gracias por haberme dado siempre alas para volar, raíces para volver y razones por las que seguir luchando y dar siempre lo mejor de mí.

TABLE OF CONTENTS

ABSTRACT	I
RESUMEN	III
RESUM	V
LIST OF ABBREVIATIONS	VII
GENERAL INTRODUCTION	IX
1. THE PLANT IMMUNE SYSTEM	1
1.1. <i>PTI: PAMP-Triggered Immunity</i>	1
1.2. <i>ETI: Effector-Triggered Immunity</i>	2
1.3. <i>Regulation of Stomatal Immunity</i>	3
<i>Pseudomonas syringae</i> pv. <i>tomato</i> DC3000 as a stomatal immunity model system.....	5
2. SECONDARY METABOLITES IN PLANT DEFENCE	6
2.1. <i>Phenolic compounds</i>	7
2.1.1. Salicylic acid	7
2.1.2. Gentisic acid	8
2.2. <i>Volatile Organic Compounds (VOCs)</i>	9
2.2.1. Green Leaf Volatiles (GLVs)	9
3. USE OF ELICITORS AGAINST BIOTIC AND ABIOTIC STRESSES	11
3.1. <i>Natural elicitors</i>	11
3.2. <i>Synthetic elicitors</i>	12
OBJECTIVES	15
CHAPTER I	19
LIST OF ABBREVIATIONS.....	23
ABSTRACT.....	25
1. INTRODUCTION	25
2. MATERIALS AND METHODS	27
3. RESULTS	33
4. DISCUSSION	49
5. REFERENCES	55
SUPPLEMENTARY MATERIALS	61
CHAPTER II	65
LIST OF ABBREVIATIONS.....	69
ABSTRACT.....	71
1. INTRODUCTION	71
2. MATERIALS AND METHODS	73

3. RESULTS	78
4. DISCUSSION	92
5. REFERENCES.....	95
SUPPLEMENTARY MATERIALS.....	101
CHAPTER III	107
LIST OF ABBREVIATIONS.....	110
ABSTRACT.....	111
1. INTRODUCTION.....	111
2. MATERIALS AND METHODS	113
3. RESULTS	115
4. DISCUSSION	120
5. REFERENCES.....	123
SUPPLEMENTARY MATERIALS.....	127
GENERAL DISCUSSION.....	131
GENERAL CONCLUSIONS.....	139
REFERENCES	145
ANNEX I	
ANNEX II	

ABSTRACT

In response to biotic and abiotic stress, plants synthesize defence proteins and chemical compounds from diverse nature. These compounds can act directly, through antioxidant, antifungal or antibacterial properties, or indirectly as defensive metabolites. Among these group of defensive metabolites, phenolic compounds and volatile organic compounds (VOCs) present a major role.

Our research group have a strong background in studying the role of plant secondary metabolites in plant defence mechanisms. On one hand, gentisic acid (GA) was first described as a signal molecule that acts complementary to salicylic acid (SA) in systemic infections. Furthermore, SA conversion to GA through the salicylate 5-hydroxylase enzyme (S5H) has received much attention. For this purpose, S5H-silenced transgenic tomato plants (*RNAi_S5H*) have been phenotypically, molecularly, and chemically characterized against both, bacterial and viroidal inoculations. *RNAi_S5H* tomato plants resulted in enhanced resistance to both *Pseudomonas syringae* pv. *tomato* DC3000 (*Pst* DC3000) and Citrus Exocortis Viroid (CEVd). Moreover, metabolomics analysis of these transgenic plants upon bacterial and viroid infections revealed differences related to SA metabolism, suggesting that SA homeostasis is specific for each tomato-pathogen interaction [1].

On the other hand, some esters of (*Z*)-3-hexenol were identified to be differentially emitted by tomato cv. Rio Grande plants upon infection with the avirulent strain of the bacterium *Pst* DC3000 [2]. Particularly, treatments with the volatile (*Z*)-3-hexenyl butyrate (HB) resulted in significant stomatal closure, defence genes induction and enhanced resistance to the bacteria. Moreover, the efficacy of this compound as a stomata closer was tested in different agronomic crop as Arabidopsis, Medicago, Zea, Citrus y Nicotiana plants, postulating HB as a new universal stomata closer [3, 108; annex I]. Due to its potent properties, the signalling pathway of the HB-mediated stomata closure has been deciphered by using different genetic, biochemical, and pharmacological approaches. The perception of this volatile by plant receptors appeared to initiate different defence signalling events, including the activation of Ca²⁺ permeable channels or reactive oxygen species (ROS) burst. Moreover, HB triggered the activation of the mitogen-activated protein kinases MPK3 and MPK6, inducing stomatal closure independently of abscisic acid (ABA) biosynthesis and signalling. Additionally, HB efficacy has been also tested in field conditions and against both biotic and abiotic stresses, and also during ripening, proposing HB as a new natural phytoprotector for the sustainable control of stresses in agriculture [4].

RESUMEN

En respuesta a estreses de tipo biótico y abiótico, las plantas sintetizan proteínas de defensa y compuestos químicos de diversa naturaleza. Estos compuestos pueden actuar de manera directa, a través de propiedades antioxidantes, antifúngicas o antibacterianas, o actuar como metabolitos defensivos indirectos. Dentro de este último grupo de compuestos defensivos, cabe destacar a los compuestos fenólicos y los compuestos orgánicos volátiles (VOCs).

En nuestro grupo de investigación se ha profundizado en el estudio de estos metabolitos secundarios implicados en la respuesta defensiva de las plantas. Por una parte, se identificó el ácido gentísico (GA) como una molécula señal que actúa de manera complementaria al ácido salicílico (SA) en infecciones de tipo sistémico. Además, se ha tratado de profundizar en el estudio de la biosíntesis del GA a través de la enzima salicilato 5-hidroxilasa (S5H), encargada de la conversión de SA a GA. Para ello, se ha llevado a cabo la caracterización fenotípica, molecular y química de plantas transgénicas de tomate que tienen silenciado el gen *S5H* mediante la técnica de RNA de interferencia (*RNAi_S5H*) frente a infecciones de tipo bacteriano y viroidal. Las plantas de tomate *RNAi_S5H* presentaron un aumento de resistencia frente a *Pseudomonas syringae* pv. *tomato* DC3000 (*Pst* DC3000) y el viroide de la exocortis de los cítricos (CEVd). Del mismo modo, se llevaron a cabo análisis metabolómicos de estas plantas transgénicas *RNAi_S5H* tras ambas infecciones, observándose diferencias relacionadas con el metabolismo del SA, que parecen indicar que la homeostasis del SA es específica para cada interacción tomate-patógeno [1].

Por otra parte, se identificaron algunos ésteres de (*Z*)-3-hexenol que eran emitidos de manera diferencial tras la infección bacteriana con la cepa avirulenta de *Pst* DC3000 en plantas de tomate cv. Rio Grande [2]. Concretamente, tratamientos exógenos con el compuesto volátil butanoato de (*Z*)-3-hexenilo (HB) fueron capaces de inducir de manera significativa el cierre de estomas, la activación de genes defensivos y un aumento en la resistencia frente a la infección bacteriana. La eficacia de este compuesto como inductor de cierre estomático fue comprobada en diferentes cultivos agronómicos, como *Arabidopsis*, *Medicago*, *Zea*, *Citrus* y *Nicotiana*, confirmando su papel como un inductor de cierre estomático universal [3, 108; anexo I]. Dado el potencial de este compuesto en agricultura, se emplearon aproximaciones genéticas, bioquímicas y farmacológicas para descifrar el mecanismo de señalización del cierre estomático mediado por HB. Una vez el volátil es percibido por los receptores de la planta, se activan diferentes componentes de la cascada de señalización defensiva, como canales permeables de Ca^{2+} o la producción de especies reactivas de oxígeno (ROS). Asimismo, el HB es capaz de desencadenar la activación de las proteínas quinasas activadas por mitógenos MPK3 y MPK6, induciendo el cierre estomático de una manera independiente a la síntesis y señalización mediada por ácido abscísico (ABA). Por último, la eficacia del HB fue evaluada en condiciones de campo frente a estreses tanto

de tipo biótico como abiótico y en procesos de desarrollo como la maduración, proponiendo un uso del HB como un nuevo compuesto fitoprotector natural para el control de estreses de forma sostenible en agricultura [4].

RESUM

En resposta a estressos de tipus biòtic i abiòtic, les plantes sintetitzen proteïnes de defensa i compostos químics de diversa naturalesa. Aquests compostos poden actuar de manera directa, a través de propietats antioxidants, antifúngiques o antibacterianes, o actuar com a metabòlits defensius indirectes. Dins d'aquest últim grup de compostos defensius, cal destacar als compostos fenòlics i els compostos orgànics volàtils (VOCs).

En el nostre grup d'investigació s'ha aprofundit en l'estudi d'aquests metabòlits secundaris implicats en la resposta defensiva de les plantes. D'una banda, es va identificar l'àcid gentísic (GA) com una molècula senyal que actua de manera complementària a l'àcid salicílic (SA) en infeccions de tipus sistèmic. A més, s'ha tractat d'aprofundir en l'estudi de la biosíntesi del GA a través d l'enzim salicilato 5-hidroxilasa (S5H), encarregada de la conversió de SA a GA. Per a això, s'ha dut a terme la caracterització fenotípica, molecular i química de plantes de transgèniques de tomaca que tenen silenciada el gen *S5H* mitjançant la tècnica d'RNA d'interferència (*RNAi_S5H*) enfront d'infeccions de tipus bacterià i viroidal. Les plantes de tomaca *RNAi_S5H* van presentar un augment de resistència enfront de *Pseudomonas syringae* pv. *tomato* DC3000 (*Pst* DC3000) i el viroide de la exocortis dels cítrics (CEVd). De la mateixa manera, es van dur a terme anàlisis metabolòmics d'aquestes plantes transgèniques *RNAi_S5H* després de totes dues infeccions, observant-se diferències relacionades amb el metabolisme del SA, que sembla indicar que l'homeòstasi del SA és específica per a cada interacció tomaca-patògena [1].

D'altra banda, es van identificar alguns èsters de (*Z*)-3-hexenol que eren emesos de manera diferencial després de la infecció bacteriana amb el cep avirulent de *Pst* DC3000 en plantes de tomaca cv. Rio Gran [2]. Concretament, tractaments exògens amb el compost volàtil butanoato de (*Z*)-3-hexenil (HB) van ser capaces d'induir de manera significativa el tancament d'estomes, l'activació de gens defensius i un augment en la resistència enfront de la infecció bacteriana. L'eficàcia d'aquest compost com a inductor de tancament estomàtic va ser comprovada en diferents cultius agronòmics, com *Arabidopsis*, Medicago, Zea, Citrus i Nicotiana, confirmant el seu paper com un inductor de tancament estomàtic universal [3, 108; annex I]. Donat el potencial d'aquest compost en agricultura, es van emprar aproximacions genètiques, bioquímiques i farmacològiques per a desxifrar el mecanisme de senyalització del tancament estomàtic mediat per HB. Una vegada el volàtil és percebut pels receptors de la planta, s'activen diferents components de la cascada de senyalització defensiva, com a canals permeables de Ca^{2+} o la producció d'espècies reactives d'oxigen (ROS). Així mateix, el HB és capaç de desencadenar l'activació de les proteïnes cinases activades per mitògens MPK3 i MPK6, induint el tancament estomàtic d'una manera independent a la síntesi i senyalització mediada per l'àcid abscísic (ABA). Finalment, l'eficàcia del HB va ser avaluada en condicions de camp enfront d'estressos tant de tipus biòtic com abiòtic, i en processos de desenvolupament com la maduració, proposant un l'ús del HB com a

nou compost fitoprotector natural per al control d'estressos de manera sostenible en agricultura [4].

LIST OF ABBREVIATIONS

AAT: Alcohol Acyltransferase	LOX: Lipoxygenase
ABA: Abscisic acid	MAPKs: Mitogen-Activated Proteins Kinases
ADH: Alcohol Dehydrogenase	MeJA: Methyl Jasmonate
AOS: Allene Oxide Synthase	MEP: Methylerythritol Phosphate
Avr: avirulence	MeSA: Methyl Salicylate
BABA: β -Aminobutyric Acid	MVA: Mevalonic Acid
BAK1: BRI1-Associated receptor Kinase 1	NLRs: Nucleotide-binding domain Leucine-rich repeat Receptors
BIK1: Botrytis Induced Kinase 1	OPDA: Oxo-Phytodienoic Acid
BTH: Benzo-(1,2,3)-thiadiazole-7-methionine S-methyl	OST1: Open Stomata 1
Ca²⁺: calcium	PAL: Phenylalanine Ammonia-Lyase
CERK1: Chitin Elicitor Kinase Receptor 1	PAMPs: Pathogen Associated Molecular Patterns
CEVd: Citrus Exocortis Viroid	PP2Cs: type 2C protein phosphatases
COR: Coronatine	PRRs: Pattern Recognition Receptors
CPKs: calcium-dependent protein kinases	PRs: Pathogenesis-Related Proteins
DAMPs: Danger-Associated Molecular Patterns	PRXs: Peroxidases
DHBA: 2,5-Dihydroxybenzoate	<i>Pst:</i> <i>Pseudomonas syringae</i> pv. <i>tomato</i>
DIECA: Sodium Diethyldithiocarbamate	PTI: PAMP-Triggered Immunity
DPI: Diphenyleiodonium chloride	PUFAs: Polyunsaturated Acids
EFR: EF-Tu Receptor	RBOHD: Respiratory Burst Oxidase Homolog D
ETI: Effector-Triggered Immunity	RLCKs: Receptor Like Cytoplasmatic Kinases
Flg22: Flagellin 22	RES: Reactive Electrophile Species
FLS2: Flagellin-Sensing 2	RLKs: Receptor-Like Kinases
GA: Gentisic Acid	RLPs: Receptor-Like Proteins
GABA: γ -aminobutyric acid	RNAi_SIS5H: RNAi <i>SIS5H</i> -silenced transgenic tomato plants
GC-MS: Gas Chromatography Mass Spectrometry	ROS: Reactive Oxygen Species
GLVs: Green Leaf Volatiles	S3H: Salicylate-3-Hydroxylase
HB: Hexenyl Butyrate	S5H: Salicylate-5-Hydroxylase
HP: Hexenyl Propionate	SA: Salicylic Acid
HPL: Hydroperoxide Lyase	SAG: Salicylic Acid Glucoside
HR: Hypersensitive Response	SAMT: S-Adenosyl Methionine
IC: Isochorismate	SAR: Systemic Acquired Resistance
Ica: Inward Calcium	SHAM: Salicylhydroxamic acid
JA: Jasmonic Acid	
JAs: Jasmonates	

SLAC1: Slow Anion Channel-Associated 1

SLAH3: SLAC1 homolog 3

SnRK2s: SNF1-related protein kinases 2

SnRKs: sucrose nonfermenting protein kinases

ToMV: Tomato Mosaic Virus

VOCs: Volatile Organic Compounds

General Introduction

1. The Plant Immune System

In natural ecosystems, plants are exposed to an endless barrage of external threats, including biotic and abiotic stresses. In response to this changeable environment, plants have evolved a highly and sophisticated defensive system to ensure their survival. The long and close story of plant–pathogen interactions led to the evolution of multiple alertness mechanisms in the plant.

Regarding biotic stresses, plants are constantly dealing with numerous microbial organisms, such as fungi, oomycetes, bacteria, viruses, and viroids. Plants immune response against pathogens relies on a complex network of constitutive and inducible defensive barriers. The “static” or constitutive defences, follow a non-host resistance strategy and include physical barriers such as the rigid cell wall, waxy cuticles, and antimicrobial secondary metabolites synthesis. Although these protectant barriers block most of the pathogenic offensives, some of them can overcome the constitutive defensive system, activating the plant immune system.

Plant innate immunity involves two defensive levels: the first line is initiated by the detection of Pathogen Associated Molecular Patterns (PAMPs) through cell-surface Pattern Recognition Receptors (PRRs) and is known as “PAMP-Triggered Immunity” (PTI); and the second one is activated by the effectors of successful pathogens which are specifically recognized by the plant resulting in “Effector-Triggered Immunity” (ETI) [5].

1.1. PTI: PAMP-Triggered Immunity

PTI constitutes the first layer of plant immunity in order to restrict pathogen invasion. This line of defence is canonically triggered after the recognition of different evolutionarily conserved molecules, named as PAMPs such as fungal chitin, glycoproteins from oomycetes or bacterial flagellin. Plants also perceive host-derived molecules released by pathogen invasion, like cell wall fragments, referred as Danger-Associated Molecular Patterns (DAMPs). PAMPs and DAMPs are recognized by PRRs, that are mainly plasma membrane-associated receptors, belonging to Receptor-Like Kinases (RLKs) or Receptor-Like Proteins (RLPs) receptor classes. An example of this interaction is the recognition of a part of bacterial flagellin by the FLAGELLIN-SENSING 2 (FLS2) receptor [6,7]. Other well-known PRRs from *Arabidopsis thaliana* plants include EF-Tu receptor EFR, and the Chitin Elicitor Kinase Receptor CERK1 [8,9]. Upon binding of ligands, most PRRs recruit co-receptors to activate downstream immune responses, as the association between FLS2 and the receptor kinase BRI1-ASSOCIATED RECEPTOR KINASE 1 (BAK1) [10,11]. Receptor-Like Cytoplasmatic Kinases (RLCKs) also play a pivotal role in defence signalling, since they phosphorylate and activate downstream

components. In this sense, Botrytis-Induced Kinase 1 (BIK1) is a central element integrating signals from different PRRs, as FLS2, EFR and CERK1 [12,13]. The establishment of heteromeric receptor complexes triggers an array of plant defence responses to halt pathogen spread and colonization, including the production of reactive oxygen species (ROS), callose deposition, lignine synthesis, the generation of secondary messengers or the synthesis of PRs (Pathogenesis-Related Proteins) defence proteins [8,14,15].

1.2. ETI: Effector-Triggered Immunity

Plants are able to activate molecular defence pathways upon contact with pathogen, leading to PTI. However, some pathogens may counter this defence by releasing specific effector molecules, referred to as avirulence (Avr) proteins, that are able to suppress PTI. In this contest between host plants and pathogens, plants have evolved resistance (R) genes encoding specific receptors, termed as Nucleotide-binding domain Leucine-rich repeat Receptors (NLRs), which detect pathogenic effectors, activating the second layer of plant immunity known as ETI [5]. Therefore, in this context two different outcomes will occur: an incompatible interaction between pathogen Avr and plants R proteins that will trigger ETI and plant resistance; or the absence of an effective Avr or R gene products, defined as a compatible interaction that will result in pathogen infection and colonization. [16]. An example of incompatible interaction is the recognition of AvrRpt2 and AvrRpm1 *Pseudomonas syringae* effectors by the NLR receptors RPS2 and RPM1, respectively, triggering ETI in Columbia 0 (Col-0) *Arabidopsis thaliana* plants [5].

Upon NLRs selective recognition of pathogen effectors and ETI establishment, robust and specific defence responses are activated as the hypersensitive response (HR) which involves a rapid localized programmed cell death, isolating pathogens during the early steps of infection [17] or a broad-spectrum disease resistance against secondary infections, known as Systemic Acquired Resistance (SAR) [18].

Originally, it was thought that ETI was activated only after PTI suppression and effectors recognition, leading to the interpretation that PTI had little effect on the ETI-mediated immune response. However, increasing evidence indicates a possible crosstalk and cooperation between PTI and ETI. Both defensive responses lead to several overlapping downstream outputs, transcriptional reprogramming and phytohormone signalling. Although some immune responses elicited by PTI and ETI are similar, the duration and amplitude of ETI responses are larger than PTI ones, postulating that ETI is an “accelerated and amplified PTI” and collaborating to ensure effective immunity [19–21].

1.3. Regulation of Stomatal Immunity

Stomata are natural openings surrounded by guard cells, located on the leaf surface, which are mainly involved in transpiration and gas exchange during photosynthesis. Guard cells control stomatal opening and closure in response to various stimuli, as light, humidity, CO₂, or pathogens attack. Guard cells movements are regulated by different ion channels, transporters, and pumps [22,23] that are controlled by different protein kinase and phosphatase networks, as sucrose non-fermenting protein kinases (SnRKs) and calcium-dependent protein kinases (CPKs) [24].

Regarding pathogen attack, many pathogens, such as bacteria, fungi, oomycetes and virus, use stomatal pores as entry gates for penetration and colonization into inner leaf tissues [25,26]. As a counteract measure, plants close their stomata to limit pathogen entry, a defensive response known as stomatal immunity. In plants, stomatal immunity starts from the perception of pathogens by PRRs, activating different key immune signalling events, including rapid phosphorylation of RLCKs, calcium (Ca²⁺) influx across the plasma membrane, production of reactive oxygen species (ROS) and activation of mitogen-activated protein kinases (MAPKs), CPKs cascades and defensive genes expression, in order to trigger stomatal closure [27–29].

As aforementioned, RLCKs play a central role in defensive mechanisms and stomatal immunity. Upon pathogen perception by the receptor complex FLS2-BAK1, BIK1 phosphorylation triggers two essential processes in stomatal immunity: ROS production, through activation of NADPH oxidase Respiratory Burst Oxidase Homolog D (RBOHD), and Ca²⁺ influx [27] (Figure 1).

Plant MAPKs cascade also play a significant role in stomatal immunity signalling pathways. In particular, two MAPKs cascades are activated upon ligand perception: the one formed by MEKK1, MKK1/2 and MPK4; and the second composed of MKK4/5 and MPK3/6 [30–32]. Particularly, the MAP3K kinase known as YODA has been described to regulate plant immune responses conferring broad-spectrum disease resistance [33]. Finally, activation of MAPKs cascades includes different defensive phenomena as stomatal closure, defence gene activation, phytoalexin accumulation, cell wall modification and the synthesis or signalling of defence hormones, such as ethylene, jasmonic acid (JA) and salicylic acid (SA).

Moreover, stomatal immunity is tightly regulated by major plant hormones such as abscisic acid (ABA), SA and JA. ABA is the main phytohormone involved in stomatal closure under abiotic stresses, such as drought. The major ABA signalling pathway consists of three core components: the ABA receptors, the type 2C protein phosphatases (PP2Cs) and the SNF1-related protein kinases 2 (SnRK2s) [34,35], that phosphorylates downstream substrates, thereby promoting stomatal closure [36]. However, the role of ABA in stomatal immunity has been extensively discussed. It is suggested that, at the pre-invasion stage, ABA promotes resistance to bacterial inoculation, acting as a positive regulator of stomatal defence [37,38]. Nonetheless, at the post-invasive stage ABA

suppress callose deposition and SA-mediated plant resistance, thus promoting bacterial infection [39,40].

Although ABA-induced stomatal closure shares core signalling components, current experimental evidence suggests that there is an ABA-independent pathway controlling stomatal immunity. In this sense, both PAMP- and ABA-induced stomatal closure converge at the level of Open Stomata 1 (OST1), a serine/threonine protein kinase that belongs to the SnRK2 family [41], triggering the activation of both S-type anion channels, Slow Anion Channel-associated 1 (SLAC1) and SLAC1 homolog 3 (SLAH3) [42–44]. However, there are some differences in the stomatal immunity signalling of both pathways. In the case of ROS production, during PTI-mediated stomatal closure, ROS burst is produced by the activation of the NADPH oxidase RBOHD that is directly phosphorylated by the plasma-associated kinase BIK1, as mentioned before, while ABA-induced ROS production is carried out via OST1, which phosphorylates and activates RBOHF/RBOHD [45,46]. Additionally, as aforementioned, MPK3 and MPK6 positively regulate flg22-triggered stomatal closure in a partially redundant manner, but they are not involved in ABA-mediated stomatal closure. In this sense, MPK9 and MPK12 act redundantly as positive regulators of ABA- and ROS-mediated stomatal immunity, but they seem not to be involved in flg22-induced stomatal closure [47–49] (Figure 1).

SA the main phytohormone involved in biotic stress caused by biotrophic pathogens, is also required for stomatal immunity, since SA-deficient mutants are defective in stomatal defence [50,51]. It has been proposed that SA accumulation during stomatal defence is activated by MPK3/6 which induced the specific guard cell lipoxygenase LOX1, producing reactive electrophile species oxylipin (RES oxylipin) [47]. Recently, researchers have suggested that SA activates peroxidase-mediated ROS production and CPKs, thus integrating SA and ABA signalling via CPKs, and finally phosphorylating and activating SLAC1 [52]. Although SA-responsive genes are induced in guard cells after pathogen exposure, the SA-induced stomatal closure signalling pathway remains to be clarified in detail [53,54].

Finally, JA signalling plays a central role in plant defences against necrotic pathogens and herbivores. However, there is no consensus regarding stomatal immunity. Several several researchers observed that its methylated derivative, methyl jasmonate (MeJA) was shown to trigger stomatal closure in epidermal peels by the activation of slow-type anion channels through a process that requires calcium channels, NO accumulation and ROS production by NADPH oxidases (RBOH D and F) [55–57]. Nonetheless, other research groups could not confirm the MeJA-triggered stomatal closure in *Arabidopsis* [47] or suggested that MeJA had a significantly lower potency in promoting stomatal closure compared with ABA or the precursor of JA, 12-oxo-phytodienoic acid [58].

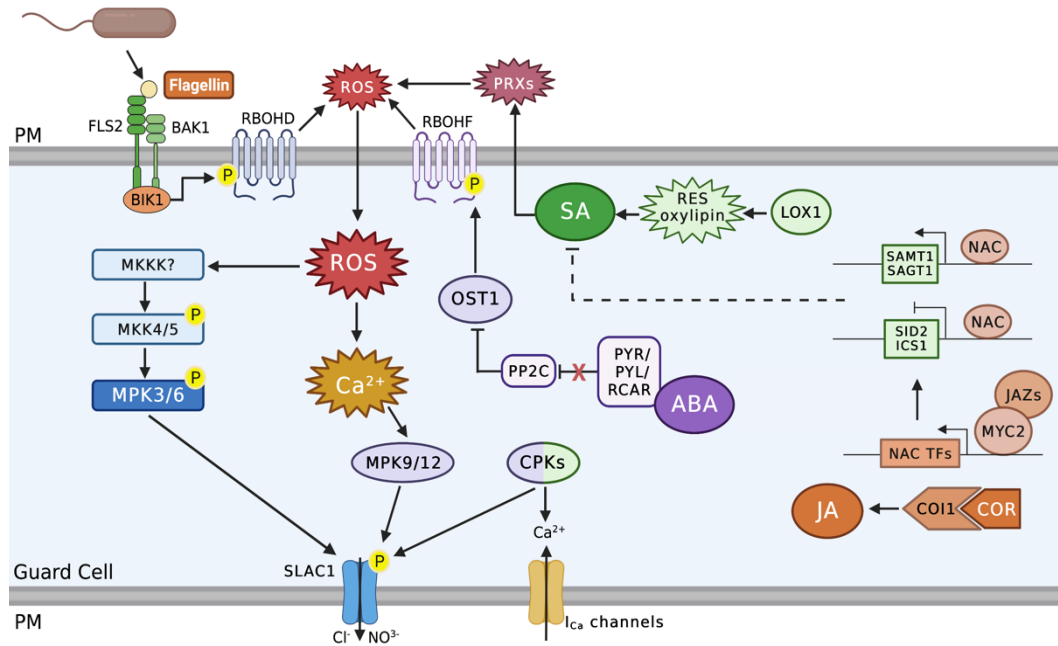


Figure 1. Signalling Pathways Regulating Stomatal Immunity against *Pseudomonas syringae* infection. Upon pathogen perception stomatal closure is mediated by ABA, PAMPs/DAMPs, SA and JA signalling pathways. ROS are produced by the NADPH oxidase RBOHD, RBOHF or by apoplastic peroxidases (PRXs). RBOHF and PRXs are specifically required for ABA- and SA-mediated ROS production, respectively. After pathogens entry, ABA signalling pathway is turned on, allowing OST1 to activate NADPH oxidases RBOHD and RBOHF ROS production. ABA-mediated ROS burst activates downstream targets such as MPK9/12 and CPKs, that finally phosphorylate and activate SLAC1. On the other hand, SA-mediated stomatal closure is activated by LOX1 and subsequent RES oxylipins production. Furthermore, MPK3/6 are activated by PAMPs and ROS burst, acting upstream or independently of RES oxylipins. Downstream secondary messengers such as H_2O_2 , and Ca^{2+} as well as inward calcium I_{Ca} channels and the S-type anion efflux channel SLAC1 are largely shared by PAMPs, ABA, and SA signalling pathways in guard cells. However, *Pst* phytotoxin coronatine targets the COI1 receptor or JAZ transcriptional repressors to activate JA signalling. Activation of JA signalling leads to MYC2 activation and subsequently, modulation of the expression of NAC transcription factors, which, in turn, NAC TFs repress the expression of the SA biosynthesis gene SID2/ICS1 and activate the expression of SA metabolism genes SAMT1 and SAGT1 resulting in lowered SA accumulation and inhibition of PAMP-triggered stomatal closure. Finally, COR also inhibits NADPH oxidase-dependent ROS production in guard cells which, along with SA signalling inhibition, triggers stomatal re-opening.

***Pseudomonas syringae* pv. *tomato* DC3000 as a stomatal immunity model system**

Pseudomonas syringae is one of the best-characterized plant pathogens, constituting a model for bacterial pathogenicity and plant-microbe interactions. *P. syringae* strains are grouped depending on host specificity into pathovars, dividing each pathovar into multiple races on the basis of differential interactions with cultivars of a plant species [59]. Specifically, *Pseudomonas syringae* pathovar *tomato* DC3000 (*Pst* DC3000) not only affects its natural host tomato, but also *Arabidopsis thaliana* plants, what has allowed the characterization of molecular mechanisms by which this strain causes disease in plants [60]. *Pst* DC3000 is described as a hemibiotrophic pathogen, since its disease cycle is divided into two spatially and temporarily interconnected lifestyles: an

initial epiphytic phase when bacteria live on the surface of healthy plant tissues; and the endophytic phase, when bacterial colonies enter the plant through natural openings, as stomata or accidental wounds, colonizing the apoplast [61].

A general model of stomatal movements in plant defence against *Pst* DC3000 has been widely studied. Particularly, it is well described that in *Arabidopsis* plants infected with *Pst* DC3000, the bacterial PAMP flg22 is recognized by the receptor complex FLS2-BAK1. Subsequently, BIK1, which is a direct substrate of the receptor complex, phosphorylates NADPH oxidase, inducing ROS production. Furthermore, flg22-induced defensive pathway also trigger transient elevation of cytosolic Ca²⁺, which, together with ROS production and MAPKs activation, particularly MPK3 and MPK6, ultimately induces stomatal closure. As aforementioned, SA plays a major role in flg22-induced and FLS2-mediated stomatal closure [25,37,46,54,62], but ABA and JA modes of action in *Pst* DC3000 infection have been extensively discussed.

Upon flg22 recognition by the receptor complex FLS2-BAK1 and PTI establishment, *Pst* DC3000 synthesizes the phytotoxin coronatine (COR), a virulence effector as a counter defence strategy. COR mimics the active form of JA, activating JA-signalling pathway and exploiting the endogenous antagonistic interaction between JA and SA signalling, that leads to the suppression of SA-dependent stomatal closing [37,63,64] (Figure 1). Furthermore, COR inhibits NADPH oxidase-dependent ROS production in guard cells, which, along with SA signalling inhibition, trigger stomatal re-opening [65]. A recent study also reported that not only JA through COR, but also ABA mediate the inactivation of the MPK3 and MPK6, promoting *Pst* DC3000 virulence. Moreover, to counteract bacterial suppression of MAPKs, host plant blocks JA signalling pathway upon ETI establishment [66]. These results demonstrate the highly interconnected network of plant immune signalling pathways, and how it can be exploited by host plants and pathogens.

2. Secondary metabolites in plant defence

An important defensive response during PTI and ETI establishment is the production of secondary metabolites. In this framework, plants are able to produce more than 100.000 chemically and structurally diversified secondary metabolites, which are generated from different primary metabolites or their biosynthetic intermediates. Secondary metabolites are generally non-essential molecules in basic plant growth and development processes, playing major roles as defensive metabolites by acting as toxins, growth inhibitors or attracting attackers' natural enemies [67–69]. Alkaloids, terpenoids, glucosinolates, quinones or phenolics, belong to this large group. Because of its interest in the plant defensive response, this thesis focusses the attention on two main groups: phenolics and Volatile Organic Compounds (VOCs).

2.1. Phenolic compounds

Phenolic compounds are a large and diverse group of chemicals that, structurally, comprise an aromatic ring, bearing one or more hydroxyl substituents, that are present in plant seeds, leaves, bark, and flowers. They are mainly biosynthesized from the pentose phosphate, shikimate and phenylpropanoid pathways [70,71]. Phenolics present a variety of biological functions, including anti-inflammatory, anti-cancerous, antibacterial, antifungal, and antioxidant properties [72]. Compounds as flavonoids, cinnamic acids, lignins and lignans, anthocyanins, tannins or the phytohormone SA belong to this family.

2.1.1. Salicylic acid

Salicylic acid (2-hydroxybenzoic acid) is a main phytohormone involved in different physiological and biochemical processes, as seed germination, storage, or fruit ripening, but its best-known function is as a defence-related compound. In plant immunity, SA was described to be essential in the establishment of the programmed cell death at the infection sites (HR), which also can result in the activation of SAR, providing both local and systemic plant resistance upon herbivores or pathogens attack [73–75]. Both HR and SAR are characteristic of the latterly called ETI.

This phytohormone can be biosynthesized by two distinct biochemical routes: the isochorismate (IC) and the phenylalanine ammonia-lyase (PAL) pathways. Although both biosynthetic paths are originated from the same primary precursor, the chorismate, more than 90% of SA accumulation in response to hemi- and biotrophic pathogens attack occurs through ICS [76–78] (Figure 2).

Due to its cytotoxic effect, the balance between SA biosynthesis and catabolism should be fine-tuned. For this reason, this phenolic undergoes several chemical modifications including glycosylation, methylation, amino acid conjugation or hydroxylation. Most of them render SA inactive, but at the same time they allow a balance between its accumulation, function and mobility [74,79]. For example, after glucosylation, SA is chemically inactive and it allows vacuolar storage of large quantities of SA glucoside (SAG) [80,81]. The methylation increases SA membrane permeability making it volatile (MeSA) [82]. This derivative can be released from the plant acting as signal molecule in plant–insect interactions. Finally, hydroxylation of SA is suggested to be the major pathway for SA catabolism and results in 2,3- and 2,5- dihydroxybenzoic acids [83,84] (Figure 2).

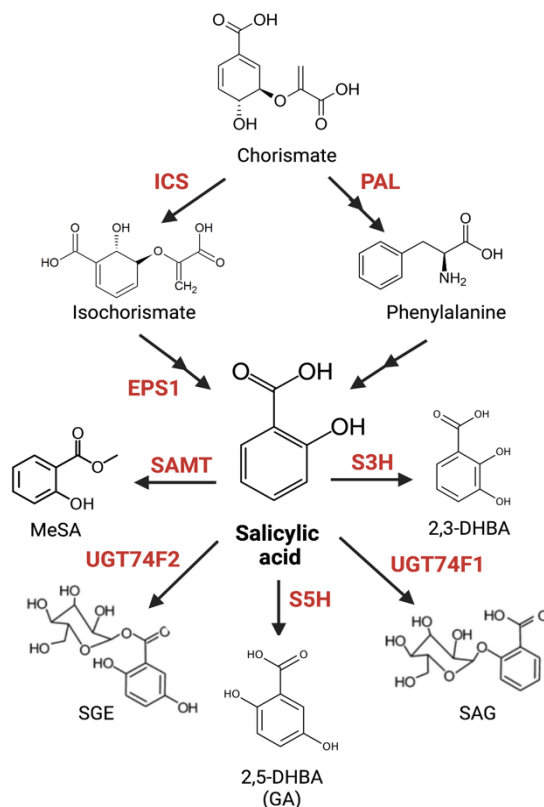


Figure 2. Salicylic acid biosynthesis and catabolism. SA is synthesized from the primary metabolic precursor chorismate via 2 distinct pathways, isochorismate (ICS) and phenylalanine ammonia-lyase (PAL) pathways. Due to its cytotoxic effect, SA is chemically modified into different derivatives: methylation converts SA into the volatile compound methyl salicylate (MeSA) with the enzyme S-adenosyl methionine (SAMT); glycosylation through UDP-glucosyltransferases 74F1 and 74F2 (UGT74F1/2) glycosyltransferases; 2,3- and 2,5-dihydroxybenzoate (DHBA) or gentisic acid (GA) through the salicylate-3 and salicylate-5- hydroxylases (S3H, S5H), respectively.

2.1.2. Gentisic acid

Gentisic acid (GA; 2,5-dihydroxybenzoic acid) is a phenolic compound present in plants, animals and microorganisms [85–87]. There are many studies published about GA biological properties such as anti-inflammatory, antimutagenicity, hepatoprotective, neuroprotective, antimicrobial, and especially antioxidant, which proposed its potential uses in the treatment of diseases [88]. Regarding plant immunity, GA accumulation was first described upon compatible plant-pathogen interactions such as those produced by citrus exocortis viroid (CEVd) and tomato mosaic virus (ToMV) in tomato plants, increasing GA accumulation more than 150-fold compared with non-infected plants [89]. Moreover, exogenous treatments with this compound induced the expression of PR defensive genes, gene silencing mechanisms and plant resistance in different plants species, as *Solanum lycopersicum*, *Cucumis sativus* and *Gynura aurantiaca* [89–91], thus confirming the role of GA as a defensive molecule.

2.2. Volatile Organic Compounds (VOCs)

Volatile Organic Compounds (VOCs) are one of the most relevant secondary metabolites produced by plants. They are defined as lipophilic compounds, with low molecular weights and high vapor pressures, physical properties that allow them to freely cross cellular membranes and be released into the surrounding environment [92]. VOCs represent a vast family, with more than 1700 identified volatiles in different plants species, and they are emitted from flowers, leaves, fruits, stem and even roots both angiosperms and gymnosperms [93].

Plant VOCs have different functions in plant-pollinator, plant-plant, plant-herbivore and plant-pathogen interactions. Regarding defence against pathogens, VOCs can act directly triggering plant defence signalling or as bactericides by inhibiting pathogen's growth; on indirectly, by attracting pathogen's natural predators [94,95]. VOCs can also prime defences in neighboring plants, constituting the main system of interplant communication [96,97].

Despite being a highly diverse and large family, their biosynthetic pathways are conserved across plant species. The four major VOCs biosynthetic pathways are the shikimate/phenylalanine for production of phenylpropanoids, mevalonic acid (MVA), methylerythritol phosphate (MEP) or terpenes biosynthesis and lipoxygenase (LOX) pathway that induce the production of methyl jasmonate and Green Leaf Volatiles (GLVs) respectively [93]. Due to their interest as multifunctional weapons of plants against herbivores and pathogens, this thesis focuses on GLVs.

2.2.1. Green Leaf Volatiles (GLVs)

Green Leaf Volatiles are compounds that consist of six carbon aldehydes, alcohols, and their acyl esters, derived from fatty acids via oxylipin/lipoxygenase (LOX) pathway [98]. Under biotic and abiotic stress conditions, the degradation of membrane lipids is initiated by phospholipases, releasing free polyunsaturated acids (PUFAs), which are the substrates for the oxylipin pathway. Plant LOXs can be classified in 9-LOXs and 13-LOXs, depending on the oxygenation position of the hydrocarbon backbone. 13-LOX oxidates the PUFAS into the corresponding 13-hydroxyperoxides that are substrates of two different pathways. On one hand, allene oxide synthase (AOS) can act on 13-hydroxyperoxide to produce oxo-phytodienoic acid (OPDA), JA, and its methyl ester MeJA, collectively named jasmonates (JAs), which play a major role in the activation of wound- and herbivore-induced responses. On the other hand, 13-hydroxyperoxide can be also cleaved by a hydroperoxide lyase (HPL) to yield C6-volatile aldehydes, as (*Z*)-3-hexenal. These aldehydes can be converted into alcohols by the action of alcohol dehydrogenase (ADH), or into esters by the enzyme alcohol acyltransferase (AAT) [93,99–101] (Figure 3). GLVs biosynthetic pathway is latent, and quickly activated when plant tissues are damaged, leading to the production of a massive amount of GLVs within seconds to a few minutes [99,102].

The role of plant GLVs in plant-herbivore interaction has been extensively studied, while its defensive role against pathogens has received less attention. However, different studies have shown positive correlation between GLV emission and pathogen resistance through direct antibacterial activities and/or as signalling molecules that induce plant defences [97,103–105]. In previous works, a non-targeted GC-MS metabolomics analysis allowed the identification of some esters of (*Z*)-3-hexenol that were differentially emitted by tomato cv. Rio Grande plants upon infection with the avirulent strain of the bacterium *Pst* DC3000, which leads to the establishment of ETI. Differential volatile production correlated with the transcriptional activation of GLVs biosynthesis genes after bacterial inoculation. Particularly genes encoding for lipoxygenase F (*TomloxF*) [106] and an alcohol acyltransferase (*AAT1*) [107], displayed induction patterns statistically correlated with the emission of the GLV esters in both interactions, becoming higher during ETI establishment. [2].

Moreover, we observed that treatments of plants with different GLV esters as (*Z*)-3-hexenyl propionate (HP) and, to a greater extent with (*Z*)-3-hexenyl butyrate (HB), promotes stomata-closing, PR gene induction and enhanced resistance to the bacterial infection with *Pst* DC3000. The efficacy of HB as a stomata closer was tested in different plant species as *Arabidopsis*, *Medicago*, *Zea*, *Citrus* y *Nicotiana* plants, postulating HB as a new universal stomata closer [3; annex I] and patenting its use [108].

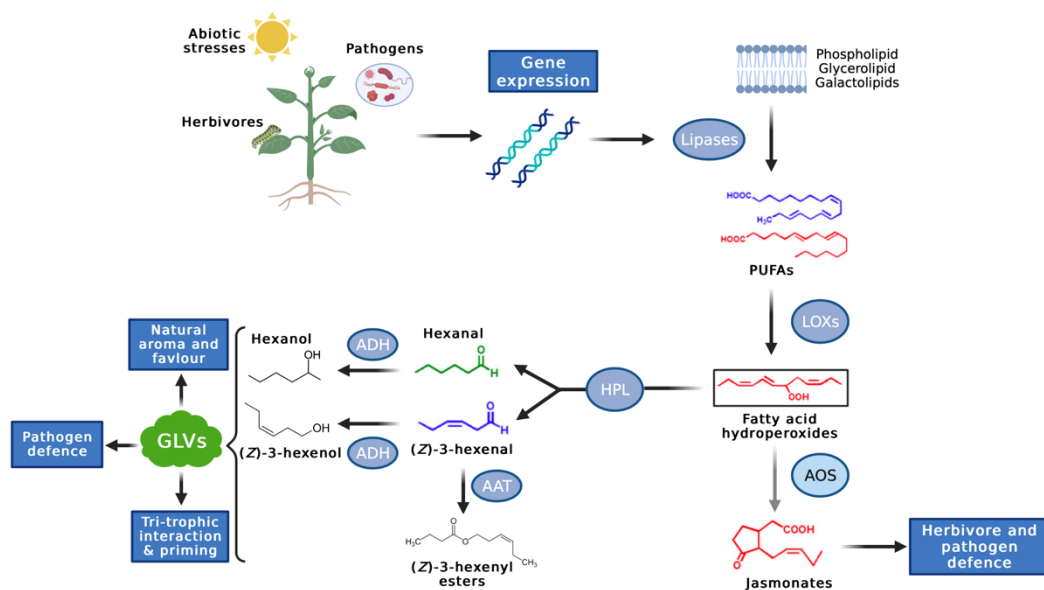


Figure 3. GLVs biosynthetic pathway. Under biotic and abiotic conditions, polyunsaturated fatty acids (PUFAs) are substrates for lipoxygenases (LOX). Subsequently, by the action of hydroperoxide lyase (HPL), alcohol dehydrogenase (ADH) and alcohol acyltransferase (AAT) enzymes, GLVs are released.

3. Use of elicitors against biotic and abiotic stresses

As aforementioned, during their lifespan, plants are constantly exposed to a range of different biotic and abiotic stresses that may occur simultaneously, affecting plant fitness. Moreover, industrialization, urbanization and climate change exacerbate the detrimental effects of these stresses, threatening global food security [109,110]. For this reason, much attention is now directed towards the development of new sustainable strategies for enhancing plant tolerance to multiple biotic and abiotic stresses.

To achieve tolerance to both biotic and/or abiotic stresses, different methodologies have been applied, from conventional and contemporary breeding procedures to genetic engineering approaches. The exploitation of the sophisticated plant defensive immune system has emerged as a promising strategy. These approaches involve the use of elicitors, which can be defined as compounds that can stimulate stress responses in plants, leading to enhanced synthesis and accumulation of secondary metabolites or target bioactive compounds [111]. In some cases, treatments with elicitors can induce “priming” in plants, a mechanism in which plants are able to better or/and more rapidly display defence responses, enhancing resistance in the case of biotic stresses, or acclimation for abiotic stresses [18,112–114].

Depending on their origin, elicitors can be classified into natural or synthetic elicitors. Several cases of both type of elicitor compounds are reviewed hereafter.

3.1. Natural elicitors

Natural elicitors can be derived from animals, microorganisms or plants and, according to their chemical properties, they can be classified into proteins, oligosaccharides, glycopeptides, lipids and other compounds acting as signal molecules [115–117].

Regarding biotic stresses, plant elicitors are defined as any compound that can activate plant immune system by interacting with endogenous plant defence proteins or inducing endogenous plant defence signals to trigger defence responses [118]. Different studies have tested the power and effectiveness of various natural elicitors derived from pathogens such as chitin [119], ethylene-inducing xylanase [120], peptidoglycans [121], and even different compounds present in the saliva of insects, as inceptin or volicitin [122–124]. Signal molecules that differentially accumulate in the plant as a consequence of pathogenic infections or abiotic stresses, can be also considered as elicitors, since they produce the activation of the plant defensive response after its exogenous application [125,126]. In this sense, different signal molecules that are accumulated after pathogenic infections as glycerol-3-phosphate, hexanoic, nonanedioic or azelaic acid, and the phytohormones JA, SA and their respective methylated derivatives, MeJA and MeSA are considered as potential plant elicitors [127–131].

Regarding abiotic stresses, metabolic pathways are dynamically altered in response to environmental stress, including primary and secondary metabolites, and hormone-related mechanisms. Many reports have demonstrated that exogenous application of primary metabolites help plants to better tolerate abiotic stresses. This is the case of treatments and with 5-aminolevulinic acid, a precursor in chlorophyll biosynthesis, able to improve UV-B tolerance, drought or salinity in lettuce potato [132,133]. The exogenous application of proline has also been extensively reported to act as external osmotic protective, improving plant growth, yield and stress tolerance under adverse environmental conditions [134]. In general terms, several studies have pointed out the promising role of signal molecules of diverse nature as hydrogen sulfide, molecular hydrogen, nitric oxide, hydrogen peroxide, melatonin, chitosan, silicon, ascorbic acid, tocopherols, and trehalose as promising elicitors that enhance the salinity tolerance of crop plants [135].

Finally, some volatile compounds act as natural elicitors as well, e.g. 1,3-propanediol, 3-pentanol, 2-butanone, albuterol or different GLVs [136–139]. Although some reports suggested that the use of elicitors in agricultural application can induce resistance up to 85%, the shortage of general knowledge about biological elicitor's capability restricts the use of these compounds [140]. In the same way as under biotic stress conditions, plant subjected to abiotic stress also emit a variety of VOCs. In this sense, GLVs play pivotal roles in priming acclimation to abiotic stresses, although the molecular mechanism is not well understood. In this sense, (*E*)-2-hexenal is commercialized as a biostimulant for heat tolerance. Furthermore, (*Z*)-3-hexenyl acetate exogenous application enhance antioxidants systems and trigger the accumulation of osmolites in peanut seedling, and reduces the damage resulting from chilling in maize [141,142].

3.2. Synthetic elicitors

An alternative strategy for the use of natural elicitors is the discovery of new small molecules that activate plant defence responses by mimicking interaction of natural priming agents or different defence signalling molecules [118]. A large variety of synthetic SA analogues have been used as synthetic elicitors, as 2,6-dichloroisonicotinic acid, Benzo-(1,2,3)-thiadiazole-7-methionine S-methyl (BTH) and acibenzolar-S-methyl mimic the pathogen-induced SAR [128]. Furthermore, there is a vast repertoire of synthetic elicitors that induce plant defence signalling either by activating other hormonal pathways, as JA or ethylene, or by activating different defensive mechanisms [118].

Since abiotic stresses are considered as a major factor limiting crop yield and quality, the development of new and effective strategies to mitigate the effects of these stresses is essential. A highly promising strategy is the use of huge chemical libraries to identify small molecules functioning as agonists for the main phytohormone involved in adaptive responses toward environmental stresses, ABA. In this sense, Pyrabactin was the first identified ABA agonist small molecule, functioning as synthetic elicitor through the ABA-

receptors PYR1 and PYL1 [143,144]. Besides pyrabactin, quinabactin, also known as AM1, is another ABA agonist that elicits stomatal closure and exogenous treatments with quinabactin resulted in delayed wilting in *Arabidopsis thaliana* and soybean, maize and barley plants exposed to water stress [145–147]. Ultimately, mandipropamid is being used as a commercial agrochemical that functions as a selective agonist of the ABA-engineered PYR1 receptor, increasing drought tolerance in crops [148].

Although different parameters as the mode of application, the integration of chemical priming and environmental data need to be further studied, the use of synthetic elicitors in order to enhance plant resistance, tolerance and acclimation against multiple biotic and abiotic stresses is highly promising [125,126].

Despite the effectiveness of elicitors as a management tactic, the use of these compounds can harbor some drawbacks since the activation of any defence responses are costly, and this energy investments leads to growth penalty due to resource restrictions. These plant growth-defence tradeoffs have profound implications in agriculture and crop production [149,150]. For instance, JA prolonged induced defence response led to inhibition of leaf growth, photosynthesis and leaf development [151,152]. Furthermore, elicitor efficacy will strongly depend on the identities of the crop, the pest, and the elicitor involved [153].

Collectively, crops are exposed to multiple aggressions which cause a decrease in agricultural productivity, resulting in severe economic losses and an increase in production costs. The problems they provoke and the difficulty of controlling them, along with a tendency towards a greater social and environmental awareness, demonstrate the need to fight them through different sustainable strategies.

The study of both the molecular basis of the defence, as well as the signalling routes, have led to the development of different approaches to combat stresses in agriculture. A directly applied strategy to increase tolerance lies in the identification of signal molecules capable of inducing the defensive response. This could lead to the development of plant elicitors that could be applied on crops. The identification, development, and application of plant elicitors against both, biotic and abiotic stresses, can serve agricultural production, facilitating important contributions to ensure widespread food safety and sustainable agriculture development.

Objectives

Plant secondary metabolites are essential in plant defence response against biotic and abiotic stresses. For this reason, understanding the physiology, biochemistry, and ecological functions of secondary metabolites offers an opportunity to develop new strategies to protect plants against different stresses. The aim of this thesis is to further analyze the role of two secondary metabolites, the phenolic compound SA and the Volatile Organic Compound (VOC) (*Z*-3-hexenyl butyrate (HB), in plant immune system by using different biotechnological approaches.

Therefore, we proposed the following main objectives:

1. To study the pathogen-triggered salicylic acid metabolism in tomato by the phenotypic, chemical, and genetic characterization of salicylic acid 5-hydroxylase-silenced (*RNAi_SIS5H*) transgenic tomato plants, which are impaired in salicylic acid (SA) catabolism.
2. To study of the mode of action and potential applications in agriculture of (*Z*-3-hexenyl butyrate by addressing the following specific objectives:
 - 2.1. Characterization of the HB-mediated stomatal immunity signalling pathway, by using chemical inhibitors and mutants of the main components in plant defence signalling mechanisms.
 - 2.2. Evaluation and optimization of HB applications in agriculture, by testing HB efficacy in plant-pathogen interactions, and exploring novel potential HB uses against different stresses and developmental processes.

Chapter I

Role of SA in different tomato-pathogen interactions

Research article

SIS5H silencing reveals specific pathogen-triggered salicylic acid metabolism in tomato

Celia Payá, Samuel Minguillón, Marta Hernández, Silvia Maria Miguel, Laura Campos, Ismael Rodrigo, José María Bellés JM, Maria Pilar López-Gresa and Purificación Lisón *

Instituto de Biología Molecular y Celular de Plantas (IBMCP), Consejo Superior de Investigaciones Científicas (CSIC), Universitat Politècnica de València (UPV), Ciudad Politécnica de la Innovación (CPI) 8 E, Ingeniero Fausto Elio s/n, 46011 Valencia, Spain

*Corresponding autor: plison@ibmcp.upv.es

Ph.D candidate contribution

C. P. had a main role in the following activities: performing the experiments, data collection, data analysis, data visualization, figures editing and manuscript review.

Citation: Payá, C.; Minguillón, S.; Hernández, M.; Miguel, S.M.; Campos, L.; Rodrigo, I.; Bellés, J.M.; López-Gresa, M.P.; Lisón, P. SIS5H Silencing Reveals Specific Pathogen-Triggered Salicylic Acid Metabolism in Tomato. *BMC Plant Biol* **2022**, *22*, doi:10.1101/2022.03.03.482652.

List of Abbreviations

2,3-DHBA:	2,3-dihydroxybenzoic acid
2,5-DHBA:	2,5-dihydroxybenzoic acid
CEVd:	Citrus Exocortis Viroid
CFUs:	Colony Forming Units
DMR6:	Downy Mildew Resistant 6
EPS1:	Enhanced Pseudomonas Susceptibility 1
GA:	Gentisic Acid
hpi:	Hours Post Inoculation
HPLC-MS:	High-Performance Liquid Chromatography
hpt:	Hours Post Treatment
IC:	Isochorismate
ICS:	Isochorismate Synthase
MeSA:	Methyl Salicylate
PAL:	Phenylalanine Ammonia-Lyase
PCA:	Principal Component Analysis
PRs:	Pathogenesis-Related Proteins
<i>Pst:</i>	<i>Pseudomonas syringae</i> pv. <i>tomato</i>
qRT-PCR:	quantitative Real Time PCR
<i>RNAi_SIS5H:</i>	<i>RNAi SIS5H</i> -silenced transgenic tomato plants
ROS:	Reactive Oxygen Species
S3H:	salicylate 3-hydroxylase
S5H:	salicylate 5-hydroxylase
SA:	Salicylic Acid
SAG:	Salicylic Acid 2- <i>O</i> - β -D-Glucoside
SAMT:	Salicylic Acid carboxyl Methyltransferase
SAR:	Systemic Acquired Response
SGE:	Salicylate Glucose Ester
ToMV:	Tomato Mosaic Virus
TSWV:	Tomato Spotted Wilt Virus
UPLC-MS:	Ultra-Performance Liquid Chromatography-Cass Cpectrometry
wpi:	Weeks Post Inoculation
WT:	Wild Type

Abstract

Background

Salicylic acid (SA) is a major plant hormone that mediates the defence pathway against pathogens. SA accumulates in highly variable amounts depending on the plant-pathogen system, and several enzyme activities participate in the restoration of its levels. Gentisic acid (GA) is the product of the 5-hydroxylation of SA, which is catalysed by S5H, an enzyme activity regarded as a major player in SA homeostasis. GA accumulates at high levels in tomato plants infected by Citrus Exocortis Viroid (CEVd), and to a lesser extent upon *Pseudomonas syringae* DC3000 pv. *tomato* (*Pst*) infection.

Results

We have studied the induction of tomato *SIS5H* gene by different pathogens, and its expression correlates with the accumulation of GA. Transient over-expression of *SIS5H* in *Nicotiana benthamiana* confirmed that SA is processed by *SIS5H* *in vivo*. *SIS5H*-silenced tomato plants were generated, displaying a smaller size and early senescence, together with hypersusceptibility to the necrotrophic fungus *Botrytis cinerea*. In contrast, these transgenic lines exhibited an increased defence response and resistance to both CEVd and *Pst* infections. Alternative SA processing appears to occur for each specific pathogenic interaction to cope with SA levels. In *SIS5H*-silenced plants infected with CEVd, glycosylated SA was the most discriminant metabolite found. Instead, in *Pst*-infected transgenic plants, SA appeared to be rerouted to other phenolics such as feruloyldopamine, feruloylquinic acid, feruloylgalactarate and 2-hydroxyglutarate.

Conclusions

Using *SIS5H*-silenced plants as a tool to unbalance SA levels, we have studied the re-routing of SA upon CEVd and *Pst* infections and found that, despite the common origin and role for SA in plant pathogenesis, there appear to be different pathogen-specific, alternate homeostasis pathways.

Keywords: Defence, metabolomics, pathogen, phenolics, plant stress, salicylic acid, tomato

1. Introduction

Salicylic acid (SA or 2-hydroxy benzoic acid) is a phenolic compound present in many plants, and involved in different physiological and biochemical processes, being the activation of inducible defence programs its best characterized function. SA was first

described to act in tobacco as an inducer of plant disease resistance to tobacco mosaic virus [1]. Subsequently, evidence suggesting SA is a signal molecule comes from the landmark studies in tobacco mosaic virus-resistant tobacco and cucumber upon infection with necrotizing pathogens [2,3]. The essential role of SA in plant defence was definitively demonstrated by using transgenic tobacco plants unable to accumulate SA, which resulted to be incapable to establish the well-known systemic acquired resistance (SAR), an induced defence that confers long-lasting protection against a broad spectrum of pathogens [4,5]. To date, many other studies have been published to point out SA as the best known defence-related hormone [6,7].

This phenolic compound is biosynthesized in plants from phenylalanine through the route of the phenylpropanoids (PAL pathway) or from isochorismate (IC pathway). Loss-of-function of some genes from both pathways results in an increased plant susceptibility to pathogens, indicating that both the IC and PAL pathways contribute to SA accumulation and function in response to biotic stresses. Nevertheless, the main source of SA when the plant faces a pathogenic infection and SAR is established mostly depends on the IC pathway in *Arabidopsis thaliana* [8,9], being the pathway downstream of IC completely deciphered [10,11]. In this sense, upon stress situations, ICS1 and ICS2 isochorismate synthase activities isomerise chorismate into IC. In plants, IC is conjugated to the amino acid L-glutamate by an isochorismoyl-9-glutamate (IC-9-Glu) that can spontaneously break down into SA. Besides, EPS1 (Enhanced Pseudomonas Susceptibility 1) is an IC-9-Glu pyruvoyl-glutamate lyase that can enhance the conversion of IC-9-Glu into SA more effectively [12].

Due to its cytotoxic effects, plants maintain SA homeostasis by fine-tuning the balance between the biosynthesis and catabolism of this phytohormone. In this way, SA can be chemically modified into different bio-active derivatives, through glycosylation, methylation, sulfonation, amino acid conjugation, and hydroxylation [7]. Most of the SA present in the plant is glycosylated into SA 2-O- β -D-glucoside (SAG) [2,13] and, to a lesser extent, into salicylate glucose ester (SGE) [14], being both stored in the vacuole. These conjugates constitute a reserve of inactive SA that can be released slowly in its active form when the plant needs it by the action of glucosyl hydrolases [15,16]. In addition to this, SA can be conjugated with amino acids such as aspartic acid into SA-Asp [17], converted into SA-2-sulfonate by sulfotransferases [18], or methylated to form methyl salicylate (MeSA) by salicylic acid carboxyl methyltransferase (SAMT), this latter modification increasing SA membrane permeability and facilitating their mobilization. In SAR, MeSA acts as a phloem-based mobile signal that, after its hydrolysis to SA, triggers resistance [19,20].

Regarding SA hydroxylation, a salicylate 3-hydroxylase (AtS3H) was described in *Arabidopsis*. This hydroxylase is induced by SA and converts this compound into both 2,5-dihydroxybenzoic acid (2,5-DHBA) and 2,3-dihydroxybenzoic acid (2,3-DHBA) *in vitro*, and only into 2,3-DHBA *in vivo*. Studies with *s3h* mutants and the gain-of-function lines revealed that S3H regulates *Arabidopsis* leaf longevity by mediating SA catabolism

[21]. DMR6 (Downy Mildew Resistant 6) oxygenase has been proven essential in plant immunity of *Arabidopsis* [22] and has been later described as a salicylic acid 5-hydroxylase (AtS5H) that catalyses the formation of 2,5-DHBA displaying higher catalytic efficiency than S3H. The *Arabidopsis* *s5h* mutants and *s5hs3h* double mutants over accumulate SA and display phenotypes such as a smaller size, early senescence, and enhanced resistance to *Pseudomonas syringae* pv. *tomato* DC3000 [23]. More recently, the tomato DMR6 orthologs *SIDMR6-1* and *SIDMR6-2* have been identified, also displaying SA 5-hydroxylase activity. Tomato *SIDMR6-1* mutants, obtained by CRISPR/Cas9 system, exhibited broad spectrum disease resistance, correlating this resistance with increased SA levels and transcriptional activation of immune response upon *Xanthomonas gardneri* infection [24]. Therefore, preventing SA hydroxylation confers resistance to pathogens both in *Arabidopsis* and tomato, standing 2,3-DHBA and 2,5-DHBA for deactivated forms of SA. The main function of these hydroxylated forms is to prevent SA from over-accumulating, thus constituting a mechanism by which plants fine-tune SA homeostasis [21,23–25].

The 2,5-DHBA or gentisic acid (GA) has been described in animal tissues [26], in microorganisms [27], and plants [28]. Similar to SA, GA accumulates as glycoconjugates in plants, primarily as GA 5-*O*- β -D-glucosides, GA 5-*O*- β -D-xylosides, or GA 2-*O*- β -D-xylosides [29–32]. It is also known that exogenous application of GA to tomato (*Solanum lycopersicum*), cucumber (*Cucumis sativus*), and *Gynura aurantiaca* induces the expression of a distinct subset of PR defensive genes compared with the genes induced by SA, as well as mechanisms of gene silencing, and plant resistance [33–35].

The accumulation of SA and GA varies up to 100-fold in different plant species [23]. In tomato, that range of difference also occurs among different types of infections, being the accumulation of GA much higher than the SA itself in all of them [33,36–38]. These differences raise the hypothesis that plants regulate SA homeostasis differently upon specific pathogenic attacks, instead of displaying common pathways to metabolise SA. Since the conversion of SA into GA appears to play an essential role in SA homeostasis, our objective was to delve into the defensive role of a tomato salicylic acid 5-hydroxylase, and our results provide new insights into the SA metabolism of tomato plants facing different infections.

2. Materials and Methods

2.1. Plant materials and growth conditions

Tomato Rio Grande plants, containing the *Pto* resistance gene (gently provided by Dr. Selena Giménez, Centro Nacional de Biotecnología, Madrid, Spain), were used to establish the virulent and avirulent interaction upon bacterial infections. In the rest of experiments, transgenic tomato (*Solanum lycopersicum*) plants silencing the endogenous salicylate 5-hydroxylase gene (*SIS5H*) and the cultivar MoneyMaker (gently

provided by Dr. Prof. Jonathan Jones, The Sainsbury Laboratory, Norwich, UK), the isogenic parental line of *RNAi_SIS5H*, were used.

Tomato seeds were surface sterilized with sodium hypochlorite. After sterilization, seeds were sown in 12 cm-diameter pots and grown in standard greenhouse conditions, with a temperature between 25-30 °C, a relative humidity of 50-70 % and long day photoperiod (16 h light/8 h darkness).

For transient expression experiments, *Nicotiana benthamiana* plants were cultivated in the same conditions as tomato plants.

2.2. Vector construction

The full-length cDNA (1014 bp) of salicylate 5-hydroxylase gene (*SIS5H*; Solyc03g080190) was amplified by RT-PCR from leaves of Moneymaker tomato plants infected with CEVd, 4 weeks after inoculation, using 5' ATGGAAACCAAAGTTATTTTC-3' as the forward primer and 5'-GTTCTTGAAAAGTTCCAAAC-3' as the reverse primer. The resulting PCR product was cloned into the pCR8/GW/TOPO entry vector (Invitrogen), following the manufacturer's protocol, and was sequenced. Then *SIS5H* was subcloned in the pGWB8 Gateway binary vector. This vector carries the CaMV35S promoter and the hexahistidine tag (6XHis) which is attached to the C-terminus of the recombinant protein.

In order to generate the *SIS5H*-silenced transgenic tomato plants, the method described by Helliwell and Waterhouse was followed. Briefly, a selected 400 bp sequence of *SIS5H* was amplified from the full-length cDNA clone using the forward primer 5'-GGCTCGAGTCTAGAGGGAAATTCGTCAA-3', which introduced restriction sites *XhoI* and *XbaI*, and the reverse primer 5'-CCGAATTCGGATCCACCGTTACTTTACTGC-3', which added restriction sites *BamHI* and *EcoRI*. The PCR product was first cloned in the pGEM T Easy vector (Promega) and sequenced. After digestion with the appropriate restriction enzymes and purification, the two *SIS5H* fragments were subcloned into the pHANNIBAL vector in both the sense and the antisense orientations. Finally, the constructs made in pHANNIBAL were subcloned as a *NotI* flanked fragment into pART27 binary vector to produce highly effective intron-containing "hairpin" RNA silencing constructs. This vector carries the neomycin phosphotransferase gene (NPT II) as a transgenic selectable marker.

2.3. *Nicotiana benthamiana* agroinfiltration and tomato transformation

The pGWB8-SIS5H construction and the pGWB8 empty vector were transformed into the *Agrobacterium tumefaciens* C58 strain, while the pART27-SIS5H construction was transformed into *A. tumefaciens* LBA4404. Leaves of 4-week-old *N. benthamiana* plants were infiltrated with the *A. tumefaciens* C58 strain carrying pGWB8-SIS5H or the empty vector, along with a 1:1 ratio of the C58 strain carrying the p19 plasmid, which encodes

the silencing suppressor protein p19. Tomato MoneyMaker cotyledons were co-cultured with *A. tumefaciens* LBA4404 carrying the pART27-SIS5H construction to generate the RNAi *SIS5H*-silenced transgenic tomato plants (*RNAi_SIS5H*). The tomato transformants were selected in kanamycin-containing medium and propagated in soil. MoneyMaker wild-type tomato plants regenerated *in vitro* from cotyledons under the same conditions as the transgenic lines were used as controls in subsequent analyses. The transgenic plants generated in this study have been produced, identified and characterized in our laboratory and are to be used exclusively for research purposes.

2.4. Production of S5H recombinant protein in *Nicotiana benthamiana*

Agroinfiltration of *N. benthamiana* leaves with *Agrobacterium tumefaciens* C58, carrying either *pGWB8-SIS5H* or *pGWB8* empty vector was performed. Three days after the agro-inoculation, plants were embedded in a solution of 1 mM SA (see SA treatments) and samples were collected 24 upon the treatment. For western blot analysis, 5 g of frozen agroinfiltrated *N. benthamiana* leaves were ground and resuspended in 1 mL of extraction buffer (50 mM Tris-HCl, pH 7.5, containing 15 mM 2-mercaptoethanol). Proteins were separated by SDS-PAGE and stained with Coomassie Brilliant Blue R-250 or transferred to nitrocellulose filters (OPTITRAN, Schleicher&Schuell). S5H recombinant protein was examined by using specific anti-His mouse antibody (Novagen).

2.5. SA treatments

The SA treatments were carried out by stem-feeding. Four-week-old tomato plants or agro-inoculated *N. benthamiana* plants were excised above cotyledons, and stem cuts were immediately immersed in a 2 mM or 1 mM SA solution, respectively. After 30 min, all the stems were transferred to water, and leaf samples from three biological replicates were taken at 0, 0.5, 1, 6, 24 and 48 h post-treatment.

2.6. Viroid inoculation

For these assays, tomato plants were grown on a growth chamber with a temperature between 28 °C/24 °C and a relative humidity of 60%/85% (day/night). Viroidal inoculum was prepared from leaves of CEVd-infected tomato plants as previously described [36] and the first cotyledon and leaf of each plant were inoculated using carborundum as abrasive. Mock plants were inoculated with sterile water. Disease and symptom severity was recorded periodically. Leaf samples from six infected or mock-inoculated plants were harvested at 2- and 3-weeks post inoculation (wpi).

2.7. *Pseudomonas syringae* inoculation

The bacterial strain used in this study was *Pseudomonas syringae* pv. *tomato* DC3000 (*Pst*). For incompatible interaction, the infection was performed by the bacterial strain Pst DC3000 that contains deletions in genes *avrPto* and *avrPtoB* (*Pst* DC3000 Δ *avrPto*/ Δ *avrPtoB*) [188].

Pathogen inoculation was performed in 4-week-old tomato plants by immersion, as previously described [3]. For mock treatments, plants were immersed in 10 mM sterile $MgCl_2$ containing 0.05% Silwet L-77. The third and fourth leaves from six plants per treatment and genotype were harvested 24 h after inoculation.

2.8. *Botrytis cinerea* inoculation assays

The *B. cinerea* strain used was CECT2100 (Spanish Type Culture Collection). Fungal hyphae were grown on potato dextrose agar for 14 days at 24 °C in darkness. Spore suspensions were prepared by scraping surface plates, washing with sterile water, and filtering through cotton. Finally, the concentration was adjusted to 10^6 spores/mL. Three leaflets per plant were spotted with a 5 mL droplet of the spore suspension. All the experiments were carried out into inoculation chambers to maintain the proper high humidity conditions. Photographs, lesion size measurements and sampling were performed at 5 days after inoculation.

2.9. Determination of chlorophyll content

Chlorophyll quantification was carried out by the method of Arnon [80]. Frozen leaf tissue was homogenized with 80% acetone and then incubated overnight at 4 °C. Then, samples were centrifuged and the absorbance of the extracted solution was measured at 645 and 663 nm. Determination of chlorophyll a, b and total concentration was determined according to Arnon's equations.

2.10. Extraction and HPLC analysis of salicylic and gentisic acids

Extraction of free and total SA and GA from tomato leaflets was performed according to our previously published protocol [35]. Aliquots of 30 μ L were injected through a Waters 717 autosampler into a reverse-phase Sun Fire 5-mm C18 column (4.6 mm x 150 mm) equilibrated in 1% (v/v) acetic acid at room temperature. A 20-min linear gradient of 1% acetic acid to 100% methanol was applied using a 1525 Waters Binary HPLC pump at a flow rate of 1 mL/min. SA and GA were detected with a 2475 Waters Multi- λ Fluorescence detector (λ excitation 313 nm; λ emission 405 nm) and were quantified with the Waters Empower Pro software using authentic standard compounds (SA sodium salt and GA, Sigma–Aldrich, Madrid, Spain). Standard curves were performed for each compound using similar concentration ranges to those detected in

the samples. Data were corrected for losses in the extraction procedure, and recovery of metabolites ranged between 50 and 80%.

2.11. UPLC-ESI-QTOF-MS analysis

For UPLC-MS analysis, frozen tomato leaves (100 mg) were ground into powder in liquid nitrogen and extracted in 1 mL of methanol/water (80:20, v/v) for chromatographic analysis.

UPLC separations were performed on a reverse phase Poroshell 120 EC-C18 column (3 x 100 mm, 2.7 μm) (Agilent Technologies) operating at 30 °C and a flow rate of 0.4 mL/min. The mobile phases used were acidified water (0.1 % formic acid) (Phase A) and acidified acetonitrile (0.1 % formic acid) (Phase B). Compounds were separated using the following gradient conditions: 0–10 min, 1–18 % phase-B; 10–16 min, 18–38 % phase- B; 16–22 min, 38–95 % phase-B. Finally, the phase B content was returned to the initial conditions (1 % phase-B) for 1 min and the column re-equilibrated for five minutes more. 7 μL of the sample was injected using flow through needle (FTN) injection with a 15 mL syringe. The sample compartment in the auto sampler was maintained at 7.0 °C.

The UPLC system was coupled to a quadrupole-time-of-flight (maXis Impact HR Q-ToF-MS, (Bruker Daltonik GmbH, Bremen, Germany) orthogonal accelerated Q-ToF mass spectrometer, was performed using HR-ToF-MS in negative electrospray ionization mode using broadband collision induced dissociation (bbCID). High and low collision energy data were collected simultaneously by alternating the acquisition between MS and bbCID conditions.

Parameters for analysis were set using negative ion mode, with spectra acquired over a mass range from 50 to 1200 m/z . The optimum values of the ESI-MS parameters were: capillary voltage, -4.0 kV; drying gas temperature, 200 °C; drying gas flow, 9.0 L/min; nebulising gas pressure, 2 bars; collision RF, 150 Vpp; transfer time 72 μs , and pre-pulse storage, 5 μs .

At some stage in the UHPLC method development, an external apparatus calibration was performed using a KD Scientific syringe pump (Vernon Hills, IL) directly linked to the interface, passing a solution of sodium formate with a flow rate of 180 $\mu\text{L}/\text{h}$. The instrument was calibrated externally before each sequence with a 10 mM sodium formate solution.

Using this method, an exact calibration curve based on numerous cluster masses each differing by 68 Da (CHO_2Na) was obtained. Due to the compensation of temperature drift in the Q-TOF, this external calibration provided accurate mass values for a complete run without the need for a dual sprayer set up for internal mass calibration.

2.12. Non-targeted metabolomics analysis and quality control

All samples were injected in the same batch and the order of sample injection was randomized to avoid sample bias. A mixture with one replicate of each group of samples was used as “quality control” (QC) and was injected at the beginning, in the middle and at the end of the batch. Besides, methanol/water injections were included every five samples as a blank run to avoid the carry-over effect.

For the untargeted analysis of the polar and semi-polar profiles, the QToF-MS data were processed with XCMS online resources (<https://xcmsonline.scripps.edu>) with the appropriate script for the alignment of chromatograms and the quantification of each MS feature [190]. The resulting dataset was submitted to a Principal Component Analysis (PCA) study by the SIMCA-P software (v. 11.0, Umetrics, Umeå, Sweden) using unit variance (UV) scaling.

Metabolite identification was based on comparison of accurate mass, retention time, MS/MS fragments and CCS values with online reference databases including Respect (<https://spectra.psc.riken.jp/>), Metlin (<https://metlin.scripps.edu/>), HMDB (<https://hmdb.ca/>), Lipidmap (<https://www.lipidmaps.org/>), in-house databases based on commercial standards and theoretical MS/MS tags, and bibliographies. The CCS value acceptable error was <5% with MS tolerance of 5p.p.m., and MS/MS tolerance of <10 mDa, at least one major fragment was found.

2.13. RNA extraction and quantitative RT-PCR analysis

The total RNA of tomato leaves was extracted using the TRIzol reagent (Invitrogen, Carlsbad, CA, United States), following the manufacturer’s protocol. RNA was then precipitated by adding one volume of 6 M LiCl and keeping it on ice for 4 h. Afterward the pellet was washed using 3 M LiCl and was dissolved in RNase-free water. Finally, to remove any contaminating genomic DNA, 2 U of TURBO DNase (Ambion, Austin, TX, United States) were added per microliter of RNA. For the quantitative RT-PCR (qRT-PCR) analysis, one microgram of total RNA was employed to obtain the corresponding cDNA target sequences using an oligo(dT)18 primer and the PrimeScript RT reagent kit (Perfect Real Time, Takara Bio Inc., Otsu, Shiga, Japan), following the manufacturer’s directions. Quantitative PCR was carried out as previously described [35]. A housekeeping gene transcript, actin or elongation factor 2, was used as the endogenous reference. The PCR primers were designed using the online service Primer3 (<https://primer3.ut.ee/>) and are listed in Table S1.

2.14. Statistical analysis

The statistical analysis of two or more variables was carried out by using Student’s *t*-test or analysis of variance (ANOVA), respectively, employing the Prism 9 software

(<https://www.graphpad.com/>). Tukey's post hoc tests were performed in ANOVA analyses. In all the analyses, a p -value < 0.05 was considered statistically significant.

3. Results

3.1. Identification of the tomato pathogen-induced ortholog of *Arabidopsis thaliana* *S5H*

To identify the enzyme responsible for the conversion of SA into GA in tomato, a Blastp analysis was performed in Sol Genomics databases (<https://solgenomics.net/>) by using the *AtS5H/DMR6* sequence (At5g24530). A phylogenetic tree was built including the closest tomato sequences (Figure S S1). The Solyc03g080190 was selected as a candidate for SH5 role in tomato, since it resulted to be one of the closest in the phylogenetic tree, and it presented the highest identity percentage (67.35%), in contrast to the 62.43% of identity displayed by the Solyc06g073080 sequence, also near in the phylogenetic tree. The Blastp analysis of the Solyc03g080190 in The Arabidopsis Information Resource (www.arabidopsis.org) confirmed the selected candidate, being *AtS5H/DMR6* the closest gene to Solyc03g080190 (*SIS5H*) in *Arabidopsis thaliana*. Finally, this sequence coincided with At5g24530 tomato ortholog proposed by *EnsemblePlants* (<http://plants.ensembl.org/index.html>) and with *SIDMR6-1*, which has been recently proposed as the *DMR6* ortholog in tomato and which displayed salicylic acid 5-hydroxylase activity [165].

According to available transcriptome data, *SIDMR6-1* expression has been described to be induced in response to several pathogens [24]. To confirm the pathogen triggered *SIS5H* induction, and to extend the study of expression to other pathogens which provoke the accumulation of SA and GA, tomato plants were subjected to infection either with Citrus Exocortis Viroid (CEVd), Tomato Spotted Wilt Virus (*TSWV*), Tomato Mosaic Virus (*ToMV*) or a virulent and an avirulent strain of *Pseudomonas syringae* pv. *tomato* DC3000 (*Pst*) (see Materials and Methods). Leaf samples were collected at the indicated time points and *SIS5H* expression levels were analysed by qRT-PCR in those tomato-pathogen interactions (Figure 1A to 1D). The induction of *SIS5H* was observed upon all the pathogen infections in the analysed samples, reaching levels up to 5 times higher in CEVd-infected or *Pst*-infected plants than those observed in the non-infected plants, and around 2 times higher in the case of *TSWV* or *ToMV* infections. It is worthy to note that these induction patterns correlated with symptomatology, producing infection with CEVd the most severe disease symptoms and being *ToMV* infection practically symptomless [39]. Regarding the bacterial infection, *SIS5H* expression levels were higher in the tomato plants inoculated with the virulent bacteria (*Pst* DC3000 Δ AvrPto) as compared to the avirulent infection at 48 hours post inoculation (hpi), therefore confirming this tendency.

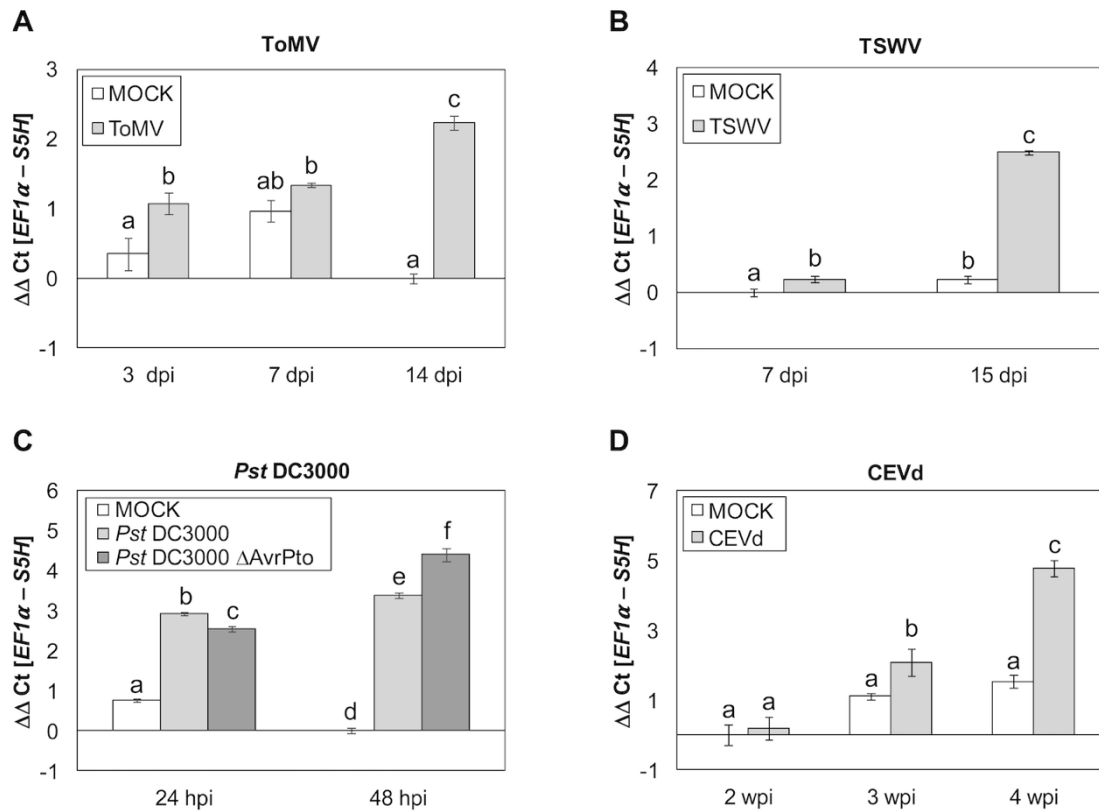


Figure 1. *SIS5H* expression patterns induced by different pathogens. Expression of *SIS5H* gene after inoculation with Tomato Mosaic Virus (ToMV, **A**); Tomato Spotted Wilt Virus (TSWV, **B**); *Pseudomonas syringae* pv. *tomato* DC3000 (*Pst*DC3000 **C**) and Citrus Exocortis Viroid (CEVd, **D**) at different times post-inoculation. MOCK represents the mock-inoculated plants. The qRT-PCR values were normalized with the level of expression of the elongation factor 1 gene. The data are presented as means \pm standard deviation of a representative experiment ($n=3$). An ANOVA test was performed and statistically significant differences (p -value < 0.05) between infected or mock-treated plants at different time points are represented by different letters.

To study the induction of *SIS5H* by its own substrate, SA treatments were performed, and samples were collected at different time points (see Materials and Methods). As Figure S2A shows, a statistically significant induction of *SIS5H* was detected by qRT-PCR at 6 hours post treatment (hpt) when compared with non-treated plants, presenting the maximal induction at 1 hpt. *PR1* activation was used as a positive control for the treatments, presenting a significant induction at 24 hpt (Figure S2B).

All these data confirm that *SIS5H* is involved in the plant response to pathogens, extending its putative role to different tomato-pathogen interactions.

3.2. Overexpression of *SIS5H* in *Nicotiana benthamiana* decreases SA levels *in vivo*

To confirm the *SIS5H* biochemical activity *in vivo*, *Nicotiana benthamiana* plants were agroinoculated with a construction carrying the *SIS5H* cDNA containing a His tag under

the *35S CaMV* promoter. These plants (*pGWB8-SIS5H*) and the corresponding control plants inoculated with the empty plasmid (*pGWB8*) were then embedded with SA (see Materials and Methods). The accumulation of the recombinant protein was confirmed by western blot analysis in *pGWB8-SIS5H* plants, and levels of free and total SA were measured (Figure S3). As expected, levels of free and total SA were almost 3 times lower in *pGWB8-SIS5H* plants, being these differences statistically significant, and thus confirming that SA is a substrate for SIS5H *in vivo*. However, no differences in neither the GA nor in 2,3-DHBA accumulation were detected between *pGWB8* and *pGWB8-SIS5H Nicotiana benthamiana* plants (Figure S3D).

3.3. Silencing *SIS5H* increases resistance to CEVd in tomato

To gain further insights into the *in vivo* role of SIS5H, silenced transgenic MoneyMaker tomato plants were generated by following an RNAi strategy (see Materials and Methods). The generated tomato lines *RNAi_SIS5H* were characterized, and several independent transgenic lines were confirmed. Homozygous lines *RNAi_SIS5H 14* and *RNAi_SIS5H 16* both carrying one copy of the transgene, were selected for further studies.

To extend the role of *SIS5H* in plant defence, the tomato-CEVd interaction was selected, since GA -the proposed product of S5H activity- had been described to accumulate at very high levels in CEVd-infected tomato plants [33,36–38]. Therefore, wild type (WT) and *RNAi_SIS5H* transgenic plants were inoculated with CEVd and checked for the development of symptoms. The characteristic symptomatology of CEVd-infected tomato plants consists of epinasty, stunting, leaf rugosity, midvein necrosis and chlorosis [40]. As Figure 2A shows, differences in the percentage of plants displaying symptoms were observed in both *RNAi_SIS5H* transgenic lines with respect to the parental tomato plants. Particularly, transgenic line *RNAi_SIS5H 16* displayed only 35% of plants showing symptoms at 1.9 weeks post inoculation (wpi), while almost 75% of non-transgenic plants exhibited them. Moreover, at 2.3 wpi all the WT plants displayed symptoms while around 20% of the *RNAi_SIS5H* remained symptomless. These results indicate a delay in symptom appearance in CEVd-infected *RNAi_SIS5H* tomato plants.

To confirm the differences in the disease development observed, a scale of the disease severity was established, scoring symptoms from mild (mild epinasty) to very severe (midvein necrosis and chlorosis), at different time points (see Materials and Methods). As Figure 2B shows, differences were observed between WT and *RNAi_SIS5H* transgenic tomato plants from 2.3 to 3.6 wpi. Moreover, *RNAi_SIS5H 16* transgenic line did not display very severe symptoms at 3 wpi, whilst 30% parental plants exhibited severe symptoms at the same time point. Therefore, the observed differences in symptom severity confirmed the partial reduction in the susceptibility of *RNAi_SIS5H* tomato plants to CEVd infection. Interestingly, transgenic plants appeared to display a

higher internode length when compared to the control plants. This phenotype was quantified as significant in further studies (Figure S6B).

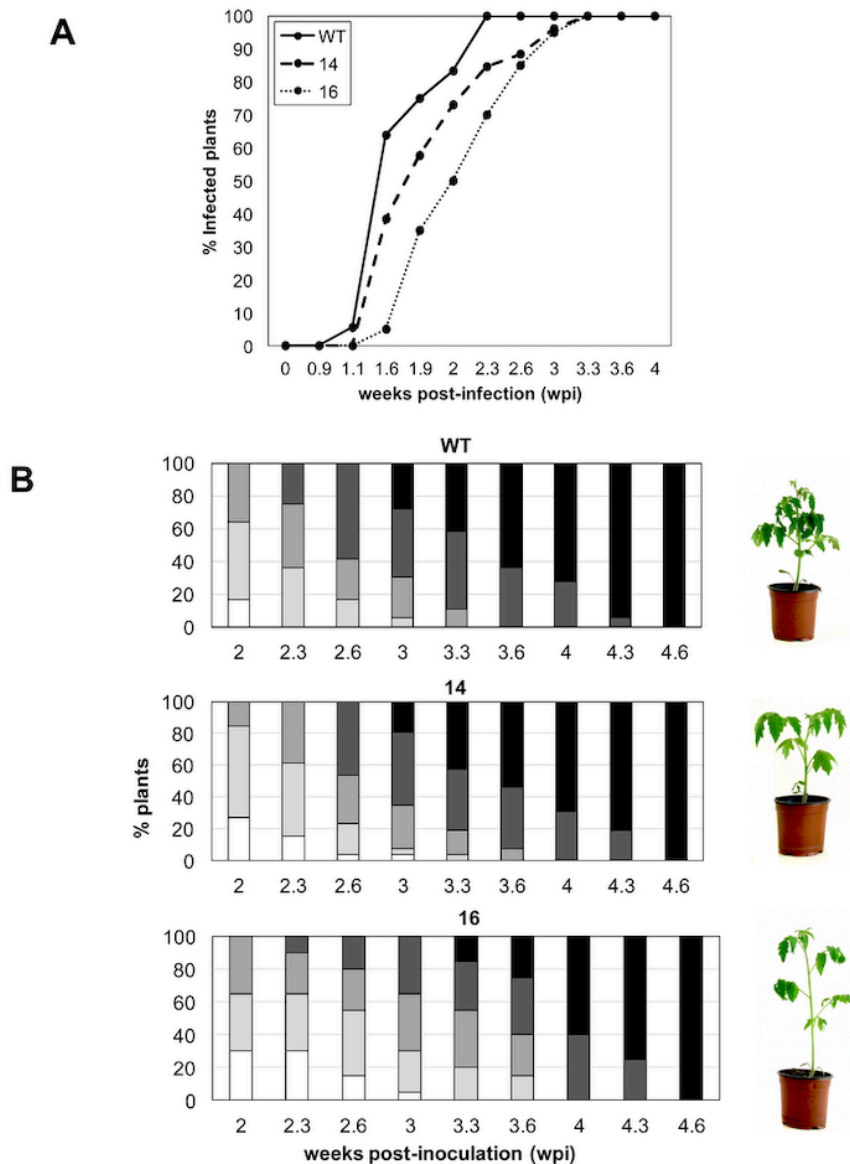


Figure 2. Symptomatology of wild type (WT) and *RNAi_SIS5H* (lines 14 and 16) tomato plants infected with CEVd. (A) Disease development in WT and *RNAi_SIS5H* 14 and *RNAi_SIS5H* 16 plants infected with CEVd. Evolution of the percentage of tomato plants showing symptoms at the indicated time points (wpi). **(B)** Representative images and disease severity of CEVd infected WT and *RNAi_SIS5H* plants. Symptomatology was established using the following scale: no symptoms (white), mild epinasty (light grey), severe epinasty and stunting (grey), leaf rugosity (dark grey), midvein necrosis and chlorosis (black). Data correspond to one representative experiment.

Finally, to confirm the enhanced resistance, the presence of pathogen was measured at 3 weeks post-inoculation (wpi), detecting a statistically significant decrease in the CEVd accumulation in both *RNAi_SIS5H* transgenic lines (Figure 3A).

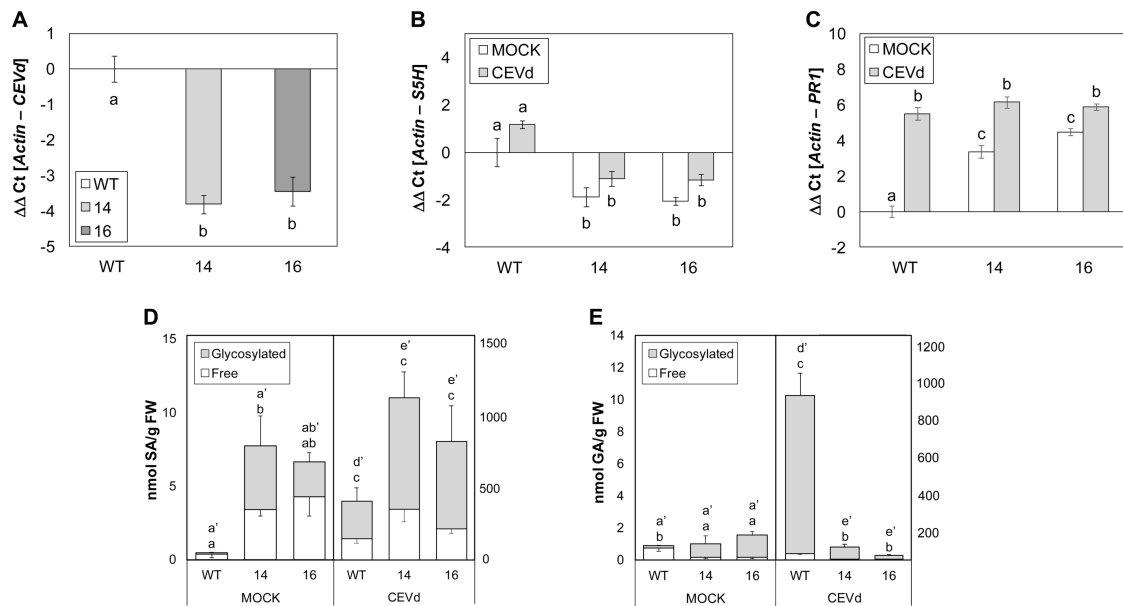


Figure 3. Characterization of wild type (WT) and transgenic *RNAi_SIS5H* (lines 14 and 16) tomato plants infected with Citrus Exocortis Viroid (CEVd). Tomato plants were inoculated with CEVd. Leaf samples were taken 3 weeks after inoculation and analyzed for *CEVd* (A), *S5H* (B) and *PR1* (C) gene expression, and phenolic compound accumulation (Salicylic Acid, SA, D; Gentisic Acid, GA, E). MOCK represents the non-inoculated plants. The qRT-PCR values were normalized with the level of expression of the actin gene. The data are presented as means \pm standard deviation of a representative experiment ($n > 3$). Statistically significant differences (p -value < 0.05) between genotypes and infected or mock-treated plants are represented by different letters. Significant differences in SA and GA accumulation are analysed in free (x) and total (x') phenolic compounds.

Our results appear to indicate *S5H* silencing reduces tomato susceptibility to CEVd, confirming the role of *SIS5H* in the plant defence response.

3.4. Silencing *SIS5H* causes an activation of plant defence upon CEVd infection

To analyse *SIS5H* expression levels in the RNAi transgenic plants infected with CEVd, qRT-PCR from WT, *RNAi_SIS5H 14* and *RNAi_SIS5H 16* plants, were performed at 2 weeks after the inoculation with CEVd (Figure 3B). Levels of *SIS5H* expression were significantly lower in both mock and viroid infected transgenic lines, than the corresponding WT tomato plants. To find out if *RNAi_SIS5H* transgenic lines exhibited an activation of the defensive response against CEVd, the expression of the pathogenesis related protein 1 (*PR1*; accession X71592), which has been described as a classical marker of plant defence rapidly induced in CEVd-infected tomato plants [41, 42], was also studied by qRT-PCR at 2 wpi. As expected, *PR1* was induced by CEVd in WT plants, but also in both *RNAi_SIS5H* transgenic lines (Figure 3C). Interestingly, levels of expression of *PR1* were already higher in mock-infected *SIS5H*-silenced tomato plants. These results appear to indicate that *SIS5H* silencing provokes the activation of the SA-mediated plant defence.

To better characterise the plant response of the *RNAi_SIS5H* transgenic lines upon CEVd infection, the expression of several defence genes was also studied at 3 wpi both in mock and infected plants. Regarding the gene silencing mechanisms that are activated by CEVd in WT plants, a significant reduction in *DCL1* and *DCL2* induction was observed in CEVd-infected *RNAi_SIS5H* lines when compared to the corresponding WT plants, thus indicating a correlation between the amount of CEVd and the induction of these two dicers (Figure S4A and S4B). However, no significant differences were observed in the *RDR1* induction pattern in the transgenic plants, which displayed a significant induction of this gene upon viroid infection (Figure S4C). As far as jasmonic acid (JA) response is concerned, a statistically significant reduction of the JA-induced proteinase inhibitor *TCI21* [43], was observed in both mock-inoculated *RNAi_SIS5H* lines when compared with WT (Figure S4D), indicating that the final JA-mediated response is repressed in these tomato transgenic plants.

Therefore, we have observed that *RNAi_SIS5H* transgenic lines display constitutive *TCI21* repression as well as *PR1* overexpression, thus suggesting an increase of SA levels in these transgenic lines.

3.5. Levels of SA and GA are altered in *RNAi_SIS5H* transgenic tomato plants upon CEVd infection

Free and total levels of SA and its hydroxylated product GA were quantified in the wild-type and *RNAi_SIS5H* transgenic lines upon viroid infection at 3 wpi (Figures 3D and 3E). As expected, free and total SA and GA levels were higher in all the CEVd-infected plants.

In CEVd-inoculated plants, levels of total SA in both *RNAi_SIS5H* transgenic infected lines resulted to be significantly higher when compared with those observed in control infected plants, reaching 1000 nmol/g fresh weight whilst levels in control infected plants barely reached 400 nmol/g fresh weight (Figure 3D). SA levels in non-pathogenic (mock) conditions were slightly higher in both transgenic lines, being statistically not significant when compared with wild-type plants.

Once detected the over-accumulation of SA, we studied the levels of GA, which is the product of the S5H activity. As Figure 3E shows, a drastic reduction of total GA levels was observed upon viroid-infected in both *RNAi_SIS5H* transgenic lines as compared to the levels detected in the infected WT tomato plants (10-fold). Interestingly, this significant reduction was also observed in free GA corresponding to mock conditions. The presence of 2,3-DHBA was measured in all samples, and the levels were negligible. The higher levels of SA and the lower accumulation of GA found in the CEVd-infected *RNAi_SIS5H* transgenic lines confirm the decrease of the salicylate 5-hydroxylase activity *in vivo* and explain the observed enhanced resistance and activation of the SA-mediated plant defence in these transgenic plants.

3.6. Infection with *Pseudomonas syringae* pv. *tomato* DC3000 produces specific phenolic accumulation pattern in *RNAi_SIS5H* transgenic tomato plants

Bacterial infection of tomato plants produces lower accumulation of SA when compared with levels produced by CEVd infection [37]. To study the role of *SIS5H* in this tomato-pathogen interaction, WT and *RNAi_SIS5H* transgenic tomato plants were infected with the virulent strain of *Pst*, and bacterial counting from infected leaves was carried out at 24 hours after infection (hpi). As shown in Figure 4A, a significant 10-fold decrease in the number of colony forming units (CFUs) was observed in infected tissues of the different transgenic lines with respect to their genetic background, confirming that transgenic plants *RNAi_SIS5H* also exhibited resistance against *Pst*.

SIS5H silencing in tomato plants upon bacterial infection was also confirmed by qRT-PCR, being differences in *SIS5H* expression in bacterial infected *RNAi_SIS5H* transgenic plants statistically significant compared to the expression levels observed in the infected WT (Figure 4B). Similar to what was observed upon viroid infection; *PR1* expression was already higher in mock-inoculated *SIS5H*-silenced tomato plants and was significantly induced by bacteria in both WT and *RNAi_SIS5H* transgenic lines (Figure 4C).

In a similar manner to that performed with CEVd-infected plants, SA and GA levels were measured in both WT and *RNAi_SIS5H* transgenic plants upon bacterial infection (Figure 4D and E). In *Pst*-tomato interaction, the levels of free and total SA were induced by the hemibiotrophic pathogen in all the analysed plants. As previously observed in mock-inoculated plants for CEVd infection, no statistically significant differences were observed in mock-inoculated transgenic plants, when compared with WT. Nevertheless, the slight overaccumulation of free SA in both mock-inoculated transgenic plants could explain the *PR1* induction observed in these plants (Figure 4C). Strikingly unlike what was observed upon CEVd infection, the bacteria produced a significant reduction of free and total SA levels in both *RNAi_SIS5H* transgenic lines when compared with levels observed in *Pst*-infected WT plants (Figure 4D). Regarding GA, only WT tomato plants showed a statistical accumulation of total GA levels after bacterial infection, thus indicating that the product of *SIS5H* is also reduced in *RNAi_SIS5H* transgenic plants upon bacterial infection (Figure 4E).

The reduction of SA levels observed in *RNAi_SIS5H* transgenic lines upon bacterial infection indicates that SA undergoes a specific catabolic process upon pathogen infection in these transgenic plants.

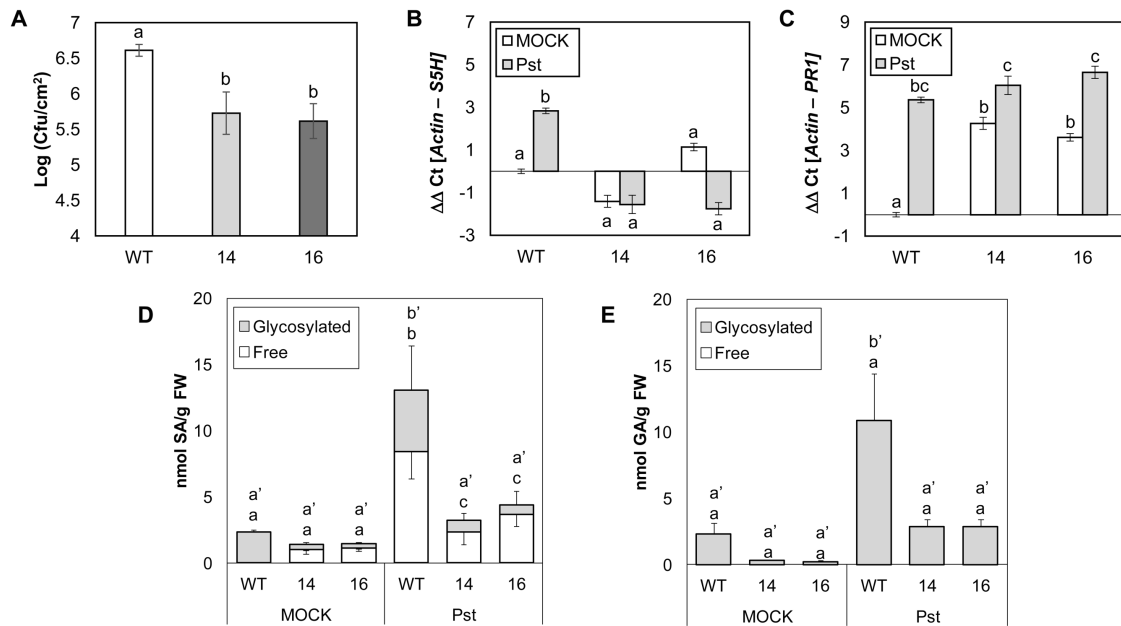


Figure 4. Characterization of wild type (WT) and transgenic *RNAi_SIS5H* (lines 14 and 16) tomato plants infected with *Pseudomonas syringae* pv. *tomato* DC3000. Tomato plants were inoculated with *Pst* DC3000 by immersion. Leaf samples were taken 24 hours after bacterial infection and analyzed for bacterial growth (A), *S5H* (B) and *PR1* (C) gene expression, and accumulation of phenolic compounds (Salicylic Acid, SA, D; Gentic Acid, GA, E). MOCK represents the non-inoculated plants. The qRT-PCR values were normalized with the level of expression of the actin gene. The data are presented as means \pm standard deviation of a representative experiment ($n > 3$). Statistically significant differences (p -value < 0.05) between genotypes and infected or mock-treated plants are represented by different letters. Significant differences in SA and GA accumulation are analysed in free (x) and total (x') phenolic compounds.

3.7. A metabolomic analysis of the *RNAi_SIS5H* transgenic tomato plants upon viroid and bacterial infection reveals differences in SA metabolism upon pathogen attack

To better understand the SA metabolism in *RNAi_SIS5H* transgenic lines upon each infection, a metabolomic study based on ultra-performance liquid chromatography-mass spectrometry (UPLC-MS) was performed. For viroid infection, 8-day-old tomato plants were used, and samples were collected 3 weeks after CEVd inoculation (wpi), while bacterial infection was carried out on 5-week-old tomato plants and the harvesting time was 24 h after *Pst* infiltration (hpi). Then, hydroalcoholic extracts from control and infected *RNAi_SIS5H* tomato leaves were analysed by UPLC-MS, and multivariate data analysis was employed to deal with the large number of mass data. Specifically, a principal component analysis (PCA) was first applied to identify metabolic changes after viroid and bacterial infection of tomato plants (Figure 5A). An extensive separation between both tomato interactions was observed by PC1 due to the different experimental conditions: temperature and plant age. Reaching the PC3, the metabolic changes in tomato leaves produced by both pathogens were explained, being greater those caused

by viroid inoculation. To exclude the differences due to this biological variability, two different PCA were therefore applied separately on each tomato-interaction.

In particular, the first two components of the PCA score plot of viroid-tomato interaction (Figure S5A) divided the observations by the infection (mock vs. infected plants; PC1) and genotype (WT vs. transgenic plants; PC2). In order to elucidate the SA metabolism in tomato plants against CEVd, a PCA of both infected WT and transgenic *RNAi_SIS5H* plants was performed (Figure 5B). For the identification of the metabolites accumulated in the infected *SIS5H* silenced lines (14 and 16), the positive PC1 loading plot was analysed. Interestingly, the glycosylated form of SA (SAG) was the most accumulated compound in the transgenic plants (fold change transgenic lines vs. WT: 3.0; *p*-value 0,009). These results are in accordance with the total SA accumulation measured by HPLC-fluorescence in CEVd infected *RNAi_SIS5H* plants (Figure 3D).

In the case of bacteria-tomato interaction, the PC3 of PCA (Figure S5B) explained the different metabolic content of transgenic tomato plants from WT, while PC1 clearly discriminated the metabolome of the infected *RNAi_SIS5H* line 16. Similarly to CEVd interaction, the PCA of infected tomato plants was required to investigate the role of SA in the bacterial infected tomato plants (Figure 5C). By analysing the negative PC1 and PC2 loading plot, the metabolites accumulated in both transgenic lines were identified. In contrast to CEVd infection, SAG accumulation was not induced by *Pst* in both transgenic lines according to the results obtained using fluorescence-based detection (Figure 4D). In tomato-bacteria interaction, some of the compounds over-accumulated in the transgenic infected leaves were identified as feruloyldopamine (fold change between transgenic lines and WT: 5.3; *p*-value 0.003), feruloylquinic acid (fold change: 5.1; *p*-value 0.006), feruloylgalactarate (fold change: 3.4; *p*-value 0.01) and 2-hydroxyglutarate (fold change: 1.4; *p*-value 0.04).

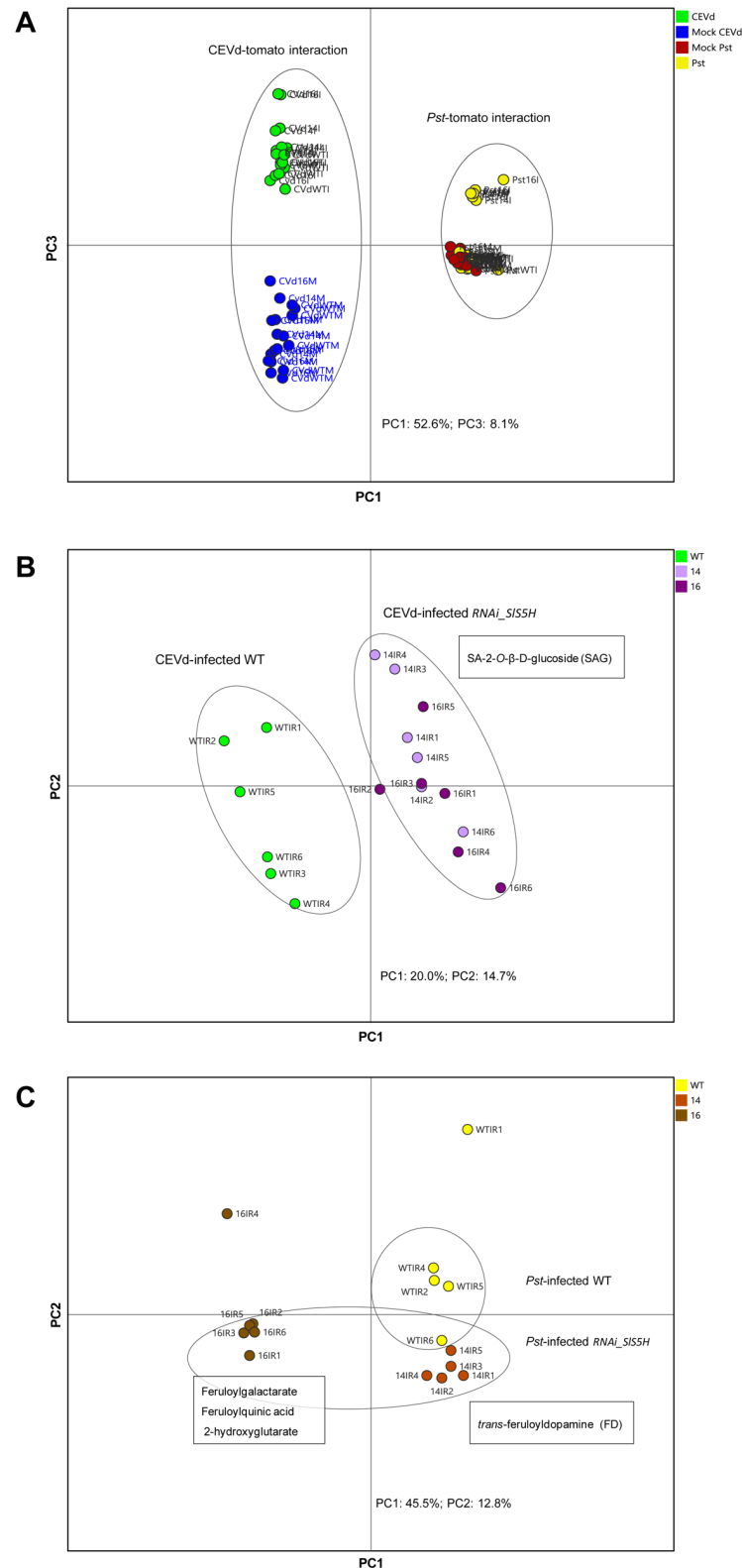


Figure 5. PCA Score plots based on whole range of on the whole array of the mass spectra within a m/z range from 100 to 1500 using unit variance (UV) scaling method of methanolic extracts from tomato leaves. (A) Green: Infected by CEVd (3 wpi); Blue: Mock for CEVd infection; Yellow: Infected by Pst (24 hpi); Red: Mock for bacterial infection. (B) Green: Wild type (WT); light purple: CEVd infected *RNAi_SIS5H* 14 at 3 wpi; dark purple: CEVd infected *RNAi_SIS5H* 16 at 3 wpi. (C) Yellow: Wild type (WT); orange: Pst infected *RNAi_SIS5H* 14 at 24 hpi; brown: Pst infected *RNAi_SIS5H* 16 at 24 hpi.

3.8. *SIS5H* silencing reveals differences in SA biosynthesis gene expression upon pathogen attack

To study differential expression of genes participating in SA biosynthesis and how they are affected by silencing *SIS5H*, qRT-PCR were performed for *ICS* (Solyc06g071030 or XM_019214145), *PAL* (Solyc09g007890 or NM_001320040), *EPS1* (Solyc08g005890 or XP_004244447), *SAMT* [44], and the glycosyltransferases of phenolic compounds *GAGT* [31] and *Twil* [45] in samples corresponding to CEVd or *Pst* infections for both WT and *RNAi_SIS5H* transgenic plants (Figure 6).

As Figure 6A shows, a significant induction in *ICS* was observed in WT plants upon CEVd infection, being that induction impaired in the transgenic lines, thus suggesting that the SA biosynthesis is down-regulated when the SA hydroxylation is prevented, which may lead to SA over-accumulation. Contrasting with CEVd infection, a clear reduction of *ICS* expression was detected upon bacterial infection, in both WT and transgenic lines. However, this decrease of expression was not statistically significant in the transgenic plants (Figure 6B).

As far as *PAL* pattern of expression is concerned, whilst CEVd infection caused a significant reduction in both transgenic lines compared to infected WT, no significant differences caused by *Pst* infection were observed (Figures 6C and 6D).

The last step in the SA biosynthesis through the isochorismate pathway involves the conversion of isochorismate-9-glutamate into SA, being performed by *EPS1*. Whilst WT plants appear not to display any significant induction of *EPS1* by CEVd, bacterial infection clearly provoked the induction of this gene. This pattern was completely opposite in both *RNAi_SIS5H* transgenic lines, since they showed a slight induction of *EPS1* upon CEVd infection, being impaired in the expression of *EPS1* upon bacterial infection (Figures 6E and 6F).

Moreover, a reduction of *SAMT* expression upon CEVd infection was measured in all the genotypes, with no significant differences observed between WT and transgenic plants. In contrast, *SAMT* induction caused by bacterial infection was lower in transgenic plants, showing statistically significant differences between the induction observed in infected WT and *RNAi_SIS5H 16* transgenic plants (Figure 6H).

Finally, as far as the glycosyltransferases of phenolic compounds *GAGT* and *Twil* are concerned, whilst no statistical differences were observed in the transgenic plants infected with *Pst*, a slight increase in the induction of both glycosyltransferases was observed upon viroid infection (Figures 6I-L).

Although the differences observed in both viroid and bacterial infections were not statistically significant for all the analysed genes, a noticeable variation in the pattern of expression of several genes participating in SA metabolism was detected upon infection

by these two pathogens, thus suggesting that SA homeostasis has specific differences for each tomato-pathogen interaction.

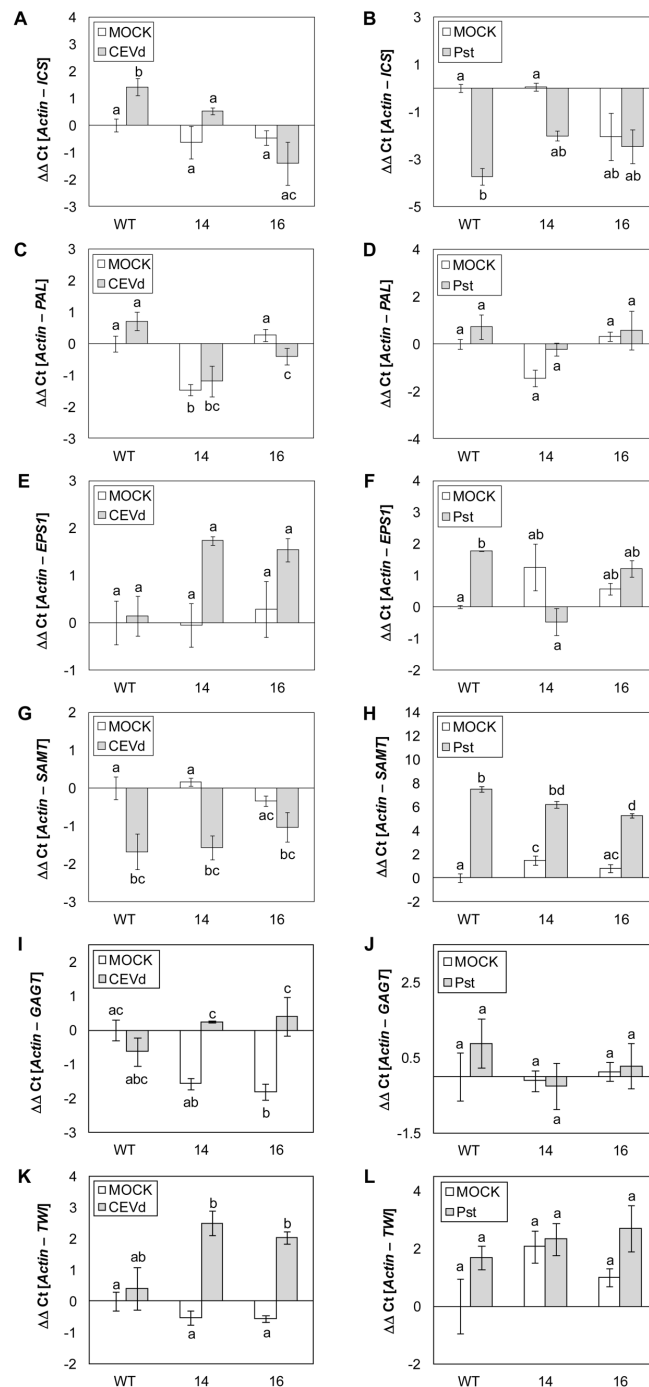


Figure 6. Differences in the pattern of induction of SA metabolism genes upon viroidal (CEVd) and bacterial (Pst) inoculation in wild type (WT) and *RNAi_SIS5H* (lines 14 and 16) transgenic tomato plants by qRT-PCR. *ICS* (A), *PAL* (C), *EPS1* (E), *SAMT* (G), *GAGT* (I) and *TWI* (K) tomato gene expression levels 3 weeks post-inoculation with CEVd; *ICS* (B), *PAL* (D), *EPS1* (F), *SAMT* (H), *GAGT* (J) and *TWI* (L) gene expression levels 24 hours after inoculation with the bacteria *Pseudomonas syringae* DC3000; MOCK represents the mock-inoculated plants. The qRT-PCR values were normalized with the level of expression of the actin gene. The expression levels correspond to the mean \pm the standard error of a representative experiment ($n=3$). Statistically significant differences (p -value < 0.05) between genotypes and infected or mock-inoculated plants are represented by different letters.

3.9. *SIS5H* silencing causes repression of the JA defence response

Once confirmed that *SIS5H* silencing provokes an activation of the SA-mediated defence, we studied the possible cross-talk with the JA-mediated response. To that purpose, control and *RNAi_SIS5H* transgenic lines were wounded, and the induction of *TCI21* was studied at 24 h after wounding (Figure 7A). As expected, *TCI21* was highly induced by wounding in WT plants, whilst *RNAi_SIS5H* wounded plants displayed only a slight induction of *TCI21*, which was comparable to non-wounded plants, thus indicating that JA response is repressed in these transgenic plants. Interestingly, a higher induction of *PR1* was detected in the *SIS5H*-silenced plants both in non-wounded and upon wounding when compared with the WT plants (Figure 7B), reinforcing the observed activation of SA-mediated defence in the *RNAi_SIS5H* transgenic plants.

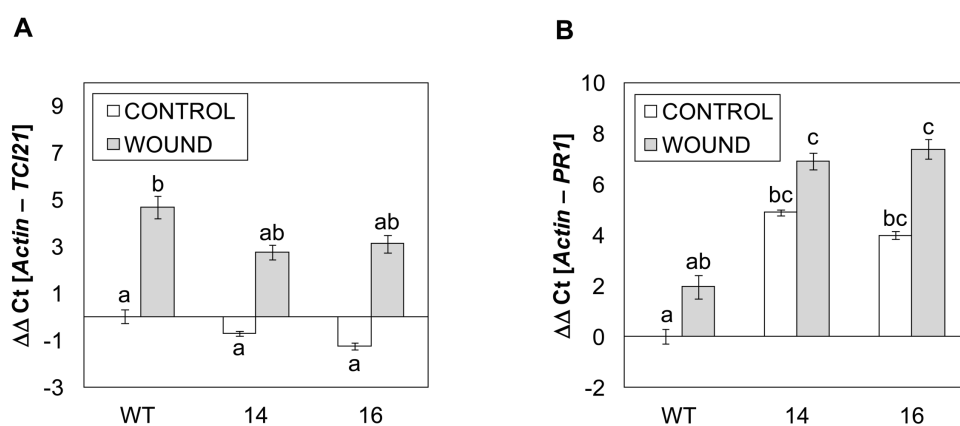


Figure 7. Expression of the tomato *TCI21* (A) and *PR1* (B) genes in wild type plants (WT) and the *RNAi_SIS5H* (lines 14 and 16) transgenic tomato plants in control (CONTROL) and wounded (WOUND) plants. Samples were taken 24 h after wounding; CONTROL represents the non-wounded plants. The qRT-PCR values were normalized with the level of expression of the actin gene. The expression levels correspond to the mean \pm the standard error of a representative experiment ($n=3$). Statistically significant differences (p -value < 0.05) between genotypes and infected or mock-inoculated plants are represented by different letters.

Since JA response appeared to be repressed in *RNAi_SIS5H* transgenic lines, the phenotype against the necrotrophic fungal pathogen *Botrytis cinerea* was explored (Figure 8A). Although no statistically significant differences were found in the size of necrotic lesions between the transgenic lines and the corresponding parental plants (Figure 8B), both *RNAi_SIS5H* transgenic lines displayed an increase in the susceptibility against *Botrytis cinerea*, as suggested by the increase in the yellowish area shown by the transgenic plants. To better quantify this effect, chlorophyll content was measured in control and transgenic plants infected with the fungus. As Figure 8C shows, *RNAi_SIS5H* transgenic lines accumulated significant lower levels of chlorophyll B and total chlorophylls, therefore confirming the observed increased susceptibility of *RNAi_SIS5H* transgenic lines against *Botrytis cinerea*.

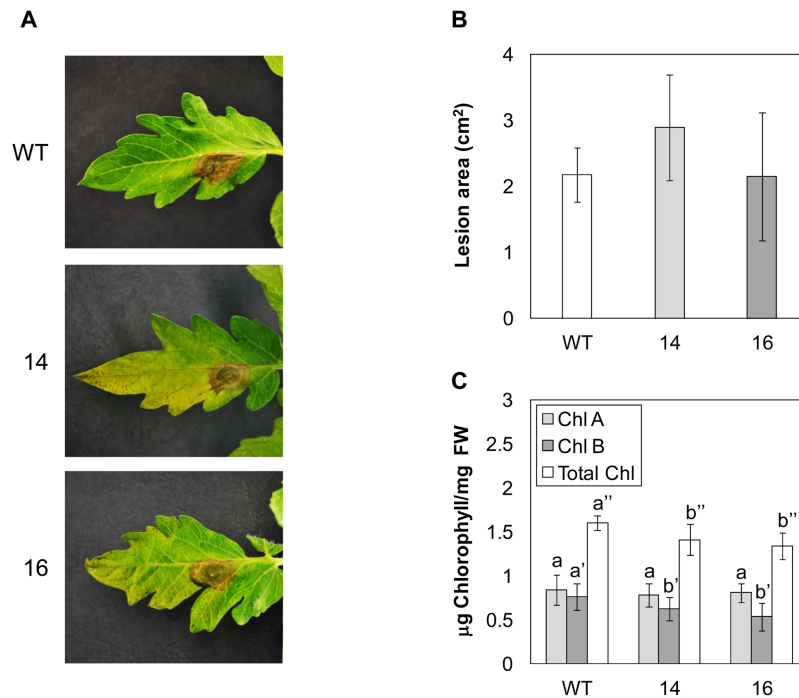


Figure 8. Response of wild type plants (WT) and *RNAi_S5H* transgenic lines 14 and 16 to *Botrytis cinerea* infection. Representative images (A), lesion area (B) and chlorophyll content (C) of plants infected with *B. cinerea* 5 days after fungal inoculation. Bars represent the mean \pm the standard deviation of a representative experiment (n=6). Significant differences between genotypes are represented different by letters since p -value < 0.05.

3.10. Silencing of *SIS5H* results in early senescence

Previous research on salicylate hydroxylase activity in *Arabidopsis* reported that the deficiency in this enzyme provokes an advanced senescent response [21, 23]. However, no noticeable phenotypic differences have been reported in *SIDMR6-1* tomato mutants [24].

To study the developmental phenotype of *RNAi_SIS5H* transgenic tomato plants, 5 individuals for each genotype were grown for 10 weeks, and the percentages of leaflets displaying different senescence stages were recorded. As Figure 9A shows, *RNAi_SIS5H* transgenic plants displayed an earlier chlorosis, even leading to the leaf collapse. Particularly, in 10-week-old plants we observed that control plants still possess approximately 50% of the green leaves, while hardly any leaf of the transgenic lines remained green, turning the entire observed leaves to different intensities of yellow and brown, eventually leading to leaf fall (Figure 9B).

To better characterize the phenotype of the *RNAi_SIS5H* transgenic tomato plants, we measured weight and conductivity at 10 weeks after germination, observing a significant weight reduction in the transgenic plants (Figure S6A). Moreover, electrolyte leakage, which is a hallmark of cell death, was also significantly increased in both transgenic lines silencing *SIS5H* (Figure S6C). Finally, the chlorophyll content was also

measured, observing significant lower levels of chlorophyll B and total chlorophylls in *RNAi_SIS5H* transgenic tomato leaves (Figure S6D).

To reinforce the data obtained by phenotypic visualization, a gene expression analysis for *PR1* as well as the senescence markers *SAG12* (AT5G45890 tomato ortholog; Solyc02g076910) and *NOR* [46] was carried out by qRT-PCR at 4 weeks after germination. As shown in Figure 9C, a significant increase of *PR1* expression was observed in *RNAi_SIS5H* transgenic lines with respect to control plants, which correlates with the higher SA levels previously observed in mock-inoculated plants (Figure 4D). In parallel with *PR1* expression levels, both senescence markers *SAG12* (Figure 9D) and *NOR* (Figure 9E) were differentially upregulated in the *RNAi_SIS5H* transgenic leaves, confirming the developmental phenotype of early senescence observed in these plants.

Levels of free and total SA and GA were measured at different stages of development (Figure 10). To that purpose, samples were collected at the indicated time points and free and total levels of both phenolics were measured by HPLC in both control and *RNAi_SIS5H* transgenic tomato plants. In general, levels of SA were higher in the transgenic plants impaired in 5-hydroxylation, being differences in total SA with control plants statistically significant at 10 weeks after germination. However, levels of GA were found to be lower at every time points, being total GA levels statistically significant from 6 weeks after germination, which confirms that the reduction of GA in these transgenic plants is consistent and reproducible in all the analysed samples.

Therefore, our results appear to indicate that over-accumulation of SA in the *RNAi_SIS5H* transgenic tomato plants provokes toxicity, which may explain their lower growth rates and early senescence.

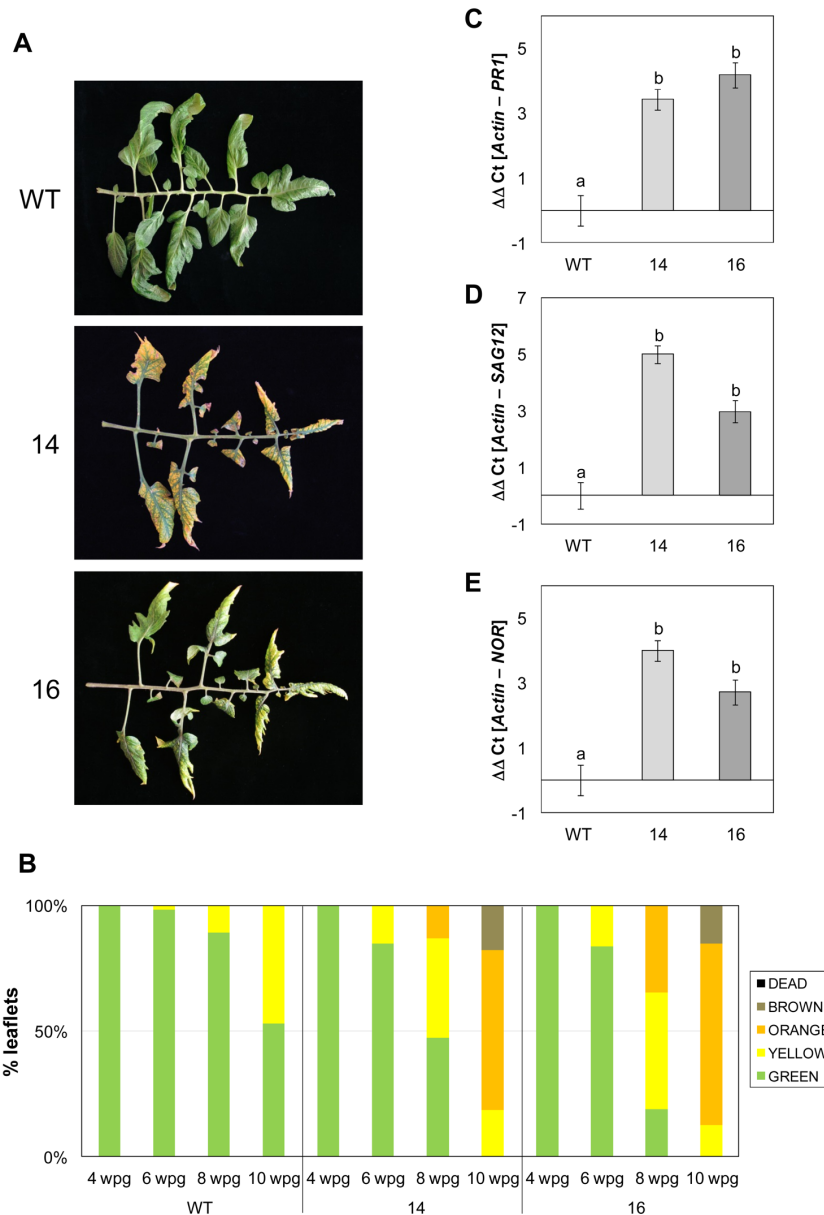


Figure 9. Early senescent phenotype and senescence-related gene expression analysis in WT and *RNAi_S5H* transgenic lines 14 and 16. (A) Representative images and (B) evolution of senescence in WT and *RNAi_S5H* tomato leaflets. The percentage of leaflets of same appearance with respect to the total of leaflets corresponding to the third, fourth and fifth leaves of the WT and *RNAi_SIS5H* transgenic tomato plants at 4-, 6-, 8- and 10-weeks post-germination (wpg) is shown. "GREEN" refers to the natural color of the tomato leaves, "YELLOW" when the leaves begin to age and acquire yellowish spots, "ORANGE" is the time when the leaf turns completely yellow, "BROWN" when necrotic lesions appear due to aging and "DEAD" defines those leaves that have detached from the plant or that are completely necrotic. Expression levels of *PR1* (C), *SAG12* (D) and *NOR* (E) are shown for WT plants and *RNAi_SIS5H* transgenic lines 14 and 16, 4 weeks after germination. The qRT-PCR values were normalized with the level of expression of the actin gene. The expression levels correspond to the mean \pm the standard error of a representative experiment ($n=3$). Statistically significant differences (p -value < 0.05) between genotypes are represented by different letters.

4. Discussion

Resistance to pathogens is associated with SA-mediated activation of plant immune response, being SA a key defence phytohormone with many potential derived applications in agriculture [6]. The fine-tuned regulation of SA accumulation constitutes an important point in plant immunity [47,48]. This regulation can occur at different levels, including the control of its biosynthesis as well as its catabolism. Hydroxylation of SA to form 2,3-DHBA and GA can be considered part of its catabolism, but these forms also constitute a temporary source for SA, since their production could be reversible. Here we study the effect of the impairment of SA hydroxylation in tomato plants subjected to CEVd and *Pst* infections, which produce high and low levels of GA, respectively [33,36–38]. Collectively, our findings provide insight into the modulation of SA metabolism upon biotic stress and provide new insights to previous results on this topic [9,47].

The SA-5 hydroxylation is performed by *AtS5H/DMR6* in *Arabidopsis thaliana*, displaying *s5h* mutants over accumulation of SA and enhanced resistance to *Pst* [23]. We have identified the tomato *S5H* ortholog and studied its induction upon different pathogen infections which provoke SA and GA accumulation, including CEVd, TSWV, ToMV and a virulent and an avirulent strain of *Pst* (Figure 1). Similar results have been reported by Thomazella et al. (2021) from publicly available transcriptome data, including the bacteria *Xanthomonas gardneri* and *Pst*, the oomycete *Phytophthora capsici*, and the fungus *Moniliophthora perniciosa* as pathogens that trigger *SIS5H-DMR6-1* induction. In general terms our data suggest a correlation between *SIS5H* induction and symptomatology. In accordance, its induction correlates not only with symptom development but also with SA and GA accumulation in tomato, since both phenolics have been described to accumulate at very high levels in tomato plants infected by CEVd [33,36–38] which provokes a high induction of *SIS5H* itself. According to that, *SIS5H* was also found to be induced by its own substrate at 6 hpt (Figure S2A), thus indicating a SA-mediated regulation of *SIS5H* expression. However, the higher induction of *SIS5H* at 24 h upon avirulent bacterial infection (Figure 1B) appear to indicate that the role of this gene is more than detoxifying elevated levels of SA generated. Whether that regulation is direct or may occur through the participation of different molecular elements remains unclear. Our results reinforce the role of *SIS5H*, also known as *SIDMR6-1*, in SA metabolism.

SIDMR6-1 was described to be a 2-oxoglutarate-Fe(II) oxygenase acting on SA to produce GA *in vitro* [24]. Here we confirm its *in vivo* SA 5-hydroxylase activity, by transiently overexpressing *SIS5H* in *Nicotiana benthamiana*. Plants agro-inoculated with a *35S:SIS5H* construction and further embedded with SA displayed lower levels of free and total SA, confirming that this phytohormone is a substrate for *SIS5H in vivo*, although a GA over-production was not detected (Figure S3). These results agree with those previously described in SA-treated *Nicotiana tabacum* plants which did not display GA accumulation [33], probably indicating that this GA is rapidly catabolised in SA-embedded plants belonging to the *Nicotiana* genus. Our results confirm the extraordinary

versatility of SA metabolism in different plant species, differences being reported in SA and GA accumulation of up to 100-fold [23].

Given the quantitative importance of GA accumulation in CEVd-infected tomato plants [33,36–38], we decided to study the role of *SIS5H* in this interaction by analysing the phenotype of *RNAi_SIS5H* transgenic tomato plants upon viroid infection. *SIS5H* silencing resulted in a very low GA accumulation, and produced an enhanced resistance to CEVd, reducing both symptoms and viroid accumulation (Figures 2 and 3A). Our results further extend the described broad spectrum resistance mediated by inhibition of SA hydroxylation [24] to a non-coding, RNA pathogen.

This enhanced resistance observed in *SIS5H*-silenced plants was accompanied by an induction of the SA-mediated plant defence response, since *PR1* expression was higher in viroid infected *RNAi_SIS5H* transgenic tomato plants when compared to the corresponding infected non-transgenic plants (Figure 3C). In contrast, activation of the silencing mechanisms through *DCL1* and *DCL2* was reduced in *RNAi_SIS5H* transgenic tomato plants (Figure S4A and S4B), thus indicating these mechanisms are related to the viroid progression, which is limited in the transgenic plants, but not to the SA accumulation itself. In contrast, a correlation between SA accumulation and activation of silencing mechanisms has been previously described (Campos et al., 2014), thus suggesting a role of SA in plant silencing. Besides, the JA-mediated response appeared to be down-regulated in the *RNAi_SIS5H* transgenic tomato plants, displaying a lower induction of *TCI21* upon CEVd infection and wounding (Figures S4D and 7A), and showing higher susceptibility to *Botrytis cinerea* (Figure 8). The reciprocal antagonism between JA and SA [49] and the higher induction of *PR1* in the transgenic lines points to a SA overaccumulation, which could be responsible for the observed SA-mediated plant resistance to CEVd. According to this, *RNAi_SIS5H* transgenic tomato plants displayed higher levels of total SA and significantly lower levels of total and free GA, confirming the decrease of *SIS5H* activity *in vivo*. The enhanced resistance of *Sldmr6-1* lines to different classes of pathogens, such as bacteria, oomycetes and fungi has also been correlated with increased SA levels and transcriptional activation of immune responses [24].

Tomato plants infected with *Pst* have been described to display a different pattern of accumulation of both SA and GA when compared to CEVd infected tomato plants, reaching SA levels less than 10 nmol/g, and around 40 nmol/g for GA [37], which are much lower than those detected upon CEVd infection [33,36–38]. To test the effect of *SIS5H* impairment on the tomato response to bacteria, similar studies to those performed for CEVd were carried out. Our results were in accordance with the enhanced *PR1* induction (Figure 4C), enhanced resistance (Figure 4A), and reduced GA accumulation in *RNAi_SIS5H* transgenic tomato plants triggered by bacteria (Figure 4E). Unlike CEVd infection, an increase in SA accumulation was not detected in transgenic tomato plants upon *Pst* infection, thus indicating that the catabolism of SA shows particularities that are dependent on the plant-pathogen interaction (Figure 4D).

The availability of different SA-deficient mutants and *NahG* transgenic plants in *Arabidopsis thaliana* background has provided vast information on the SA metabolism in response to bacterial infection in this species [7,12]. However, fewer studies have been done on the role of SA in tomato plants in response to bacteria. Therefore, to better understand the modulation of SA metabolism by *Pst* infection in tomato, and to compare it with that activated by CEVd, metabolomic analyses were performed using our *SIS5H*-silenced plants as a tool to study the effect of the altered levels of SA. Our metabolomic assay confirmed that the glycosylated form of SA was the most accumulated compound in the *RNAi_SIS5H* transgenic tomato upon viroid infection (Figure 5B), whereas the glycosylated GA is described to be the most accumulated compound in CEVd-infected WT plants [38], thus confirming *in vivo* the proposed SA 5-hydroxylase activity for *SIS5H*. Strikingly, the impairment of SA 5-hydroxylation in tomato plants uncovered alternative SA homeostasis routes upon *Pst* infection, since *RNAi_SIS5H* transgenic plants over-accumulated feruloyldopamine, feruloylquinic acid, feruloylgalactarate and 2-hydroxyglutarate (Figure 5C).

Feruloyldopamine is a hydroxycinnamic acid amide (HCAA) known to accumulate in tomato plants infected with a high *Pst* bacterial titre, thus producing a hypersensitive-like response [50,51]. It is worthy to note that this HCAA accumulation was accompanied by a rapid and sharp production of SA. These results appear to indicate that SA over-accumulation produced by bacterial infection could trigger the accumulation of this HCAA to prevent a toxic SA effect. The acyl-quinic acids are a diverse group of plant-derived compounds produced principally through esterification of an hydroxycinnamic acid and quinic acid [52]. Particularly, the flavonoid feruloylquinic acid has been described to accumulate in barley leaves upon ultraviolet and photosynthetically active radiation suggesting a protective role [53]. In *Coffea canephora*, feruloylquinic acid is accumulated in juvenile leaves associated with chloroplasts, therefore suggesting a protective role against photooxidative damage [54]. Feruloylgalactarate results from the reaction of feruloyl-CoA with galactaric acid. The accumulation of hydroxycinnamic acids esters of quinic acid and glucaric acids has also been described in tomato plants infected with *Ralstonia solanacearum*, the causal agent of bacterial wilt, a highly destructive bacterial disease [55]. Finally, the accumulation of 2-hydroxyglutarate has been proposed to be linked to light-dependent photorespiration, it is related to oxidative stress and is considered as a marker for senescence in plants [56,57]. In this respect, the expression of 2-hydroxyglutarate dehydrogenase increases gradually during developmental and dark-induced senescence in *Arabidopsis thaliana* [58].

The accumulation of all these compounds may be somehow related with photooxidative damages, caused by biotic and abiotic stresses or senescence. There is a well-known interplay between SA and reactive oxygen species (ROS), being ROS signals involved both upstream and downstream SA signalling [59]. Therefore, the observed over-accumulation of these metabolites in the *RNAi_SIS5H* plants upon bacterial infection could be exerting a protective role against the photooxidative damage

provoked by the transient over-accumulation of SA which could be promoting ROS production, as previously described [59]. On the other hand, there is a biosynthetic connection between SA and these phenolic compounds, displaying age-related differences in their biosynthesis in *Solanum lycopersicum* cv. *amateur* infected by *Pst* [60]. Therefore, the accumulation of feruloyldopamine, feruloylquinic acid and feruloylgalactarate could also be the result of the SA catabolism.

The specific pathogen-triggered SA metabolism observed in this study, was accompanied with noticeable differences in the pattern of induction of SA biosynthesis genes provoked by the CEVd and *Pst* (Figure 6). Regarding *ICS* and *EPS1* expression levels, a significant induction was observed in WT plants after viroid and bacterial infection, respectively. However, no differences were observed after CEVd and *Pst* infection in transgenic plants when compared with mock controls. *ICS* encodes an isochorismate synthase in the plastids, being required for SA biosynthesis [7]. The impairment of its induction in transgenic plants upon CEVd infection appears to indicate a negative feed-back produced by SA over-accumulation (Figure 6A). However, this negative feed-back was not detected neither in transgenic plants upon bacterial infection, where the levels of SA were lower than after a viroid infection (Figure 7A), nor at *EPS1* level, which is described to act at the cytoplasm [12]. *EPS1* was significantly induced by *Pst* in WT tomato plants, while *RNAi_SIS5H* plants did not display that induction. In the same way, a reduction of the *PAL* expression was observed in transgenic plants upon CEVd infection coinciding with SA over-accumulation, and no differences in *PAL* induction were detected in tomato-*Pst* interaction. Regarding WT tomato plants, *PAL* was not induced by any of the pathogens studied here, indicating that the main source of SA upon infection is also dependent on the IC pathway in tomato plants, as previously described in Arabidopsis [8,9].

Finally, the *SAMT* regulation was opposite depending on the attack of the different studied pathogens in WT plants. While viroid caused a significant *SAMT* repression, bacterial infection produced *SAMT* induction. The reduced expression of *SAMT* upon CEVd inoculation could be due to the lower amount of its substrate which is redirected to form SAG (Figures 3D and 5B), since a correlation between SA and MeSA accumulations has been previously described [61]. However, the *SAMT* induction in tomato plants upon bacterial infection matches with the increase in the production of methyl salicylate (MeSA), salicylaldehyde, and ethyl salicylate described in this virulent plant-pathogen interaction (López-Gresa, 2017). The lower induction of *SAMT* upon *Pst* infection in transgenic plants could also be due to the lower amount of its substrate. Together, these results confirm the versatility of the SA metabolism in response to different pathogens.

These specific differences in tomato SA metabolism generated by both pathogens could also be explained by SA bacterial metabolism itself. Whilst CEVd is a non-coding pathogen totally dependent on host transcriptional machinery, *Pst* possesses its own SA biosynthetic pathway which is different from plants [62]. Moreover, plant SA

accumulation is a target of suppression by *Pst* [63], and the bacterial wilt pathogen *Ralstonia solanacearum* has been described to degrade plant SA in order to protect itself from inhibitory levels of this compound as well as to enhance its virulence on plant hosts [64]. Therefore, while the observed SA metabolism caused by CEVd infection is totally plant-dependent, the participation of the *Pst* SA metabolism could in part explain the differences observed in *Pst*-infected *RNAi_SIS5H* tomato plants, including the lack of SA accumulation.

The role of SA on leaf senescence has long been described [65]. In this sense, impairment of S3H or S5H in *Arabidopsis* provokes an advanced senescent response [21,23]. However, no distinctive phenotypic differences regarding senescence were reported for *SIDMR6-1* tomato mutant [24]. Here we have studied the effect of *SIS5H* silencing on the development of tomato plants, observing an early senescence phenotype provoked by SA over-accumulation (Figure 9). These differences could be due to the tomato variety employed for the studies, since Fla. 8000 was used by Thomazella et al. (2021) and MoneyMaker tomato plants were used in our studies. Additionally, the differences between CRISPR knock out and RNAi silencing approaches could also be considered. According to our results, a higher induction of both *SAG12* and *NOR* senescence markers [46], as well as *PR1*, a molecular marker for the defence response (Conejero et al., 1990), was detected in both transgenic plants silencing *SIS5H* (Figure 9). As previously stated, the toxic effect of SA over-accumulation, also responsible for the observed cell death and the decrease in chlorophyll, could be related with ROS accumulation [59]. Our results provide genetic evidence that *SIS5H* has an important role in regulating the onset and rate of leaf senescence in tomato by fine-tuning the endogenous levels of SA.

Conclusions

Through the balance between *de novo* biosynthesis, catabolism and reversible deactivation, plants manage to maintain their endogenous levels of SA. Hydroxylation of SA to produce GA is performed by S5H, which has been described as DMR6 in *Arabidopsis* [67] and tomato [24]. Infections with CEVd and *Pst* produce high and low levels of GA, respectively [33,36–38], thus constituting excellent models to study the role of S5H in tomato plants. Here we demonstrate that the impairment of SA hydroxylation increases resistance to CEVd and *Pst* in tomato. Surprisingly, the observed resistance is accompanied by an increase in SA levels in *RNAi_SIS5H* plants only upon CEVd, but not upon *Pst* infection, where SA appeared to be rerouted to other phenolics involved in defence. Our results indicate there is an additional complexity level associated to pathogen-induced specific SA homeostasis, suggesting that the framework of SA biology, which is established mainly for *Pst*-infected *Arabidopsis thaliana* plants, needs to be considered for each specific plant-pathogen interaction.

Declarations

Ethics approval and consent to participate

Experimental research and field studies on plants (either cultivated or wild), including the collection of plant material, complied with relevant institutional, national, and international guidelines and legislation.

Consent for publication

Not applicable

Availability of data and materials

Material will be available upon request to authors after MTA signature. The datasets generated and/or analysed during the current study are not publicly available since they are stored in our local computers and are available from the corresponding author on reasonable request. The database links mentioned in the manuscript are listed below:

<https://solgenomics.net/>

www.arabidopsis.org

<http://plants.ensembl.org/index.html>

<https://xcmsonline.scripps.edu>

<https://spectra.psc.riken.jp/>

<https://metlin.scripps.edu/>

<https://hmdb.ca/>

<https://www.lipidmaps.org/>

<https://primer3.ut.ee/>

<https://www.graphpad.com>

Competing interests

The authors declare that they have no competing interests

Funding

This work was supported by Grant PID2020-116765RB-I00 funded by MCIN/AEI/10.13039/501100011033 and Grant AICO/2017/048 from the Generalitat Valenciana. Work in the lab is also supported by grant PROMETEU/2021/056 by Generalitat Valenciana. C.P. was a recipient of a predoctoral contract of the Generalitat Valenciana (ACIF/2019/187).

Acknowledgements

We would like to thank the “Metabolomics Platform of CEBAS-CSIC” (Centro de

Edafología y Biología Aplicada del Segura, Murcia, Spain), especially to Dr. José E. Yuste (Technical Coordinator) for his excellent support in the phenolics identification of this study.

5. References

1. White, R.F. Acetylsalicylic Acid (Aspirin) Induces Resistance to Tobacco Mosaic Virus in Tobacco. *Virology* **1979**, *99*, 410–412, doi:[https://doi.org/10.1016/0042-6822\(79\)90019-9](https://doi.org/10.1016/0042-6822(79)90019-9).
2. Malamy, J.; Hennig, J.; Klessig, D.F. Temperature-Dependent Induction of Salicylic Acid and Its Conjugates during the Resistance Response to Tobacco Mosaic Virus Infection. *Plant Cell* **1992**, *4*, 359, doi:10.1105/TPC.4.3.359.
3. Métraux, J.P.; Signer, H.; Ryals, J.; Ward, E.; Wyss-Benz, M.; Gaudin, J.; Raschdorf, K.; Schmid, E.; Blum, W.; Inverardi, B. Increase in Salicylic Acid at the Onset of Systemic Acquired Resistance in Cucumber. *Science (80-.)*. **1990**, *250*, 1004–1006, doi:10.1126/science.250.4983.1004.
4. Gaffney, T.; Friedrich, L.; Vernooij, B.; Negrotto, D.; Nye, G.; Uknes, S.; Ward, E.; Kessmann, H.; Ryals, J. Requirement of Salicylic Acid for the Induction of Systemic Acquired Resistance. *Science (80-.)*. **1993**, *261*, 754–756, doi:10.1126/science.261.5122.754.
5. Delaney, T.P.; Uknes, S.; Vernooij, B.; Friedrich, L.; Weymann, K.; Negrotto, D.; Gaffney, T.; Gut-Rella, M.; Kessmann, H.; Ward, E.; et al. A Central Role of Salicylic Acid in Plant Disease Resistance. *Science* **1994**, *266*, 1247–1250, doi:10.1126/SCIENCE.266.5188.1247.
6. Klessig, D.F.; Choi, H.W.; Dempsey, D.A. Systemic Acquired Resistance and Salicylic Acid: Past, Present, and Future. *Mol. Plant. Microbe. Interact.* **2018**, *31*, 871–888, doi:10.1094/MPMI-03-18-0067-CR.
7. Ding, P.; Ding, Y. Stories of Salicylic Acid: A Plant Defence Hormone. *Trends Plant Sci.* **2020**, *25*, 549–565, doi:<https://doi.org/10.1016/j.tplants.2020.01.004>.
8. Wildermuth, M.C.; Dewdney, J.; Wu, G.; Ausubel, F.M. Isochorismate Synthase Is Required to Synthesize Salicylic Acid for Plant Defence. *Nature* **2001**, *414*, 562–565, doi:10.1038/35107108.
9. Zhang, Y.; Li, X. Salicylic Acid: Biosynthesis, Perception, and Contributions to Plant Immunity. *Curr Opin Plant Biol* **2019**, *50*, 29–36, doi:10.1016/j.pbi.2019.02.004.
10. Rekhter, D.; Lüdke, D.; Ding, Y.; Feussner, K.; Zienkiewicz, K.; Lipka, V.; Wiermer, M.; Zhang, Y.; Feussner, I. Isochorismate-Derived Biosynthesis of the Plant Stress Hormone Salicylic Acid. *Science* **2019**, *365*, 498–502, doi:10.1126/SCIENCE.AAW1720.
11. Torrens-Spence, M.P.; Bobokalonova, A.; Carballo, V.; Glinkerman, C.M.; Pluskal, T.; Shen, A.; Weng, J.K. PBS3 and EPS1 Complete Salicylic Acid Biosynthesis from Isochorismate in Arabidopsis. *Mol. Plant* **2019**, *12*, 1577–1586, doi:10.1016/J.MOLP.2019.11.005/ATTACHMENT/C57285CC-8B6B-45E6-9674-4E245F50DBCE/MMC4.XLSX.
12. Zeier, J. Metabolic Regulation of Systemic Acquired Resistance. *Curr. Opin. Plant Biol.* **2021**, *62*, 102050, doi:10.1016/J.PBI.2021.102050.
13. Enyedi, A.J.; Yalpani, N.; Silverman, P.; Raskin, I. Localization, Conjugation, and Function of Salicylic Acid in Tobacco during the Hypersensitive Reaction to Tobacco Mosaic Virus. *Proc. Natl. Acad. Sci. U. S. A.* **1992**, *89*, 2480, doi:10.1073/PNAS.89.6.2480.
14. Edwards, R. Conjugation and Metabolism of Salicylic Acid in Tobacco. *J. Plant Physiol.* **1994**, *143*, 609–614, doi:10.1016/S0176-1617(11)81146-6.

15. Dean, J. V.; Mohammed, L.A.; Fitzpatrick, T. The Formation, Vacuolar Localization, and Tonoplast Transport of Salicylic Acid Glucose Conjugates in Tobacco Cell Suspension Cultures. *Planta* **2005**, *221*, 287–296, doi:10.1007/s00425-004-1430-3.
16. Canet, J. V.; Dobón, A.; Ibáñez, F.; Perales, L.; Tornero, P. Resistance and Biomass in Arabidopsis: A New Model for Salicylic Acid Perception. *Plant Biotechnol J* **2010**, *8*, 126–141, doi:10.1111/j.1467-7652.2009.00468.x.
17. Zhang, Z.; Li, Q.; Li, Z.; Staswick, P.E.; Wang, M.; Zhu, Y.; He, Z. Dual Regulation Role of *GH3.5* in Salicylic Acid and Auxin Signalling during Arabidopsis-*Pseudomonas Syringae* Interaction. *Plant Physiol.* **2007**, *145*, 450–464, doi:10.1104/pp.107.106021.
18. Baek, D.; Pathange, P.; Chung, J.S.; Jiang, J.; Gao, L.; Oikawa, A.; Hirai, M.Y.; Saito, K.; Pare, P.W.; Shi, H. A Stress-Inducible Sulphotransferase Sulphonates Salicylic Acid and Confers Pathogen Resistance in Arabidopsis. *Plant Cell Env.* **2010**, *33*, 1383–1392, doi:10.1111/j.1365-3040.2010.02156.x.
19. Shulaev, V.; Silverman, P.; Raskin, I. Airborne Signalling by Methyl Salicylate in Plant Pathogen Resistance. *Nat.* **1997**, *385*, 718–721, doi:10.1038/385718a0.
20. Park, S.W.; Kaimoyo, E.; Kumar, D.; Mosher, S.; Klessig, D.F. Methyl Salicylate Is a Critical Mobile Signal for Plant Systemic Acquired Resistance. *Science* (80-.). **2007**, *318*, 113–116, doi:10.1126/science.1147113.
21. Zhang, K.; Halitschke, R.; Yin, C.; Liu, C.J.; Gan, S.S. Salicylic Acid 3-Hydroxylase Regulates Arabidopsis Leaf Longevity by Mediating Salicylic Acid Catabolism. *Proc Natl Acad Sci U S A* **2013**, *110*, 14807–14812, doi:10.1073/pnas.1302702110.
22. van Damme, M.; Huibers, R.P.; Elberse, J.; Van den Ackerveken, G. Arabidopsis DMR6 Encodes a Putative 2OG-Fe(II) Oxygenase That Is Defence-Associated but Required for Susceptibility to Downy Mildew. *Plant J* **2008**, *54*, 785–793, doi:10.1111/j.1365-313X.2008.03427.x.
23. Zhang, Y.; Zhao, L.; Zhao, J.; Li, Y.; Wang, J.; Guo, R.; Gan, S.; Liu, C.-J.; Zhang, K. S5H/DMR6 Encodes a Salicylic Acid 5-Hydroxylase That Fine-Tunes Salicylic Acid Homeostasis. *Plant Physiol.* **2017**, *175*, 1082–1093.
24. Thomazella, D.; Seong, K.; Mackelprang, R.; Dahlbeck, D.; Geng, Y.; Gill, U.; Qi, T.; Pham, J.; Giuseppe, P.; Lee, C.; et al. Loss of Function of a DMR6 Ortholog in Tomato Confers Broad-Spectrum Disease Resistance. *Proc. Natl. Acad. Sci. U. S. A.* **2021**, *118*, doi:10.1073/PNAS.2026152118.
25. Bartsch, M.; Bednarek, P.; Vivancos, P.D.; Schneider, B.; von Roepenack-Lahaye, E.; Foyer, C.H.; Kombrink, E.; Scheel, D.; Parker, J.E. Accumulation of Isochorismate-Derived 2,3-Dihydroxybenzoic 3-O-Beta-D-Xyloside in Arabidopsis Resistance to Pathogens and Ageing of Leaves. *J Biol Chem* **2010**, *285*, 25654–25665, doi:10.1074/jbc.M109.092569.
26. Lutwak-Mann, C. The Excretion of a Metabolic Product of Salicylic Acid. *Biochem J* **1943**, *37*, 246–248, doi:10.1042/bj0370246.
27. Walker, N.; Evans, W.C. Pathways in the Metabolism of the Monohydroxybenzoic Acids by Soil Bacteria. *Biochem J* **1952**, *52*, xxiii–xxiv.
28. Ibrahim, R.K.; Towers, G.H.N. Conversion of Salicylic Acid to Gentisic Acid and O-Pyrocatechuic Acid, All Labelled with Carbon-14, in Plants. *Nature* **1959**, *184*, 1803, doi:10.1038/1841803a0.
29. Fayos, J.; Bellés, J.M.; López-Gresa, M.P.; Primo, J.; Conejero, V. Induction of Gentisic Acid 5-O-Beta-D-Xylopyranoside in Tomato and Cucumber Plants Infected by Different Pathogens. *Phytochemistry* **2006**, *67*, 142–148, doi:10.1016/J.PHYTOCHEM.2005.10.014.
30. Dean, J. V.; Delaney, S.P. Metabolism of Salicylic Acid in Wild-Type, *Ugt74f1* and *Ugt74f2*

- Glucosyltransferase Mutants of *Arabidopsis Thaliana*. *Physiol Plant* **2008**, *132*, 417–425, doi:10.1111/j.1399-3054.2007.01041.x.
31. Tárraga, S.; Lisón, P.; López-Gresa, M.P.; Torres, C.; Rodrigo, I.; Bellés, J.M.; Conejero, V. Molecular Cloning and Characterization of a Novel Tomato Xylosyltransferase Specific for Gentisic Acid. *J Exp Bot* **2010**, *61*, 4325–4338, doi:10.1093/jxb/erq234.
 32. Li, X.; Svedin, E.; Mo, H.; Atwell, S.; Dilkes, B.P.; Chapple, C. Exploiting Natural Variation of Secondary Metabolism Identifies a Gene Controlling the Glycosylation Diversity of Dihydroxybenzoic Acids in *Arabidopsis Thaliana*. *Genetics* **2014**, *198*, 1267–1276, doi:10.1534/genetics.114.168690.
 33. Bellés, J.M.; Garro, R.; Fayos, J.; Navarro, P.; Primo, J.; Conejero, V. Gentisic Acid As a Pathogen-Inducible Signal, Additional to Salicylic Acid for Activation of Plant Defences in Tomato. *Mol. Plant-Microbe Interact.* **1999**, *12*, 227–235, doi:10.1094/MPMI.1999.12.3.227.
 34. Bellés, J.M.; Garro, R.; Pallas, V.; Fayos, J.; Rodrigo, I.; Conejero, V. Accumulation of Gentisic Acid as Associated with Systemic Infections but Not with the Hypersensitive Response in Plant-Pathogen Interactions. *Planta* **2006**, *223*, 500–511, doi:10.1007/s00425-005-0109-8.
 35. Campos, L.; Granell, P.; Tarraga, S.; Lopez-Gresa, P.; Conejero, V.; Belles, J.M.; Rodrigo, I.; Lison, P. Salicylic Acid and Gentisic Acid Induce RNA Silencing-Related Genes and Plant Resistance to RNA Pathogens. *Plant Physiol Biochem* **2014**, *77*, 35–43, doi:10.1016/j.plaphy.2014.01.016.
 36. López-Gresa, M.P.; Lisón, P.; Yenush, L.; Conejero, V.; Rodrigo, I.; Belles, J.M. Salicylic Acid Is Involved in the Basal Resistance of Tomato Plants to Citrus Exocortis Viroid and Tomato Spotted Wilt Virus. *PLoS One* **2016**, *11*, e0166938, doi:10.1371/journal.pone.0166938.
 37. López-Gresa, M.P.; Lisón, P.; Campos, L.; Rodrigo, I.; Rambla, J.L.; Granell, A.; Conejero, V.; Belles, J.M. A Non-Targeted Metabolomics Approach Unravels the VOCs Associated with the Tomato Immune Response against *Pseudomonas Syringae*. *Front Plant Sci* **2017**, *8*, 1188, doi:10.3389/fpls.2017.01188.
 38. López-Gresa, M.P.; Payá, C.; Rodrigo, I.; Bellés, J.M.; Barceló, S.; Hae Choi, Y.; Verpoorte, R.; Lisón, P. Effect of Benzothiadiazole on the Metabolome of Tomato Plants Infected by Citrus Exocortis Viroid. *Viruses* **2019**, *11*, doi:10.3390/v11050437.
 39. López-Gresa, M.P.; Lisón, P.; Kim, H.K.; Choi, Y.H.; Verpoorte, R.; Rodrigo, I.; Conejero, V.; Bellés, J.M. Metabolic Fingerprinting of Tomato Mosaic Virus Infected *Solanum Lycopersicum*. *J. Plant Physiol.* **2012**, *169*, 1586–1596, doi:10.1016/J.JPLPH.2012.05.021.
 40. Prol, F. V.; López-Gresa, M.P.; Rodrigo, I.; Bellés, J.M.; Lisón, P. Ethylene Is Involved in Symptom Development and Ribosomal Stress of Tomato Plants upon Citrus Exocortis Viroid Infection. *Plants (Basel)* **2020**, *9*, doi:10.3390/plants9050582.
 41. Granell, A.; Bellés, J.M.; Conejero, V. Induction of Pathogenesis-Related Proteins in Tomato by Citrus Exocortis Viroid, Silver Ion and Ethephon. *Physiol. Mol. Plant Pathol.* **1987**, *31*, 83–90, doi:https://doi.org/10.1016/0885-5765(87)90008-7.
 42. Tornero, P.; Rodrigo, I.; Conejero, V.; Vera, P. Nucleotide Sequence of a cDNA Encoding a Pathogenesis-Related Protein, P1-P14, from Tomato (*Lycopersicon Esculentum*). *Plant Physiol* **1993**, *102*, 325.
 43. Lison, P.; Rodrigo, I.; Conejero, V. A Novel Function for the Cathepsin D Inhibitor in Tomato. *Plant Physiol* **2006**, *142*, 1329–1339, doi:10.1104/pp.106.086587.
 44. Tieman, D.; Zeigler, M.; Schmelz, E.; Taylor, M.G.; Rushing, S.; Jones, J.B.; Klee, H.J. Functional Analysis of a Tomato Salicylic Acid Methyl Transferase and Its Role in Synthesis of the Flavor Volatile Methyl Salicylate. *Plant J.* **2010**, *62*, 113–123, doi:10.1111/J.1365-313X.2010.04128.X.

45. Campos, L.; López-Gresa, M.P.; Fuertes, D.; Bellés, J.M.; Rodrigo, I.; Lisón, P. Tomato Glycosyltransferase Twi1 Plays a Role in Flavonoid Glycosylation and Defence against Virus. *BMC Plant Biol.* **2019**, *19*, doi:10.1186/S12870-019-2063-9.
46. Ma, X.; Balazadeh, S.; Mueller-Roeber, B. Tomato Fruit Ripening Factor NOR Controls Leaf Senescence. *J. Exp. Bot.* **2019**, *70*, 2727–2740, doi:10.1093/JXB/ERZ098.
47. Huang, X.X.; Zhu, G.Q.; Liu, Q.; Chen, L.; Li, Y.J.; Hou, B.K. Modulation of Plant Salicylic Acid-Associated Immune Responses via Glycosylation of Dihydroxybenzoic Acids. *Plant Physiol.* **2018**, *176*, 3103–3119, doi:10.1104/PP.17.01530.
48. Chen, L.; Wang, W.S.; Wang, T.; Meng, X.F.; Chen, T.T.; Huang, X.X.; Li, Y.J.; Hou, B.K. Methyl Salicylate Glucosylation Regulates Plant Defence Signalling and Systemic Acquired Resistance. *Plant Physiol.* **2019**, *180*, 2167–2181, doi:10.1104/PP.19.00091.
49. Thaler, J.S.; Humphrey, P.T.; Whiteman, N.K. Evolution of Jasmonate and Salicylate Signal Crosstalk. *Trends Plant Sci.* **2012**, *17*, 260–270, doi:10.1016/J.TPLANTS.2012.02.010.
50. Zacarés, L.; López-Gresa, M.P.; Fayos, J.; Primo, J.; Bellés, J.M.; Conejero, V. Induction of P-Coumaroyldopamine and Feruloyldopamine, Two Novel Metabolites, in Tomato by the Bacterial Pathogen *Pseudomonas Syringae*. *Mol. Plant. Microbe. Interact.* **2007**, *20*, 1439–1448, doi:10.1094/MPMI-20-11-1439.
51. López-Gresa, M.P.; Torres, C.; Campos, L.; Lisón, P.; Rodrigo, I.; Bellés, J.M.; Conejero, V. Identification of Defence Metabolites in Tomato Plants Infected by the Bacterial Pathogen *Pseudomonas Syringae*. *Environ. Exp. Bot.* **2011**, *74*, 216–228, doi:10.1016/J.ENVEXPBOT.2011.06.003.
52. Clifford, M.N.; Jaganath, I.B.; Ludwig, I.A.; Crozier, A. Chlorogenic Acids and the Acyl-Quinic Acids: Discovery, Biosynthesis, Bioavailability and Bioactivity. *Nat. Prod. Rep.* **2017**, *34*, 1391–1421, doi:10.1039/C7NP00030H.
53. Klem, K.; Holub, P.; Štroch, M.; Nezval, J.; Špunda, V.; Tříška, J.; Jansen, M.A.K.; Robson, T.M.; Urban, O. Ultraviolet and Photosynthetically Active Radiation Can Both Induce Photoprotective Capacity Allowing Barley to Overcome High Radiation Stress. *Plant Physiol. Biochem.* **2015**, *93*, 74–83, doi:10.1016/J.PLAPHY.2015.01.001.
54. Mondolot, L.; La Fisca, P.; Buatois, B.; Talansier, E.; De Kochko, A.; Campa, C. Evolution in Caffeoylquinic Acid Content and Histolocalization During *Coffea Canephora* Leaf Development. *Ann. Bot.* **2006**, *98*, 33–40, doi:10.1093/AOB/MCL080.
55. Zeiss, D.R.; Mhlongo, M.I.; Tugizimana, F.; Steenkamp, P.A.; Dubery, I.A. Metabolomic Profiling of the Host Response of Tomato (*Solanum Lycopersicum*) Following Infection by *Ralstonia Solanacearum*. *Int. J. Mol. Sci.* **2019**, *Vol. 20*, Page 3945 **2019**, *20*, 3945, doi:10.3390/IJMS20163945.
56. Kuhn, A.; Engqvist, M.K.M.; Jansen, E.E.W.; Weber, A.P.M.; Jakobs, C.; Maurino, V.G. D-2-Hydroxyglutarate Metabolism Is Linked to Photorespiration in the Shm1-1 Mutant. *Plant Biol.* **2013**, *15*, 776–784, doi:10.1111/PLB.12020.
57. Sipari, N.; Lihavainen, J.; Shapiguzov, A.; Kangasjärvi, J.; Keinänen, M. Primary Metabolite Responses to Oxidative Stress in Early-Senescing and Paraquat Resistant Arabidopsis *Thaliana* Rcd1 (Radical-Induced Cell Death1). *Front. Plant Sci.* **2020**, *11*, 194, doi:10.3389/FPLS.2020.00194/BIBTEX.
58. Engqvist, M.K.M.; Kuhn, A.; Wienstroer, J.; Weber, K.; Jansen, E.E.W.; Jakobs, C.; Weber, A.P.M.; Maurino, V.G. Plant D-2-Hydroxyglutarate Dehydrogenase Participates in the Catabolism of Lysine Especially during Senescence. *J. Biol. Chem.* **2011**, *286*, 11382–11390, doi:10.1074/JBC.M110.194175/ATTACHMENT/97BF4533-D615-497F-8167-

4598C2A15D12/MMC1.ZIP.

59. Herrera-Vásquez, A.; Salinas, P.; Holuigue, L. Salicylic Acid and Reactive Oxygen Species Interplay in the Transcriptional Control of Defence Genes Expression. *Front. Plant Sci.* **2015**, *6*, 1–9, doi:10.3389/FPLS.2015.00171/BIBTEX.
60. Dadáková, K.; Heinrichová, T.; Lochman, J.; Kašparovský, T. Production of Defence Phenolics in Tomato Leaves of Different Age. *Molecules* **2020**, *25*, doi:10.3390/MOLECULES25214952.
61. Hernández-Aparicio, F.; Lisón, P.; Rodrigo, I.; Bellés, J.M.; López-Gresa, M.P. Signalling in the Tomato Immunity against *Fusarium Oxysporum*. *Molecules* **2021**, *26*, doi:10.3390/MOLECULES26071818.
62. Mishra, A.K.; Baek, K.H. Salicylic Acid Biosynthesis and Metabolism: A Divergent Pathway for Plants and Bacteria. *Biomol.* **2021**, Vol. 11, Page 705 **2021**, *11*, 705, doi:10.3390/BIOM11050705.
63. Wilson, D.C.; Carella, P.; Cameron, R.K. Intercellular Salicylic Acid Accumulation during Compatible and Incompatible *Arabidopsis-Pseudomonas Syringae* Interactions. <https://doi.org/10.4161/psb.29362> **2014**, *9*, doi:10.4161/PSB.29362.
64. Lowe-Power, T.M.; Jacobs, J.M.; Ailloud, F.; Fochs, B.; Prior, P.; Allen, C. Degradation of the Plant Defence Signal Salicylic Acid Protects *Ralstonia Solanacearum* from Toxicity and Enhances Virulence on Tobacco. *MBio* **2016**, *7*, doi:10.1128/MBIO.00656-16.
65. Morris, K.; Mackerness, S.A.H.; Page, T.; Fred John, C.; Murphy, A.M.; Carr, J.P.; Buchanan-Wollaston, V. Salicylic Acid Has a Role in Regulating Gene Expression during Leaf Senescence. *Plant J.* **2000**, *23*, 677–685, doi:10.1046/J.1365-313X.2000.00836.X.
66. Conejero, V., Bellés, J. M., García-Breijo, F., Garro, R., Hernández-Yago, J., Rodrigo, I., & Vera, P. *Recognition and Response in Plant-Virus Interactions.*; Fraser RSS, E., Ed.; Berlin Heidelberg: Springer Verlag, 1990;
67. Zhang, Y.; Zhao, L.; Zhao, J.; Li, Y.; Wang, J.; Guo, R.; Gan, S.; Liu, C.J.; Zhang, K. S5H/DMR6 Encodes a Salicylic Acid 5-Hydroxylase That Fine-Tunes Salicylic Acid Homeostasis. *Plant Physiol* **2017**, *175*, 1082–1093, doi:10.1104/pp.17.00695.
68. Nakagawa, T.; Suzuki, T.; Murata, S.; Nakamura, S.; Hino, T.; Maeo, K.; Tabata, R.; Kawai, T.; Tanaka, K.; Niwa, Y.; et al. Improved Gateway Binary Vectors: High-Performance Vectors for Creation of Fusion Constructs in Transgenic Analysis of Plants. *Biosci. Biotechnol. Biochem.* **2007**, *71*, 2095–2100, doi:10.1271/BBB.70216.
69. Helliwell, C.; Waterhouse, P. Constructs and Methods for High-Throughput Gene Silencing in Plants. *Methods* **2003**, *30*, 289–295, doi:10.1016/S1046-2023(03)00036-7.
70. Gleave, A.P. A Versatile Binary Vector System with a T-DNA Organisational Structure Conducive to Efficient Integration of Cloned DNA into the Plant Genome. *Plant Mol. Biol.* **1992**, *206* **1992**, *20*, 1203–1207, doi:10.1007/BF00028910.
71. Lakatos, L.; Szittyá, G.; Silhavy, D.; Burgyán, J. Molecular Mechanism of RNA Silencing Suppression Mediated by P19 Protein of Tombusviruses. *EMBO J.* **2004**, *23*, 876, doi:10.1038/SJ.EMBOJ.7600096.
72. Ellul, P.; Garcia-Sogo, B.; Pineda, B.; Ríos, G.; Roig, L.A.; Moreno, V. The Ploidy Level of Transgenic Plants in *Agrobacterium*-Mediated Transformation of Tomato Cotyledons (*Lycopersicon Esculentum* Mill.) Is Genotype and Procedure Dependent [Corrected]. *Theor. Appl. Genet.* **2003**, *106*, 231–238, doi:10.1007/S00122-002-0928-Y.
73. Yang, H.; Morita, A.; Matsubayashi, Y.; Nakamura, K.; Sakagami, Y. A Rapid and Efficient System of *Agrobacterium* Infection-Mediated Transient Gene Expression in Rice Oc Cells and Its Application for Analysis of the Expression and Antisense Suppression of Preprophytosulfokine, a Precursor of

- Phytosulfokine-a, Encoded by OsPSK Gene. *Plant Cell Physiol.* **2000**, *41*, 811–816, doi:10.1093/PCP/41.6.811.
74. Conejero, V.; Semancik, J.S. Exocortis Viroid: Alteration in the Proteins of *Gynura Aurantiaca* Accompanying Viroid Infection. *Virology* **1977**, *77*, 221–232, doi:10.1016/0042-6822(77)90420-2.
 75. Towbin, H.; Staehelin, T.; Gordon, J. Electrophoretic Transfer of Proteins from Polyacrylamide Gels to Nitrocellulose Sheets: Procedure and Some Applications. *Proc. Natl. Acad. Sci. U. S. A.* **1979**, *76*, 4350–4354, doi:10.1073/PNAS.76.9.4350.
 76. Campos, L.; López-Gresa, M.P.; Fuertes, D.; Bellés, J.M.; Rodrigo, I.; Lisón, P. Tomato Glycosyltransferase *Twi1* Plays a Role in Flavonoid Glycosylation and Defence against Virus. *BMC Plant Biol* **2019**, *19*, 450, doi:10.1186/s12870-019-2063-9.
 77. Semancik, J.S.; Roistacher, C.N.; Rivera-Bustamante, R.; Duran-Vila, N. Citrus Cachexia Viroid, a New Viroid of Citrus: Relationship to Viroids of the Exocortis Disease Complex. *J. Gen. Virol.* **1988**, *69*, 3059–3068, doi:10.1099/0022-1317-69-12-3059.
 78. Ntoukakis, V.; Mucyn, T.S.; Gimenez-Ibanez, S.; Chapman, H.C.; Gutierrez, J.R.; Balmuth, A.L.; Jones, A.M.; Rathjen, J.P. Host Inhibition of a Bacterial Virulence Effector Triggers Immunity to Infection. *Science (80-.)*. **2009**, *324*, 784–787, doi:10.1126/science.1169430.
 79. López-Gresa, M.P.; Payá, C.; Ozáez, M.; Rodrigo, I.; Conejero, V.; Klee, H.; Bellés, J.M.; Lisón, P. A New Role for Green Leaf Volatile Esters in Tomato Stomatal Defence against *Pseudomonas Syringae* Pv. Tomato. *Front. Plant Sci.* **2018**, *871*, doi:10.3389/fpls.2018.01855.
 80. Arnon, D.I. Copper Enzymes in Isolated Chloroplasts. Polyphenoloxidase in *Beta Vulgaris*. *Plant Physiol.* **1949**, *24*, 1–15, doi:10.1104/PP.24.1.1.
 81. Rambla, J.L.; López-Gresa, M.P.; Bellés, J.M.; Granell, A. Metabolomic Profiling of Plant Tissues. *Methods Mol. Biol.* **2015**, *1284*, 221–235, doi:10.1007/978-1-4939-2444-8_11.
 82. Campos, L.; Lisón, P.; López-Gresa, M.P.; Rodrigo, I.; Zacarés, L.; Conejero, V.; Bellés, J.M. Transgenic Tomato Plants Overexpressing Tyramine N-Hydroxycinnamoyltransferase Exhibit Elevated Hydroxycinnamic Acid Amide Levels and Enhanced Resistance to *Pseudomonas Syringae*. *Mol. Plant. Microbe. Interact.* **2014**, *27*, 1159–1169, doi:10.1094/MPMI-04-14-0104-R.

Supplementary Materials

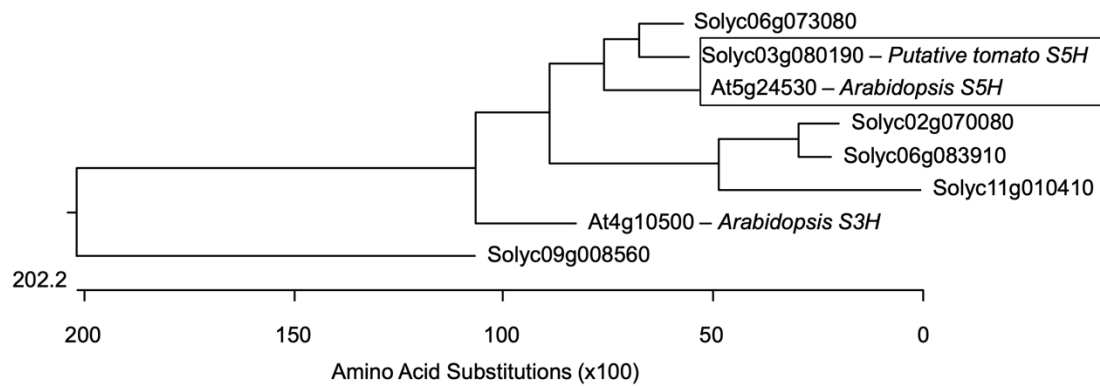


Figure S1. Phylogenetic analysis of *AtS5H* orthologs in tomato. The box in the phylogenetic tree highlights *AtS5H* from *Arabidopsis thaliana* (At5g24530) and its closest homolog in tomato (Solyc03g080190). The multiple alignment was made using ClustalW and the dendrogram was built using the MegAlign program from the Lasergene package (DNASTAR, Madison, Wisconsin, USA).

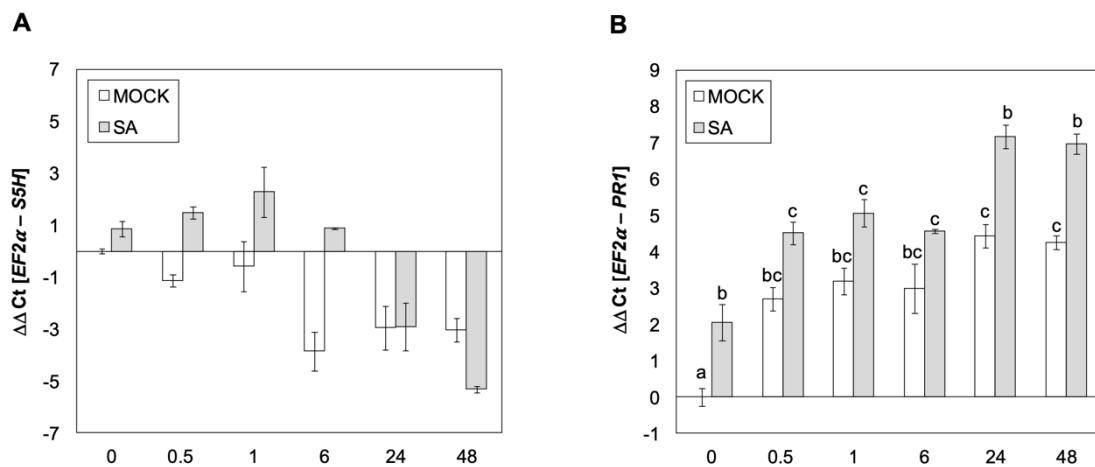


Figure S2. SA-induced expression of *SIS5H* in wild type (WT) tomato plants. *SIS5H* (A) and *PR1* (B) expression of tomato plants treated with 2 mM of SA (SA) or water (MOCK) by stem feeding at 0, 0.5, 1, 6, 24 and 48 hours post-treatment. The qRT-PCR values were normalized with the level of expression of the actin gene. The expression levels correspond to the mean \pm the standard error of a representative experiment ($n=3$). Significant differences between mock and infected or treated plants at different time points are represented by different letters when p -value < 0.05 . No statistical differences were observed regarding *SIS5H* gene expression.

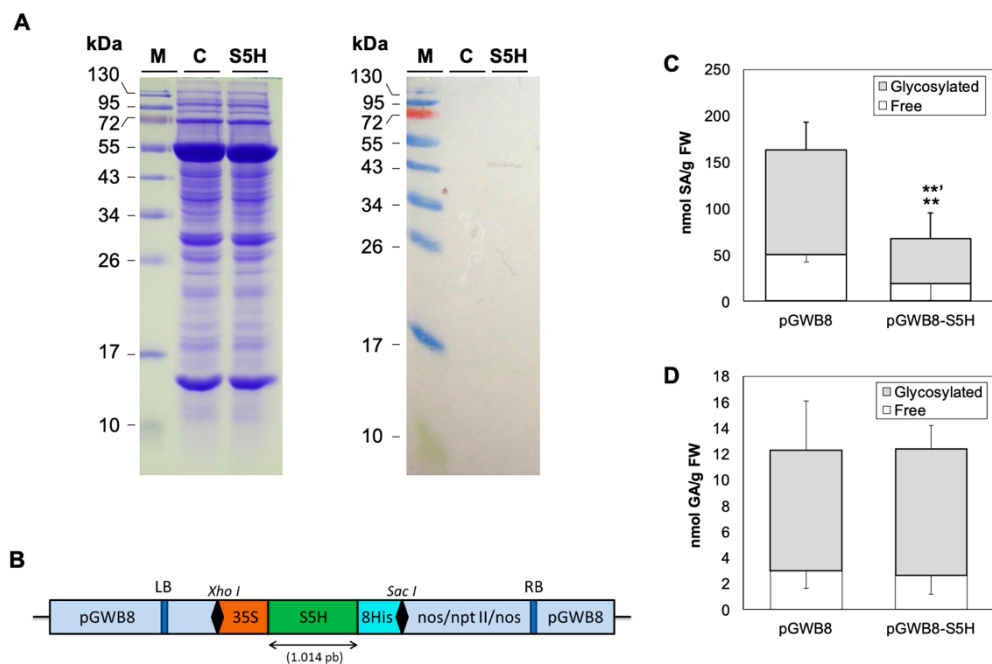


Figure S3. S5H *in vivo* activity in *Nicotiana benthamiana* plants. (A) SDS-PAGE (left panel) and western blot analysis (right panel) of *N. benthamiana* plants agroinoculated with pGWB8 empty vector (C) or pGWB8-SIS5H (S5H). **(B)** Diagram of the cloning cassette. Panels on the right show the nanomoles of SA **(C)** and GA **(D)** per gram of fresh weight in *Nicotiana benthamiana* leaves embedded with SA and agroinoculated with the construction pGWB8-S5H, compared with its control (plasmid pGWB8 without insert). The results correspond to a representative experiment (n=3). Student's *t*-statistic analysis shows the mean \pm standard deviation since *p*-value < 0.001 in free (**) and total (***) SA accumulation. No statistical differences were observed for GA accumulation. 2,3-DHBA was not detected.

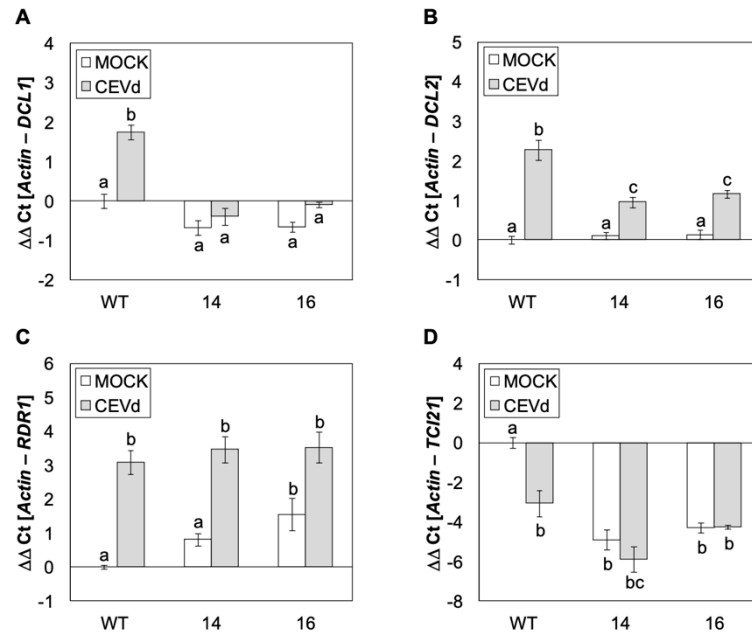


Figure S4. Gene expression analysis of wild type (WT) and *RNAi_SIS5H* (lines 14 and 16) transgenic tomato plants, mock-inoculated (MOCK) and inoculated with CEVd (CEVd). *DCL1* (A), *DCL2* (B), *RDR1* (C) and *TCI21* (D) gene expression was analyzed 3 weeks after viroid infection. The qRT-PCR values were normalized with the level of expression of the actin gene. The expression levels correspond to the mean \pm the standard error of a representative experiment ($n=3$). The significant differences between different genotypes and infected or mock-inoculated plants are represented by different letters since p -value < 0.05 .

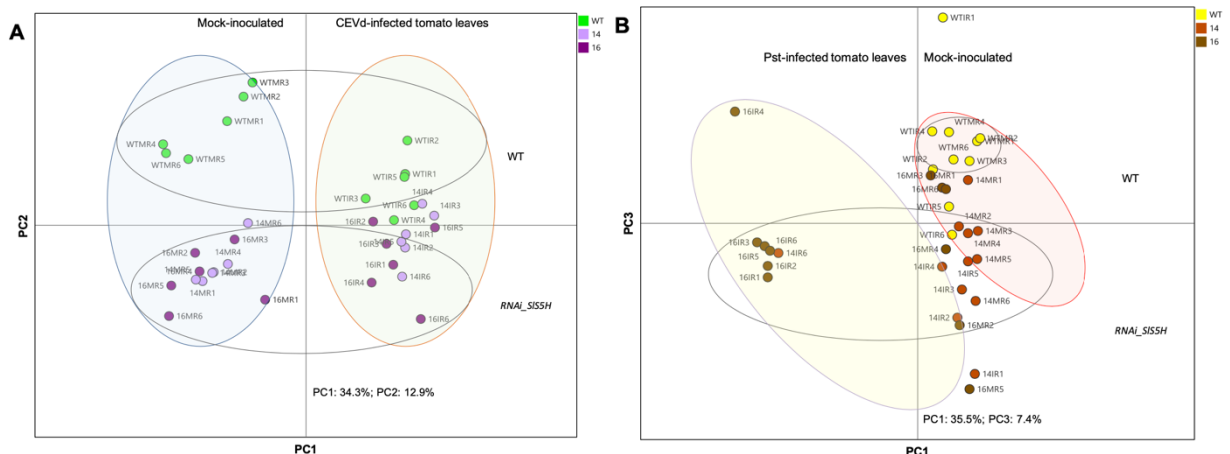


Figure S5. Score plot of PCA based on whole range of on the whole array of the mass spectra within a m/z range from 100 to 1500 using unit variance (UV) scaling method of methanolic extracts from tomato leaves. (A) CEVd infected plants at 3 wpi, green: wild type (WT); light purple: *RNAi_SIS5H* 14; dark purple: *RNAi_SIS5H* 16; (B) *Pst* infected plants at 24 hpi, yellow: wild type (WT); orange: *RNAi_SIS5H* 14; brown: *RNAi_SIS5H* 16.

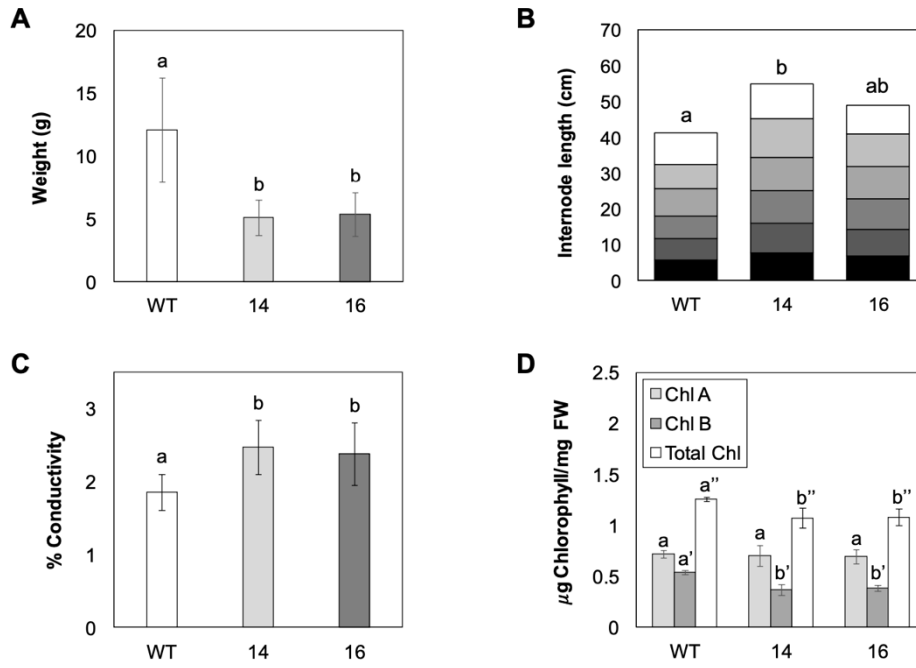


Figure S6. Analysis of phenotypic differences between WT and *RNAi_S5H* transgenic lines 14 and 16. Differences related to weight (**A**), internode length (**B**), conductivity (**C**) and chlorophyll content (**D**) in WT and *RNAi_SIS5H* 14 and 16 transgenic plants were measured 10 weeks after germination. Bars represent the mean \pm the standard deviation of a representative experiment (n=6).

Chapter II

HB: signalling mechanisms and agricultural
applications (I)

Research article

Signalling mechanisms and agricultural applications of (Z)-3-Hexenyl Butyrate-mediated stomatal closure

Celia Payá¹, Julia Pérez Pérez¹, Francisco Vera¹, Borja Belda¹, Lucía Jordá², Giovanni Pensabene³, Ismael Rodrigo¹, José M^a Bellés¹, M^a Pilar López-Gresa^{1*} and Purificación Lisón^{1*}.

¹Instituto de Biología Molecular y Celular de Plantas (IBMCP), Consejo Superior de Investigaciones Científicas (CSIC), Universitat Politècnica de València (UPV), Ciudad Politécnica de la Innovación (CPI) 8 E, Ingeniero Fausto Elio s/n, 46011 Valencia, Spain.

²Centro de Biotecnología y Genómica de Plantas (CBGP, UPM-INIA), Universidad Politécnica de Madrid (UPM) – Instituto Nacional de Investigación y Tecnología Agraria y Alimentaria (INIA), Madrid, Spain

³ Químicas Meristem S. L., Valencia, Spain.

*These authors contributed equally to this work

*Corresponding autor: plison@ibmcp.upv.es

Ph.D candidate contribution

C. P. had a main role in the following activities: performing the experiments, data collection, data analysis, data visualization, drafting figures and manuscript, manuscript review and editing.

AUTHOR'S VERSION

Manuscript submitted in *Plant, Cell & Environment*

List of Abbreviations

ABA: Abscisic Acid	RBOHD: Respiratory Burst Oxidase Homolog D
BABA: β -Aminobutyric Acid	RBOHF: Respiratory Burst Oxidase Homolog F
BAK1: BRI1-Associated receptor Kinase 1	ROS: Reactive Oxygen Species
BIK1: Botrytis Induced Kinase 1	SA: Salicylic Acid
BP: Biological Processes	SAR: Systemic Acquired Resistance
BTH: Benzo-(1,2,3)-thiadiazole-7-methionine S-methyl	SHAM: Salicylhydroxamic acid
Ca²⁺: calcium	SLAC1: Slow Anion Channel-Associated 1
CC: Cellular Components	SLAH3: SLAC1 homolog 3
DAD: Days After Drought	VOCs: Volatile Organic Compounds
DAMPs: Danger-Associated Molecular Patterns	
DEGs: Differentially Expressed Genes	
DPI: Diphenyleiodonium chloride	
EFRs: Ethylene Responsive Factors	
EGTA: Ethylene-bis(oxyethylenenitrilo)tetraacetic acid	
ETI: Effector-Triggered Immunity	
<i>flc:</i> <i>flacca</i>	
Fig22: Flagellin 22	
FLS2: Flagellin-Sensing 2	
GLVs: Green Leaf Volatiles	
HB: (<i>Z</i>)-3-Hexenyl Butyrate	
MAMPs: Microbe-Associated Molecular Patterns	
MAPKs: Mitogen-Activated Protein Kinases	
MF: Molecular Functions	
NLRs: Nucleotide-binding domain Leucine-rich repeat Receptors	
NO: Nitric Oxide	
OST1: Open Stomata 1	
PAMPs: Pathogen-Associated Molecular Patterns	
PRRs: Pattern Recognition Receptors	
PRs: Pathogenesis-Related Proteins	
<i>Pst:</i> <i>Pseudomonas syringae</i> pv. <i>tomato</i>	
PTI: PAMP-Triggered Immunity	
qRT-PCR: Quantitative Real Time PCR	

Abstract

It is well known that plants respond to various stresses by releasing volatile organic compounds (VOCs). Green leaf volatiles (GLVs), which are commonly produced across different plant species after tissue damage, comprise an important group within VOCs. Among them, (*Z*)-3-hexenyl butyrate (HB) was described as a natural stomatal closure inducer, playing an important role in stomatal immunity, although its mechanism of action is unknown. Here, through different genetic, pharmacological and biochemical approaches we uncover that HB perception initiates different defence signalling events such as activation of Ca²⁺ permeable channels, mitogen-activated protein kinases (MPKs) and production of NADPH oxidase-mediated reactive oxygen species (ROS). Furthermore, HB-mediated stomata closure resulted to be independent of abscisic acid (ABA) biosynthesis and signalling. Additionally, exogenous treatments with this volatile alleviate water stress and improve fruit productivity in tomato plants. HB efficacy was also tested under open field conditions, leading to enhanced resistance against *Phytophthora* spp. and *Pseudomonas syringae* infection in potato and tomato plants, respectively. Collectively, our results provide insights into HB signalling transduction pathway, confirming its role in stomatal closure and plant immune system activation, and proposing HB as a new phytoprotector for the sustainable control of biotic and abiotic stresses in agriculture.

1. Introduction

Plants have evolved a complex and efficient innate immune system to deal with pathogen attacks. Two different defensive layers are involved in plant immune responses [1]. The first line of plant innate immunity is established upon the recognition by receptors on the plasma membrane (pathogen recognition receptors; PRRs) of conserved microbial features, called as pathogen- and microbe-associated molecular patterns (PAMPs and MAMPs), activating the PAMP-triggered immunity (PTI) [2,3]. At this level, plants are also able to perceive through different PRRs, molecules known as damage molecular patterns (DAMPs), released from plant cells upon pathogen attack. This specific recognition trigger also a PTI response known as DAMP-triggered immunity (DTI) [4]. The second layer is started by the recognition of virulence factors, also called effectors, by intracellular receptors (nucleotide-binding, leucine-rich repeat receptors; NLRs), activating the effector triggered immunity (ETI) [5,6]. Although both types of immune responses involve different activation mechanisms, PTI and ETI share many downstream components and responses, such as reactive oxygen species (ROS) production, increases in cytosolic calcium (Ca²⁺) levels or activation of mitogen-activated protein kinases (MPK) cascades. Amplitudes and dynamics differ in each defensive level, postulating that ETI is an “accelerated and amplified PTI” [7].

Many foliar pathogens, including bacteria, are unable to directly penetrate plant tissues and they use natural openings such as stomata that represent one of the most important passages for the entry of bacterial pathogens. As a countermeasure, plants have evolved a mechanism to rapidly close their stomata upon PAMPs/MAMPs perception limiting bacterial entrance, a defensive response known as stomatal immunity [8]. The bacterial MAMP flg22, an immunogenic epitope of the bacterial flagellin, is recognized by the PRRs receptor FLAGELLIN- SENSITIVE2 (FLS2) and the coreceptors BRI1-ASSOCIATED RECEPTOR KINASE1 (BAK1) and BOTRYTIS—INDUCED KINASE 1 (BIK1) [9–12]. This recognition by the FLS2 complex triggers a cascade of signalling events including increases of Ca²⁺ influx, ROS burst through the activation of plant NADPH oxidases, MAPK cascades and activation/inhibition of ion channels, all leading to stomatal immunity [13].

The phytohormone abscisic acid (ABA) is essential in stomatal defence during plant immunity [14]. In fact, ABA-induced stomatal closure shares a common signalling pathway with PAMP-induced stomatal closure, including ROS burst, nitric oxide (NO) intermediate accumulation, activation of S-type anion channels, or the inhibition of K⁺ channels [13]. Besides, both signals converge at the level of open stomata 1 (OST1), a serine/threonine protein kinase also known as SnRK2.6 that activates S-type anion channels like the slow anion channel-associated 1 (SLAC1) and SLAC1 homolog 3 (SLAH3), and the R-/QUAC-type anion channel QUAC1 [15–18]. Despite this, there are some differences in the canonical stomatal immunity signalling components in both PTI and ABA signalling pathways. ABA-induced ROS production depends on the kinase OST1, which phosphorylates and activates RBOHF/RBOHD. However, during PTI stomatal closure, ROS are produced by the activation of the NADPH oxidase RBOHD that is directly phosphorylated by the plasma-membrane-associated kinase BIK1 [12,13]. Furthermore, MPKs are known to play a specific role in stomatal immunity. MPK3 and MPK6 positively regulate flg22-triggered stomatal closure in a partially redundant manner, but they are not involved in ABA-mediated stomatal closure [15,19]. Intriguingly, MPK9 and MPK12 act redundantly as positive regulators of ABA- and ROS-mediated stomatal immunity, acting downstream of ROS production and Ca²⁺ fluxes, while they seem not to be involved in the flg22-induced stomatal closure [15,20,21]. It has been also reported that not only JA through the phytotoxin coronatine which is produced by various strains of *Pseudomonas syringae*, but also ABA mediate the inactivation of the MPK3 and MPK6, promoting *Pseudomonas syringae* DC3000 pv. *tomato* (*Pst* DC3000) virulence. Moreover, to counteract bacterial suppression of MAPKs, host plant block JA signalling pathway upon ETI establishment [22]. These results demonstrate the highly interconnected network of plant immune signalling pathways, and how it can be exploited by host plants and pathogens.

After pathogen invasion, plant metabolic pathways are dramatically reprogrammed, triggering the accumulation of a plethora of secondary metabolites to cope with this stress. The defensive metabolites may act through direct mechanisms as antimicrobial

or antifungal agents *per se*, or through indirect mechanisms, participating in the signalling/amplification of the plant defence responses. Due to its gaseous nature, volatile organic compounds (VOCs) act as fast signalling molecules that activate plant defensive response pathways between distant organs, and they even allow communication between different plants [23–25]. Several studies have demonstrated that VOCs are able to induce defences against herbivorous insects, pathogens, and even environmental stresses [24,26–28]. Defence priming against pathogens induced by VOCs has been considered as a sort of “green vaccination” [27,29].

A non-targeted GC-MS metabolomics analysis revealed the VOCs profile associated with the immune response of tomato cv. Rio Grande plants upon infection with either virulent or avirulent strains of the model bacterial pathogen *Pst* DC3000. In the case of the avirulent infection which leads to the establishment of ETI, the VOC profile of immunized plants was characterized by esters of (*Z*)-3-hexenol with acetic, propionic, isobutyric or butyric acids, and several monoterpenoids such as linalool or α -terpineol [30]. The defensive role of these compounds was tested through exogenous application in tomato plants and, among all these compounds, treatments with (*Z*)-hexenyl butyrate (HB) resulted in the transcriptional upregulation of defensive genes, stomatal closure and enhanced resistance to the bacterial infection with *Pst* DC3000, confirming the role of HB as a natural defence elicitor [31]. Additionally, HB-mediated stomatal closure was effective in different plant species, which also led to accelerated ripening in *Vitis vinifera* [31,32].

In this study, we investigated the signalling mechanisms underlying HB-mediated stomatal closure and plant immunity. The results showed that HB triggers stomatal closure not only in an ABA-independent manner, but through Ca^{2+} , ROS and MAPK-signalling cascade activation. Furthermore, we tested the efficacy of this compound in water stress and its effectiveness was also assessed against both biotic and abiotic stresses under field conditions. Taken together, we propose a new role for HB as a natural priming agent against biotic and abiotic stresses.

2. Materials and Methods

2.1. Plant Material and Growth Conditions

In this study *Solanum lycopersicum* (tomato) var. MoneyMaker were used. Tomato ABA-deficient mutants *flacca* (*flc*) and their corresponding parental and Lukullus plants, were kindly provided by Jorge Lozano (IBMCP, Valencia Spain). Tomato seeds were chemically sterilized with a 1:1 mixture of sodium hypochlorite and distilled water. After sterilization, seeds were placed in 12 cm-diameter pots containing vermiculite:peat (1:1). Plants were grown under greenhouse conditions with 16/8 h (26/30° C) photoperiod and a relative humidity between 50-70%.

In the case of drought experiments, water stress was simulated by quitting irrigation during 6 days in the case of stressed plants, whilst control plants were normally watered. HB-treatments were performed every 2 days, until the end of the experiments.

Arabidopsis thaliana (*Arabidopsis*) were also employed. All the *Arabidopsis* plants are in Columbia (Col-0) ecotype background, including Col-0 and *mpk3*, *mpk6* mutants. They were grown in a chamber under short-day conditions (10/14 h; 23/19°C light/darkness), with a relative humidity ranging from 50 to 60%.

2.2. HB treatments under greenhouse conditions

Treatments were carried out on 4-week-old tomato plants either in closed chambers or by spray. Tomato plants were placed into 121 L methacrylate chambers containing hydrophilic cotton swabs soaked with 5 µM of (*Z*)-3-hexenyl butyrate (HB; Sigma-Aldrich, Saint Louis, MO, USA) or distilled water in the case of control plants. Methacrylate chambers were hermetically sealed during the 24 h treatment. In the case of spray treatments, tomato plants were pre-treated by spray with HB at a concentration of 2 mM or distilled water (mock), containing 0.05% Tween 20 as wetting agent, and placed into methacrylate chambers as described.

2.3. Bacterial inoculation assays

The bacterial strain used in this study was *Pst* DC3000 (kindly provided by Dr. Selena Giménez, Centro Nacional de Biotecnología, Madrid, Spain). Bacteria were grown in LB agar medium supplemented with rifampicin (10 mg/mL) and kanamycin (0.5 mg/mL) during 48 h at 28°C. An independent colony was transferred into King's B liquid medium containing rifampicin and were grown at 28°C. After 48 h, bacteria were centrifugated and resuspended in 10 mM sterile MgCl₂ to an OD₆₀₀=0.1, which corresponds to a final inoculum concentration of 5 × 10⁷ CFU/mL approximately. For dip inoculation assays in *Arabidopsis thaliana* plants, *Pst* DC3000 suspension (OD₆₀₀= 0.2) in 19 mM MgCl₂ containing 0.05% Silwet L-77 was sprayed onto 4-weeks old plants. Then, the bacterial growth experiments were carried out by sampling three leaf discs (1 cm² each) from each inoculated plant. Finally, samples were grounded in 10 mM MgCl₂, serial dilutions were done and plated on King's B medium supplemented with rifampicin. Bacterial colonies were counted 48 h after serial dilutions.

2.4. Stomatal Aperture Measurement

To measure stomatal aperture in tomato plants, nail polish was applied in the abaxial part of five leaves from three independent plants. Once the layer was dried, leaves were peeled off and epidermal strips were obtained.

In the case of leaf discs, they were taken from 3- to 4-week old plants and floated in Murashige & Skoog medium (MS) for 3 h under light, in order to induce stomatal opening. Then, stomata closer elicitors (HB, ABA and flg22) were added to the medium at the appropriated concentration for 3 h. For chemical inhibitors, 2 mM salicylhydroxamic acid (SHAM), 20 μ M diphenyleiodonium chloride (DPI), 2 mM EGTA and 20 μ M PD980059 were added 30 minutes before incubation with the elicitors.

In both cases, samples were then visualized under a Leica DC5000 microscope (Leica Microsystems S.L.U.) and pictures of different regions were analyzed with *ImageJ* software. Aperture ratio was measured as stomata width/length from at least 50 stomata per plant and/or treatment, considering a value of 1 as a totally opened stomata.

2.5. Ion leakage estimation

Five leaf discs were excised by a 1 cm² diameter stainless steel cork borer, then immersed in tubes containing 40 mL of deionized water and shaken at 200 rpm for 2 h at 28°C. The conductivity of the solution (L1) was measured with a conductivity meter (DDS-11A, Shanghai Leici Instrument Inc., Shanghai, China). After that, the solution was boiled for 15 min, cooled to room temperature, and the conductivity of killed tissues (L2) was measured. Ion leakage was calculated as the ratio of L1 to L2.

2.6. RNA Isolation and qRT-PCR analysis

Total RNA of tomato leaves was extracted using TRIzol reagent (Invitrogen, Carlsbad, CA, USA), following the manufacturer's protocol. RNA was then precipitated by adding one volume of 6 M LiCl and keeping it on ice for 4 h. Afterward the pellet was washed using 3 M LiCl and was dissolved in RNase-free water. Finally, in order to remove any contaminating genomic DNA, 2 U of TURBO DNase (Ambion, Austin, TX, USA) were added per microliter of RNA. For the quantitative RT-qPCR analysis, one microgram of total RNA was employed to obtain the corresponding cDNA target sequences using an oligo(dT)₁₈ primer and the PrimeScript RT reagent kit (Perfect Real Time, Takara Bio Inc., Otsu, Shiga, Japan), following the manufacturer's directions. Quantitative PCR was carried out as previously described [33]. The housekeeping gene transcript actin was used as the endogenous reference. The PCR primers were designed using the online service Primer3 (<https://primer3.ut.ee/>) and are listed in Table S1.

2.7. RNA-seq Analysis

Six individual MoneyMaker tomato plants of 4 weeks-old were placed into methacrylate chambers and treated with HB or distilled water as described above. Twenty-four hours post-treatments leaves samples were collected, and total RNA was extracted and analyzed using a 2100 Agilent Bioanalyzer (Agilent Technologies, Inc.,

Santa Clara, CA, USA) to check RNA integrity and quality. RNASeq and bioinformatics analysis were performed by Genomics4All (Madrid, Spain). Samples were sequenced with x50 tomato genome coverage using 1 x 50 bp reads. Raw data was aligned to *Solanum lycopersicum* genome using HISAT2 v2.1.0 [34]. StringTie was used to obtain the differential expression. Data and transcript-level expression analysis, and functional enrichment analysis were performed following previously described protocols [35–38]. GO enrichment analysis were performed with Panther Classification System (<http://pantherdb.org>) [39].

2.8. MPK Phosphorylation Assay

Leaf discs were taken from 3- to 4-week-old tomato and *Arabidopsis thaliana* plants and floated on MS medium for 3 h under light. Then, flg22 1 μM , ABA 10 μM and HB 50 μM treatments were added, and samples were taken 15, 30 and 60 minutes after treatments, and they were frozen in liquid nitrogen. Frozen leaf samples were homogenized and proteins extracts were obtained by Laemmli extraction method. Briefly, leaf disc powder (100 mg) was mixed with 150 μL 2x Laemmli buffer and incubated on ice for 20 min, vortexing every 5 min. Samples were thereafter boiled for 10 min, cooled on ice for 5 min, and centrifuged at 12000g for 5 min at 4°C to clear homogenates. The resulting supernatants (10 μL) were analyzed by Western Blot with Phospho-p44/42 MAPK (Erk1/2) (Thr202/Tyr204) (Cell Signalling, 1679101S; dilution 1:1,000) primary antibodies and peroxidase-conjugated goat anti-rabbit IgG (Jacksons, 111035144; dilution 1:20,000) secondary antibodies.

2.9. Open-field HB treatments

2.9.1. Biotic stress

The trial of tomato plants inoculated with *Pseudomonas syringae* was performed under open field conditions in Torrellano (Alicante, Spain, 38°17'39"N, 0°35'11"O, 68 m.a.s.l.). The tomato plants were transplanted on August 26th, 2020 and the commercial variety Muchamiel was used. The experiment comprised 6 plots (10 plants each) treated with HB at 0.5, 5, 10 and 50 mM, plus another plot that was treated with the commercial pesticide OXICOOP 50 as a positive control, and one plot was left untreated. Treatment applications were carried out using a motorized knapsack sprayer. Three applications were carried out, the application A being preventive and subsequent applications (B and C) were carried out with 6 to 8 days interval coinciding with the persistence of the effect of HB [31].

To determine the efficacy of HB for the control of *Downy mildew* in potatoes, an independent open field condition trial was performed in Borbotó (Valencia, Spain, 39°30'55"N, 0°23'27"O, 22 m.a.s.l.). The potato plants were transplanted on February 18th 2019 and the variety used was Vivaldi. The experimental design used was randomized block with 6 plots (one plot per treatment) and 60 plants in each one. Foliar

treatments were performed following the same methodology and strategy than in the case of the tomato experiment, but in this case ORO-COBRE ZINEB was used as positive control. Four applications were carried out, being application A before disease appears, and following applications (A, B, C and D) with 7 ± 1 days intervals.

In both experiments, the efficacy (E) of the treatments was calculated according to the Abbott's formula [40], using the percentage of leaf area affected in control (C) and treated (T) groups. The following formula was used:

$$E = \frac{(C - T)}{C} \times 100$$

Tomato and potato-pathogen inoculation trials were performed in accordance with EPPOs: PP1/135(4), PP1/152(4) and PP1/181(4). Specific EPPOs: PP1/2(4).

2.9.2. Abiotic stress

This experiment was carried out at Picanya, located in Valencia, Spain ([39°26'08"N, 0°26'09"O](#), 14.9 m.a.s.l.). Due to the volatility of the compound, the field trial was performed in two independent greenhouses, one for HB treatments and the other one for control treatments. The experimental design used was randomized blocks (9 m²) with 4 biological replicates per treatment. Plants were sprayed with HB at 5 mM every two weeks. To provoke water stress, irrigation was completely stopped. The soil capacity was continuously monitored and once it reached 50, the water regime was re-established. Different parameters were assessed like plant height, number of flowers, number of set fruits and vigor. Moreover, at harvest, total and yield was analyzed per categories as follows: small size (25-50 mm diameter, 25-100 g weight); medium size (50-75 mm diameter, 100-200 g weight); big size (75-100 mm diameter, 200-300 g weight); and extra size (>100 mm diameter, >300 g weight).

In all the field trials, time units are referred as follows: X DA Y, being X day (0, 7 and 18); DA Days After; Y day of treatment (A, B, C and D).

Abiotic stress trials were performed under General Standards, in accordance with EPPO Guidelines PP 1/153(4), PP 1/181(4), PP 1/135 (5) and PP 1/239(2).

2.10. Statistical Analysis

The statistical analysis of two or more variables was carried out by using Student's *t*-test or analysis of variance (ANOVA), respectively employing the GraphPad's Prism 9 software. In all the analyses, a *p*-value < 0.05 was considered statistically significant.

3. Results

3.1. Treatments with HB induce transcriptomic changes related to plant immunity and photosynthesis

To provide insight into the molecular mechanisms underlying the tomato plant response to HB, an RNA-seq analysis was performed on leaves tissues from mock and HB-treated tomato plants. After trimming and filtering data, a total of 1456 genes were found to be differentially expressed (DEGs) between HB- and control-treated plants, indicating that HB treatments produce an outstanding effect at the transcriptional level. To classify DEGs, a GO enrichment analysis for biological processes (BP), cellular components (CC) and molecular functions (MF) was performed for up- and down-regulated DEGs, independently.

Among the upregulated genes, 1122 DEGs were annotated being the BP category the most enriched one. In this regard, most of the DEGs were putatively involved in organonitrogen compound metabolic processes (GO:1901564), chitin metabolic process (GO:0006030) or amino glycan and amino sugar metabolic processes (GO: 0006040, GO:0006022). MF category included chitinase activity (GO:0004568), chitin binding (GO:00080761) or endopeptidase activity (GO: 0004175), which are mainly related to pathogen defensive responses (Figure 1A). On the other hand, only 334 downregulated DEGs were annotated, and most of them were associated with the CC category mainly related to plastoglobule (GO:0010287), photosystem (GO:0009521) and chloroplast (GO:0009507). Indeed, the most enriched groups when biological processes were assessed were related to photosynthesis (GO:0015979) and the only enriched MF term was chlorophyll binding (GO:0016168) (Figure 1B). Both defensive- and photosynthesis-related gene expression were confirmed by RT-qPCR, observing a statistically significant induction for the pathogenesis-related genes *PR1* (X68738) and *PR5* (X70787), as well as a gene coding for a putative PRR immune leucine-rich repeat receptor-like kinase (Solyc12g036793) and also a gene involved in heavy metal resistance and detoxification (Solyc06g066590). Besides, a reduction in the expression of genes encoding chlorophyll binding proteins (Solyc06g069730; Solyc06g069000; Solyc12g011280) was also validated (Figure S1). Therefore, RNA-seq transcriptomic analysis revealed that HB treatments induced plant defensive responses against pathogens as well as photosynthesis reprogramming.

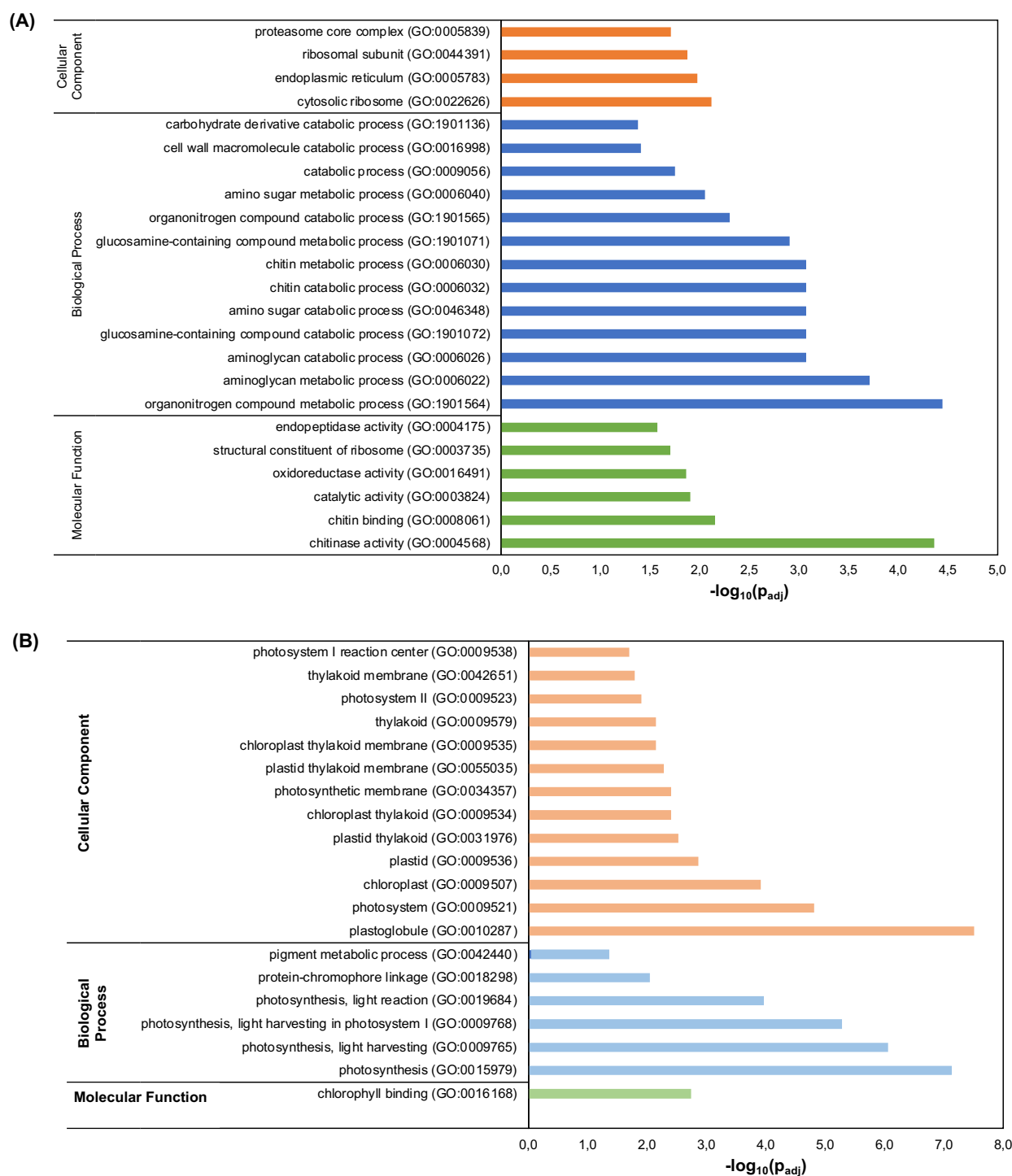


Figure 1. Transcriptomic analysis confirm the role of HB in plant immunity. Functional profiling analysis of upregulated **(A)** and downregulated **(B)** DEGs between HB- and control-treated plants.

3.2. ROS production via NADPH oxidases and Ca²⁺ signalling but not ABA are required for HB-mediated stomatal closure

To decipher the signalling pathway by means of which HB mediates stomatal closure, an appropriate method was developed for stomatal measurement analyses (Materials and Methods). In these experiments, we studied the effect of HB in comparison with the positive controls for stomatal closure flg22 and ABA, considering both dose-response and time-course assays of these compounds to optimize the different treatments (Figure S2).

Once set up, we studied whether ABA was necessary for the HB-dependent stomata closure. For this purpose, we took advantage of both *flacca* (*flc*) tomato mutants that are impaired in ABA biosynthesis and their corresponding parental Lukullus wildtype (WT) plants [41]. As expected, HB, flg22 and ABA treatments promoted stomatal closure in WT plants. In *flc* mutants, the stomatal aperture ratio in mock conditions was significantly higher compared to WT plants, probably due to a reduction of the ABA levels. However, ABA treatments in *flacca* mutants closed the stomata to the same extent than flg22 and HB, suggesting that ABA biosynthesis is not required for flg22- and HB-mediated stomatal closure (Figure 2A).

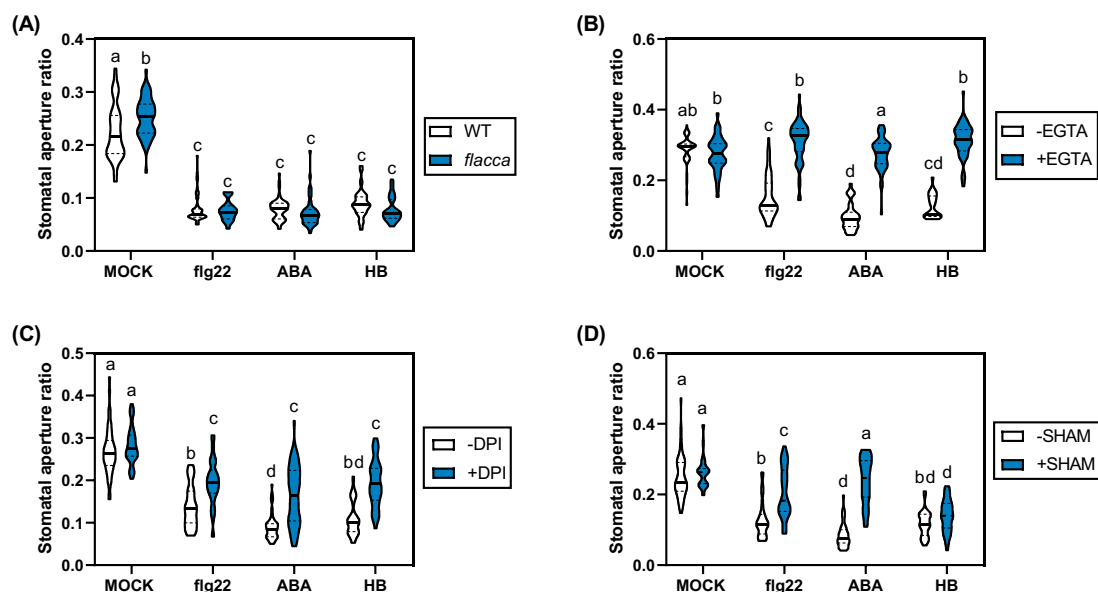


Figure 2. HB-mediated stomatal closure requires Ca²⁺ signalling and ROS production by NADPH oxidases, but not ABA biosynthesis. (A) Lukullus (WT) and *flacca* tomato leaf discs were floated on liquid MS for 3 h under light. Then, 1 μ M flg22, 10 μ M ABA and 50 μ M HB were applied and stomatal aperture ratio was determined 2 h after treatments. In the case of chemical inhibitors experiments, 2 mM EGTA (B), 20 μ M DPI (C) and 2 mM SHAM (D) were added before elicitors treatments. Violin plots represents the stomatal aperture ratio of 50 stomata for each treatment. Different letters indicate statistically significant differences for each genotype and treatment ($p < 0.05$, two-way ANOVA with Tukey HSD Test).

As aforementioned, Ca^{2+} and ROS also play a pivotal role in the stomatal response, acting as secondary messengers upon pathogen attack. Therefore, we decided to analyze the role of these signalling molecules in the HB-mediated stomatal closure. For this purpose, we performed pre-treatments with the specific Ca^{2+} ion chelator EGTA (ethylene-bis(oxyethylenitrilo)tetraacetic acid), and the ROS production inhibitors DPI (Diphenyleneiodonium, which inhibits NADPH oxidase) or SHAM (salicylhydroxamic acid, acting on peroxidases) before triggering the stomatal closure with either HB, flg22 or ABA. Pre-treatments with EGTA completely abolished the stomatal closure mediated by all, HB, flg22 and ABA treatments, indicating that Ca^{2+} signalling is essential for stomatal closure (Figure 2B). Interestingly, pre-treatments with DPI partially abrogated the stomatal closure induced by HB, flg22 and ABA, suggesting that NADPH-dependent ROS production is partially necessary for this process (Figure 2C). However, unlike flg22 and ABA treatments, SHAM did not inhibit HB-induced stomatal closure, indicating that stomatal closure promoted by HB is independent of ROS production by peroxidases (Figure 2D).

Our results seem to indicate that HB-mediated stomatal closure requires Ca^{2+} fluxes and is partially dependent on ROS generation by NADPH oxidases but is nevertheless independent of ABA biosynthesis and ROS generated through peroxidases.

3.3. Activation of MPK3 and MPK6 is essential for HB-mediated stomatal immunity

To test whether HB intracellular signalling occurs through activation of MPK-cascades, we analyzed the phosphorylation of MPK3 and MPK6 in tomato and *Arabidopsis thaliana* leaf discs after treatments with flg22, ABA and HB. Regarding tomato samples, 15 minutes after treatments HB induced MPK3 phosphorylation, and this activation persisted until 60 minutes after treatments (Figure 3A). Nevertheless, in *Arabidopsis thaliana* samples MPK3/6 phosphorylation was observed at 60 minutes after HB treatments, suggesting that MPKs activation phenomenon occurs earlier in tomato than in *Arabidopsis thaliana* plants (Figure 3B).

To confirm the importance of MPK3/6 activation in HB-mediated stomatal immunity, pre-treatments with the MPKs inhibitor PD98059 on tomato leaf discs were performed. After PD98059 application, flg22, ABA and HB treatments diminished their ability to induce stomatal closure, confirming that MAPKs play a pivotal role in all the elicited stomatal responses (Figure 3C). Furthermore, treatments with PD98059 were also carried out *in planta* (See Materials and Methods). In this regard, application of PD98059 diminished HB enhanced resistance to bacterial infection (Figure 3D). These results indicated that HB induces stomatal immunity partially via activation of the MPK3/6 signalling cascades in tomato plants, without discarding that other mechanisms should also be involved in the HB-mediated stomatal immunity.

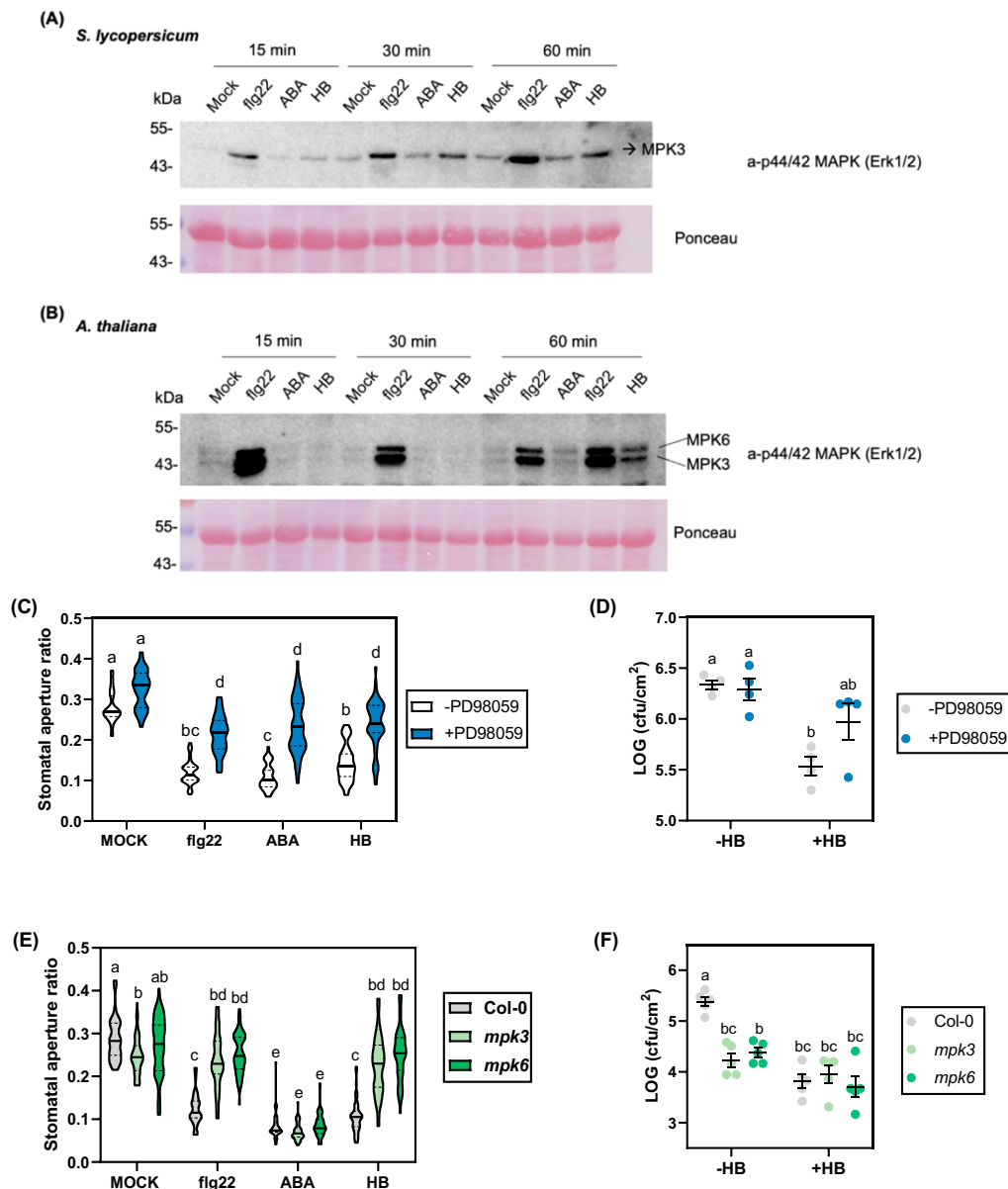


Figure 3. Activation of MPK3 and MPK6 is involved in HB-mediated stomatal immunity. MPK activation assay in tomato **(A)** and *Arabidopsis thaliana* **(B)** leaf discs 15, 30 and 60 minutes after treatments with 1 μ M flg22, 10 μ M ABA and 50 μ M HB. MPK activation was detected by immunoblot analysis using the Phospho-p44/42 MAPK (Erk1/2; Thr-202/Tyr204) rabbit monoclonal antibody. Western blot experiments were performed three times and yielded similar results. **(C)** Stomatal aperture ratio was measured in tomato leaf discs floated on MS liquid for 3 h under light, pre-treated with the MPKs inhibitor PD98059 20 μ M and followed by treatments with 1 μ M flg22, 10 μ M ABA and 50 μ M HB for 2 h. **(D)** Growth of *Pst* DC3000 on tomato leaves of control (-HB) and HB-treated (+HB) after treatments with the MPKs inhibitor PD98059. Plants were sprayed with PD98059 100 μ M for 3 hours, subsequently treated with HB 5 μ M or water for 24 h into methacrylate chambers, and then dip inoculated with *Pst* DC3000. Bacterial growth measurements were done 24 h after inoculation. **(E)** Stomatal aperture ratio of *Arabidopsis* Col-0, *mpk3* and *mpk6* mutants leaf discs 2 h after treatments with flg22, ABA and HB. **(F)** Growth of *Pst* DC3000 on *Arabidopsis thaliana* leaves of control (-HB) and HB-treated (+HB) 3 days after inoculation. Plants were treated with HB 5 μ M or water for 24 h into methacrylate chambers, and then infected by spray with *Pst* DC3000. In stomatal aperture experiments, 50 stomata were measured per each treatment and condition (violin plots). Data correspond to at least four independent plants \pm SEM of a representative experiment. Statistically significant differences are represented by different letters ($p < 0.05$, two-way ANOVA with Tukey HSD).

To better characterize this phenomenon, a genetic approach in *Arabidopsis thaliana* *mpk3* and *mpk6* mutants was performed. To do this, the stomatal behavior was analyzed as described in Materials and Methods. As expected, ABA treatments reduced dramatically stomatal aperture in both *Arabidopsis* mutants and WT plants. In contrast, and in accordance with chemical inhibitor experiments performed in tomato plants, stomata aperture ratio was identical to that observed in mock-treated plants not only in *flg22*- but also in HB- treated *mpk3* and *mpk6* mutants, whilst treatments were efficient in the corresponding WT *Arabidopsis* plants (Figure 3E). The incapacity of HB in closing stomata in *mpk3* and *mpk6* mutants resulted in non-enhanced resistance to bacterial infection with *Pst* DC3000 after HB treatments (Figure 3F).

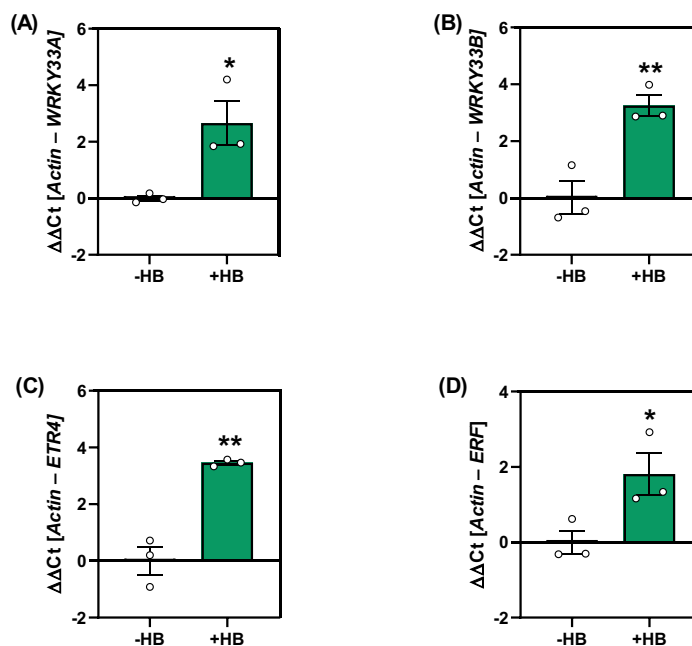


Figure 4. HB treatments induce MPK3/6-mediated downstream signalling. Real-time qPCR analysis of *WRKY33A* (A), *WRKY33B* (B), *ETR4* (C) and an ethylene responsive factor (*ERF*) (D) gene expression in HB-treated plants. Expression levels are relative to tomato mock plants and normalized to the tomato actin gene. Data represent the mean of three independent plants \pm SEM. Asterisk (*) and double asterisks (**) indicate statistical significant differences with $p \leq 0.05$ and $p \leq 0.01$, respectively (Student's t-test).

Additionally, the expression of MPK3/6 target genes was also explored upon HB treatment. As shown in Figures 4A and 4B, HB treatments of tomato plants significantly induced *SIWRKY33A* and *SIWRKY33B* transcription factors, which correspond to tomato orthologs of *AtWRKY33*. This gene has been described to work downstream of MPK3/MPK6 in the reprogramming of the expression of genes involved in camalexin biosynthesis and pipelicolic acid in *Arabidopsis* [42–44]. Since MPK3/6 seem to play a central role in the regulation of the ethylene response pathway [45], ethylene signalling-related genes like the ethylene receptor *ETR4* and an ethylene responsive factor (*ERF*) were also analyzed, observing a significant induction of the expression of both genes

(Figures 4C and 4D). Taken together, these results indicate that MPK3/6 are involved in HB-mediated stomatal immunity.

3.4. HB treatments confer drought tolerance in tomato

The robust effect of HB in promoting the closure of stomata prompted us to study the effect of HB on drought tolerance. To that purpose, well-watered as well as drought-stressed tomato plants were periodically treated with HB and stomatal opening and closing dynamics were monitored. Three days after drought exposure (DAD), stomatal aperture ratio in HB-treated plants was lower than in control-treated plants, confirming the role of HB as stomatal closure inducer in tomato plants, even in drought conditions. It should be noted that HB treatments in well-watered conditions caused similar stomatal closure to those control-treated plants subjected to drought. Moreover, at 6 DAD, stomatal behavior in all treatments and conditions was similar to that observed at 3 DAD (Figure 5A), excepting control plants exposed to drought, in which it was not possible to take leaf samples due to the wilt phenotype of the plants.

To correlate the HB-mediated stomatal closure upon drought conditions with the water content of tomato plants, we also measured the fresh weight at 3 and 6 DAD. At 6 DAD, control-treated plants under drought conditions showed an approximately 50% reduction in the fresh weight. Nevertheless, in the case of HB-treated plants, no statistically significant differences were observed between well-watered plants and those that were under water deficit conditions (Figure 5B).

Finally, plasma membrane damage was also evaluated by measuring electrolyte leakage. In severe drought conditions (6 DAD), no significant differences were observed between HB-treated plants. However, control-treated plants subjected to drought displayed a higher percentage of ion leakage than the rest of treatments, suggesting the role of HB in cell membrane protection and stabilization (Figure 5C). Nonetheless, no differences were found between treatments and conditions related to chlorophyll content, indicating that water-stressed plants had a withered appearance, but they were not collapsed (Figure S3).

To further analyze the mode of action of HB in an ABA-independent manner, water deprivation experiments were carried out in *flc* mutant plants (Figure S4). Due to ABA-deficient plants wilt phenotype, samples were only taken at 3 DAD since they were collapsed at 6 DAD. As we previously observed (Figure 5A), stomatal closure in HB-treated WT plants was similar to non-treated WT plants subjected to drought. Besides, HB treatments in *flacca* plants slightly triggered stomatal closure (Figure S4A), confirming the previous results observed in disc treatments (Figure 2). Regarding weight loss, no significant differences were found (Figure S4B). Our results suggest that HB treatments conferred drought tolerance in tomato plants in an ABA-independent manner.

Finally, membrane damage was also evaluated through electrolyte leakage. In severe drought conditions (6 DAD), no significant differences were shown between HB-

treated plants. However, control-treated plants subjected to drought displayed higher percentage of ion leakage than the rest of treatments, considering the role of HB in cell membrane protection and stabilization (Figure 5C). No differences were found between treatments and conditions related to chlorophyll content, suggesting that water-stressed plants had a withered appearance, but they were not collapsed (Figure S3).

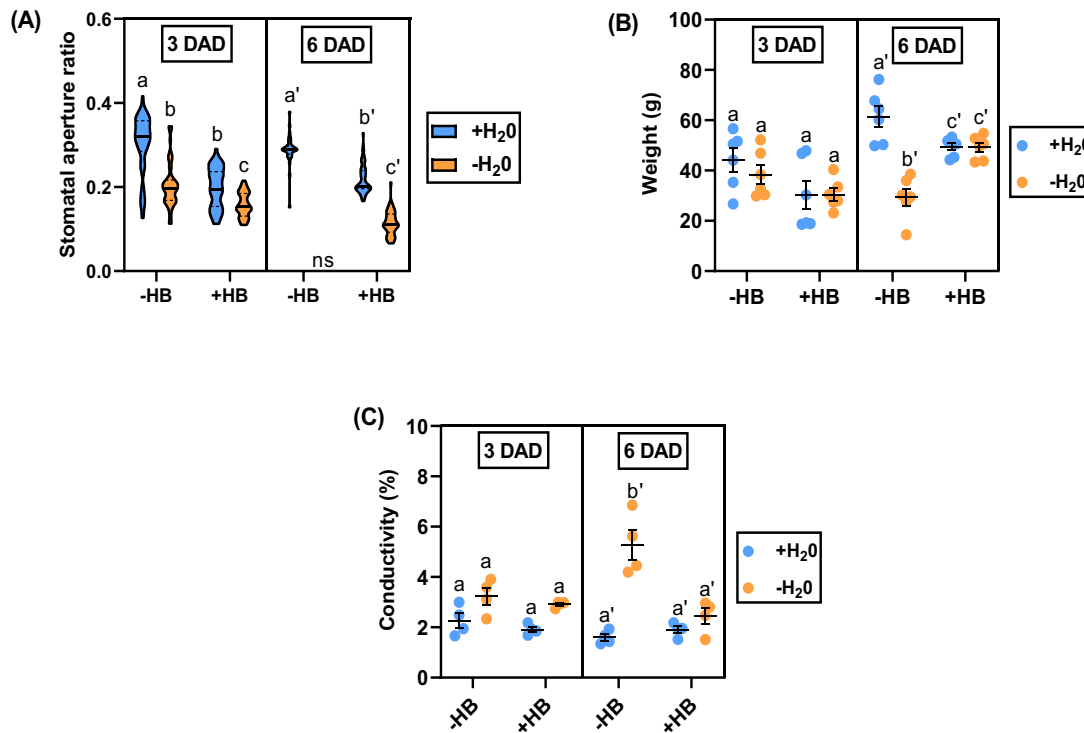


Figure 5. HB treatments induce tolerance to drought in tomato plants. Differences related to stomatal aperture ratio (A), weight (B) and ion leakage (C) in tomato plants treated (+HB) or not (-HB) with HB, in normal (+H₂O) or water stressed conditions (-H₂O). Samples were taken 3 or 6 days after exposure (DAD) to drought conditions. Data in (B) and (C) correspond to six independent plants \pm SEM of a representative experiment. 50 stomata were measured per each treatment and condition (violin plots). Different letters indicate statistically significant differences for each genotype and treatment ($p < 0.05$, two-way ANOVA with Tukey HSD).

To further analyze the mode of action of HB in an ABA-independent manner, water deprivation experiments were carried out in *flc* mutant plants (Figure S4). Due to ABA-deficient plants wilt phenotype, samples were only taken at 3 DAD since they were collapsed at 6 DAD. As we previously observed (Figure 5A), stomatal closure in HB-treated WT plants was similar to non-treated WT plants subjected to drought. Besides, HB treatments in *flacca* plants slightly triggered stomatal closure (Figure S4A), confirming the previous results observed in disc treatments (Figure 2). Regarding weight loss, no significant differences were found (Figure S4B). Our results suggest that HB treatments conferred drought tolerance in tomato plants in an ABA-independent manner.

3.5. Tomato plants treated with HB show lower proline content under drought conditions

To better understand the role of HB in drought tolerance, proline biosynthesis and accumulation were analyzed, since proline is a well-known osmoprotectant [46]. As expected, tomato non-treated plants that were subjected to water deprivation accumulated higher proline levels than well-watered plants. However, when HB-treated plants were analyzed, no statistical differences were found between non-stressed and water-stressed plants (Figure 6A).

Remarkably, a similar trend was observed regarding proline biosynthesis, in which Δ^1 -Pyrroline-5-Carboxylate Synthetase 1 (*P5CS1*) is the rate-limiting enzyme [47,48]. We observed that tomato *P5CS1* gene expression was significantly induced under drought conditions in both HB and non-treated plants. Nevertheless, *P5CS1* expression was lower in the case of HB-treated plants and the expression level was statistically similar to watered, non-treated plants (Figure 6B). Therefore, HB effect appears to alleviate the drought stress, since mechanisms counteracting against the water deprivation are less activated in HB-treated plants.

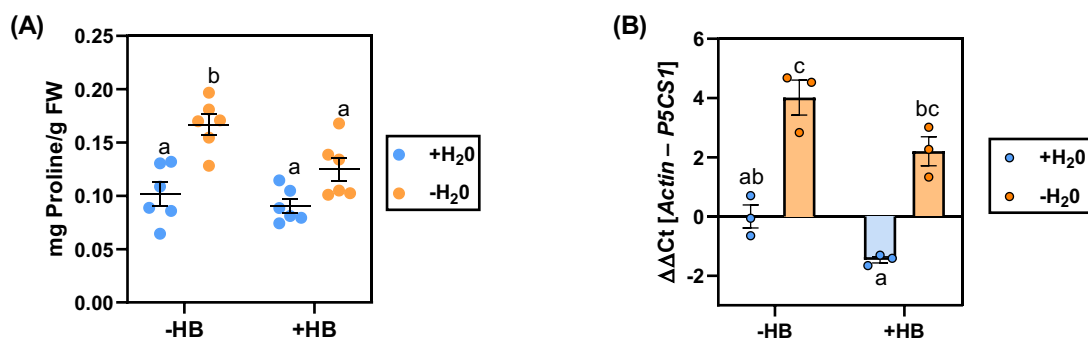


Figure 6. Tomato plants treated with HB have lower proline content under drought conditions. Tomato plants were periodically sprayed (+HB) or not (-HB) with 2 mM HB, and plants were subjected (-H₂O) or not (+H₂O) to 6 days of water deprivation. **(A)** Tomato leaves proline content. Data correspond to average of six independent plants \pm SEM of a representative experiment. **(B)** *P5CS1* gene relative expression. RT-qPCR values were normalized with the level of expression of the actin gene. Bars represent the mean \pm SEM of a representative experiment. Different letters indicate statistically significant differences for each genotype and treatment ($p < 0.05$, two-way ANOVA with Tukey HSD).

3.6. Transcriptomic changes in HB treatments under water stress revealed a repression of ABA biosynthesis

To provide insight into the molecular responses of the plants exposed to HB subjected or not to water deprivation, a further RNA-seq analysis was performed. A gene clustering analysis with DEGS from both RNA-seq, was performed for discovering groups of correlated genes between different treatments (non-treated and HB-treated) and conditions (well-watered and non-watered plants). Following this approach, 16 clusters

were generated (Figure S5). According to cluster trends we grouped them in 3 groups of interest: first DEGS that share the same response to HB in well-watered and non-watered conditions (clusters 7, 10, 12 and 16), second DEGS that only respond to HB in non-stress conditions (clusters 5 and 6) and third DEGS that only respond to HB in water deficit conditions (clusters 2 and 3). To elucidate the function of these three groups of genes, a GO enrichment analysis for biological processes was executed. Interestingly, no GO term was enriched in the first group that share the same response in both watering conditions. Regarding DEGs that only respond after HB treatments in well-watered conditions (clusters 5 and 6), we found GO terms related to apocarotenoid and abscisic acid metabolism, which correlated well with the previously observed results indicating that the HB mode of action was independent of ABA (Figure 7A).

To further study the relationship between HB and ABA, DEGS that only respond to HB in well-watered conditions from the enriched category related to abscisic acid metabolic processes (GO:0009687), previously cited were identified. This set has 3 genes that were involved in different critical steps of ABA biosynthesis, like 9-cis-epoxycarotenoid dioxygenase (*NCED*; *Solyc07g056570*), zeaxanthin epoxidase (*Solyc02g090890*), and ABA 8'-hydroxylase (*Solyc04g078900*). The pattern of expression of these genes was analyzed by RT-qPCR, observing a tendency of down-regulation upon HB treatments in watered plants, that confirms their behavior in the RNA-seq (Figures 7B, 7C and 7D). Since our results revealed a down-regulation of genes involved in ABA biosynthesis, we explored the levels of ABA accumulation in HB-treated or non-treated, and well-watered or non-watered plants. In our experiments, we did not observe significant differences in ABA content between non- and HB-treated plants under well-watered conditions. Surprisingly, we observed that water-stressed plants treated with HB significantly accumulated less ABA than the stressed untreated plants, being levels similar to those observed in non-stressed plants (Figure 7E). Also, we analyzed the expression of marker genes of ABA signalling [48], such as Responsive to ABA 18 (*RAB18*), the transcription factor *MYB44*, and a *late embryogenesis abundant* (*LEA*) protein in tomato plants at 6 DAD. Drought treatment induced the expression levels of *RAB18* and *LEA* in non- and HB-treated plants. Interestingly, *LEA* gene induction in HB-treated plants was higher than in non-treated plants for both watered and drought stress conditions (Figure S6). The higher induction of *LEA* in water-stressed plants treated with HB (Figure S6) which accumulate lower levels of ABA (Figure 7E) appears to reinforce that HB induces the abiotic response in an ABA-independent manner.

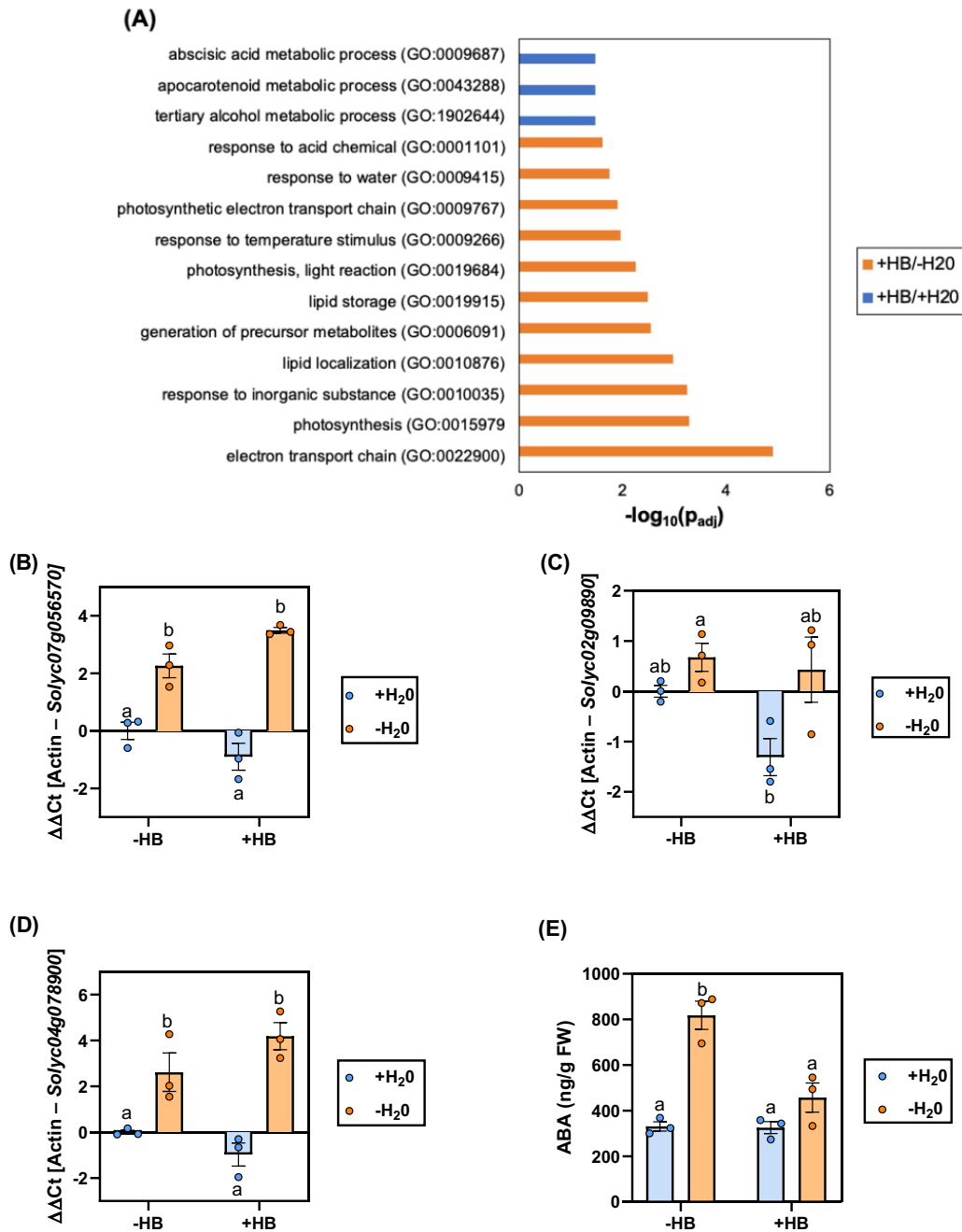


Figure 7. ABA biosynthetic pathway is repressed by HB treatments. Plants were treated (+HB) or not (-HB) with 2mM HB and were subjected to water deprivation (-H₂O) for 6 days or normally watered (+H₂O). **(A)** Functional analysis profiling of RNA-Seq data comparing different treatments (+/-HB) and conditions (+/-H₂O). Real-time qPCR analysis of *Solyc07g056570* **(B)**, *Solyc02g09890* **(C)** and *Solyc04g078900* **(D)** genes. Expression levels are relative to tomato non-treated and watered plants and normalized to the tomato actin gene. **(E)** ABA accumulation in tomato leaves upon different treatments and conditions. Data correspond to the averages of three independent plants \pm SEM of a representative experiment. Different letters indicate statistically significant differences for each genotype and treatment ($p < 0.05$, two-way ANOVA with Tukey HSD).

3.7. HB application improves productivity under limited water conditions

A high yield is a crucial factor for profitable crop production. For this reason, we considered whether drought tolerance conferred by HB treatments in tomato plants could contribute to improve productivity. To this end, we carried out treatments in an experimental field located in Pincanya (Spain) under limited water availability (50%).

On one hand, we examined tomato fruits setting along the experimental trial. As Figure 8A shows, water stressed HB-treated plants developed significantly more flowers than non-treated plants almost during all the experimental trial. Related to this, we detected a set of genes involved in flower development that were altered by HB treatments under drought conditions in the RNA-seq analysis (Figure S7). Besides, the observed higher amount in flowers turned into higher fruit yield at 12 DA-F (Days After treatment F, See Materials and Methods) (Figure 8B).

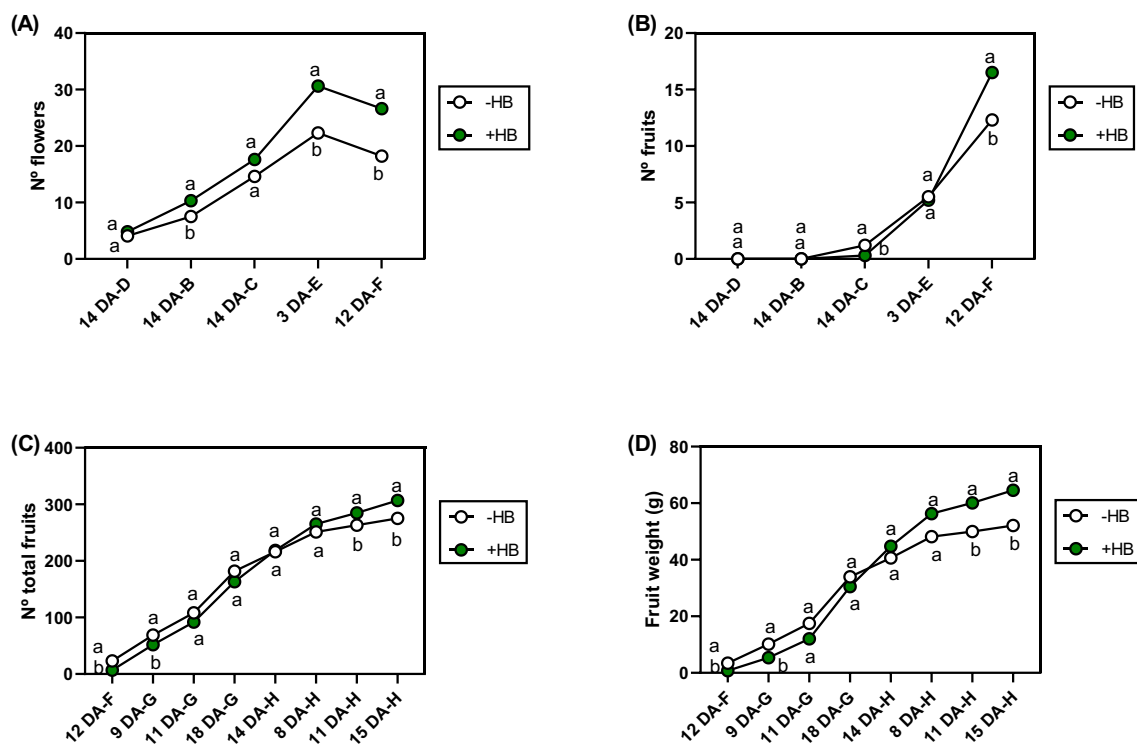


Figure 8. HB treatments in tomato plants improve productivity under drought conditions in open field experiments. Number of flowers (A), number of set fruits (B), total harvested fruits (C) and mean fruit weight (D) of tomato plants under limited water availability conditions (50%) and treated (+HB) or not (-HB) with HB. Points represent mean values. Different letters indicate significant differences at each time point ($p < 0.05$, two-way ANOVA with Tukey HSD).

On the other hand, we assessed the number of fruits and total productivity at different time points. At the beginning of the harvesting period, the number of fruits in HB-treated plants was lower than non-treated plants. However, from the fifth harvest (14 DA-H), the number of fruits in HB-treated plants became similar to the untreated tomato plants. At the end of the harvesting period, HB treatments produced higher yield (23%) than non-treated plants (Figure 8C). Furthermore, the same trend was observed regarding fruit

weight (Figure 8D), thus indicating that periodic HB treatments can improve tomato fruit size and productivity under drought conditions. The harvested fruits were also classified depending on their size into extra, class I, class II or class III. Both fruit weight and fruit number were higher in the extra and class I groups, in tomato plants treated with HB subjected to drought conditions (Figure S8). Our results indicate that HB treatments increase productivity and quality of the fruits in water-stressed tomato plants.

3.8. HB treatments lead to pathogen resistance

Since HB application activates defence-related genes and confers resistance to the bacteria *Pst* DC3000 under greenhouse conditions with controlled inoculations [31], experimental trials were carried out to assess whether HB defensive effects have potential uses in agriculture. The first trial was performed to confirm the agricultural applications of HB in tomato plants against *Pst* DC3000. For this purpose, tomato plants were treated periodically with different HB concentrations (0.05, 5, 50 and 500 mM), using the commercial pesticide OXICOOP 50 as positive control.

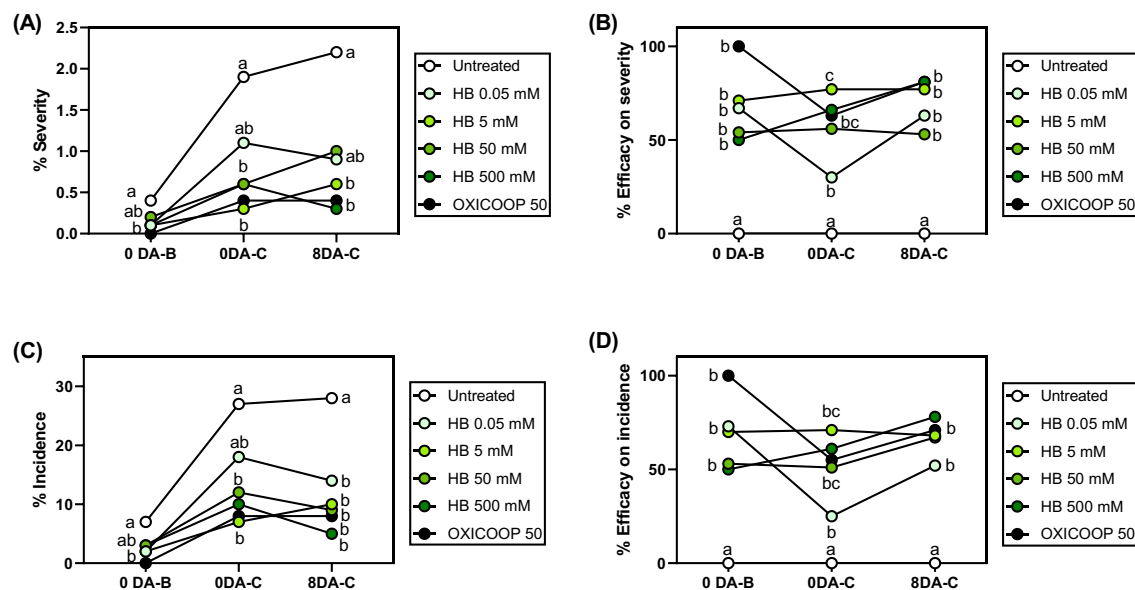


Figure 9. HB application enhances resistance to *Pseudomonas syringae* in tomato plants.

Percentage of severity (A), efficacy on severity (B), incidence (C) and efficacy on incidence (D) of untreated plants, HB weekly-treated plants at different concentrations (0.05, 5, 50, 500 mM) and plants treated with OXICOOP 50. An ANOVA test was performed, and different letters indicate statistical significances with a $p < 0.05$.

The applications started as preventive and were performed as a broadcast foliar application on the tomato plants before appearance of bacterial disease symptoms (see Materials and Methods). On each assessment date, the percentage of leaves presenting symptoms per plot (incidence) and the leaf area infected (severity) were evaluated on 10 plants per plot. At the beginning of the experiment, HB-treated plants did not show

differences with respect to untreated plants in the percentage of severity or incidence of the bacterial infection. Nonetheless, at 0 DA-C and 8 DA-C intermediate and high concentrations of HB acted in a similar way to the commercial pesticide OXICOOP 50, being the efficacy of incidence between 68 and 78% for high dose of HB treatments and between 77-81% at last assessment considering percentage of infected leaf (Figure 9).

Furthermore, we tested the efficacy of HB in a different plant-pathogen interaction in which stomatal immunity is crucial, that is potato defence against *Phytophthora infestans*. For this end, the same approach as tomato against *Pst* field trial was followed but employing OROCOBRE as a commercial positive control treatment. Regarding the percentage of damaged leaf area, all plots showed statistical differences compared to the untreated control check since 6 DA-D. The best results were obtained with the 500 mM HB treatment, reaching efficacies near to 70% at the end of trial, surpassing the performance of the reference OROCOBRE which efficacy was around 52% at the end of trial (Figures 10A and 10B). Regarding symptomatology in potato plants, HB treatments showed statistical significances since the beginning of the trial, obtaining similar efficacy on downy mildew incidence than treatments with the commercial fungicide (Figures 10C and 10D).

Therefore, our results indicated that HB can be efficiently used to prevent diseases in agriculture caused by pathogens whose entrance is through stomata.

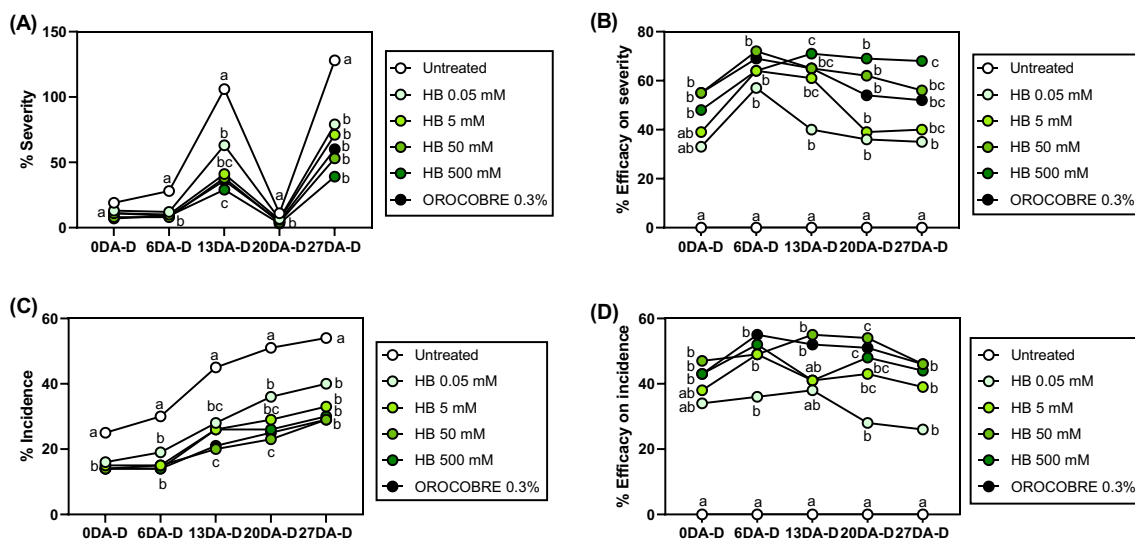


Figure 10. HB treatments confer resistance to the oomycete *Phytophthora infestans* in potato plants under open field conditions. Percentage of (A) severity, (B) efficacy on severity, (C) incidence and (D) efficacy on incidence of untreated plants, HB weekly-treated plants at different concentrations (0.05, 5, 50, 500 mM) and plants treated with OXICOOP 50. An ANOVA test was performed, and different letters indicate statistical significances with a $p < 0.05$.

4. Discussion

Climate change is one of the greatest challenges of our time. The impacts of climate change are affecting crop production and increasing pressure on natural ecosystems and resources [49]. Abiotic stresses, including drought, heat, or salinity, together with biotic stresses, represent the major threats for crop yield so new different strategies are emerging to increase crop adaptation for future climatic conditions. One of the most powerful and promising alternatives for crop protection is related with the exploitation of plant defence responses [50]. Plants have developed a two-tier accurate and sophisticated innate immune system, consisting of PTI mediated by PRRs, and NLRs-mediated ETI for detecting pathogenic effectors [1]. Although the two defensive barriers involve different activation mechanisms, PTI and ETI converge into many similar downstream responses although the kinetics and amplitude of the responses are different [7,51]. The shared defence signalling network is mainly composed by the activation of MAPKs, ROS production, Ca²⁺ influx, activation/inhibition of ion channels and transcriptomic reprogramming which causes the accumulation of secondary metabolites to manage stress. Plant innate immune machinery also involves the rapid closure of stomata, a response known as stomatal immunity, in order to restrict pathogen invasion [8].

In previous studies, we identified different GLVs that were emitted when tomato plants efficiently resisted bacterial infection with *Pst* DC3000. particularly, the volatile HB stood out due to its properties as a stomatal closure compound and defence-related gene inducer, but the detailed mechanisms of HB in plant immunity still remain undeciphered [31]. In this work, a transcriptomic analysis revealed that HB treatments triggered the activation of different processes that were related to plant defence mechanisms such as chitin catabolism, glucosamine and aminoglycan metabolism or endopeptidase activity, re-confirming the HB-mediated defensive genes induction (Figure 1A, and Figure S1).

The role of stomata as active defensive barriers in plant immunity has been extensively studied. Specifically, in the infections caused by *Pst* DC3000, bacterial flagellin epitope flg22 triggers stomata closure through the recognition by the receptor complex FLS2-BAK1, the subsequent NADPH oxidase-dependent ROS production and the activation of MAPK signalling cascades, mainly via MPK3 and MPK6 [11,52,53]. Furthermore, ABA biosynthesis and signalling are essential to stomatal immunity [8,19,54]. However, it has been demonstrated that PAMPs- and ABA-mediated stomatal immunity pathways are independent. Contrary to PAMP-mediated stomatal closure, ABA signalling pathway leads to ROS production via the Open Stomata 1 (OST1) kinase, that leads to MPK9 and MPK12 activation, triggering ABA-mediated stomata closure [15,19–21]. Besides, both phytohormones ABA and jasmonate, the signalling pathways of which are often exploited by pathogens, transcriptionally activate a common family of protein phosphatases that suppress immune-associated MPK3 and MPK6 kinases [22]. Our results showed that HB treatments induce stomatal closure as effectively as ABA and

flg22 (Figure S2). Nonetheless, HB treatments in ABA-deficient mutants triggered stomatal closure (Figure 2A), demonstrating that HB-mediated stomatal closure is ABA-independent. Moreover, chemical approaches also indicated that, similarly to flg22, HB treatments induced stomatal closure and plant defence signalling through NADPH-oxidase ROS production and Ca^{2+} ion permeable channels (Figures 2, B, C and D). Furthermore, we have also observed that MPK3 and MPK6 activation is essential for HB-triggered stomatal immunity (Figure 3). Our results correlate with other studies that have shown that GLV exposure induced the activation of these downstream responses. For instance, exposure of *Arabidopsis* plants to (*E*)-2-hexenal and (*E*)-2-hexenol involved membrane potential depolarization through an increase in cytosolic Ca^{2+} via ROS-activated calcium channels [55]. Besides, maize and *Arabidopsis* plants exposed to (*Z*)-3-hexenol and (*E*)-2-hexenal, respectively, increased the transcript abundance of different genes involved in defence signalling [56,57]. The facts that GLVs are formed from plant endogenous components, they are emitted upon pathogen infection, and exogenous application activate defence signalling mechanisms suggest that GLVs, and particularly HB, can act as DAMPs [58]. DAMPs are danger signals released by plants upon pathogen attack that have a relevant role amplifying the immune responses.

Drought is considered as one of the most significant factors limiting crop productivity, and new strategies are needed to cope with this global threat [59]. In response to drought stress conditions, the first option for plants is to partially close stomata to prevent water loss via transpiration [60–62]. In this study, we have shown that stomatal aperture ratio of HB-treated tomato plants was similar to the stomatal aperture ratio of plants that were subjected to water stress (Figure 5A), a phenomenon that led to minimize weight loss and ion leakage after 6 days of water deprivation (Figures 5 B and C), indicating that HB-mediated stomatal closure was also effective in drought. Besides, the HB-treatments under both irrigation and drought conditions did not penalize the plant in terms of chlorophyll content (Figure S3). It was also noteworthy that HB application under drought conditions highly induced the expression of a *LEA* family genes (Figure S6C), which are thought to participate in membrane protein stability, osmotic adjustment and macromolecular stabilization [46,63,64] denoting that HB-mediated drought tolerance in tomato plants could be not only due to stomatal closure, but also due to the role of HB as an osmoprotectant compound. In fact, some mechanisms that balance out the water deprivation, such as proline biosynthesis and accumulation, are less activated in HB-treated plants (Figure 6).

ABA is a pivotal hormone governing plant response to drought. Under limited water availability conditions, plants show the induction of ABA biosynthetic enzymes, such as 9-cis-epoxycarotenoid dioxygenase (NCED1), that result in high levels of ABA accumulation [65]. In the same manner than in biotic stress experiments, interconnection between HB and ABA was studied in *flc* mutants, thus exogenous HB application in *flc* mutants subjected to water deficit confirmed that HB-mediated stomatal closure under drought conditions was independent of ABA biosynthesis (Figure S4). Moreover, the

transcriptomic analysis of non- and HB-treated tomato plants under normal or water stress conditions revealed that HB application down-regulated the expression of different ABA *de novo* biosynthetic genes, as zeaxanthin epoxidase (*Solyc02g090890*) and 9-cis-epoxycarotenoid dioxygenase (*Solyc07g056570*) and catabolism genes like ABA 8'-hydroxylase (*Solyc04g078900*) (Figure 7) that are dominant contributors to ABA homeostasis in Arabidopsis and tomato plants [66–69]. This gene repression correlated with the low accumulation of ABA in HB-treated plants compared to non-treated under drought conditions (Figure 7E). These results, together with the high induction of *LEA* family genes, lower levels of proline accumulation and *P5C1* gene expression in water stressed HB-treated plants (Figure 6), appear to indicate that drought stress mechanisms were not activated in HB-treated plants, suggesting that HB signalling is interfering in ABA homeostasis. All these data suggests that HB alleviates drought stress in tomato plants mainly due to HB-induced stomatal closure.

The application of osmoprotectants and biostimulants to confer plant tolerance to different biotic and abiotic stresses through priming is a promising alternative to conventional techniques. The priming mechanism enables plants to respond more robustly and rapidly, which results in an enhanced resistance or tolerance to a stress condition [50,70,71]. Most-known priming compounds are synthetic SA analogs, such as (1,2,3)thiadiazole-7-carbothioic acid *S*-methyl ester (BTH) or 2,6-dichloroisonicotinic acid and its methyl ester (both referred to as INA) which trigger the activation of systemic acquired resistance (SAR), and the non-protein amino acid β -aminobutyric acid (BABA) that protects plants against various biotic and abiotic stresses in a plethora of plant species [72–76]. Many VOCs have also been described as priming compounds. Hexanoic acid can activate broad-spectrum defences by inducing callose deposition and activating SA and JA signalling pathways. Besides, its efficiency has been demonstrated in a wide range of host plants and pathogens [77,78]. Another example of VOCs as priming agents against abiotic factors is the GLV (*Z*)-3-hexenyl acetate, since maize seeds primed with this volatile exhibited cold tolerance [28]. In greenhouse conditions, our laboratory demonstrated the induction of resistance against bacterial infection of a similar compound, (*Z*)-3-hexenyl butyrate (HB), through stomata closure [31]. In this study, the enhanced resistance to pathogens and tolerance to drought conditions caused by the HB has also been demonstrated in field conditions. Regular exogenous HB treatments in tomato plants under limited water availability conditions resulted in greater number and size of tomato fruits compared to non-treated plants (Figures 8 B, C and D; Figure S6). HB efficacy in field was also demonstrated in the previously analyzed tomato-bacteria interaction and also against potato late blight caused by *Phytophthora infestans*, obtaining in both cases highest efficacies than commercial agrochemicals (Figures 9 and 10) with the added advantage of being non-toxic unlike most conventional pesticides. According to these results, HB is proposed as a promising natural priming compound against biotic and abiotic stress.

In summary, the results obtained in this work provide evidence for the role of HB in stomatal immunity in tomato and Arabidopsis plants, being ROS generation by NADPH oxidases, Ca²⁺ fluxes, MPK3/6 activation, but not ABA, essential for HB-mediated stomatal immunity. Moreover, HB-induced stomatal closure resulted in enhanced resistance and tolerance to pathogen infection and drought in field conditions, proposing HB as a novel natural priming agent candidate and a promising strategy for sustainable agriculture.

5. References

1. Jones, J.D.G.; Dangl, J.L. The Plant Immune System. *Nature* **2006**, *444*, 323–329, doi:10.1038/nature05286.
2. Boutrot, F.; Zipfel, C. Function, Discovery, and Exploitation of Plant Pattern Recognition Receptors for Broad-Spectrum Disease Resistance. *Annu. Rev. Phytopathol.* **2017**, *55*, 257–286, doi:10.1146/annurev-phyto-080614-120106.
3. Zhang, J.; Zhou, J.M. Plant Immunity Triggered by Microbial Molecular Signatures. *Mol. Plant* **2010**, *3*, 783–793, doi:10.1093/mp/ssq035.
4. Bjornson, M.; Pimprikar, P.; Nürnberger, T.; Zipfel, C. The Transcriptional Landscape of Arabidopsis Thaliana Pattern-Triggered Immunity. *Nat. plants* **2021**, *7*, 579–586, doi:10.1038/s41477-021-00874-5.
5. Cui, H.; Tsuda, K.; Parker, J.E. Effector-Triggered Immunity: From Pathogen Perception to Robust Defence. *Annu. Rev. Plant Biol.* **2015**, *66*, 487–511, doi:10.1146/annurev-arplant-050213-040012.
6. Wang, W.; Feng, B.; Zhou, J.M.; Tang, D. Plant Immune Signalling: Advancing on Two Frontiers. *J. Integr. Plant Biol.* **2020**, *62*, 2–24, doi:10.1111/jipb.12898.
7. Yuan, M.; Ngou, B.P.M.; Ding, P.; Xin, X.F. PTI-ETI Crosstalk: An Integrative View of Plant Immunity. *Curr. Opin. Plant Biol.* **2021**, *62*, 102030, doi:10.1016/j.pbi.2021.102030.
8. Melotto, M.; Underwood, W.; Koczan, J.; Nomura, K.; He, S.Y. Plant Stomata Function in Innate Immunity against Bacterial Invasion. *Cell* **2006**, *126*, 969–980, doi:10.1016/j.cell.2006.06.054.
9. Gómez-Gómez, L.; Boller, T. FLS2: An LRR Receptor-like Kinase Involved in the Perception of the Bacterial Elicitor Flagellin in Arabidopsis. *Mol. Cell* **2000**, *5*, 1003–1011, doi:10.1016/s1097-2765(00)80265-8.
10. Chinchilla, D.; Bauer, Z.; Regenass, M.; Boller, T.; Felix, G. The Arabidopsis Receptor Kinase FLS2 Binds Flg22 and Determines the Specificity of Flagellin Perception. *Plant Cell* **2006**, *18*, 465–476, doi:10.1105/tpc.105.036574.
11. Chinchilla, D.; Zipfel, C.; Robatzek, S.; Kemmerling, B.; Nürnberger, T.; Jones, J.D.G.; Felix, G.; Boller, T. A Flagellin-Induced Complex of the Receptor FLS2 and BAK1 Initiates Plant Defence. *Nature* **2007**, *448*, 497–500, doi:10.1038/nature05999.
12. Kadota, Y.; Sklenar, J.; Derbyshire, P.; Stransfeld, L.; Asai, S.; Ntoukakis, V.; Jones, J.D.; Shirasu, K.; Menke, F.; Jones, A.; et al. Direct Regulation of the NADPH Oxidase RBOHD by the PRR-Associated Kinase BIK1 during Plant Immunity. *Mol. Cell* **2014**, *54*, 43–55, doi:10.1016/j.molcel.2014.02.021.
13. Arnaud, D.; Hwang, I. A Sophisticated Network of Signalling Pathways Regulates Stomatal Defences to Bacterial Pathogens. *Mol. Plant* **2015**, *8*, 566–581, doi:10.1016/j.molp.2014.10.012.

14. Bharath, P.; Gahir, S.; Raghavendra, A.S. Abscisic Acid-Induced Stomatal Closure: An Important Component of Plant Defence Against Abiotic and Biotic Stress. *Front. Plant Sci.* **2021**, *12*, 1–18, doi:10.3389/fpls.2021.615114.
15. Montillet, J.L.; Leonhardt, N.; Mondy, S.; Tranchimand, S.; Rumeau, D.; Boudsocq, M.; Garcia, A.V.; Douki, T.; Bigeard, J.; Laurière, C.; et al. An Abscisic Acid-Independent Oxylin Pathway Controls Stomatal Closure and Immune Defence in *Arabidopsis*. *PLoS Biol.* **2013**, *11*, 13–15, doi:10.1371/journal.pbio.1001513.
16. Mustilli, A.C.; Merlot, S.; Vavasseur, A.; Fenzi, F.; Giraudat, J. *Arabidopsis* OST1 Protein Kinase Mediates the Regulation of Stomatal Aperture by Abscisic Acid and Acts Upstream of Reactive Oxygen Species Production. *Plant Cell* **2002**, *14*, 3089–3099, doi:10.1105/tpc.007906.
17. Vahisalu, T.; Kollist, H.; Wang, Y.-F.; Nishimura, N.; Chan, W.-Y.; Valerio, G.; Lamminmäki, A.; Brosché, M.; Moldau, H.; Desikan, R.; et al. SLAC1 Is Required for Plant Guard Cell S-Type Anion Channel. *Nature* **2008**, *452*, 487–491, doi:10.1038/nature06608.SLAC1.
18. Chong, L.; Xu, R.; Ku, L.; Zhu, Y. Beyond Stress Response: OST1 Opening Doors for Plants to Grow. *Stress Biol.* **2022**, *2*, 44, doi:10.1007/s44154-022-00069-8.
19. Su, J.; Zhang, M.; Zhang, L.; Sun, T.; Liu, Y.; Lukowitz, W.; Xu, J.; Zhang, S. Regulation of Stomatal Immunity by Interdependent Functions of a Pathogen-Responsive MPK3/MPK6 Cascade and Abscisic Acid. *Plant Cell* **2017**, *29*, 526–542, doi:10.1105/tpc.16.00577.
20. Jammes, F.; Yang, X.; Xiao, S.; Kwak, J.M. Two *Arabidopsis* Guard Cell-Preferential MAPK Genes, MPK9 and MPK12, Function in Biotic Stress Response. *Plant Signal. Behav.* **2011**, *6*, 1875–1877, doi:10.4161/psb.6.11.17933.
21. Jammes, F.; Song, C.; Shin, D.; Munemasa, S.; Takeda, K.; Gu, D.; Cho, D.; Lee, S.; Giordo, R.; Sritubtim, S.; et al. MAP Kinases MPK9 and MPK12 Are Preferentially Expressed in Guard Cells and Positively Regulate ROS-Mediated ABA Signalling. *Proc. Natl. Acad. Sci. U. S. A.* **2009**, *106*, 20520–20525, doi:10.1073/pnas.0907205106.
22. Mine, A.; Berens, M.L.; Nobori, T.; Anver, S.; Fukumoto, K.; Winkelmüller, T.M.; Takeda, A.; Becker, D.; Tsuda, K. Pathogen Exploitation of an Abscisic Acid- and Jasmonate-Inducible MAPK Phosphatase and Its Interception by *Arabidopsis* Immunity. *Proc. Natl. Acad. Sci. U. S. A.* **2017**, *114*, 7456–7461, doi:10.1073/pnas.1702613114.
23. Heil, M.; Bueno, J.C.S. Within-Plant Signalling by Volatiles Leads to Induction and Priming of an Indirect Plant Defence in Nature. *Proc. Natl. Acad. Sci. U. S. A.* **2007**, *104*, 5467–5472, doi:10.1073/pnas.0610266104.
24. Baldwin, I.T.; Halitschke, R.; Paschold, A.; Von Dahl, C.C.; Preston, C.A. Volatile Signalling in Plant-Plant Interactions: “Talking Trees” in the Genomics Era. *Science (80-)*. **2006**, *311*, 812–815, doi:10.1126/science.1118446.
25. Dudareva, N.; Klempien, A.; Muhlemann, J.K.; Kaplan, I. Biosynthesis, Function and Metabolic Engineering of Plant Volatile Organic Compounds. *New Phytol.* **2013**, *198*, 16–32, doi:10.1111/nph.12145.
26. Ameye, M.; Audenaert, K.; De Zutter, N.; Steppe, K.; Van Meulebroek, L.; Vanhaecke, L.; De Vleeschauwer, D.; Haesaert, G.; Smaghe, G. Priming of Wheat with the Green Leaf Volatile Z-3-Hexenyl Acetate Enhances Defence against *Fusarium Graminearum* but Boosts Deoxynivalenol Production. *Plant Physiol.* **2015**, *167*, 1671–1684, doi:10.1104/pp.15.00107.
27. Brill, F.; Loreto, F.; Baccelli, I. Exploiting Plant Volatile Organic Compounds (VOCS) in Agriculture to Improve Sustainable Defence Strategies and Productivity of Crops. *Front. Plant Sci.* **2019**, *10*, 1–8, doi:10.3389/fpls.2019.00264.

28. Cofer, T.M.; Engelberth, M.; Engelberth, J. Green Leaf Volatiles Protect Maize (*Zea Mays*) Seedlings against Damage from Cold Stress. *Plant Cell Environ.* **2018**, *41*, 1673–1682, doi:10.1111/pce.13204.
29. Luna, E. Using Green Vaccination to Brighten the Agronomic Future. *Outlooks Pest Manag.* **2016**, *27*, 136–140.
30. López-Gresa, M.P.; Lisón, P.; Campos, L.; Rodrigo, I.; Rambla, J.L.; Granell, A.; Conejero, V.; Bellés, J.M. A Non-Targeted Metabolomics Approach Unravels the VOCs Associated with the Tomato Immune Response against *Pseudomonas Syringae*. *Front. Plant Sci.* **2017**, *8*, 1–15, doi:10.3389/fpls.2017.01188.
31. López-Gresa, M.P.; Payá, C.; Ozáez, M.; Rodrigo, I.; Conejero, V.; Klee, H.; Bellés, J.M.; Lisón, P. A New Role for Green Leaf Volatile Esters in Tomato Stomatal Defence against *Pseudomonas Syringae* Pv. Tomato. *Front. Plant Sci.* **2018**, *871*, 1–12, doi:10.3389/fpls.2018.01855.
32. Payá, C.; Pilar López-Gresa, M.; Intrigliolo, D.S.; Rodrigo, I.; Bellés, J.M.; Lisón, P. (Z)-3-Hexenyl Butyrate Induces Stomata Closure and Ripening in *Vitis Vinifera*. *Agronomy* **2020**, *10*, doi:10.3390/agronomy10081122.
33. Campos, L.; Lisón, P.; López-Gresa, M.P.; Rodrigo, I.; Zacarés, L.; Conejero, V.; Bellés, J.M. Transgenic Tomato Plants Overexpressing Tyramine N-Hydroxycinnamoyltransferase Exhibit Elevated Hydroxycinnamic Acid Amide Levels and Enhanced Resistance to *Pseudomonas Syringae*. *Mol. Plant. Microbe. Interact.* **2014**, *27*, 1159–1169, doi:10.1094/MPMI-04-14-0104-R.
34. Kim, D.; Langmead, B.; Salzberg, S.L. HISAT: A Fast Spliced Aligner with Low Memory Requirements. *Nat. Methods* **2015**, *12*, 357–360, doi:10.1038/nmeth.3317.
35. Kovaka, S.; Zimin, A. V.; Perte, G.M.; Razaghi, R.; Salzberg, S.L.; Perte, M. Transcriptome Assembly from Long-Read RNA-Seq Alignments with StringTie2. *Genome Biol.* **2019**, *20*, 1–13, doi:10.1186/s13059-019-1910-1.
36. Perte, M.; Perte, G.M.; Antonescu, C.M.; Chang, T.C.; Mendell, J.T.; Salzberg, S.L. StringTie Enables Improved Reconstruction of a Transcriptome from RNA-Seq Reads. *Nat. Biotechnol.* **2015**, *33*, 290–295, doi:10.1038/nbt.3122.
37. Perte, M.; Kim, D.; Perte, G.M.; Leek, J.T.; Salzberg, S.L. Transcript-Level Expression Analysis of RNA-Seq Experiments with HISAT, StringTie and Ballgown. *Nat. Protoc.* **2016**, *11*, 1650–1667, doi:10.1038/nprot.2016.095.
38. Raudvere, U.; Kolberg, L.; Kuzmin, I.; Arak, T.; Adler, P.; Peterson, H.; Vilo, J. G:Profiler: A Web Server for Functional Enrichment Analysis and Conversions of Gene Lists (2019 Update). *Nucleic Acids Res.* **2019**, *47*, W191–W198, doi:10.1093/nar/gkz369.
39. Mi, H.; Muruganujan, A.; Huang, X.; Ebert, D.; Mills, C.; Guo, X.; Thomas, P.D. Protocol Update for Large-Scale Genome and Gene Function Analysis with the PANTHER Classification System (v.14.0). *Nat. Protoc.* **2019**, *14*, 703–721, doi:10.1038/s41596-019-0128-8.
40. Abbott, W.S. A Method of Computing the Effectiveness of an Insecticide. *J. Econ. Entomol.* **1925**, *18*, 265–267, doi:10.1093/jee/18.2.265a.
41. Tal, M. Abnormal Stomatal Behavior in Wilty Mutants of Tomato. *Plant Physiol.* **1966**, *41*, 1387–1391, doi:10.1104/pp.41.8.1387.
42. Zhou, J.; Wang, J.; Zheng, Z.; Fan, B.; Yu, J.Q.; Chen, Z. Characterization of the Promoter and Extended C-Terminal Domain of Arabidopsis WRKY33 and Functional Analysis of Tomato WRKY33 Homologues in Plant Stress Responses. *J. Exp. Bot.* **2015**, *66*, 4567–4583, doi:10.1093/jxb/erv221.
43. Mao, G.; Meng, X.; Liu, Y.; Zheng, Z.; Chen, Z.; Zhang, S. Phosphorylation of a WRKY Transcription Factor by Two Pathogen-Responsive MAPKs Drives Phytoalexin Biosynthesis in Arabidopsis. *Plant*

- Cell* **2011**, *23*, 1639–1653, doi:10.1105/tpc.111.084996.
44. Wang, Y.; Schuck, S.; Wu, J.; Yang, P.; Döring, A.C.; Zeier, J.; Tsuda, K. A Mpk3/6-Wrky33-Ald1-Pipelicolic Acid Regulatory Loop Contributes to Systemic Acquired Resistance[Open]. *Plant Cell* **2018**, *30*, 2480–2494, doi:10.1105/tpc.18.00547.
 45. Hahn, A.; Harter, K. Mitogen-Activated Protein Kinase Cascades and Ethylene: Signalling, Biosynthesis, or Both? *Plant Physiol.* **2009**, *149*, 1207–1210, doi:10.1104/pp.108.132241.
 46. Ozturk, M.; Turkyilmaz Unal, B.; García-Caparrós, P.; Khursheed, A.; Gul, A.; Hasanuzzaman, M. Osmoregulation and Its Actions during the Drought Stress in Plants. *Physiol. Plant.* **2021**, *172*, 1321–1335, doi:https://doi.org/10.1111/ppl.13297.
 47. Kaur, G.; Asthir, B. Proline: A Key Player in Plant Abiotic Stress Tolerance. *Biol. Plant.* **2015**, *59*, 609–619, doi:10.1007/s10535-015-0549-3.
 48. Gonzalez-Guzman, M.; Rodriguez, L.; Lorenzo-Orts, L.; Pons, C.; Sarrion-Perdigones, A.; Fernandez, M.A.; Peirats-Llobet, M.; Forment, J.; Moreno-Alvero, M.; Cutler, S.R.; et al. Tomato PYR/PYL/RCAR Abscisic Acid Receptors Show High Expression in Root, Differential Sensitivity to the Abscisic Acid Agonist Quinabactin, and the Capability to Enhance Plant Drought Resistance. *J. Exp. Bot.* **2014**, *65*, 4451–4464, doi:10.1093/jxb/eru219.
 49. *FAO Crops and Climate Change Impact Briefs*; 2022; ISBN 9789251355107.
 50. Alagna, F.; Balestrini, R.; Chitarra, W.; Marsico, A.D.; Nerva, L. *Getting Ready with the Priming: Innovative Weapons against Biotic and Abiotic Crop Enemies in a Global Changing Scenario*; Elsevier Inc., 2020; ISBN 9780128178935.
 51. Tsuda, K.; Katagiri, F. Comparing Signalling Mechanisms Engaged in Pattern-Triggered and Effector-Triggered Immunity. *Curr. Opin. Plant Biol.* **2010**, *13*, 459–465, doi:10.1016/j.pbi.2010.04.006.
 52. Li, L.; Li, M.; Yu, L.; Zhou, Z.; Liang, X.; Liu, Z.; Cai, G.; Gao, L.; Zhang, X.; Wang, Y.; et al. The FLS2-Associated Kinase BIK1 Directly Phosphorylates the NADPH Oxidase RbohD to Control Plant Immunity. *Cell Host Microbe* **2014**, *15*, 329–338, doi:10.1016/j.chom.2014.02.009.
 53. Beckers, G.J.M.; Jaskiewicz, M.; Liu, Y.; Underwood, W.R.; He, S.Y.; Zhang, S.; Conrath, U. Mitogen-Activated Protein Kinases 3 and 6 Are Required for Full Priming of Stress Responses in *Arabidopsis thaliana*. *Plant Cell* **2009**, *21*, 944–953, doi:10.1105/tpc.108.062158.
 54. Du, M.; Zhai, Q.; Deng, L.; Li, S.; Li, H.; Yan, L.; Huang, Z.; Wang, B.; Jiang, H.; Huang, T.; et al. Closely Related NAC Transcription Factors of Tomato Differentially Regulate Stomatal Closure and Reopening during Pathogen Attack. *Plant Cell* **2014**, *26*, 3167–3184, doi:10.1105/tpc.114.128272.
 55. Asai, N.; Nishioka, T.; Takabayashi, J.; Furuichi, T. Plant Volatiles Regulate the Activities of Ca²⁺-Permeable Channels and Promote Cytoplasmic Calcium Transients in *Arabidopsis* Leaf Cells. *Plant Signal. Behav.* **2009**, *4*, 294–300, doi:10.4161/psb.4.4.8275.
 56. Mirabella, R.; Rauwerda, H.; Allmann, S.; Scala, A.; Spyropoulou, E.A.; de Vries, M.; Boersma, M.R.; Breit, T.M.; Haring, M.A.; Schuurink, R.C. WRKY40 and WRKY6 Act Downstream of the Green Leaf Volatile E-2-Hexenal in *Arabidopsis*. *Plant J.* **2015**, *83*, 1082–1096, doi:https://doi.org/10.1111/tpj.12953.
 57. Engelberth, J.; Contreras, C.F.; Dalvi, C.; Li, T.; Engelberth, M. Early Transcriptome Analyses of Z-3-Hexenol-Treated Zea Mays Revealed Distinct Transcriptional Networks and Anti-Herbivore Defence Potential of Green Leaf Volatiles. *PLoS One* **2013**, *8*, e77465.
 58. Duran-Flores, D.; Heil, M. Sources of Specificity in Plant Damaged-Self Recognition. *Curr. Opin. Plant Biol.* **2016**, *32*, 77–87, doi:https://doi.org/10.1016/j.pbi.2016.06.019.

59. Konapala, G.; Mishra, A.K.; Wada, Y.; Mann, M.E. Climate Change Will Affect Global Water Availability through Compounding Changes in Seasonal Precipitation and Evaporation. *Nat. Commun.* **2020**, *11*, 3044, doi:10.1038/s41467-020-16757-w.
60. Torres-Ruiz, J.M.; Diaz-Espejo, A.; Morales-Sillero, A.; Martín-Palomo, M.J.; Mayr, S.; Beikircher, B.; Fernández, J.E. Shoot Hydraulic Characteristics, Plant Water Status and Stomatal Response in Olive Trees under Different Soil Water Conditions. *Plant Soil* **2013**, *373*, 77–87.
61. Clauw, P.; Coppens, F.; De Beuf, K.; Dhondt, S.; Van Daele, T.; Maleux, K.; Storme, V.; Clement, L.; Gonzalez, N.; Inzé, D. Leaf Responses to Mild Drought Stress in Natural Variants of Arabidopsis. *Plant Physiol.* **2015**, *167*, 800–816, doi:10.1104/pp.114.254284.
62. Pirasteh-Anosheh, H.; Saed-Moucheshi, A.; Pakniyat, H.; Pessarakli, M. Stomatal Responses to Drought Stress. *Water Stress Crop Plants* 2016, 24–40.
63. Jiang, Y.; Huang, B. Protein Alterations in Tall Fescue in Response to Drought Stress and Abscisic Acid. *Crop Sci.* **2002**, *42*, 202–207, doi:https://doi.org/10.2135/cropsci2002.2020.
64. Ling, H.; Zeng, X.; Guo, S. Functional Insights into the Late Embryogenesis Abundant (LEA) Protein Family from *Dendrobium Officinale* (Orchidaceae) Using an *Escherichia Coli* System. *Sci. Rep.* **2016**, *6*, 39693, doi:10.1038/srep39693.
65. Dar, N.A.; Amin, I.; Wani, W.; Wani, S.A.; Shikari, A.B.; Wani, S.H.; Masoodi, K.Z. Abscisic Acid: A Key Regulator of Abiotic Stress Tolerance in Plants. *Plant Gene* **2017**, *11*, 106–111, doi:https://doi.org/10.1016/j.plgene.2017.07.003.
66. Burbidge, A.; Grieve, T.M.; Jackson, A.; Thompson, A.; McCarty, D.R.; Taylor, I.B. Characterization of the ABA-Deficient Tomato Mutant *Notabilis* and Its Relationship with Maize Vp14. *Plant J.* **1999**, *17*, 427–431, doi:https://doi.org/10.1046/j.1365-313X.1999.00386.x.
67. Iuchi, S.; Kobayashi, M.; Tajiri, T.; Naramoto, M.; Seki, M.; Kato, T.; Tabata, S.; Kakubari, Y.; Yamaguchi-Shinozaki, K.; Shinozaki, K. Regulation of Drought Tolerance by Gene Manipulation of 9-Cis-Epoxycarotenoid Dioxygenase, a Key Enzyme in Abscisic Acid Biosynthesis in Arabidopsis. *Plant J.* **2001**, *27*, 325–333, doi:https://doi.org/10.1046/j.1365-313x.2001.01096.x.
68. Saito, S.; Hirai, N.; Matsumoto, C.; Ohgashi, H.; Ohta, D.; Sakata, K.; Mizutani, M. Arabidopsis CYP707As Encode (+)-Abscisic Acid 8'-Hydroxylase, a Key Enzyme in the Oxidative Catabolism of Abscisic Acid. *Plant Physiol.* **2004**, *134*, 1439–1449, doi:10.1104/pp.103.037614.
69. Kushiro, T.; Okamoto, M.; Nakabayashi, K.; Yamagishi, K.; Kitamura, S.; Asami, T.; Hirai, N.; Koshiba, T.; Kamiya, Y.; Nambara, E. The Arabidopsis Cytochrome P450 CYP707A Encodes ABA 8'-Hydroxylases: Key Enzymes in ABA Catabolism. *EMBO J.* **2004**, *23*, 1647–1656, doi:10.1038/sj.emboj.7600121.
70. Conrath, U.; Beckers, G.J.M.; Flors, V.; García-Agustín, P.; Jakab, G.; Mauch, F.; Newman, M.A.; Pieterse, C.M.J.; Poinssot, B.; Pozo, M.J.; et al. Priming: Getting Ready for Battle. *Mol. Plant-Microbe Interact.* **2006**, *19*, 1062–1071, doi:10.1094/MPMI-19-1062.
71. Beckers, G.J.M.; Conrath, U. Priming for Stress Resistance: From the Lab to the Field. *Curr. Opin. Plant Biol.* **2007**, *10*, 425–431, doi:https://doi.org/10.1016/j.pbi.2007.06.002.
72. Kohler, A.; Schwindling, S.; Conrath, U. Benzothiadiazole-Induced Priming for Potentiated Responses to Pathogen Infection, Wounding, and Infiltration of Water into Leaves Requires the NPR1/NIM1 Gene in Arabidopsis. *Plant Physiol.* **2002**, *128*, 1046–1056, doi:10.1104/pp.010744.
73. Bektas, Y.; Eulgem, T. Synthetic Plant Defence Elicitors. *Front. Plant Sci.* **2015**, *5*, 1–9, doi:10.3389/fpls.2014.00804.
74. Martínez-Aguilar, K.; Ramírez-Carrasco, G.; Hernández-Chávez, J.L.; Barraza, A.; Alvarez-Venegas, R. Use of BABA and INA As Activators of a Primed State in the Common Bean (*Phaseolus*

- Vulgaris L.). *Front. Plant Sci.* **2016**, *7*, 1–17, doi:10.3389/fpls.2016.00653.
75. Jisha, K.C.; Puthur, J.T. Seed Priming with Beta-Amino Butyric Acid Improves Abiotic Stress Tolerance in Rice Seedlings. *Rice Sci.* **2016**, *23*, 242–254, doi:https://doi.org/10.1016/j.rsci.2016.08.002.
76. Thevenet, D.; Pastor, V.; Baccelli, I.; Balmer, A.; Vallat, A.; Neier, R.; Glauser, G.; Mauch-Mani, B. The Priming Molecule β -Aminobutyric Acid Is Naturally Present in Plants and Is Induced by Stress. *New Phytol.* **2017**, *213*, 552–559, doi:https://doi.org/10.1111/nph.14298.
77. Aranega-Bou, P.; de la O Leyva, M.; Finiti, I.; García-Agustín, P.; Gonzalez-Bosch, C. Priming of Plant Resistance by Natural Compounds. Hexanoic Acid as a Model. *Front. Plant Sci.* **2014**, *5*, doi:10.3389/fpls.2014.00488.
78. Llorens, E.; Camañes, G.; Lapeña, L.; García-Agustín, P. Priming by Hexanoic Acid Induce Activation of Mevalonic and Linolenic Pathways and Promotes the Emission of Plant Volatiles. *Front. Plant Sci.* **2016**, *7*, 1–12, doi:10.3389/fpls.2016.00495.

Supplementary Materials

Table S1. Primer sequences used for quantitative RT-PCR analysis of the selected tomato genes.

Gene	Forward primer (5'-3')	Reverse primer (5'-3')
<i>Actin</i>	CTAGGGTGGGTTTCGCAGGAGATGATGC	GTCTTTTTGACCCATACCCACCATCACAC
<i>ERF</i>	GTTTGAGGCCCAAAAGGAA	TCAAGTGGCGTTCTCAACAG
<i>ETR4</i>	CTGCAGATTGGAATGAATGG	ATAAGGCACCGTCAACATCA
<i>MYB44</i>	GGGAGTCGAACAAAAGCAAC	TCCAAGCCCTAAACCACTTG
<i>LEA</i>	TTCCCTGCTGACAAAGCTAGAGCA	AGGGTGCAGATGAAACTGATCCGA
<i>P5CS1</i>	ACCTTAATCTGGAGGCTTGA	AATTATTTACCCACCTGCC
<i>RAB18</i>	CCTGGGATGCATTGAACACC	CACGGGACACCATAACACAC
<i>Solyc12g036793</i>	TCATTGCCCTTGTGTTCTTG	TGTTTGGGTCTGCCACATTA
<i>Solyc06g066590</i>	ATGACGGCGTTCTTACCTTG	GCAGGCATCATCAGCATGTA
<i>Solyc10g006900</i>	ACCACGAAGAGACTGGCATC	ATGGAGGGAAAAGGAGCCTA
<i>Solyc06g069730</i>	CCCTGGAAGTGTGAACCAAG	TGCAAAGTTGAGTGGGTTGA
<i>Solyc12g011280</i>	TAGGCCCATCTCTGGTGAG	GCAAAAGTTTCAGGGTCAGC
<i>Solyc02g090890</i>	GGTGGGTTAGTGTGTTGCTTTG	GGTGGGTTAGTGTGTTGCTTTG
<i>Solyc07g056570</i>	TACGTTCGAAACGGAGCTAAC	CGTAACTAGCCGACCCATTT
<i>Solyc04g078900</i>	CTCAAGACCCTAATGCCTTCTT	CATCACACATGGACAACCTAGA
<i>X68738</i>	ACTCAAGTAGTCTGGCGCAACTC	AGTAAGGACGTTGTCCGATCGAGT
<i>X70787</i>	TTCGAGGTACGCAACAACCTG	ATGCATTGATGACCCATGTTT
<i>WRKY33A</i>	GCATTACTGTCAACCATCGC	AACTTCGCGGATTCTCACTT
<i>WRKY33B</i>	CCACAACAGTCTGAAATGGG	CAGCAAAGCAATGACTCCAT

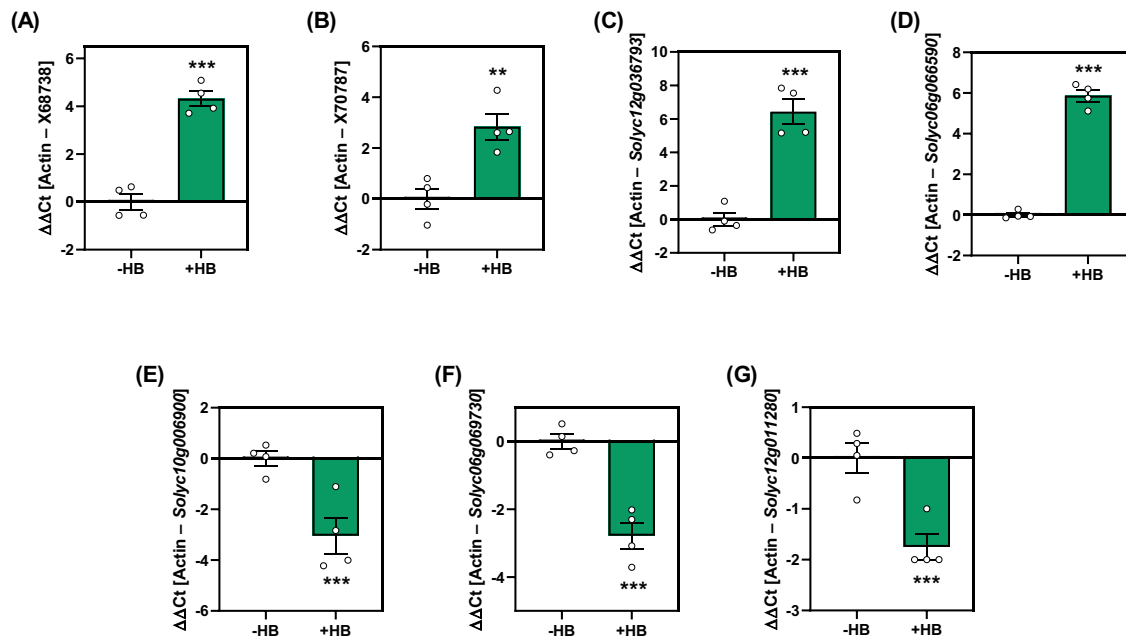


Figure S1. Validation of RNA-seq data by RT-qPCR. 4 weeks-old tomato plants were treated (+HB) or not (-HB) with 5 μM HB into methacrylate chambers. Gene expression analysis of the *PR1* (*X68738*), *PR5* (*X70787*), a pathogen recognition receptor (*Solyc12g036793*), plant cadmium resistance 2 (*Solyc06g066590*) and chlorophyll binding genes (*Solyc06g069730*; *Solyc06g069000*; *Solyc12g011280*) was examined by RT-qPCRs using total RNA from leaves. The RT-qPCR values were normalized with the level of expression of the actin gene. Data represent the mean \pm SEM of a representative experiment ($n=4$). Double (**) and triple (***) asterisks indicate significant differences between treatments with $p < 0.01$ and $p < 0.001$, respectively (Student's *t*-test).

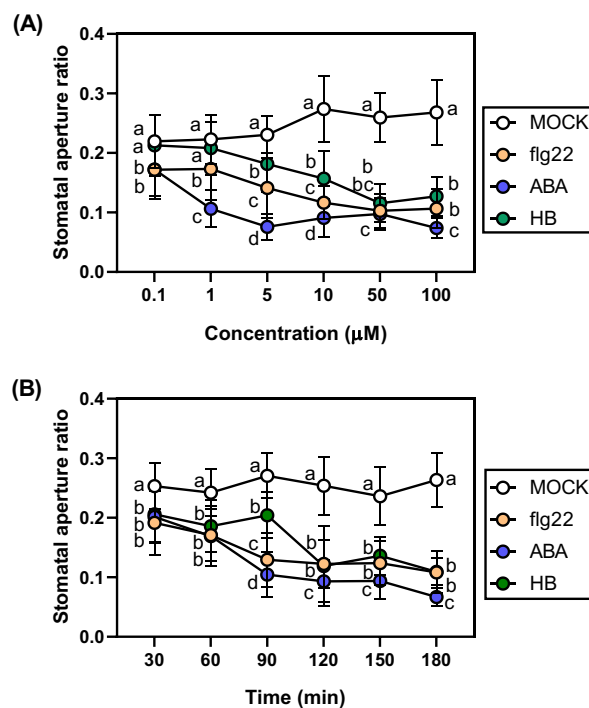


Figure S2. Dose (A) and time (B) effect of HB, flg22 and ABA in tomato leaves stomatal aperture. Data represent the mean \pm SEM of a representative experiment ($n=50$). Different letters indicate statistically significant differences for each treatment at each time point ($p < 0.05$, one-way ANOVA with Tukey HSD Test).

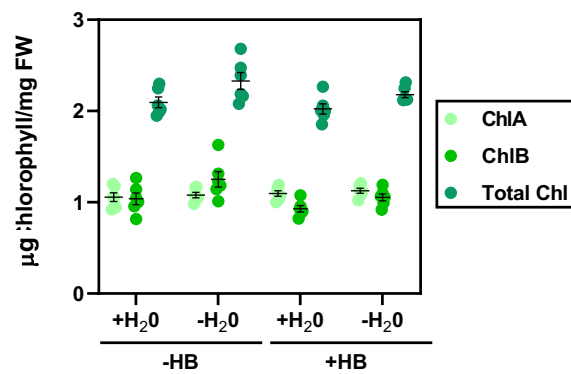


Figure S3. Effect of HB treatments on chlorophyll content in tomato leaves. Chlorophyll a, chlorophyll b and total chlorophyll content in tomato plants treated (+HB) or not (-HB) with HB, in normal (+H₂O) or water stressed conditions (-H₂O). Data correspond to six independent plants \pm SEM of a representative experiment. No statistically significant differences were found.

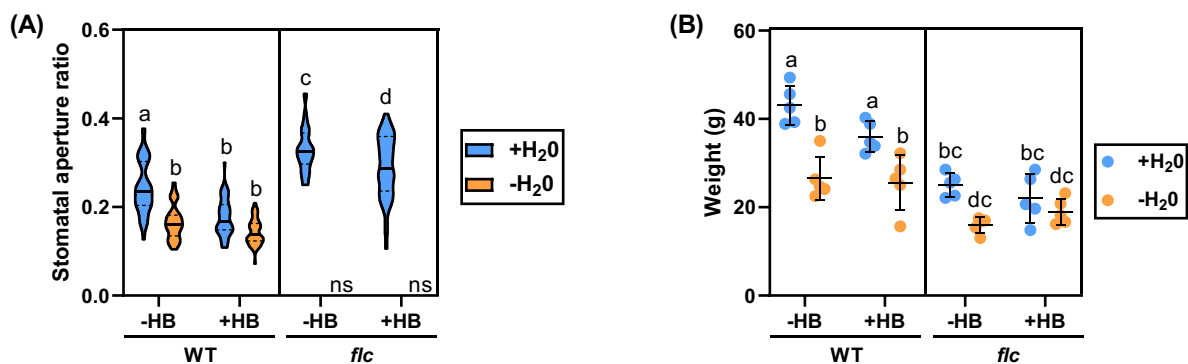


Figure S4. Effect of HB treatments in ABA-deficient mutants. Differences related to stomatal aperture ratio (A) and weight (B) in Lukullus (WT) and flaca (*flc*) tomato plants treated (+HB) or not (-HB) with HB, in normal (+H₂O) or water stressed conditions (-H₂O). Samples were taken after 3 days after exposure to drought conditions. Bars represent the mean \pm SEM of a representative experiment ($n=6$). In stomatal aperture assays, 50 stomata were measured in each treatment and condition (violin plots). Statistically significant differences are represented by different letters ($p < 0.05$, one-way ANOVA with Tukey HSD Test).

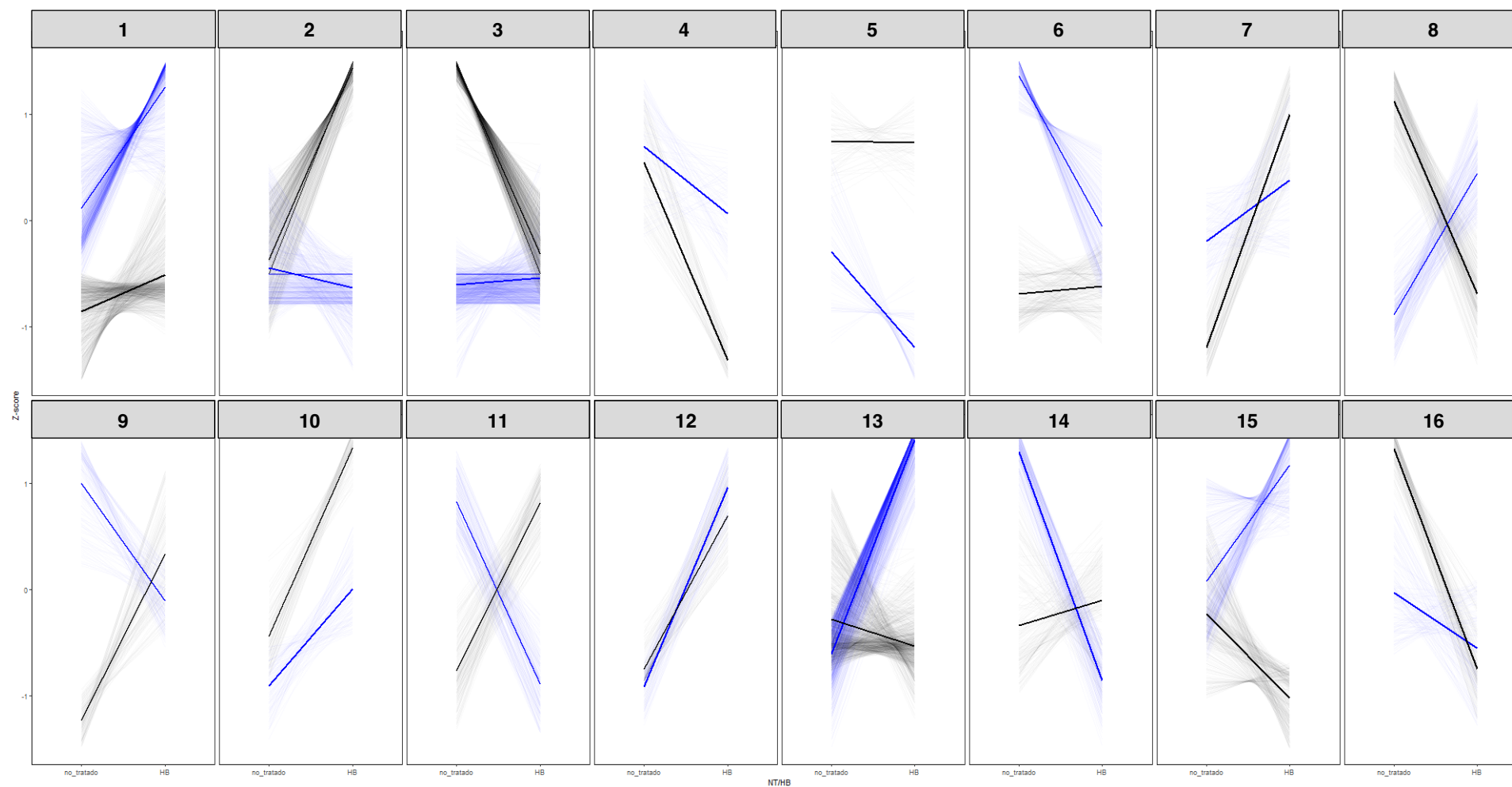


Figure S5. Cluster analysis of RNAseq data of tomato plants under different treatments (+/-HB) and conditions (+/-H₂O). Plants were treated (+HB) or not (-HB) with 2 mM HB and were subjected to water deprivation (-H₂O) for 6 days or normally watered (+H₂O). Blue lines correspond to HB treatments relative expression, and black lines represent expression data from plants subjected to drought.

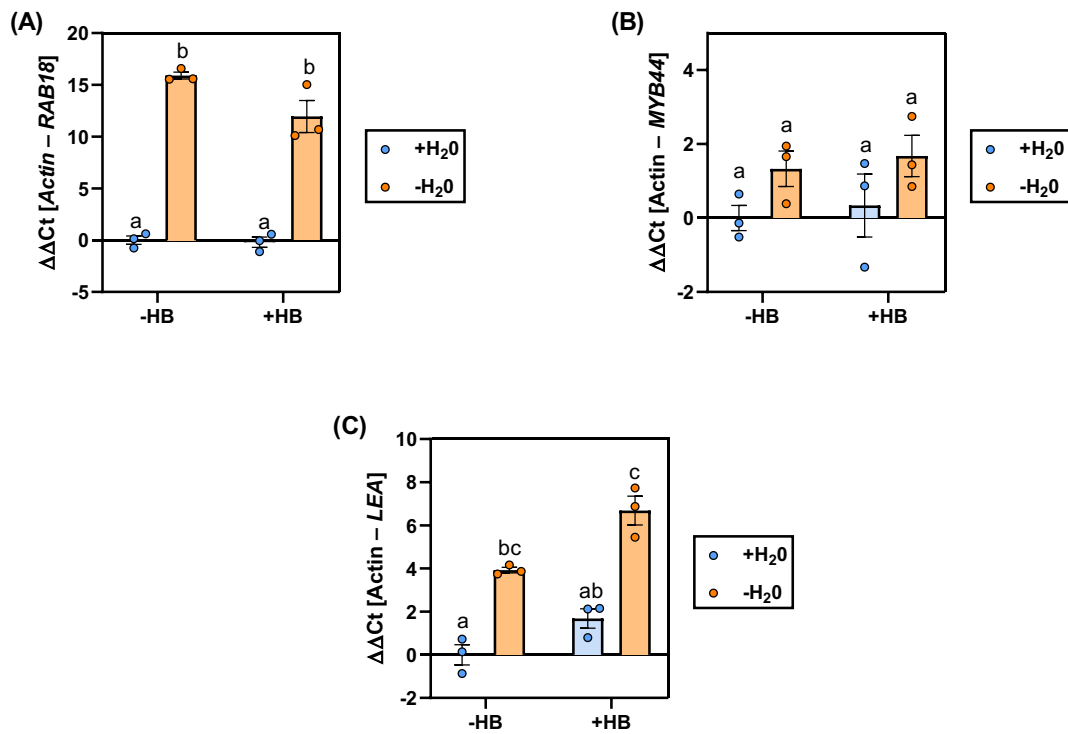


Figure S6. ABA-related genes expression profiles in tomato plants treated with HB. Plants were treated with HB (+HB) or water (-HB) periodically. Water-stressed plants were subjected to water deficit for 6 days. *RAB18* (A), *MYB44* (B) and *LEA* family (C) gene relative expression in plants under normal (+H₂O) or water deficit conditions (-H₂O). Gene expression analysis were examined by RT-qPCRs using total RNA from leaves. The RT-qPCR values were normalized with the level of expression of the actin gene. Bars represent the mean \pm the standard deviation of a representative experiment (n=3). Different letters indicate statistically significant differences for each treatment and condition ($p < 0.05$, one-way ANOVA with Tukey HSD Test).

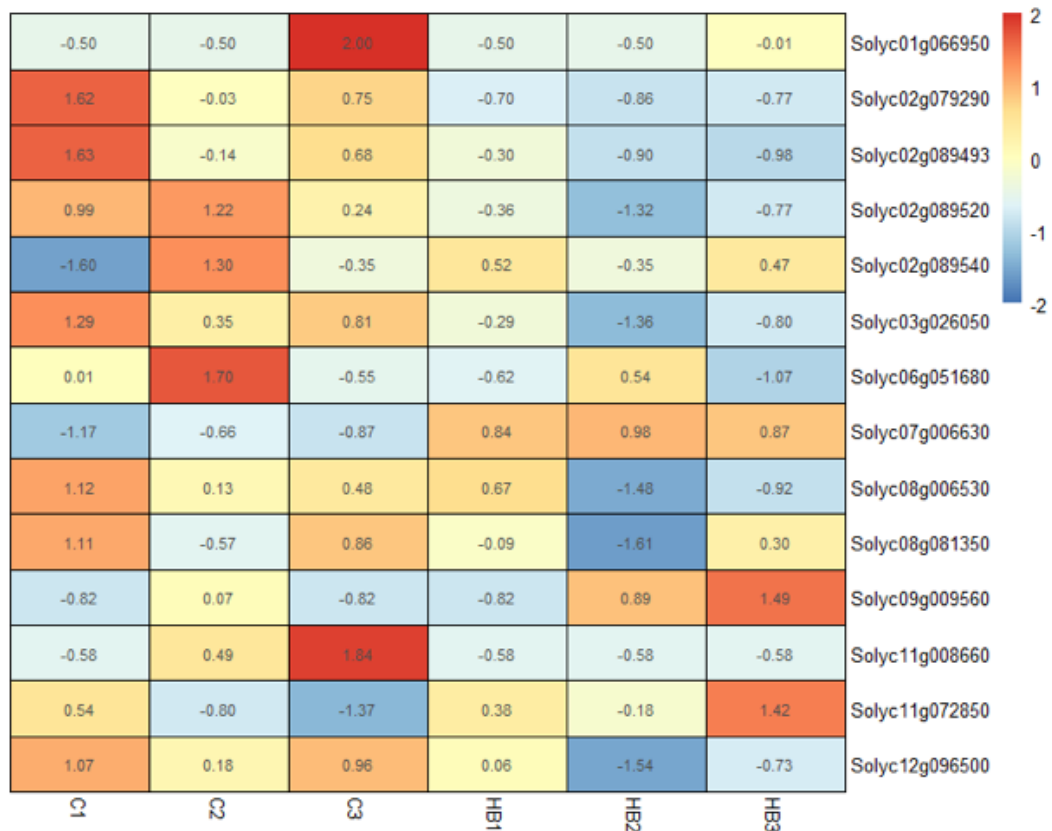


Figure S7. Heat map of flowering related genes from the RNA-seq from non-watered plants experiment. The numbers in each box represent the ratio between the FPKM of each replicated divided the average of the fpkm from the six individual samples.

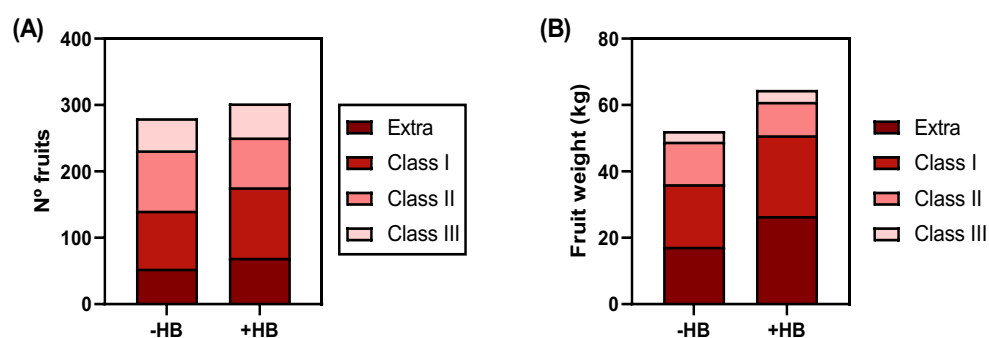


Figure S8. Total and yield per categories in tomato plants upon HB treatments under open field conditions. Tomato plants were subjected to water limitation (50%) and treated (+HB) or not (-HB) with HB. Number of harvested fruits **(A)** and total weight of harvested fruits **(B)** per categories were analyzed as follows: small size (25-50 mm diameter, 25-100 g weight); medium size (50-75 mm diameter, 100-200 g weight); big size (75-100 mm diameter, 200-300 g weight); and extra size (>100 mm diameter, >300 g weight).

Chapter III

HB: agricultural applications (II)

Research article

(Z)-3-Hexenyl Butyrate Induces Stomata Closure and Ripening in *Vitis vinifera*

Celia Payá¹, M^a Pilar López-Gresa¹, Diego S. Intrigliolo², Ismael Rodrigo¹, José M^a Bellés¹ and Purificación Lisón^{1*}

¹Instituto de Biología Molecular y Celular de Plantas (IBMCP), Consejo Superior de Investigaciones Científicas (CSIC), Universitat Politècnica de València (UPV), Ciudad Politécnica de la Innovación (CPI) 8 E, Ingeniero Fausto Elio s/n, 46011 Valencia, Spain

²Consejo Superior de Investigaciones Científicas, Centro de Edafología y Biología Aplicada del Segura, Dept. Riego 30100, Murcia, Spain

*Corresponding autor: plison@ibmcp.upv.es

Ph.D candidate contribution

C. P. had a main role in the following activities: performing the experiments, data collection, data analysis, data visualization, figures editing and manuscript review.

Citation: Payá, C.; Pilar López-Gresa, M.; Intrigliolo, D.S.; Rodrigo, I.; Bellés, J.M.; Lisón, P. (Z)-3-Hexenyl Butyrate Induces Stomata Closure and Ripening in *Vitis Vinifera*. *Agronomy* **2020**, *10*, doi:10.3390/agronomy10081122.

List of Abbreviations

ABA: Abscisic Acid

ACO: *1-Aminocyclopropane-1-carboxylic acid synthase*

ACS: *1-Aminocyclopropane-1-carboxylic acid synthase*

HB: (*Z*)-3-hexenyl butyrate

HPLC: High-Performance Liquid Chromatography

WUE: Water Use Efficiency

Abstract

Agronomy solutions for modifying pre-harvest grape ripening are needed for a more sustainable viticulture. Field experiments were performed in *Vitis vinifera* L. vines to study the effect of the previously described stomata-closing compound (*Z*)-3-hexenyl butyrate (HB). Exogenous treatments at different doses were periodically carried out using a randomized block design. Firstly, we observed that HB was able to induce stomatal closure in grapevine plants. Under field conditions, the application of HB around veraison induced a higher color intensity in berries, and vines treated at higher doses reached this stage earlier than the un-treated controls. There was also a clear increase in both grape anthocyanin concentration and total soluble solids without having a negative impact on total yield. We therefore, confirm the role of HB as a universal natural stomatal closure compound and propose a new use for HB in viticulture as a ripening inducer, by accelerating anthocyanin accumulation.

Keywords: (*Z*)-3-hexenyl butyrate; stomata; ripening; *Vitis vinifera*

1. Introduction

Grapevine (*Vitis vinifera* L.) is one of the major crops worldwide, based on the number of cultivated hectares and its socio-economic value. Grape is a non-climacteric fruit that can be used as a table fruit, a dried raisin, and also for vinification and distillation. The onset of ripening, or veraison, is a key phenological stage in grapevine's lifecycle that involves a series of biochemical, physiological and organoleptic changes. Generally, this stage is characterized by berry sugar accumulation, organic acid level reduction, synthesis of anthocyanins and changes in texture, flavor compounds and aroma volatiles [1–3].

The grape berry is probably one of the fruits whose composition is most sensitive to the natural environment. In recent years, several environmental cues influencing berry ripening have been studied, such as light, water status, temperature and pathogens. High temperatures, shade or pathogenic attack impair ripening-associated mechanisms, while moderate water deficit, UV-B radiation or low temperatures positively promote veraison [4,5]. For this reason, winegrowers search for different viticultural practices to modulate ripening. Particularly in warm climates viticulture is nowadays required to better couple berry sugar accumulation with the phenolic maturity [6]. Consumers are also demanding wines with lower alcohol content. There are numerous researchers investigating how to modulate grape ripening with field practices [7]. These new agricultural practices could embrace a general strategic response or could be focused on specific threats, aiming for the short-term optimization of grapevine development and growth, known as short-term strategies [8,9]. In this sense, a pre- and post-harvest

application of different treatments has been effective in managing grapevine stress responses and modulating ripening. For example, exogenous treatments with different phytohormones such as abscisic acid (ABA), auxins, salicylic acid or gibberellins and specifically ethylene, promote changes in total phenol content and berry sugar, acidity and color [10–14]. Other types of treatments have also been studied, such as melatonin application, that could benefit phenolic content and antioxidant activity in the “Merlot” variety [15], or the application of humic acid or polyamines to increase leaf and berry pigments [16,17]. Regarding post-harvest treatments, ethylene is the most studied compound involved in ripening [18]. For instance, in Aleatico grape berries, post-harvest treatments with ethylene affect phenols, anthocyanins and the aromatic quality of both the grapes and the wine [19,20].

Vitis species are well adapted to drought conditions since they are able to survive even under severe soil water deficit because of their deep root system, capacity to carry out some tissue osmotic adjustment, efficient control of stomatal aperture and regulation of canopy growth [21,22]. Particularly in the Mediterranean Sea basin, grapevines are cultivated under conditions of water scarcity because of climate aridity and restricted water availability for irrigation. Vine stress tolerance depends on the vine cultivar [23]. Although this genotype-related tolerance involves different aspects, they are highly linked to differences in stomatal responses to abiotic stress [24]. Regulation of stomata closure is one of the best characterized plant physiological responses against different stresses. Stomata are in charge of controlling two main plant processes: photosynthesis and transpiration. Plants modulate stomatal closure to regulate CO₂ and water evaporation in response to many environmental and biochemical stimuli such as light, humidity or pathogenic attack. Across the diversity of plant species, stomata closure leads to lower stomatal conductance, reducing CO₂ uptake and subsequently limiting photosynthesis [25,26].

As stomata are major players in plant water use, the regulation of their closure is a potential target to optimize carbon assimilation efficiency and plant productivity. Exogenous treatments using inducers of stomatal closure may constitute an alternative way for the development of new phytosanitary products that improve not only the plant tolerance against both biotic and abiotic stresses but also the plant development. In this context, the volatile compound (*Z*)-3-hexenyl butyrate (HB) was identified in tomato plants as inducer of resistance against bacterial infection [27], and was patented for its ability to produce stomatal closure (P201730685), therefore, emerging as an excellent candidate for the sustainable control of stresses in agriculture. Moreover, the efficacy of HB has also been demonstrated in several plant species belonging to the *Arabidopsis*, *Medicago*, *Zea*, *Citrus* and *Nicotiana* genus, suggesting its role as possible universal natural stomatal closure agent [28].

In this work the role of the HB as an inducer of grape ripening that may act mimicking a moderate water deficit has been studied. For that purpose, open field experiments in

grapevine crops were performed, using different HB concentrations, and evaluating the vine's phenotype and different agronomic traits over time such as yield, fruit weight, color assessment or sugar and acid content.

2. Materials and Methods

2.1. Experimental Site Description, Plant Material and Maintenance

The trial performed to determine the effect of HB on the stomata aperture ratios was carried on potted Bobal grapevines (*Vitis vinifera* L. cv Bobal grafted onto 110R) at the IVIA (Instituto Valenciano de Investigaciones Agrarias, Valencia, Spain, 39°32' N, 0°23' W) experimental farm in July 2019. Both, un-fruited newly grafted vines (young) and 8 years old mature grapevines (old) were tested. Pots used for the young vines were of 9 L (0.23 m height and 0.25 m width). Mature vines were grown in seventy L pots (0.45 m height and 0.55 m width). In both cases, pots were filled with a mix of coco fiber substrate and compost.

An additional field trial was carried out in a commercial vineyard located in Alpera (Albacete, Spain, 38°57' N, 1°13' W). The experiment was conducted during August to September 2019 and the grapevine variety used was Garnacha tintorera (*Vitis vinifera* L. cv Alicante Bouschet grafted onto 161-49R). During the trial, average air temperature was 22 °C with a total precipitation of 80 mm and these conditions were similar to the historical data, except the precipitation in September which resulted to be higher (Table S1). The vineyard soil was sandy loam with flooding irrigation applied every 2 weeks. Neither pesticides nor fertilizers were used during the trial. Test site information and maintenance are shown in Tables S2 and S3.

2.2. Experimental Design and Treatment Application

In the potted cv. Bobal vines, three young and three mature vine plants were sprayed with 5 mM HB or 50 mM HB under open field conditions in order to determine the effect of HB on stomata aperture. In addition, three untreated plants were used as negative controls. Leaves were collected 24 h after treatments and stomata aperture was measured.

The second field trial was performed in a commercial vineyard and the experimental design used was a randomized block (27 m²) designed with 6 plots with 6 plants in each one, with a 1.5 m of distance in the row and 3 m between the row. Six treatments were performed: four plots were treated with HB at 0.5, 5, 10 and 50 mM; one plot was treated with a commercial ripening inducer FRUITEL (48% Ethephon) and served as positive control; and finally, one control, untreated plot was used as a negative control. Four HB and FRUITEL applications were carried out using a motorized knapsack sprayer. The

first application was done just before veraison (application A), and subsequent applications (B, C and D applications) were sprayed with a 7-day interval, since the effect of the compound has been described to persist from 7 to 10 days after the treatment in tomato plants [28]. Time units are referred as follows: X, DA, Y, being X day (0, 7, 14); DA Days After; Y day of treatment (A, B, C and D).

In this field trial, berry samples were randomly collected weekly after the second application (0 days after application B; 0 DA-B) to determine sugar content, pH, must acidity and color. Specifically, the anthocyanin, catechin and epicatechin content as well as the glucose, fructose, malic and tartaric concentrations were evaluated at 7 DA-D. At harvest (20 days after application D, that corresponds to a crop stage scale BBCH 89, the total yield and the number of bunches per plot were also determined.

2.3. Stomatal Aperture Measurement

Grapevine leaf impressions were obtained by coating the abaxial part of five randomly selected leaves from three independent grapevines, with a thin layer of nitrocellulose-based glue (Imedio, Bolton Group, Madrid, Spain) and peeling off the dried layer carefully. Epidermal strips were mounted on glass slides and observed under a Leica DC5000 microscope (Leica Microsystems S.L.U.) [28]. Pictures of different leaf regions were analyzed using the NIH's *ImageJ* software. Stomatal aperture ratio was calculated as stomata width/stomata length in at least 50 stomata for each experimental vine. A value of 1 was considered for a totally opened stomata.

2.4. Color and Total Anthocyanin Content Assessment

To determine color differences, a total of 200 samples per plot at the same height from the ground were analyzed by using a visual scale from 0 to 10, being 0 light green berry, 10 totally purple berry and intermediate degrees within green and purple: yellow, red, light purple. For anthocyanin quantification, 100 g of frozen berry tissue was homogenized (100 mL of water added to facilitate homogenization, filtered and centrifuged in order to obtain aqueous grape extracts. Total anthocyanin quantification was determined using a previously described method [29] using a modified pH differential method. Absorbance of 6 independent grape extracts (100 μ L) was measured with a spectrophotometer at 510 and 700 nm, adding 900 μ L of 0.025 M KCl at pH 1.0 and 0.4 M CH_3COONa at pH 4.5, respectively. Absorbance readings were converted to total milligrams of cyanidin 3-glucoside per 100 g berry fresh weight using its molar extinction coefficient ($\epsilon = 26900 \text{ L mol}^{-1} \text{ cm}^{-1}$).

2.5. Sugar Content Determination

Total soluble solids ($^{\circ}$ Brix) was determined by measuring the refraction index in the grape juice coming from 200 samples. Glucose and fructose content from 6

independent grape extracts was quantified by high-performance liquid chromatography (HPLC), using a Transgenomic IC Sep ION-300 ion exclusion column (300 × 7.8 mm) coupled to a refractive index detector (Waters 2414) converting the refractive index units (RIUs) into an electrical signal (mV) [30]. The must was centrifuged, and the supernatant was isocratically eluted at 60 °C with 5 mM H₂SO₄ at 0.4 mL min⁻¹, over a total run of 30 min. The compounds were quantified with the Waters Breeze software using external standard curves converting mV into g/100 mL grape juice.

2.6. Grape Juice Acidity Analysis

The total acidity content was determined by titrating 5 mL of 200 independent grape extracts containing phenolphthalein, with a sodium hydroxide solution in continuously stirring until a specific pH end point was reached, indicated by pink color change. Malic and tartaric acids determinations from 6 independent grape extracts were quantified by HPLC as previously described (Section 2.5). The pH value was obtained directly from the extracted must using a pH-meter.

2.7. (+)-Catechin and (-)-Epicatechin Analysis

The determination of (+)-catechin and (-)-epicatechin was performed by mass spectrometry using a 1515 Waters HPLC binary pump, a 996 Waters photodiode detector (range of maxplot 240–400 nm, spectral resolution of 1.2 nm) and a ZMD Waters single quadrupole mass spectrometer equipped with an electrospray ionization ion source. Samples (20 µL) from six independent grape extracts were injected at room temperature into a reverse-phase Sun Fire 5-µm C18 (4.6 by 150 mm; Waters) column. A 20-min linear gradient of 1% (vol/vol) acetic acid (J. T. Baker) in Milli Q water to 100% methanol at a flow rate of 1 mL/min was applied. (+)-Catechin and (-)-epicatechin were quantified with Masslynx Waters software using authentic standards.

2.8. Statistical Analysis

To study the effect of the applied treatments for each assessment data, means were compared using Student–Newman–Keuls test ($p = 0.05$). Statistical analyses of two variables were performed by using Student's *t*-test. Statistical procedures were applied using the software ARM Revision 2019.

3. Results

3.1. Evaluation of HB Efficacy in Grapevine Plants under Open-Field Conditions

The capacity of HB as a natural stomatal closure compound was previously tested

in different crops including tomato, tobacco, maize, citrus or alfalfa [28]. However, HB efficacy in the genus *Vitishad* not been tested yet. To study the effect of HB on stomata closure of grapevine plants, exogenous treatments at different concentrations were performed on vines at two different developmental stages: young grapevines and old grapevines.

As shown in Figure 1, in both young and old grapevines, the application of HB at a dose of 50 mM resulted in a statistically significant stomata closure at a. However, 5 mM HB treatments only resulted to induce statistical differences on the young grapevines.

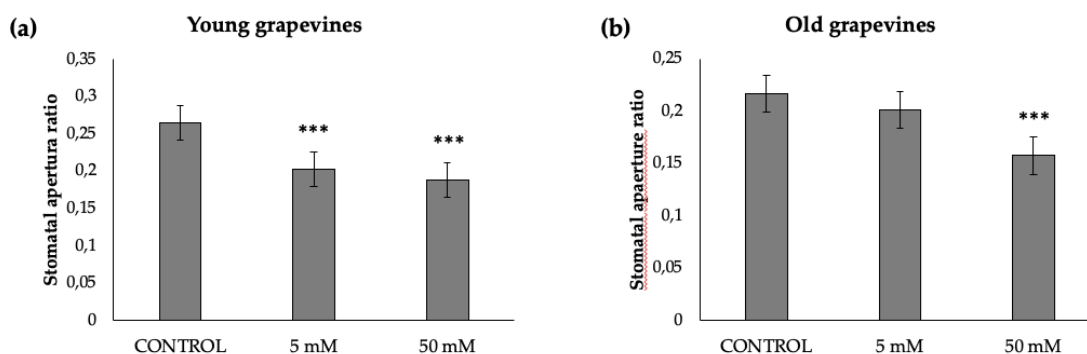


Figure 1. Effect of (*Z*)-3-hexenyl butyrate (HB) on stomatal aperture ratio of *Vitis vinifera* L. cv Bobal leaves. Stomatal aperture mean values \pm SE are shown of one representative experiment. Leaves from young grapevines (a) and old grapevines (b) were collected 24 h after treatments at different HB concentrations. Asterisks (***) indicate statistically significant differences between control and HB-treated grapevine plants at each concentration with $p < 0.001$.

3.2. Study of the effect of HB in ripening and color assessment

During ripening, a change of berry color is produced as a consequence of anthocyanins accumulation [31,32]. To study the phenotypical effect of HB-mediated stomata closure on grapevine plants, the color development of berries was firstly analyzed, by using a color scale adapted from Fernández-López et al. [32] (Figure 2a). Differences in berry color in HB-treated grapevine plants with regard to non-treated plants appeared since 0 DA-C, when almost all HB-treated plot showed a higher color intensity in berries. The positive effect of HB on berry color increased along the experiment, even surpassing the color change induced by FRUITEL which was used as the positive control. This was particularly noticeable at 7 DA-D, when statistically significant differences were observed using 5 mM HB. At this time, the increase in the color scale for HB treatments ranged within 11% to 29%, for 0.5 mM and 5 mM treatments, respectively. These results were in line with the number of days at which each treated plot reached veraison. Most of the treatments with the volatile compound hastened this process (Figure 2b). Interestingly, both 10 mM and 50 mM HB-treatments reached effects comparable to those produced by the commercial compound FRUITEL.

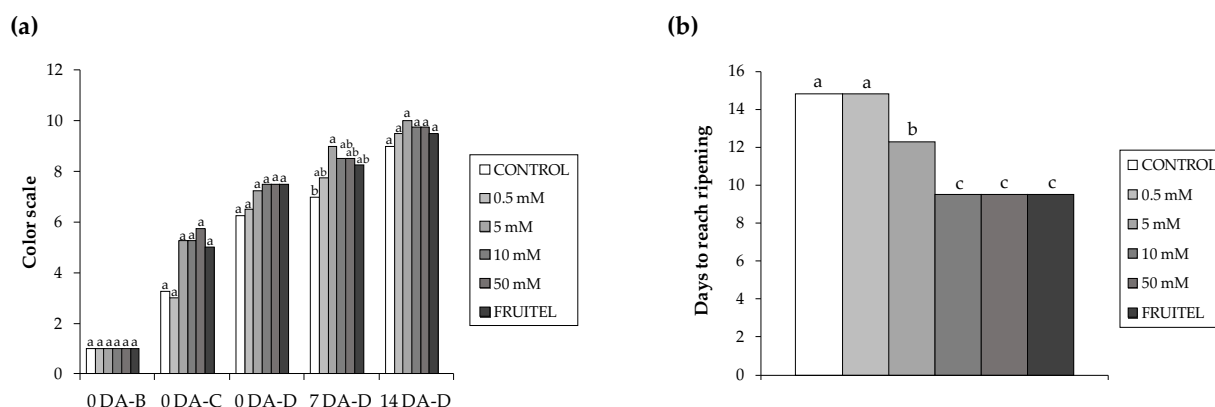


Figure 2. Color change of *Vitis vinifera* L. cv Alicante Bouschet berries of non-treated (CONTROL) plants, HB weekly-treated plants at different concentrations (0.5, 5, 10, 50 mM) and plants treated with the ripening inducer FRUITEL. (a) Evolution of color of non-treated, HB-treated and FRUITEL-treated plants. (b) Number of days until CONTROL, HB and FRUITEL treated plants reached ripening. An ANOVA test was performed, and different letters indicate statistical significances with a p-value < 0.05.

3.3. Study of phenolic compounds accumulation induced by HB treatments

In grapevine, anthocyanins accumulation initiates at veraison, and it is highly correlated with the change of berry color during ripening [31, 32]. Total anthocyanin content was analyzed in samples corresponding to 7 DA-D and 10 and 50 mM, in which we observed the greater effect in berry ripening (Figure 2a,b). Total anthocyanin content (Figure 3) was significantly and much higher in treated plants, which also correlates with the advanced color development in berries of HB-treated plants previously observed (Figure 2a).

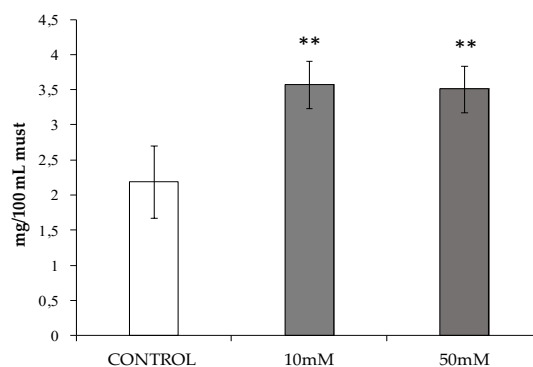


Figure 3. Total anthocyanin content was measured as mg of cyanidine-3-glucoside in 100 mL of grape juice from CONTROL and HB-treated *Vitis vinifera* L. cv Alicante Bouschet plants. Samples were collected at time 7 DA-D. Asterisks (**) indicate statistically significant differences between control and treated plants at each concentration with p < 0.01.

Different monomeric-3-flavonols, as (+)-catechin and (-)-epicatechin, are also involved in grapevine ripening, but in this case, these polyphenols decline rapidly at veraison [33]. As expected, catechin and epicatechin content was lower in berries of

plants treated with a higher dose of HB, corroborating the effect of this compound on phenolics associated to ripening phenomenon (Figure S1).

3.4. Total soluble solids determination

To further analyze the effect of HB in berry ripening, we evaluated sugar accumulation in berries, a well-described physiological process in ripening. Slight differences between treatments were observed during ripening, reaching levels comparable to those produced by FRUITEL. However, no significant differences were found in any treatment, including those performed with FRUITEL at any time studied (Figure 4a).

The must glucose and fructose concentrations were analyzed by high performance liquid chromatography. For this purpose, we evaluated 10 and 50 mM HB treatments, which seemed to display the most promising results regarding berry ripening. In this case, the must of the berries treated with HB at 50 mM showed significant differences in levels of glucose and fructose with regard to non-treated plants (Figure 4b).

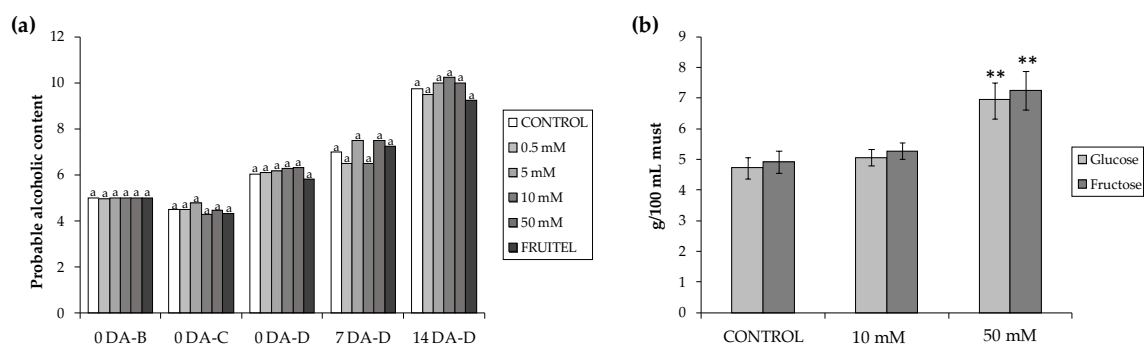


Figure 4. Effect of HB treatments on the sugar content of *Vitis vinifera* L. cv Alicante Bouschet berries. Total soluble solids (°Brix) of non-treated (CONTROL) plants, HB weekly-treated plants at different concentrations (0.5, 5, 10, 50 mM) and plants treated with the ripening inducer FRUITEL. (b) Glucose and fructose content in must of berries from CONTROL and HB-treated plants at 7 DA-D. An ANOVA test was performed, and same letter indicates no statistical significances with a p-value < 0.05. Asterisks (**) indicate statistically significant differences between control and treated plants at each concentration with p < 0.01.

3.5. Acidity evaluation

Another key process in ripening is the reduction of organic acid concentration; therefore, both total acidity values and pH were evaluated. Regarding total acidity content, differences were observed both total acidity values and pH were evaluated from the first treatment, although no statistical differences between control and HB-treated plants were found (Figure 5a). In addition, no significant differences were observed in malic nor tartaric acid accumulation (Figure S2). However, HB-treated grapevine berries presented statistically higher pH values than non-treated plants at 7

DA-D, when HB treatments at higher concentrations reached similar pH values than FRUITEL (Figure 5b).

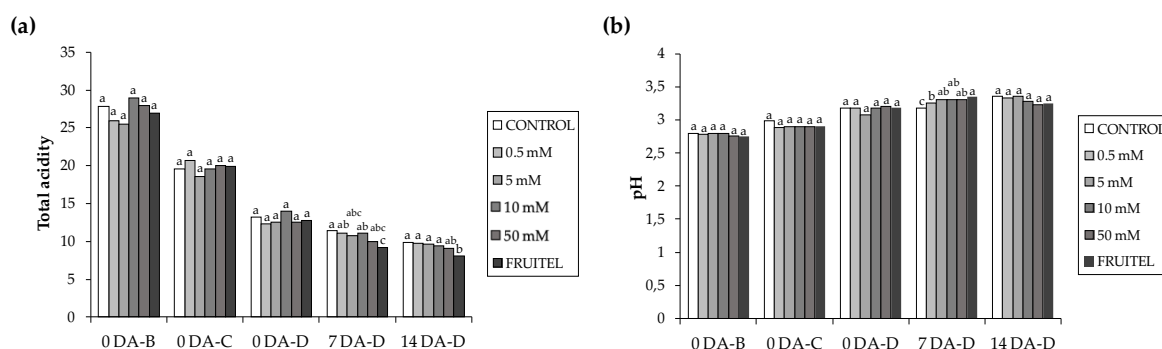


Figure 5. Acid content evolution of *Vitis vinifera* L. cv Alicante Bouschet berries of non-treated (CONTROL) plants, HB weekly-treated plants at different concentrations (0.5, 5, 10, 50 mM) and plants treated with FRUITEL. (a) Changes in total acidity content and (b) pH of berries of non-treated, HB-treated and FRUITEL-treated plants. An ANOVA test was performed, and different letters indicate statistical significances with a p-value < 0.05.

3.6. Effect of HB treatments in crop level and yield

The application of HB, even at the highest dose did not affect the grapevine yield performance (Table 1).

Table 1. Yield of *Vitis vinifera* L. cv Alicante Bouschet vines of non-treated (CONTROL) plants, HB weekly-treated plants at different concentrations (0.5, 5, 10, 50 mM) and plants treated with the ripening inducer FRUITEL. An ANOVA test was performed. The letter “a” indicates that no statistically significant differences were observed.

Treatment	Yield (kg/ha)
CONTROL	19722 a
0.5 mM	19418 a
5 mM	20530 a
10 mM	19901 a
50 mM	19912 a
FRUITEL	19802 a

4. Discussion

The impacts of climate change are reducing the capacity of natural resources (biodiversity, soil and water) to sustain the food demand of the world's increasing population. Predictable increases in temperature, changes in extreme weather events and precipitation patterns, as well as reduction in water availability may result in reduced agricultural productivity. This has prompted scientists to develop new crop varieties or manipulate potential targets in order to obtain more stress-resistant crops [34]. Stomatal closure is among the earliest plant responses to the changing environment, so stomata could be considered as potential targets for manipulation to improve plant productivity in stress conditions. We have previously identified a volatile compound emitted by infected tomato plants named as HB, which induces stomata closure in different plant species [27, 28]. In the present research HB treatments were effective in grapevines, confirming its role as universal natural stomata closer agent (Figure 1). Interestingly, this volatile resulted more effective on young plants since stomatal conductance depends on leaf and plant age mainly due to differences in biochemical limitations [35, 36]. Other exogenous treatments have also been reported to induce stomatal closure in *Vitis vinifera* plants. For instance, treatments with the well-described phytohormone involved in stomatal closure, ABA [37]; or exogenously applied sugars such as sucrose, maltose, trehalose and trehalose-6-phosphate induced a significant closure of stomata in a dose-dependent manner [38]. Moreover, the effects of pinolene as an anti-transpirant on grapevine has also been described [39, 40]. However, to our knowledge, this is the first time that a natural volatile compound is described to produce this effect on *Vitis vinifera* plants.

The obtained results might have implications for improving crop performance under soil water deficit. In semi-arid climates, tools for improving water use efficiency (WUE) are needed and, for instance, deficit irrigation is often employed as a tool to increase the intrinsic leaf gas exchange (WUE) since normally the relationship between stomatal conductance and photosynthesis is curvilinear [41]. The exogenous application of HB could be used to stimulate stomatal closure reducing water use in those periods of time when soil water content might severely limit plant performance. However, it should be considered that a reduction in stomatal conductance could impair leaf photosynthesis rates. The potential effects of HB application on the overall vine source capacity and the carbon partitioning within the vines should be investigated in order to determine the long-term effects of HB applications on vine vegetative growth, crop water use and longevity and productivity.

Once the role of HB as stomata closer was confirmed in grapevine, we studied the impact of this effect on different processes, since it was also demonstrated that HB treatments in tomato plants induced resistance against *Pseudomonas syringae* [28]. Phenotypically, grapevine plots treated regularly with HB at different concentrations

showed higher color intensity in bunches, comparable or even higher than those plots that were treated with the ripening inducer FRUITEL (Figure 2a). This change in color development also correlated with the number of days on reaching veraison (Figure 2b), proposing a new role for HB as a ripening inducer. Interestingly, effects produced by 10 mM and 50 mM treatments were very similar, thus indicating a saturation of the effect on the color, probably related with saturation on the stomata closure. Other ripening-associated phenomena such as phenolic content were also analyzed. Total anthocyanin content was significantly higher in HB-treated plots at 10 and 50 mM (Figure 3), which properly correlates with the effect of the volatile in color development. Moreover, the decrease of tannins after veraison was also confirmed in 50 mM HB treated plants, which showed reduced content of (+)-catechin and (-)-epicatechin in berries (Figure S1). The presence of these tannins also participates in wine organoleptic properties, influencing astringency and bitter perception. Higher amounts of (+)-catechin and (-)-epicatechin lead to higher intensity of oral astringency and bitterness [42]. Color development and tannin content are important in the maturity index of many fruits. To further study the role of HB in grapevine ripening, we analyzed other parameters involved in fruit ripening. It is well known that, at veraison, berry sugar contents rise while acid levels decrease. The balance between sugars and acids is considered one of the main aspects of grape and wine quality. HB treatments increased sugar content, especially at higher concentrations (Figure 4), whereas no significant differences were observed in acid contents (Figures 5 and S2). However, the musts obtained from HB-treated grapevines at 7 DA-D showed statistically higher pH values than musts of non-treated plants, reaching similar pH values than FRUITEL treatments when applied from 5 mM onwards. Several studies have described a relationship between the stomata aperture and the sugar accumulation in the grapevine. In this sense, Kaolin has been described to increase anthocyanin content without altering the sugar content, and the anti-transpirant pinolene reduced both the anthocyanin and sugar contents [39,43–45].

Exogenous pre-harvest treatments with different compounds have been widely explored and similar results have been observed. For instance, nitrogen application in grapevines delays berry sugar accumulation during ripening, but increases anthocyanin content, enhancing wine color [46]. Phytohormonal control has also been suggested as another strategy since hormones such as ABA, ethylene, brassinosteroids or gibberellins provide many signals for the onset of ripening [4,47,48]. Other compounds known as elicitors such as benzothiadiazole, methyl jasmonate, chitosan and yeast extract, have demonstrated their efficacy for increasing grape phenolic content [49–51]. HB treatments could somehow be activating ethylene biosynthesis in grapevines therefore promoting the anthocyanin accumulation in a similar manner to the the positive control (FRUITEL; [52]). Future experiments to test the possible induction of genes involved in the ethylene biosynthesis, such as *ACS* or *ACO*, will result in great interest.

In this study, we present HB as a new natural product, whose application requires practically no equipment, which acts as a stomata closing agent promoting grapevine ripening under open-field conditions. The clear increase in grape anthocyanin content in response to the HB treatment without any clear effect on grape total soluble solids is considered a very positive result for wine making and particularly for wine aging purposes. For premium wine quality, grapes need to be harvested at high sugar concentration in order to reach full grape phenolic maturity. This results in wines with too high an alcohol content. Our results suggest that HB applications could be used as a field practices to clearly increase grape color potential. Further investigation is required in other grapevine varieties, in addition to the Alicante Bouschet tested here, which has the peculiarity to accumulate anthocyanin both in the berry skin and pulp tissues. It would be also interesting to further study the effect of HB application volatile against other biotic grapevine stresses related to stomata control, such as the downy mildew. Since *Plasmopara viticola* uses stomata to penetrate into leaves [53], HB treatments could limit the entrance of the pathogen. Finally, a metabolomics study of the volatile organic compound profiles of control and HB treated grapes would result also of great interest.

Conclusions

In this study, we confirm the role of HB as both a natural stomatal closure compound, and a ripening inducer which accelerates anthocyanin accumulation under open-field conditions without having, in the short-term, a negative impact on yield. Therefore, this volatile could be used to control the physiology of ripening in *Vitis vinifera* L. by promoting veraison. Broadly, HB could also act as a phytoprotector for the sustainable control of abiotic stresses in agriculture. The present research paves the way to further longer-term studies determining the potential effects of HB application during different periods of the vine development and as a possible tool to mitigate the effects of severe soil water deficit on vine performance.

Patents: The compound (*Z*)-3-hexenyl butyrate has been patented by the Spanish Patent and Trademark Office (P201730685).

Funding: This research was funded by Grant INNVAL10/18/005 from the Agència Valenciana de la Innovació (Spain). CP was a recipient of a predoctoral contract of the Generalitat Valenciana (ACIF/2019/187). DI is supported by AEI-FEDER grant AGL2017-83738-C3-3-R.

Acknowledgments: We would like to thank the IVIA Unidad Asociada to CSIC “Riego en la agricultura mediterránea” for helping us with the fine tuning and the first trial. We also thank José Giner, Bernat Tetuán, Eduardo Ibáñez, Isidre Ferrero and José Suñer (GMW Bioscience, Valencia, Spain) for their technical support in the EOR studies.

Conflicts of Interest: The authors declare no conflict of interest. The funders had no role in the design of the study; in the collection, analyses, or interpretation of data; in the writing of the manuscript, or in the decision to publish the results.

5. References

1. Conde, C.; Silva, P.; Fontes, N.; Dias, A.C.P.; Tavares, R.M.; Sousa, M.J.; Agasse, A.; Delrot, S.; Gerós, H. Biochemical changes throughout grape berry development and fruit and wine quality. *Food* **2007**, *1*, 1–22. Available online: <http://hdl.handle.net/1822/6820> (accessed on 14 March 2020).
2. Zoccatelli, G.; Zenoni, S.; Savoï, S.; Dal Santo, S.; Tononi, P.; Zandonà, V.; Dal Cin, A.; Guantieri, V.; Pezzotti, M.; Tornielli, G. Skin pectin metabolism during the postharvest dehydration of berries from three distinct grapevine cultivars. *Aust. J. Grape Wine Res.* **2013**, *19*, 171–179. doi: 10.1111/ajgw.12014
3. Lund, S.T.; Bohlmann, J. The Molecular Basis for Wine Grape Quality-A Volatile Subject. *Science* **2006**, *311*, 804–805. <https://doi.org/10.1126/science.1118962>
4. Kuhn, N.; Guan, L.; Dai, Z.W.; Wu, B.H.; Lauvergeat, V.; Gomès, E.; Li, S.H.; Godoy, F.; Arce-Johnson, P.; de Irot, S. Berry ripening: Recently heard through the grapevine. *J. Exp. Bot.* **2014**, *65*, 4543–4559. <https://doi.org/10.1093/jxb/ert395>
5. Gerós, H.; Chaves, M.M.; Medrano, H.; Delrot, S. *Grapevine in a Changing Environment: A Molecular and Ecophysiological Perspective*; John Wiley & Sons, Ltd.: West Sussex, UK, **2016**. <https://doi.org/10.1002/9781118735985.ch1>
6. Palliotti, A.; Tombesi, S.; Silvestroni, O.; Lanari, V.; Gatti, M.; Poni, S. Changes in vineyard establishment and canopy management urged by earlier climate-related grape ripening: A review. *Sci. Hort.* **2014**, *178*, 43–54. <https://doi.org/10.1016/j.scienta.2014.07.039>.
7. Van Leeuwen, C.; Destrac-Irvine, A.; Dubernet, M.; Duchêne, E.; Gowdy, M.; Marguerit, E.; Pieri, P.; Parker, A.; de Rességuier, L.; Ollat, N. An update on the impact of climate change in viticulture and potential adaptations. *Agronomy* **2019**, *9*, 514. <https://doi.org/10.3390/agronomy9090514>
8. Schultz, H.R. Climate Change and Viticulture: Research Needs for Facing the Future. *J. Wine Res.* **2010**, *21*, 113–116. <https://doi.org/10.1080/09571264.2010.530093>
9. Fraga, H.; Malheiro, A.C.; Moutinho-Pereira, J.; Santos, J.A. An overview of climate change impacts on European viticulture. *Food Energy Secur.* **2012**, *1*, 94–110. <https://doi.org/10.1002/fes3.14>
10. Zhang, Y.; Mechlin, T.; Dami, I. Foliar Application of Abscisic Acid Induces Dormancy Responses in Greenhouse-grown Grapevines. *HortSci. Horts* **2011**, *46*, 1271–1277. <https://doi.org/10.21273/HORTSCI.46.9.1271>
11. Jung, C.J.; Hur, Y.Y.; Yu, H.-J.; Noh, J.-H.; Park, K.-S.; Lee, H.J. Gibberellin application at pre-bloom in grapevines down-regulates the expressions of *VvIAA9* and *VvARF7*, negative regulators of fruit set initiation, during parthenocarpic fruit development. *PLoS ONE* **2014**, *9*, e95634. <https://doi.org/10.1371/journal.pone.0095634>

12. Deytieux-Belleau, C.; Gagné, S.; L'Hyvernay, A.; Donèche, B.; Geny, L. Possible roles of both abscisic acid and indol-acetic acid in controlling grape berry ripening process. *OENO One* **2007**, *41*, 141–148. <https://doi.org/10.20870/oenone.2007.41.3.844>
13. El-kenawy, M. Effect of chitosan, salicylic acid and fulvic acid on vegetative growth, yield and fruit quality of Thompson seedless grapevines. *Egypt. J. Hortic.* **2017**, *44*, 45–59. <https://doi.org/10.21608/ejoh.2017.1104.1007>
14. Becatti, E.; Genova, G.; Ranieri, A.; Tonutti, P. Postharvest treatments with ethylene on *Vitis vinifera* (cv Sangiovese) grapes affect berry metabolism and wine composition. *Food Chem.* **2014**, *159*, 257–266. <https://doi.org/10.1016/j.foodchem.2014.02.169>
15. Meng, J.F.; Yu, Y.; Shi, T.C.; Fu, Y.S.; Zhao, T.; Zhang, Z.W. Melatonin treatment of pre-veraison grape berries modifies phenolic components and antioxidant activity of grapes and wine. *Food Sci. Technol.* **2019**, *39*, 35–42. <https://doi.org/10.1590/1678-457x.24517>
16. Abdel-Salam, M.M. Effect of foliar application with humic acid and two antioxidants on ruby seedless grapevine. *Middle East J. Agric. Res.* **2016**, *5*, 123–131.
17. Mirdehghan, S.H.; Rahimi, S. Pre-harvest application of polyamines enhances antioxidants and table grape (*Vitis vinifera* L.) quality during postharvest period. *Food Chem.* **2016**, *196*, 1040–1047. <https://doi.org/10.1016/j.foodchem.2015.10.038>
18. Mencarelli, F.; Bellincontro, A. Recent advances in postharvest technology of the wine grape to improve the wine aroma. *J. Sci. Food Agric.* **2018**. <https://doi.org/10.1002/jsfa.8910>
19. Bellincontro, A.; Fardelli, A.; De Santis, D.; Botondi, R.; Mencarelli, F. Postharvest ethylene and 1-MCP treatments both affect phenols, anthocyanins, and aromatic quality of Aleatico grapes and wine. *Aust. J. Grape Wine Res.* **2006**, *12*, 41–149. <https://doi.org/10.1111/j.1755-0238.2006.tb00054.x>
20. Botondi, R.; Lodola, L.; Mencarelli, F. Postharvest ethylene treatment affects berry dehydration, polyphenol and anthocyanin content by increasing the activity of cell wall enzymes in Aleatico wine grape. *Eur. Food Res. Technol.* **2011**, *232*, 679–685. <https://doi.org/10.1007/s00217-011-1437-5>
21. Williams, L.E.; Matthews, M.A. Grapevine. In *Irrigation of Agricultural Crops. Agronomy Monograph No. 30*; Stewart, B.A., Nielsen, D.R., Eds.; ASA-CSSA-SSSA: Madison, WI, USA, **1990**; pp. 1019–1055.
22. Lovisolo, C.; Hartung, W.; Schubert, A. Whole-plant hydraulic conductance and root-to-shoot flow of abscisic acid are independently affected by water stress in grapevines. *Funct. Plant Biol.* **2002**, *29*, 1349–1356. <https://doi.org/10.1071/FP02079>
23. Flexas, J.; Barón, M.; Bota, J.; Ducruet, J.M.; Gallé, A.; Galmés, J.; Jiménez, M.; Pou, A.; Ribas-Carbó, M.; Sajani, C.; et al. Photosynthesis limitations during water stress acclimation and recovery in the drought-adapted *Vitis* hybrid Richter-110 (*V. berlandierix* V. *rupestris*). *J. Exp. Bot.* **2009**, *60*, 2361–2377. <https://doi.org/10.1093/jxb/erp069>
24. Yu, D.J.; Kim, S.J.; Lee, H.J. Stomatal and non-stomatal limitations to photosynthesis in field-grown grapevine cultivars. *Biol. Plant.* **2009**, *53*, 133–137. <https://doi.org/10.1007/s10535-009-0019-x>
25. Wong, S.C.; Cowan, I.R.; Farquhar, G.D. Stomatal conductance correlates with photosynthetic capacity. *Nature* **1979**, *282*, 424–426. <https://doi.org/10.1038/282424a0>
26. Franks, P.J.; Farquhar, G.D. The mechanical diversity of stomata and its significance in gas-exchange control. *Plant Physiol.* **2007**, *143*, 78–87. <https://doi.org/10.1104/pp.106.089367>
27. López-Gresa, M.P.; Lisón, P.; Campos, L.; Rodrigo, I.; Rambla, J.L.; Granell, A.; Conejero, V.; Bellés, J.M. A non-targeted metabolomics approach unravels the VOCs associated with the tomato

- immune response against *Pseudomonas syringae*. *Front. Plant Sci.* **2017**, *8*, 1–15. <https://doi.org/10.3389/fpls.2017.01188>
28. López-Gresa, M.P.; Payá, C.; Ozáez, M.; Rodrigo, I.; Conejero, V.; Klee, H.; Bellés, J.M.; Lisón, P. A new role for green leaf volatile esters in tomato stomatal defence against *pseudomonas syringe* pv. Tomato. *Front. Plant Sci.* **2018**, *871*, 1–12. <https://doi.org/10.3389/fpls.2018.01855>
 29. Meyers, K.J.; Watkins, C.B.; Pritts, M.P.; Liu, R.H. Antioxidant and Antiproliferative Activities of Strawberries. *J. Agric. Food Chem.* **2003**, *51*, 6887–6892. <https://doi.org/10.1021/jf034506n>
 30. García-Hurtado, N.; Carrera, E.; Ruiz-Rivero, O.; López-Gresa, M.P.; Hedden, P.; Gong, F.; García-Martínez, J.L. The characterization of transgenic tomato overexpressing gibberellin 20-oxidase reveals induction of parthenocarpic fruit growth, higher yield, and alteration of the gibberellin biosynthetic pathway. *J. Exp. Bot.* **2012**, *63*, 5803–5813. <https://doi.org/10.1093/jxb/ers229>
 31. Coombe, B.G. Research on development and ripening of the grape berry. *Am. J. Enol. Vitic.* **1992**, *43*, 101–110.
 32. Fernández-López, J.A.; Almela, L.; Muñoz, J.A.; Hidalgo, V.; Carreño, J. Dependence between colour and individual anthocyanin content in ripening grapes. *Food Res. Int.* **1998**, *31*, 667–672. [https://doi.org/10.1016/S0963-9969\(99\)00043-5](https://doi.org/10.1016/S0963-9969(99)00043-5)
 33. Kennedy, J.A.; Troup, G.J.; Pilbrow, J.R.; Hutton, D.R.; Hewitt, D.; Hunter, C.R.; Ristic, R.; Iland, P.G.; Jones, G.P. Development of seed polyphenols in berries from *Vitis vinifera* L. cv. Shiraz. *Aust. J. Grape Wine Res.* **2000**, *6*, 244–254. <https://doi.org/10.1111/j.1755-0238.2000.tb00185.x>
 34. Gupta, A.; Rico-Medina, A.; Caño-Delgado, A.I. The physiology of plant responses to drought. *Science* **2020**, *368*, 266–269. <https://doi.org/10.1126/science.aaz7614>
 35. Jordan, W.R.; Brown, K.W.; Thomas, J.C. Leaf Age as a Determinant in Stomatal Control of Water Loss from Cotton during Water Stress. *Plant Physiol.* **1975**, *56*, 595–599. <https://doi.org/10.1104/pp.56.5.595>
 36. Whitehead, D.; Barbour, M.M.; Griffin, K.L.; Turnbull, M.H.; Tissue, D.T. Effects of leaf age and tree size on stomatal and mesophyll limitations to photosynthesis in mountain beech (*Nothofagus solandrii* var. *cliffortioides*). *Tree Physiol.* **2011**, *31*, 985–996. <https://doi.org/10.1093/treephys/tpr021>
 37. Tombesi, S.; Nardini, A.; Frioni, T.; Soccolini, M.; Zadra, C.; Farinelli, D.; Poni, S.; Palliotti, A. Stomatal closure is induced by hydraulic signals and maintained by ABA in drought-stressed grapevine. *Sci. Rep.* **2015**, *5*, 12449. <https://doi.org/10.1038/srep12449>
 38. Gamm, M.; Héloir, M.C.; Adrian, M. Trehalose and trehalose-6-phosphate induce stomatal movements and interfere with aba-induced stomatal closure in grapevine. *J. Int. Sci. Vigne Vin* **2015**, *49*, 165–171. <https://doi.org/10.20870/oeno-one.2015.49.3.84>
 39. Di Vaio, C.; Marallo, N.; di Lorenzo, R.; Pisciotta, A. Anti-Transpirant effects on vine physiology, berry and wine composition of cv. *Aglianico (Vitis vinifera L.) grown in South Italy*. *Agronomy* **2019**, *9*, 244. <https://doi.org/10.3390/agronomy9050244>
 40. Di Vaio, C.; Villano, C.; Lisanti, M.T.; Marallo, N.; Cirillo, A.; Di Lorenzo, R.; Pisciotta, A. Application of Anti-Transpirant to Control Sugar Accumulation in Grape Berries and Alcohol Degree in Wines Obtained from Thinned and Unthinned Vines of cv. Falanghina (*Vitis vinifera L.*). *Agronomy* **2020**, *10*, 345. <https://doi.org/10.3390/agronomy10030345>
 41. Medrano, H.; Tomás, M.; Martorell, S.; Escalona, J.-M.; Pou, A.; Fuentes, S.; Flexas, J.; Bota, J. Improving water use efficiency of vineyards in semi-arid regions. A review. *Agron. Sustain. Dev.* **2015**, *35*, 499–517. <https://doi.org/10.1007/s13593-014-0280-z>

42. Kallithraka, S.; Bakker, J.; Clifford, M.N. Evaluation of bitterness and astringency of (+)-catechin and (-)-epicatechin in red wine and in model solution. *J. Sens. Stud.* **1997**, *12*, 25–37. <https://doi.org/10.1111/j.1745-459X.1997.tb00051.x>
43. Brillante, L.; Belfiore, N.; Gaiotti, F.; Lovat, L.; Sansone, L.; Poni, S.; Tomasi, D. Comparing Kaolin and Pinolene to Improve Sustainable Grapevine Production during Drought. *PLoS ONE* **2016**, *11*, e0156631. <https://doi.org/10.1371/journal.pone.0156631>
44. Palliotti, A.; Panara, F.; Famiani, F.; Sabbatini, P.; Howell, G.S.; Silvestroni, O.; Poni, S. Postveraison Application of Antitranspirant Di-1-*p*-Menthene to Control Sugar Accumulation in Sangiovese Grapevines. *Am. J. Enol. Vitic.* **2013**, *64*, 378–385. <https://doi.org/10.5344/ajev.2013.13015>
45. Fahey, D.J.; Rogiers, S.Y. Di-1-*p*-menthene reduces grape leaf and bunch transpiration. *Aust. J. Grape Wine Res.* **2019**, *25*, 134–141. <https://doi.org/10.1111/ajgw.12371>
46. Martín, P.; Delgado, R.; González, M.R.; Gallegos, J.I. Colour of “Tempranillo” grapes affected by different nitrogen and potassium fertilization rates. *Acta Hortic.* **2004**, *652*, 153–160. <https://doi.org/10.17660/ActaHortic.2004.652.18>
47. Fortes, A.M.; Teixeira, R.T.; Agudelo-Romero, P. Complex interplay of hormonal signals during grape berry ripening. *Molecules* **2015**, *20*, 9326–9343. <https://doi.org/10.3390/molecules20059326>
48. Griesser, M.; Savoi, S.; Supapvanich, S.; Dobrev, P.; Vankova, R.; Forneck, A. Phytohormone profiles are strongly altered during induction and symptom development of the physiological ripening disorder berry shrivel in grapevine. *Plant Mol. Biol.* **2020**. <https://doi.org/10.1007/s11103-020-00980-6>
49. Portu, J.; López, R.; Baroja, E.; Santamaría, P.; Garde-Cerdán, T. Improvement of grape and wine phenolic content by foliar application to grapevine of three different elicitors: Methyl jasmonate, chitosan, and yeast extract. *Food Chem.* **2016**, *201*, 213–221. <https://doi.org/10.1016/j.foodchem.2016.01.086>
50. Gomez-Plaza, E.; Bautista-Ortín, A.B.; Ruiz-García, Y.; Fernández-Fernández, J.I.; Gil-Muñoz, R. Effect of elicitors on the evolution of grape phenolic compounds during the ripening period. *J. Sci. Food Agric.* **2017**, *97*, 977–983. <https://doi.org/10.1002/jsfa.7823>
51. Silva, V.; Singh, R.K.; Gomes, N.; Soares, B.G.; Silva, A.; Falco, V.; Capita, R.; Alonso-Calleja, C.; Pereira, J.E.; Amaral, J.S.; et al. Comparative Insight upon Chitosan Solution and Chitosan Nanoparticles Application on the Phenolic Content, Antioxidant and Antimicrobial Activities of Individual Grape Components of Sousão Variety. *Antioxidants* **2020**, *9*, 178. <https://doi.org/10.3390/antiox9020178>
52. El-Kereamy, A.; Chervin, C.; Roustan, J.-P.; Cheynier, V.; Souquet, J.-M.; Moutounet, M.; Raynal, J.; Ford, C.; Latché, A.; Pech, J.-C.; et al. Exogenous ethylene stimulates the long-term expression of genes related to anthocyanin biosynthesis in grape berries. *Physiol. Plant.* **2003**, *119*, 175–182. <https://doi.org/10.1034/j.1399-3054.2003.00165.x>
53. Allègre, M.; Héloir, M.C.; Trouvelot, S.; Daire, X.; Pugin, A.; Wendehenne, D.; Adrian, M. Are grapevine stomata involved in the elicitor-induced protection against downy mildew? *Mol. Plant-Microbe Interact.* **2009**, *22*, 977–986. <https://doi.org/10.1094/MPMI-22-8-0977>

Supplementary Materials

Table S1. Conditions during the trial.

Type of data	Long term averages		Monthly averages 2019	
Location of the weather station	Almansa (Albacete)		Almansa (Albacete)	
Meters above sea-level	676		676	
Distance to the test site [km]	10.4		10.4	
Source for the weather data	SIAR http://eportal.mapa.gob.es/websiar/Inicio.aspx		SIAR. http://eportal.mapa.gob.es/websiar/Inicio.aspx	
Long term averages (2011-2018)				
Month	Avg. Temperature [°C]		Precipitation [mm]	
August	23.9		29.3	
September	19.9		29.4	
Average during the trial				
Month	Avg. Temperature [°C]		Precipitation [mm]	
August	24.0		24.1	
September	19.9		137.1	
Conditions during the trial				
Daily	Avg. Temperature [°C]	Tmin [°C]	Tmax [°C]	Precipitation [mm]
26/7/2019	25	14.6	34.4	0
27/7/2019	24	18.5	29.3	0
28/7/2019	23.1	14.8	30.8	0
29/7/2019	24.9	15	34.3	0
30/7/2019	23.8	15.6	32.8	0
31/7/2019	21.9	16.3	27.5	0
1/8/2019	23.7	14	34	0
2/8/2019	24.9	15.8	34.2	0
3/8/2019	25.3	15	34.5	0
4/8/2019	26.9	17.3	37.5	0
5/8/2019	26.8	16.8	37.3	0
6/8/2019	28	18.1	37.9	0

7/8/2019	27.3	19.3	36.1	0
8/8/2019	27.5	17.9	36.5	0
9/8/2019	27.6	15.4	37.3	0
10/8/2019	27.6	17.6	37.4	0
11/8/2019	26.6	18.7	34.7	0
12/8/2019	23.7	16.4	30.6	0
13/8/2019	22	17.3	28.6	0
14/8/2019	23.4	14.8	33.2	0
15/8/2019	24.4	14.8	34.7	0
Date	Avg. Temperature [°C]	Tmin [°C]	Tmax [°C]	Precipitation [mm]
16/8/2019	24.2	13.9	33.8	0
17/8/2019	26.7	15.6	36.9	0
18/8/2019	27.4	16.9	37.1	0
19/8/2019	24.8	15.1	34.2	0
20/8/2019	21.4	16.3	30	5
21/8/2019	20.3	16.1	26.7	0.4
22/8/2019	21	11.2	30.9	0
23/8/2019	21	9.6	30.6	0
24/8/2019	21.5	10.6	32.4	0
25/8/2019	21.2	11.4	30.6	0
26/8/2019	20.1	13	26.9	0
27/8/2019	18.2	13.1	26.7	18.3
28/8/2019	21.3	12.9	30.6	0
29/8/2019	22.8	15.1	31.1	0.2
30/8/2019	22.8	15	32.3	0
31/8/2019	22.9	14.3	32.7	0.2
1/9/2019	23.3	15	33.4	0.2
2/9/2019	21.5	17.9	27.1	13.5
3/9/2019	22.5	17.7	30	0
4/9/2019	22.7	18.8	31.3	1.6
5/9/2019	21.1	15.9	27.7	0.2
6/9/2019	20.7	17.1	26.3	0
7/9/2019	20.6	16.6	26.4	0
8/9/2019	19.6	13.5	25.7	0
9/9/2019	21.2	15	28.9	0
10/9/2019	18.1	11.7	23.2	0.4
11/9/2019	13.6	11.1	16.7	15.5
12/9/2019	16.7	14	19.1	76.2

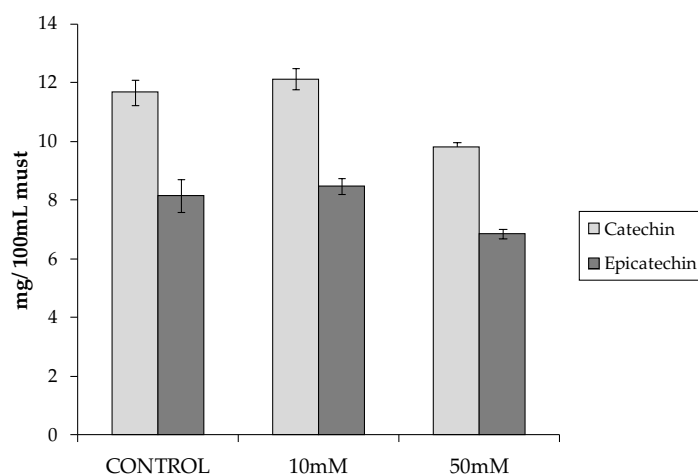


Figure S1. Catechin and epicatechin content of must from *Vitis vinifera* berries of CONTROL and HB-treated plants. Samples were collected at time 7 DA-D. No statistically significant differences were observed between control and treated plants.

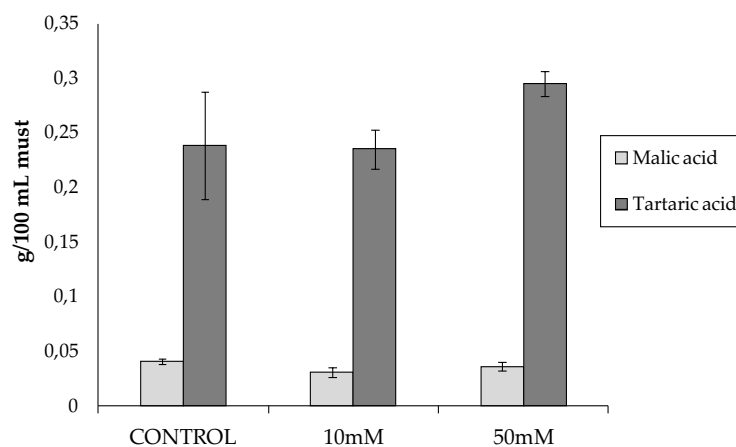


Figure S2. Malic and tartaric acid content of must from *Vitis vinifera* berries of CONTROL and HB-treated plants. Samples were collected at time 7 DA-D. No statistically significant differences were observed between control and treated plants.

General Discussion

Throughout the 20th century, there is a wide consensus that climate has globally changed, facing increases in average temperatures, accompanied by greater variations in precipitations. In addition, it is expected that these weather events will occur more frequently and severely [154–156]. This scenario will directly affect agricultural practices and production due to the increased pressure from biotic and abiotic stresses. Nowadays the use of pesticides is the main solution for crop protection against biotic stresses. However, the employment of chemicals to control pests could have a negative environmental impact, carrying out ecological consequences, so new policies are emerging towards a reduced use of conventional pesticides [157–159]. For these reasons, new methods and strategies should be developed in order to successfully control plant stresses, thus increasing agricultural productivity in a sustainable manner [160,161].

In addition to producing primary compounds that are essential for growth and development, plants synthesize a diverse and large assortment of secondary metabolites. Plant secondary metabolites have different functions in plant defence against herbivores and pathogens due to their direct toxic properties such as antimicrobial, antioxidant and antifeeding activities; or indirectly by attracting insects for seed dispersal, predators of attacking insects establishing tri-trophic interactions, or acting as defensive signal metabolites [63,69,94,162,163]. Furthermore, plant secondary metabolites also contribute to human health, due to their antibiotic, antifungal, anthelmintic, analgesic, anti-inflammatory, antitumoral, antioxidant, immunostimulant and peripheral nervous modulating effects, and event to produce of flavors and perfumes, among others [164,165].

In this context, by using two different biotechnological approaches we have further analyzed the role of two main groups of plant secondary metabolites, phenolic and volatile compounds. Specifically, we have focused our attention on the plant defensive role of both the simple phenolic salicylic acid (SA), and the green leaf volatile (GLV) (*Z*)-3-hexenyl-butyrate (HB). On one hand, we have made use of genetic methodologies in both contexts. Firstly, we have generated tomato transgenic plants with altered SA levels, which led to enhanced resistance to bacterial and viroidal inoculation, being SA catabolism specific for each interaction. Regarding VOCs, through genetic tools we have unraveled the HB-signal transduction cascade in the model specie *Arabidopsis thaliana*. On the other hand, we have complemented genetic approaches by following chemical biology strategies to uncover the downstream essential components for HB-mediated stomatal closure. Furthermore, delving into the knowledge of the HB mechanism of action, has allowed us to explore its possible applications in agriculture, not only against biotic stresses, but also against abiotic stresses and ripening.

Secondary metabolites in plant defence mechanisms: Genetic approaches

One of the key strategies enabling the study of the role of secondary metabolites in plants is the genetic manipulation of the existing metabolic pathways by overexpressing or silencing different essential components. In the **first chapter** of this project, we used this tool to generate tomato transgenic *SIS5H* plants, which have altered SA levels. Apart from the enhanced resistance to pathogens phenotype previously described [83,166], our results suggest that SA metabolism in *SIS5H*-silenced plants is specific for each tomato-pathogen interaction, indicating that there is an additional complexity regarding SA homeostasis. One of the most relevant examples of SA-genetically engineered plants are *NahG* transgenic plants, which express a salicylate hydroxylase gene from *Pseudomonas putida* which catalyzes the decarboxylative hydroxylation of salicylate into catechol and, consequently, they are unable to accumulate SA [167,168]. *NahG* transgenic plants have been excellent tools to study the role of SA in response to biotic stress and in the establishment of SAR [73,75,167]. Additionally, other studies attempted to generate transgenic plants that accumulate high levels of SA. In this sense, different SA over-accumulating *Arabidopsis* mutants, such as *pr5*, *cpr6*, *snc1* and *pi4kIIIβ1β2*, exhibited enhanced resistance to pathogens, but also presented stunted growth [169–172]. These results together with the early senescence associated to *RNAi_S5H* tomato plants appear to indicate that constitutive activation of SA biosynthesis and signalling entailed penalty development, excluding this kind of approaches as suitable biotechnological tools in agriculture.

In previous works, the role of GLV esters in plant immunity was confirmed by using transgenic antisense *AAT1* tomato plants, which exhibited a lower ratio of stomatal closure and an hypersusceptible phenotype to *Pst* DC3000 infection due to the reduction of ester emissions upon bacterial infection [3, annex I]. Moreover, we also observed that pre-treatments with HB in SA-deficient *NahG* and JA-signalling impaired *JAZ2* [173] tomato plants resulted in a significant stomatal closure, indicating that the effect of HB is SA- and JA-independent. On the other hand, in the **second chapter** of this thesis, we have employed *Arabidopsis thaliana mpk3* and *mpk6* mutants to confirm that HB-mediated stomatal closure is dependent on MPKs cascades. Despite the progress in recent years about GLVs, there are still many outstanding questions related to their perception and signalling. Several studies have also observed that GLVs exposure triggered an increase in cytosolic calcium, ROS production and increased the expression of several genes related to defence mechanisms [174–177]. However, volatile perception remains an enigma. Plant volatiles are most likely taken up by the plant via stomata or by absorption, and then, they must cross the cuticle and the cell wall to reach the plasma membrane. It is suggested that, due to its lipophilic nature, GLVs can cross plasma membranes and directly “dissolve”, or they are further metabolized by the plant cell [178,179]. Besides, there is an existing dilemma regarding how GLVs can activate plant immune system. Due to the facts that GLVs synthesis is initiated within seconds upon wounding and herbivore or pathogen attack, and these volatiles are formed from

plant endogenous components, it is suggested that GLVs can act as DAMPs [177,179,180]. Another hypothesis supports that as GLVs are generated downstream of classical DAMPs, they should be seen as second messengers rather than the initial signals [181]. In this project, we have observed that HB perception activates different defence signalling events, including the activation of Ca²⁺ permeable channels, ROS burst and phosphorylation of the mitogen-activated protein kinases MPK3 and MPK6, triggering stomatal closure. It would be highly interesting to identify HB receptor by screening different plant PRRs, supporting the idea that HB could be perceived as a DAMP rather than a second messenger.

Secondary metabolites in plant defence mechanisms: chemical biology approaches

Chemical biology is emerging as a new cross-discipline that integrates molecular biology and chemical methodologies to study physiological mechanisms at molecular level. Whereas genetics produces phenotypes based on mutations that, in turn, perturb protein expression or function, chemical genetics approaches generate phenotypes mainly by directly altering protein function, hence chemical biology can be harnessed to overcome obstacles of genetic approaches, as high redundancy in gene families or gene essentiality. A principal and ongoing area in chemical biology is the discovery of small organic molecules with different bioactivities that can act as agonists or antagonists of plant hormone biosynthesis, metabolism, and transport for studying the complex signals of plant hormones. These small molecules can also be used for discovering of new signalling pathways and regulatory factors [182,183].

SA is known as the major phytohormone involved in plant defence mechanisms against pathogens, triggering plant immunity responses that allow the establishment of disease resistance also in the distal non-inoculated region (SAR). It is widely known that exogenous SA application induces *PR* genes expression, ROS production and disease resistance against a wide range of biotrophic and hemibiotrophic fungal, bacterial, viral, as well as phloem-feeding insects in different plant species [184–186]. Although SA is a potent plant immunity inducer, its phytotoxicity and its rapid chemical modifications, mainly by glycosylation and hydroxylation, often leads to controlled concentration of the active form [114,187]. In this context, functional analogues of SA can mimic SA functions by directly interfering with SA-receptors or by triggering transcriptional and physiological SA- and SAR-related responses [118,128,188]. The nonprotein amino acid β-Aminobutyric Acid (BABA) is one of the most well-described SA analogues. The BABA-induced resistance is associated with an increase of the basal defence response in both SA-dependent and SA-independent ways. In this sense, BABA applications protected *Brassica napus* plants against the fungal pathogen *Leptosphaeria maculans* by activating SA biosynthesis and inducing *PR1* expression, but also acting as an antifungal compound [189]. Furthermore, BABA efficacy has also been demonstrated in open field experiments, enhancing resistance to *Plasmopara viticola* on grapevine, and reducing

severity of potato late blight caused by *Phytophthora infestans* [190,191]. Other SA analogues have also received much attention, as the thiazolic compound probenazole (PBZ), which was the first commercialized synthetic elicitor due to its direct antifungal properties and also its ability to induce several genes involved in plant defence [192,193]; or the benzothiadiazole (BTH), a chemical activator of disease resistance in several agronomic crops, as apple, pear or tomato, against a wide spectrum of pathogens by activating SA downstream signalling [194–197]. In this sense, BTH treatments enhance resistance to CEVd and Tomato Spotted Wilt Virus (TSWV) in tomato plants [198]. Moreover, the study of the metabolic alterations in BTH-treated tomato plants infected by CEVd, revealed γ -aminobutyric acid (GABA) as a metabolite significantly accumulated. Since treatments with GABA also reverted the hypersusceptibility to CEVd, the previously observed resistance to CEVd induced by BTH could be mediated by GABA [199] (see **annex II**).

Recent studies argue that VOCs have potential applications in agricultural, not only related to herbivores attack, but also against pathogens and environmental stresses. One of the most applied GLVs is (*Z*)-hexenyl acetate (HA), whose exogenous application prime resistance of wheat plants to the fungus *Fusarium graminearum*, but it is also effective in reducing damaged in maize plants during cold stress [200,201]. Different experimental trials have also demonstrated that VOCs can inhibit plant pathogens growth. Recently, different fungal pathogens as *Colletotrichum lindemuthianum*, *Fusarium oxysporum*, and *Botrytis cinerea* were treated with 22 different VOCs emitted from leaves, revealing that nonanal, (+)-carvone, citral, trans-2-decenal, linalool, nerolidol, or eugenol treatments significantly inhibited the growth of all these three fungal species [202]. Besides, a new role for GLVs esters in tomato stomatal defence against *Pst* DC3000 has been demonstrated. Particularly treatments with HB resulted in stomatal closure, defence gene activation and enhanced resistance to the bacteria, being the efficacy of this compound as a stomata closer extended to different plant species [3] (see **annex I**). In the **second chapter** of this thesis, we have shown that in field conditions, weekly HB treatments enhanced resistance to downy mildew in potato plants and bacterial speck in both potato and tomato crops. Furthermore, HB efficacy was tested under greenhouse and field conditions in tomato plants, improving tolerance, yield and fruit quality in drought conditions, and, ultimately, results in **chapter three** exhibited that HB application accelerated anthocyanin accumulation and improved ripening in grapevine, proposing a new use for HB in viticulture. A recent study demonstrated that exposure of sweet pepper plants to different GLVs, including HB, activated the sweet pepper immune defence system. Additionally, Y-tube olfactometer experiments showed that *Orius laevigatus*, the main natural enemy of *F. occidentalis*, a key sweet pepper pest, showed a strong preference to plants exposed to HB, confirming our previous work that HB could activate plant defence-related genes and also proposing a new role for this volatile in tri-trophic interactions in order to manage insect pests [139].

Apart from chemical treatments for priming, in **the second chapter** we have also taken advantage of chemical biology to identify the key components of the HB-mediated stomatal closure pathway. In this sense, we have used chemical inhibitors of the main elements involved in stomatal immunity regulation, as EGTA, DPI, SHAM and PD98059. These approaches have led us to conclude that HB downstream signalling is regulated by permeable Ca²⁺ channels, ROS production by NADPH oxidases and MPKs signalling cascade. Different researchers have followed similar strategies to elucidate the signalling pathways of many compounds in stomatal movement regulation, as is the case with melatonin, alanine and even the bacterial phytotoxin coronatine [65,125,203,204].

By using different biotechnological tools, we have deeply studied the role of two different groups of secondary metabolites, phenolic and volatile compounds, against different stresses, from their molecular mechanisms to different novel applications in agriculture. Our results confirm that plant secondary metabolites are high-valuable molecules that can be used for wide-ranging purposes, emerging as a promising alternative for conventional agricultural practices.

Future Perspectives

In this thesis we have further studied different plant defensive mechanisms, as the production of phenolic compounds and VOCs emission, taking advantage of them to obtain more tolerant and resistant plants. Another adaptation mechanism that plants have developed to maintain their well-being and survival is the ability to emit and intercept signalling molecules within the plant, and from other plants, which is known as intra- and inter-plant communication. The main via for plants in transmitting information is based on emission of VOCs, not only changing the volatile components but also their blend ratios. Plant-plant communication was first described in poplar and sugar maple trees, which accumulated phenolics and tannins when they were situated closed to damaged trees [205]. Since then, there is increasing evidence that plants can perceive and respond to signals released from neighboring plants, becoming interplant communication a widely recognized and accepted phenomena.

In this context, we aim to obtain tomato plants that over-emit different VOCs, named as *emitting Volatile Organic Compounds* (eVOCs), specifically (*Z*)-3-hexenol derivatives, as our main studied volatile, HB. Biosynthetic pathways of GLVs and JA have a common substrate, linolenic acid (Figure 3). For our purpose, we will use pharmacological and genetic approaches to block JA biosynthetic pathway by altering the activity of its key biosynthetic enzyme allene oxide synthase (AOS), to redirect the metabolic flux to the production of GLVs. On one hand, tomato plants will be exogenous treated with sodium diethyldithiocarbamate (DIECA), that inhibits JA pathway by shunting 13(S)-hydroperoxylinolenic acid to 13-hydroxylinolenic [206]. Application of DIECA has been shown to significantly reduce JA levels in multiple plant species and reduce the expression of some resistance gene [207–209]. On the other hand, tomato plants that

constitutively over-emit GLVs, will be generated by knocking out the tomato *AOS2* gene using CRISPR-Cas9 gene-editing technology. A similar approach was performed in *Nicotiana attenuata* (*Na*) plants by antisense expression of *NaAOS*, that led to reduced wound- and herbivore-induced JA accumulation [210].

The volatile nature of GLV esters would permit *eVOCs* plants to provide protection in non-transgenic neighboring crops. These transgenic plants could constitute a sustainability strategy because of the reduction of phytosanitary treatments in the protected crops. Collectively, the development of this project will allow to expand the knowledge about the defensive system of plants and to generate new biotechnological strategies for the control of pests and diseases.

General Conclusions

1. Tomato *SIS5H*-silenced plants resulted in enhanced resistance to bacterial and viroidal infections due to altered salicylic acid metabolism, which appear to be specific for each tomato-pathogen interaction.
2. The volatile (*Z*)-3-hexenyl butyrate could be perceived by the plant as a DAMP, triggering plant defensive mechanisms and stomatal immunity through the activation of Ca²⁺ permeable channels, reactive oxygen species burst, and mitogen-activated protein kinases MPK3 and MPK6 signalling, in an abscisic acid-independent manner.
3. HB can be considered as a natural plant priming agent, since its efficacy has been confirmed in field conditions against biotic stress, including fungal and bacterial inoculation, and water deprivation in different agronomic crops. Furthermore, HB exogenous treatments improved ripening in grapevine, uncovering a new role for this volatile in developmental processes.

General References

References

1. Payá, C.; Minguillón, S.; Hernández, M.; Miguel, S.M.; Campos, L.; Rodrigo, I.; Bellés, J.M.; López-Gresa, M.P.; Lisón, P. SIS5H Silencing Reveals Specific Pathogen-Triggered Salicylic Acid Metabolism in Tomato. *BMC Plant Biol* **2022**, *22*, doi:10.1101/2022.03.03.482652.
2. López-Gresa, M.P.; Lisón, P.; Campos, L.; Rodrigo, I.; Rambla, J.L.; Granell, A.; Conejero, V.; Bellés, J.M. A Non-Targeted Metabolomics Approach Unravels the VOCs Associated with the Tomato Immune Response against *Pseudomonas Syringae*. *Front. Plant Sci.* **2017**, *8*, 1–15, doi:10.3389/fpls.2017.01188.
3. López-Gresa, M.P.; Payá, C.; Ozáez, M.; Rodrigo, I.; Conejero, V.; Klee, H.; Bellés, J.M.; Lisón, P. A New Role for Green Leaf Volatile Esters in Tomato Stomatal Defence against *Pseudomonas Syringe* Pv. Tomato. *Front. Plant Sci.* **2018**, *871*, 1–12, doi:10.3389/fpls.2018.01855.
4. Payá, C.; Pilar López-Gresa, M.; Intrigliolo, D.S.; Rodrigo, I.; Bellés, J.M.; Lisón, P. (Z)-3-Hexenyl Butyrate Induces Stomata Closure and Ripening in *Vitis Vinifera*. *Agronomy* **2020**, *10*, doi:10.3390/agronomy10081122.
5. Jones, J.D.G.; Dangl, J.L. The Plant Immune System. *Nature* **2006**, *444*, 323–329, doi:10.1038/nature05286.
6. Chinchilla, D.; Bauer, Z.; Regenass, M.; Boller, T.; Felix, G. The Arabidopsis Receptor Kinase FLS2 Binds Flg22 and Determines the Specificity of Flagellin Perception. *Plant Cell* **2006**, *18*, 465–476, doi:10.1105/tpc.105.036574.
7. Gómez-Gómez, L.; Boller, T. FLS2: An LRR Receptor-like Kinase Involved in the Perception of the Bacterial Elicitor Flagellin in Arabidopsis. *Mol. Cell* **2000**, *5*, 1003–1011, doi:10.1016/s1097-2765(00)80265-8.
8. Zipfel, C.; Kunze, G.; Chinchilla, D.; Caniard, A.; Jones, J.D.G.; Boller, T.; Felix, G. Perception of the Bacterial PAMP EF-Tu by the Receptor EFR Restricts Agrobacterium-Mediated Transformation. *Cell* **2006**, *125*, 749–760, doi:10.1016/j.cell.2006.03.037.
9. Miya, A.; Albert, P.; Shinya, T.; Desaki, Y.; Ichimura, K.; Shirasu, K.; Narusaka, Y.; Kawakami, N.; Kaku, H.; Shibuya, N. CERK1, a LysM Receptor Kinase, Is Essential for Chitin Elicitor Signalling in Arabidopsis. *Proc. Natl. Acad. Sci.* **2007**, *104*, 19613–19618, doi:10.1073/pnas.0705147104.
10. Chinchilla, D.; Zipfel, C.; Robatzek, S.; Kemmerling, B.; Nürnberger, T.; Jones, J.D.G.; Felix, G.; Boller, T. A Flagellin-Induced Complex of the Receptor FLS2 and BAK1 Initiates Plant Defence. *Nature* **2007**, *448*, 497–500, doi:10.1038/nature05999.
11. Heese, A.; Hann, D.R.; Gimenez-Ibanez, S.; Jones, A.M.E.; He, K.; Li, J.; Schroeder, J.I.; Peck, S.C.; Rathjen, J.P. The Receptor-like Kinase SERK3/BAK1 Is a Central Regulator of Innate Immunity in Plants. *Proc. Natl. Acad. Sci. U. S. A.* **2007**, *104*, 12217–12222, doi:10.1073/pnas.0705306104.
12. Zhang, J.; Li, W.; Xiang, T.; Liu, Z.; Laluk, K.; Ding, X.; Zou, Y.; Gao, M.; Zhang, X.; Chen, S.; et al. Receptor-like Cytoplasmic Kinases Integrate Signalling from Multiple Plant Immune Receptors and Are Targeted by a *Pseudomonas Syringae* Effector. *Cell Host Microbe* **2010**, *7*, 290–301, doi:10.1016/j.chom.2010.03.007.
13. Lu, D.; Wu, S.; Gao, X.; Zhang, Y.; Shan, L.; He, P. A Receptor-like Cytoplasmic Kinase, BIK1, Associates with a Flagellin Receptor Complex to Initiate Plant Innate Immunity. *Proc. Natl. Acad. Sci. U. S. A.* **2010**, *107*, 496–501, doi:10.1073/pnas.0909705107.
14. Gimenez-Ibanez, S.; Rathjen, J.P. The Case for the Defence: Plants versus *Pseudomonas Syringae*. *Microbes Infect.* **2010**, *12*, 428–437, doi:https://doi.org/10.1016/j.micinf.2010.03.002.
15. Bigeard, J.; Colcombet, J.; Hirt, H. Signalling Mechanisms in Pattern-Triggered Immunity (PTI). *Mol. Plant* **2015**, *8*, 521–539, doi:https://doi.org/10.1016/j.molp.2014.12.022.
16. Flor, H.H. Current Status of the Gene-For-Gene Concept. *Annu. Rev. Phytopathol.* **1971**, *9*, 275–296, doi:10.1146/annurev.py.09.090171.001423.
17. Dangl, J.L.; Jones, J.D.G. Defence Responses To Infection. *Nature* **2001**, *411*.
18. Conrath, U.; Beckers, G.J.M.; Flors, V.; García-Agustín, P.; Jakab, G.; Mauch, F.; Newman, M.A.;

- Pieterse, C.M.J.; Poinssot, B.; Pozo, M.J.; et al. Priming: Getting Ready for Battle. *Mol. Plant-Microbe Interact.* **2006**, *19*, 1062–1071, doi:10.1094/MPMI-19-1062.
19. Yuan, M.; Ngou, B.P.M.; Ding, P.; Xin, X.F. PTI-ETI Crosstalk: An Integrative View of Plant Immunity. *Curr. Opin. Plant Biol.* **2021**, *62*, 102030, doi:10.1016/j.pbi.2021.102030.
 20. Tsuda, K.; Katagiri, F. Comparing Signalling Mechanisms Engaged in Pattern-Triggered and Effector-Triggered Immunity. *Curr. Opin. Plant Biol.* **2010**, *13*, 459–465, doi:10.1016/j.pbi.2010.04.006.
 21. Peng, Y.; Van Wersch, R.; Zhang, Y. Convergent and Divergent Signalling in PAMP-Triggered Immunity and Effector-Triggered Immunity. *Mol. Plant-Microbe Interact.* **2018**, *31*, 403–409, doi:10.1094/MPMI-06-17-0145-CR.
 22. Kim, T.-H.; Böhmer, M.; Hu, H.; Nishimura, N.; Schroeder, J.I. Guard Cell Signal Transduction Network: Advances in Understanding Abscisic Acid, CO₂, and Ca²⁺ Signalling. *Annu. Rev. Plant Biol.* **2010**, *61*, 561–591, doi:10.1146/annurev-arplant-042809-112226.
 23. Kollist, H.; Nuhkat, M.; Roelfsema, M.R.G. Closing Gaps: Linking Elements That Control Stomatal Movement. *New Phytol.* **2014**, *203*, 44–62, doi:https://doi.org/10.1111/nph.12832.
 24. Hrabak, E.M.; Chan, C.W.M.; Gribskov, M.; Harper, J.F.; Choi, J.H.; Halford, N.; Kudla, J.; Luan, S.; Nimmo, H.G.; Sussman, M.R.; et al. The Arabidopsis CDPK-SnRK Superfamily of Protein Kinases. *Plant Physiol.* **2003**, *132*, 666–680, doi:10.1104/pp.102.011999.
 25. McLachlan, D.H.; Kopischke, M.; Robatzek, S. Gate Control: Guard Cell Regulation by Microbial Stress. *New Phytol.* **2014**, *203*, 1049–1063, doi:10.1111/nph.12916.
 26. Grimmer, M.K.; John Foulkes, M.; Paveley, N.D. Foliar Pathogenesis and Plant Water Relations: A Review. *J. Exp. Bot.* **2012**, *63*, 4321–4331, doi:10.1093/jxb/ers143.
 27. Tang, D.; Wang, G.; Zhou, J.M. Receptor Kinases in Plant-Pathogen Interactions: More than Pattern Recognition. *Plant Cell* **2017**, *29*, 618–637, doi:10.1105/tpc.16.00891.
 28. Zhou, J.M.; Zhang, Y. Plant Immunity: Danger Perception and Signalling. *Cell* **2020**, *181*, 978–989, doi:10.1016/j.cell.2020.04.028.
 29. Boller, T.; Felix, G. A Renaissance of Elicitors: Perception of Microbe-Associated Molecular Patterns and Danger Signals by Pattern-Recognition Receptors. *Annu. Rev. Plant Biol.* **2009**, *60*, 379–407, doi:10.1146/annurev-arplant.57.032905.105346.
 30. Asai, T.; Tena, G.; Plotnikova, J.; Willmann, M.R.; Chiu, W.L.; Gomez-Gomez, L.; Boller, T.; Ausubel, F.M.; Sheen, J. Map Kinase Signalling Cascade in Arabidopsis Innate Immunity. *Nature* **2002**, *415*, 977–983, doi:10.1038/415977a.
 31. Qiu, J.L.; Zhou, L.; Yun, B.W.; Nielsen, H.B.; Fiil, B.K.; Petersen, K.; MacKinlay, J.; Loake, G.J.; Mundy, J.; Morris, P.C. Arabidopsis Mitogen-Activated Protein Kinase Kinases MKK1 and MKK2 Have Overlapping Functions in Defence Signalling Mediated by MEKK1, MPK4, and MKS1. *Plant Physiol.* **2008**, *148*, 212–222, doi:10.1104/pp.108.120006.
 32. Meng, X.; Zhang, S. MAPK Cascades in Plant Disease Resistance Signalling. *Annu. Rev. Phytopathol.* **2013**, *51*, 245–266, doi:10.1146/annurev-phyto-082712-102314.
 33. Sopena-Torres, S.; Jordá, L.; Sánchez-Rodríguez, C.; Miedes, E.; Escudero, V.; Swami, S.; López, G.; Piślewska-Bednarek, M.; Lassowskat, I.; Lee, J.; et al. YODA MAP3K Kinase Regulates Plant Immune Responses Conferring Broad-Spectrum Disease Resistance. *New Phytol.* **2018**, *218*, 661–680, doi:https://doi.org/10.1111/nph.15007.
 34. Cutler, S.R.; Rodriguez, P.L.; Finkelstein, R.R.; Abrams, S.R. Abscisic Acid: Emergence of a Core Signalling Network. *Annu. Rev. Plant Biol.* **2010**, *61*, 651–679, doi:10.1146/annurev-arplant-042809-112122.
 35. Umezawa, T.; Nakashima, K.; Miyakawa, T.; Kuromori, T.; Tanokura, M.; Shinozaki, K.; Yamaguchi-Shinozaki, K. Molecular Basis of the Core Regulatory Network in ABA Responses: Sensing, Signalling and Transport. *Plant Cell Physiol.* **2010**, *51*, 1821–1839, doi:10.1093/pcp/pcq156.
 36. Wang, P.; Xue, L.; Batelli, G.; Lee, S.; Hou, Y.-J.; Van Oosten, M.J.; Zhang, H.; Tao, W.A.; Zhu, J.-K. Quantitative Phosphoproteomics Identifies SnRK2 Protein Kinase Substrates and Reveals the Effectors of Abscisic Acid Action. *Proc. Natl. Acad. Sci.* **2013**, *110*, 11205–11210, doi:10.1073/pnas.1308974110.
 37. Melotto, M.; Underwood, W.; Koczan, J.; Nomura, K.; He, S.Y. Plant Stomata Function in Innate Immunity against Bacterial Invasion. *Cell* **2006**, *126*, 969–980, doi:10.1016/j.cell.2006.06.054.
 38. Du, M.; Zhai, Q.; Deng, L.; Li, S.; Li, H.; Yan, L.; Huang, Z.; Wang, B.; Jiang, H.; Huang, T.; et al.

- Closely Related NAC Transcription Factors of Tomato Differentially Regulate Stomatal Closure and Reopening during Pathogen Attack. *Plant Cell* **2014**, *26*, 3167–3184, doi:10.1105/tpc.114.128272.
39. De Torres-Zabala, M.; Truman, W.; Bennett, M.H.; Lafforgue, G.; Mansfield, J.W.; Rodriguez Egea, P.; Bögre, L.; Grant, M. Pseudomonas Syringae Pv. Tomato Hijacks the Arabidopsis Abscisic Acid Signalling Pathway to Cause Disease. *EMBO J.* **2007**, *26*, 1434–1443, doi:10.1038/sj.emboj.7601575.
 40. Ton, J.; Flors, V.; Mauch-Mani, B. The Multifaceted Role of ABA in Disease Resistance. *Trends Plant Sci.* **2009**, *14*, 310–317, doi:https://doi.org/10.1016/j.tplants.2009.03.006.
 41. Acharya, B.R.; Jeon, B.W.; Zhang, W.; Assmann, S.M. Open Stomata 1 (OST1) Is Limiting in Abscisic Acid Responses of Arabidopsis Guard Cells. *New Phytol.* **2013**, *200*, 1049–1063, doi:https://doi.org/10.1111/nph.12469.
 42. Vahisalu, T.; Kollist, H.; Wang, Y.-F.; Nishimura, N.; Chan, W.-Y.; Valerio, G.; Lamminmäki, A.; Brosché, M.; Moldau, H.; Desikan, R.; et al. SLAC1 Is Required for Plant Guard Cell S-Type Anion Channel. *Nature* **2008**, *452*, 487–491, doi:10.1038/nature06608.SLAC1.
 43. Mustilli, A.C.; Merlot, S.; Vavasseur, A.; Fenzi, F.; Giraudat, J. Arabidopsis OST1 Protein Kinase Mediates the Regulation of Stomatal Aperture by Abscisic Acid and Acts Upstream of Reactive Oxygen Species Production. *Plant Cell* **2002**, *14*, 3089–3099, doi:10.1105/tpc.007906.
 44. Guzel Deger, A.; Scherzer, S.; Nuhkat, M.; Kedzierska, J.; Kollist, H.; Brosché, M.; Unyayar, S.; Boudsocq, M.; Hedrich, R.; Roelfsema, M.R.G. Guard Cell SLAC1-Type Anion Channels Mediate Flagellin-Induced Stomatal Closure. *New Phytol.* **2015**, *208*, 162–173, doi:10.1111/nph.13435.
 45. Kadota, Y.; Sklenar, J.; Derbyshire, P.; Stransfeld, L.; Asai, S.; Ntoukakis, V.; Jones, J.D.; Shirasu, K.; Menke, F.; Jones, A.; et al. Direct Regulation of the NADPH Oxidase RBOHD by the PRR-Associated Kinase BIK1 during Plant Immunity. *Mol. Cell* **2014**, *54*, 43–55, doi:10.1016/j.molcel.2014.02.021.
 46. Arnaud, D.; Hwang, I. A Sophisticated Network of Signalling Pathways Regulates Stomatal Defences to Bacterial Pathogens. *Mol. Plant* **2015**, *8*, 566–581, doi:10.1016/j.molp.2014.10.012.
 47. Montillet, J.L.; Leonhardt, N.; Mondy, S.; Tranchimand, S.; Rumeau, D.; Boudsocq, M.; Garcia, A.V.; Douki, T.; Bigeard, J.; Laurière, C.; et al. An Abscisic Acid-Independent Oxylinin Pathway Controls Stomatal Closure and Immune Defence in Arabidopsis. *PLoS Biol.* **2013**, *11*, 13–15, doi:10.1371/journal.pbio.1001513.
 48. Jammes, F.; Yang, X.; Xiao, S.; Kwak, J.M. Two Arabidopsis Guard Cell-Preferential MAPK Genes, MPK9 and MPK12, Function in Biotic Stress Response. *Plant Signal. Behav.* **2011**, *6*, 1875–1877, doi:10.4161/psb.6.11.17933.
 49. Jammes, F.; Song, C.; Shin, D.; Munemasa, S.; Takeda, K.; Gu, D.; Cho, D.; Lee, S.; Giordo, R.; Sritubtim, S.; et al. MAP Kinases MPK9 and MPK12 Are Preferentially Expressed in Guard Cells and Positively Regulate ROS-Mediated ABA Signalling. *Proc. Natl. Acad. Sci. U. S. A.* **2009**, *106*, 20520–20525, doi:10.1073/pnas.0907205106.
 50. Zeng, W.; Brutus, A.; Kremer, J.M.; Withers, J.C.; Gao, X.; Jones, A.D.; He, S.Y. A Genetic Screen Reveals Arabidopsis Stomatal and/or Apoplastic Defences against Pseudomonas Syringae Pv. Tomato DC3000. *PLOS Pathog.* **2011**, *7*, e1002291.
 51. Zeng, W.; He, S.Y. A Prominent Role of the Flagellin Receptor FLAGELLIN-SENSING2 in Mediating Stomatal Response to Pseudomonas Syringae Pv Tomato DC3000 in Arabidopsis. *Plant Physiol.* **2010**, *153*, 1188–1198, doi:10.1104/pp.110.157016.
 52. Prophan, M.Y.; Munemasa, S.; Nahar, M.N.E.N.; Nakamura, Y.; Murata, Y. Guard Cell Salicylic Acid Signalling Is Integrated into Abscisic Acid Signalling via the Ca²⁺/CPK-Dependent Pathway. *Plant Physiol.* **2018**, *178*, 441–450, doi:10.1104/pp.18.00321.
 53. Zheng, X.; Zhou, M.; Yoo, H.; Pruneda-Paz, J.L.; Spivey, N.W.; Kay, S.A.; Dong, X. Spatial and Temporal Regulation of Biosynthesis of the Plant Immune Signal Salicylic Acid. *Proc. Natl. Acad. Sci.* **2015**, *112*, 9166–9173, doi:10.1073/pnas.1511182112.
 54. Melotto, M.; Zhang, L.; Oblessuc, P.R.; He, S.Y. Stomatal Defence a Decade Later. *Plant Physiol.* **2017**, *174*, 561–571, doi:10.1104/pp.16.01853.
 55. Zamora, O.; Schulze, S.; Azoulay-Shemer, T.; Parik, H.; Unt, J.; Brosché, M.; Schroeder, J.I.; Yarmolinsky, D.; Kollist, H. Jasmonic Acid and Salicylic Acid Play Minor Roles in Stomatal Regulation by CO₂, Abscisic Acid, Darkness, Vapor Pressure Deficit and Ozone. *Plant J.* **2021**, *108*, 134–150, doi:https://doi.org/10.1111/tpj.15430.
 56. Yan, S.; McLamore, E.S.; Dong, S.; Gao, H.; Taguchi, M.; Wang, N.; Zhang, T.; Su, X.; Shen, Y.

- The Role of Plasma Membrane H⁺-ATPase in Jasmonate-Induced Ion Fluxes and Stomatal Closure in *Arabidopsis thaliana*. *Plant J.* **2015**, *83*, 638–649, doi:<https://doi.org/10.1111/tpj.12915>.
57. Munemasa, S.; Oda, K.; Watanabe-Sugimoto, M.; Nakamura, Y.; Shimoishi, Y.; Murata, Y. The Coronatine-Insensitive 1 Mutation Reveals the Hormonal Signalling Interaction between Abscisic Acid and Methyl Jasmonate in *Arabidopsis* Guard Cells. Specific Impairment of Ion Channel Activation and Second Messenger Production. *Plant Physiol.* **2007**, *143*, 1398–1407, doi:[10.1104/pp.106.091298](https://doi.org/10.1104/pp.106.091298).
 58. Savchenko, T.; Kolla, V.A.; Wang, C.-Q.; Nasafi, Z.; Hicks, D.R.; Phadungchob, B.; Chehab, W.E.; Brandizzi, F.; Froehlich, J.; Dehesh, K. Functional Convergence of Oxylinin and Abscisic Acid Pathways Controls Stomatal Closure in Response to Drought. *Plant Physiol.* **2014**, *164*, 1151–1160, doi:[10.1104/pp.113.234310](https://doi.org/10.1104/pp.113.234310).
 59. Berge, O.; Monteil, C.L.; Bartoli, C.; Chandeysson, C.; Guilbaud, C.; Sands, D.C.; Morris, C.E. A User's Guide to a Data Base of the Diversity of *Pseudomonas Syringae* and Its Application to Classifying Strains in This Phylogenetic Complex. *PLoS One* **2014**, *9*, e105547.
 60. Whalen, M.C.; Innes, R.W.; Bent, A.F.; Staskawicz, B.J. Identification of *Pseudomonas Syringae* Pathogens of *Arabidopsis* and a Bacterial Locus Determining Avirulence on Both *Arabidopsis* and Soybean. *Plant Cell* **1991**, *3*, 49–59, doi:[10.1105/tpc.3.1.49](https://doi.org/10.1105/tpc.3.1.49).
 61. Melotto, M.; Underwood, W.; He, S.Y. Role of Stomata in Plant Innate Immunity and Foliar Bacterial Diseases. *Annu. Rev. Phytopathol.* **2008**, *46*, 101–122, doi:[10.1146/annurev.phyto.121107.104959](https://doi.org/10.1146/annurev.phyto.121107.104959).
 62. Su, J.; Zhang, M.; Zhang, L.; Sun, T.; Liu, Y.; Lukowitz, W.; Xu, J.; Zhang, S. Regulation of Stomatal Immunity by Interdependent Functions of a Pathogen-Responsive MPK3/MPK6 Cascade and Abscisic Acid. *Plant Cell* **2017**, *29*, 526–542, doi:[10.1105/tpc.16.00577](https://doi.org/10.1105/tpc.16.00577).
 63. Yan, J.; Zhang, C.; Gu, M.; Bai, Z.; Zhang, W.; Qi, T.; Cheng, Z.; Peng, W.; Luo, H.; Nan, F.; et al. The *Arabidopsis* CORONATINE INSENSITIVE1 Protein Is a Jasmonate Receptor. *Plant Cell* **2009**, *21*, 2220–2236, doi:[10.1105/tpc.109.065730](https://doi.org/10.1105/tpc.109.065730).
 64. Geng, X.; Jin, L.; Shimada, M.; Kim, M.G.; Mackey, D. The Phytotoxin Coronatine Is a Multifunctional Component of the Virulence Armament of *Pseudomonas Syringae*. *Planta* **2014**, *240*, 1149–1165, doi:[10.1007/s00425-014-2151-x](https://doi.org/10.1007/s00425-014-2151-x).
 65. Toum, L.; Torres, P.S.; Gallego, S.M.; Benavides, M.P.; Vojnov, A.A.; Gudesblat, G.E. Coronatine Inhibits Stomatal Closure through Guard Cell-Specific Inhibition of NADPH Oxidase-Dependent ROS Production. *Front. Plant Sci.* **2016**, *7*, 1–12, doi:[10.3389/fpls.2016.01851](https://doi.org/10.3389/fpls.2016.01851).
 66. Mine, A.; Berens, M.L.; Nobori, T.; Anver, S.; Fukumoto, K.; Winkelmüller, T.M.; Takeda, A.; Becker, D.; Tsuda, K. Pathogen Exploitation of an Abscisic Acid- and Jasmonate-Inducible MAPK Phosphatase and Its Interception by *Arabidopsis* Immunity. *Proc. Natl. Acad. Sci. U. S. A.* **2017**, *114*, 7456–7461, doi:[10.1073/pnas.1702613114](https://doi.org/10.1073/pnas.1702613114).
 67. Piasecka, A.; Jedrzejczak-Rey, N.; Bednarek, P. Secondary Metabolites in Plant Innate Immunity: Conserved Function of Divergent Chemicals. *New Phytol.* **2015**, *206*, 948–964, doi:<https://doi.org/10.1111/nph.13325>.
 68. Maag, D.; Erb, M.; Köllner, T.G.; Gershenzon, J. Defensive Weapons and Defence Signals in Plants: Some Metabolites Serve Both Roles. *BioEssays* **2015**, *37*, 167–174, doi:<https://doi.org/10.1002/bies.201400124>.
 69. Dixon, R.A. Natural Products and Plant Disease Resistance. *Nature* **2001**, *411*, 843–847, doi:[10.1038/35081178](https://doi.org/10.1038/35081178).
 70. Cheynier, V.; Comte, G.; Davies, K.M.; Lattanzio, V.; Martens, S. Plant Phenolics: Recent Advances on Their Biosynthesis, Genetics, and Ecophysiology. *Plant Physiol. Biochem.* **2013**, *72*, 1–20, doi:<https://doi.org/10.1016/j.plaphy.2013.05.009>.
 71. Balasundram, N.; Sundram, K.; Samman, S. Phenolic Compounds in Plants and Agri-Industrial by-Products: Antioxidant Activity, Occurrence, and Potential Uses. *Food Chem.* **2006**, *99*, 191–203, doi:<https://doi.org/10.1016/j.foodchem.2005.07.042>.
 72. Pereira, D.M.; Valentão, P.; Pereira, J.A.; Andrade, P.B. Phenolics: From Chemistry to Biology. *Molecules* **2009**, *14*, 2202–2211, doi:[10.3390/molecules14062202](https://doi.org/10.3390/molecules14062202).
 73. Delaney, T.P.; Uknes, S.; Vernooij, B.; Friedrich, L.; Weymann, K.; Negrotto, D.; Gaffney, T.; Gut-Rella, M.; Kessmann, H.; Ward, E.; et al. A Central Role of Salicylic Acid in Plant Disease Resistance. *Science (80-.)*. **1994**, *266*, 1247–1250, doi:[10.1126/science.266.5188.1247](https://doi.org/10.1126/science.266.5188.1247).
 74. Ding, P.; Ding, Y. Stories of Salicylic Acid: A Plant Defence Hormone. *Trends Plant Sci.* **2020**, *25*, 549–565, doi:[10.1016/j.tplants.2020.01.004](https://doi.org/10.1016/j.tplants.2020.01.004).

75. Gaffney, T.; Friedrich, L.; Vernooij, B.; Negrotto, D.; Nye, G.; Uknes, S.; Ward, E.; Kessmann, H.; Ryals, J. Requirement of Salicylic Acid for the Induction of Systemic Acquired Resistance. *Science (80-)*. **1993**, *261*, 754–756, doi:10.1126/science.261.5122.754.
76. Strawn, M.A.; Marr, S.K.; Inoue, K.; Inada, N.; Zubieta, C.; Wildermuth, M.C. Arabidopsis Isochorismate Synthase Functional in Pathogen-Induced Salicylate Biosynthesis Exhibits Properties Consistent with a Role in Diverse Stress Responses*. *J. Biol. Chem.* **2007**, *282*, 5919–5933, doi:https://doi.org/10.1074/jbc.M605193200.
77. Nawrath, C.; Métraux, J.-P. Salicylic Acid Induction–Deficient Mutants of Arabidopsis Express PR-2 and PR-5 and Accumulate High Levels of Camalexin after Pathogen Inoculation. *Plant Cell* **1999**, *11*, 1393–1404, doi:10.1105/tpc.11.8.1393.
78. Rekhter, D.; Lüdke, D.; Ding, Y.; Feussner, K.; Zienkiewicz, K.; Lipka, V.; Wiermer, M.; Zhang, Y.; Feussner, I. Isochorismate-Derived Biosynthesis of the Plant Stress Hormone Salicylic Acid. *Science (80-)*. **2019**, *365*, 498–502, doi:10.1126/science.aaw1720.
79. Dempsey, D.A.; Vlot, A.C.; Wildermuth, M.C.; Klessig, D.F. Salicylic Acid Biosynthesis and Metabolism. *Arab. B.* **2011**, *9*, e0156, doi:10.1199/tab.0156.
80. Enyedi, A.J.; Yalpani, N.; Silverman, P.; Raskin, I. Localization, Conjugation, and Function of Salicylic Acid in Tobacco during the Hypersensitive Reaction to Tobacco Mosaic Virus. *Proc. Natl. Acad. Sci.* **1992**, *89*, 2480–2484, doi:10.1073/pnas.89.6.2480.
81. Dean, J. V.; Shah, R.P.; Mohammed, L.A. Formation and Vacuolar Localization of Salicylic Acid Glucose Conjugates in Soybean Cell Suspension Cultures. *Physiol. Plant.* **2003**, *118*, 328–336, doi:https://doi.org/10.1034/j.1399-3054.2003.00117.x.
82. Snoeren, T.A.L.; Mumm, R.; Poelman, E.H.; Yang, Y.; Pichersky, E.; Dicke, M. The Herbivore-Induced Plant Volatile Methyl Salicylate Negatively Affects Attraction of the Parasitoid *Diadegma Semicausum*. *J. Chem. Ecol.* **2010**, *36*, 479–489, doi:10.1007/s10886-010-9787-1.
83. Zhang, Y.J.; Zhao, L.; Zhao, J.Z.; Li, Y.J.; Wang, J. Bin; Guo, R.; Gan, S.S.; Liu, C.J.; Zhanga, K.W. S5H/DMR6 Encodes a Salicylic Acid 5-Hydroxylase That Fine-Tunes Salicylic Acid Homeostasis. *Plant Physiol.* **2017**, *175*, 1082–1093, doi:10.1104/pp.17.00695.
84. Zhang, K.; Halitschke, R.; Yin, C.; Liu, C.J.; Gan, S.S. Salicylic Acid 3-Hydroxylase Regulates Arabidopsis Leaf Longevity by Mediating Salicylic Acid Catabolism. *Proc. Natl. Acad. Sci. U. S. A.* **2013**, *110*, 14807–14812, doi:10.1073/pnas.1302702110.
85. WALKER, N.; WILTSHIRE, G.H. The Breakdown of Naphthalene by a Soil Bacterium. *J. Gen. Microbiol.* **1953**, *8*, 273–276, doi:10.1099/00221287-8-2-273.
86. Lutwak-Mann, C. The Excretion of a Metabolic Product of Salicylic Acid. *Biochem. J.* **1943**, *37*, 246–248, doi:10.1042/bj0370246.
87. Ibrahim, Ragai K.; Towers, G.H.N. Conversion of Salicylic Acid to Gentisic Acid and O-Pyrocatechuic Acid, All Labelled with Carbon-14, in Plants. *Nature* **1959**, 4701.
88. Abedi, F.; Razavi, B.M.; Hosseinzadeh, H. A Review on Gentisic Acid as a Plant Derived Phenolic Acid and Metabolite of Aspirin: Comprehensive Pharmacology, Toxicology, and Some Pharmaceutical Aspects. *Phyther. Res.* **2020**, *34*, 729–741, doi:https://doi.org/10.1002/ptr.6573.
89. Bellés, J.M.; Garro, R.; Fayos, J.; Navarro, P.; Primo, J.; Conejero, V. Gentisic Acid As a Pathogen-Inducible Signal, Additional to Salicylic Acid for Activation of Plant Defences in Tomato. *Mol. Plant-Microbe Interact.* **1999**, *12*, 227–235, doi:10.1094/MPMI.1999.12.3.227.
90. Campos, L.; Granell, P.; Tàrraga, S.; López-Gresa, P.; Conejero, V.; Bellés, J.M.; Rodrigo, I.; Lisón, P. Salicylic Acid and Gentisic Acid Induce RNA Silencing-Related Genes and Plant Resistance to RNA Pathogens. *Plant Physiol. Biochem.* **2014**, *77*, 35–43, doi:https://doi.org/10.1016/j.plaphy.2014.01.016.
91. Bellés, J.M.; Garro, R.; Pallás, V.; Fayos, J.; Rodrigo, I.; Conejero, V. Accumulation of Gentisic Acid as Associated with Systemic Infections but Not with the Hypersensitive Response in Plant-Pathogen Interactions. *Planta* **2006**, *223*, 500–511, doi:10.1007/s00425-005-0109-8.
92. Pichersky, E.; Noel, J.P.; Dudareva, N. Biosynthesis of Plant Volatiles: Nature’s Diversity and Ingenuity. *Science (80-)*. **2006**, *311*, 808–811, doi:10.1126/science.1118510.
93. Dudareva, N.; Klempien, A.; Muhlemann, J.K.; Kaplan, I. Biosynthesis, Function and Metabolic Engineering of Plant Volatile Organic Compounds. *New Phytol.* **2013**, *198*, 16–32, doi:10.1111/nph.12145.
94. Kessler, A.; Baldwin, I.T. Defensive Function of Herbivore-Induced Plant Volatile Emissions in Nature. *Science (80-)*. **2001**, *291*, 2141–2144, doi:10.1126/science.291.5511.2141.

95. Huang, M.; Sanchez-Moreiras, A.M.; Abel, C.; Sohrabi, R.; Lee, S.; Gershenzon, J.; Tholl, D. The Major Volatile Organic Compound Emitted from Arabidopsis Thaliana Flowers, the Sesquiterpene (E)- β -Caryophyllene, Is a Defence against a Bacterial Pathogen. *New Phytol.* **2012**, *193*, 997–1008, doi:https://doi.org/10.1111/j.1469-8137.2011.04001.x.
96. Kim, J.; Felton, G.W. Priming of Antiherbivore Defensive Responses in Plants. *Insect Sci.* **2013**, *20*, 273–285, doi:https://doi.org/10.1111/j.1744-7917.2012.01584.x.
97. Hammerbacher, A.; Coutinho, T.A.; Gershenzon, J. Roles of Plant Volatiles in Defence against Microbial Pathogens and Microbial Exploitation of Volatiles. *Plant. Cell Environ.* **2019**, *42*, 2827–2843, doi:https://doi.org/10.1111/pce.13602.
98. Dudareva, N.; Negre, F.; Nagegowda, D.A.; Orlova, I. Plant Volatiles: Recent Advances and Future Perspectives. *CRC Crit. Rev. Plant Sci.* **2006**, *25*, 417–440, doi:10.1080/07352680600899973.
99. D'Auria, J.C.; Pichersky, E.; Schaub, A.; Hansel, A.; Gershenzon, J. Characterization of a BAHD Acyltransferase Responsible for Producing the Green Leaf Volatile (Z)-3-Hexen-1-Yl Acetate in Arabidopsis Thaliana. *Plant J.* **2007**, *49*, 194–207, doi:https://doi.org/10.1111/j.1365-313X.2006.02946.x.
100. ul Hassan, M.N.; Zainal, Z.; Ismail, I. Green Leaf Volatiles: Biosynthesis, Biological Functions and Their Applications in Biotechnology. *Plant Biotechnol. J.* **2015**, *13*, 727–739, doi:https://doi.org/10.1111/pbi.12368.
101. Matsui, K. Green Leaf Volatiles: Hydroperoxide Lyase Pathway of Oxylipin Metabolism. *Curr. Opin. Plant Biol.* **2006**, *9*, 274–280, doi:https://doi.org/10.1016/j.pbi.2006.03.002.
102. Matsui, K.; Engelberth, J.; Antonio, S. Green Leaf Volatiles (GLVs) Is a Generic Name for Volatile Compounds Consisting of Six ©. **2022**, 1–31.
103. Kishimoto, K.; Matsui, K.; Ozawa, R.; Takabayashi, J. Direct Fungicidal Activities of C6-Aldehydes Are Important Constituents for Defence Responses in Arabidopsis against Botrytis Cinerea. *Phytochemistry* **2008**, *69*, 2127–2132, doi:https://doi.org/10.1016/j.phytochem.2008.04.023.
104. Scala, A.; Allmann, S.; Mirabella, R.; Haring, M.A.; Schuurink, R.C. Green Leaf Volatiles: A Plant's Multifunctional Weapon against Herbivores and Pathogens. *Int. J. Mol. Sci.* **2013**, *14*, 17781–17811.
105. Ozawa, R.; Shiojiri, K.; Matsui, K.; Takabayashi, J. Intermittent Exposure to Traces of Green Leaf Volatiles Triggers the Production of (Z)-3-Hexen-1-Yl Acetate and (Z)-3-Hexen-1-Ol in Exposed Plants. *Plant Signal. Behav.* **2013**, *8*, 7–8, doi:10.4161/psb.27013.
106. Mariutto, M.; Duby, F.; Adam, A.; Bureau, C.; Fauconnier, M.-L.; Ongena, M.; Thonart, P.; Dommes, J. The Elicitation of a Systemic Resistance by Pseudomonas Putida BTP1 in Tomato Involves the Stimulation of Two Lipoxygenase Isoforms. *BMC Plant Biol.* **2011**, *11*, 29, doi:10.1186/1471-2229-11-29.
107. Goulet, C.; Kamiyoshihara, Y.; Lam, N.B.; Richard, T.; Taylor, M.G.; Tieman, D.M.; Klee, H.J. Divergence in the Enzymatic Activities of a Tomato and Solanum Pennellii Alcohol Acyltransferase Impacts Fruit Volatile Ester Composition. *Mol. Plant* **2015**, *8*, 153–162, doi:10.1016/j.molp.2014.11.007.
108. Lisón, P.; Lopez-Gresa, M.; Rodrigo, I.; Bellés, J. Use of a Compound Por Plant Protection Trough Stomata Closure and Application Method PCT/ES2018/070. **2017**.
109. Pandey, P.; Irulappan, V.; Bagavathiannan, M. V.; Senthil-Kumar, M. Impact of Combined Abiotic and Biotic Stresses on Plant Growth and Avenues for Crop Improvement by Exploiting Physio-Morphological Traits. *Front. Plant Sci.* **2017**, *8*, 1–15, doi:10.3389/fpls.2017.00537.
110. Reddy, P. *Climate Resilient Agriculture for Ensuring Food Security*; 2015; ISBN 978-81-322-2198-2.
111. Cabrera-De la Fuente, M.; González-Morales, S.; Juárez-Maldonado, A.; Leija-Martínez, P.; Benavides-Mendoza, A. Chapter 4 - Plant Nutrition and Agronomic Management to Obtain Crops With Better Nutritional and Nutraceutical Quality. In *Handbook of Food Bioengineering*; Holban, A.M., Grumezescu, A.M.B.T.-T.F., Eds.; Academic Press, 2018; pp. 99–140 ISBN 978-0-12-811517-6.
112. Mittler, R.; Blumwald, E. Genetic Engineering for Modern Agriculture: Challenges and Perspectives. *Annu. Rev. Plant Biol.* **2010**, *61*, 443–462, doi:10.1146/annurev-arplant-042809-112116.
113. Alagna, F.; Balestrini, R.; Chitarra, W.; Marsico, A.D.; Nerva, L. *Getting Ready with the Priming: Innovative Weapons against Biotic and Abiotic Crop Enemies in a Global Changing Scenario*; Elsevier Inc., 2020; ISBN 9780128178935.
114. Conrath, U.; Beckers, G.J.M.; Langenbach, C.J.G.; Jaskiewicz, M.R. Priming for Enhanced Defence.

- Annu. Rev. Phytopathol.* **2015**, *53*, 97–119, doi:10.1146/annurev-phyto-080614-120132.
115. Boutrot, F.; Zipfel, C. Function, Discovery, and Exploitation of Plant Pattern Recognition Receptors for Broad-Spectrum Disease Resistance. *Annu. Rev. Phytopathol.* **2017**, *55*, 257–286, doi:10.1146/annurev-phyto-080614-120106.
 116. Schwessinger, B.; Ronald, P.C. Plant Innate Immunity: Perception of Conserved Microbial Signatures. *Annu. Rev. Plant Biol.* **2012**, *63*, 451–482, doi:10.1146/annurev-arplant-042811-105518.
 117. Yang, B.; Yang, S.; Zheng, W.; Wang, Y. Plant Immunity Inducers: From Discovery to Agricultural Application. *Stress Biol.* **2022**, *2*, doi:10.1007/s44154-021-00028-9.
 118. Bektas, Y.; Eulgem, T. Synthetic Plant Defence Elicitors. *Front. Plant Sci.* **2015**, *5*, 1–9, doi:10.3389/fpls.2014.00804.
 119. Hayafune, M.; Berisio, R.; Marchetti, R.; Silipo, A.; Kayama, M.; Desaki, Y.; Arima, S.; Squeglia, F.; Ruggiero, A.; Tokuyasu, K.; et al. Chitin-Induced Activation of Immune Signalling by the Rice Receptor CEBiP Relies on a Unique Sandwich-Type Dimerization. *Proc. Natl. Acad. Sci.* **2014**, *111*, E404–E413, doi:10.1073/pnas.1312099111.
 120. Ron, M.; Avni, A. The Receptor for the Fungal Elicitor Ethylene-Inducing Xylanase Is a Member of a Resistance-Like Gene Family in Tomato. *Plant Cell* **2004**, *16*, 1604–1615, doi:10.1105/tpc.022475.
 121. Bertsche, U.; Mayer, C.; Götz, F.; Gust, A.A. Peptidoglycan Perception—Sensing Bacteria by Their Common Envelope Structure. *Int. J. Med. Microbiol.* **2015**, *305*, 217–223, doi:https://doi.org/10.1016/j.ijmm.2014.12.019.
 122. War, A.R.; Taggar, G.K.; Hussain, B.; Taggar, M.S.; Nair, R.M.; Sharma, H.C. Plant Defence against Herbivory and Insect Adaptations. *AoB Plants* **2018**, *10*, ply037, doi:10.1093/aobpla/ply037.
 123. Shinya, T.; Hojo, Y.; Desaki, Y.; Christeller, J.T.; Okada, K.; Shibuya, N.; Galis, I. Modulation of Plant Defence Responses to Herbivores by Simultaneous Recognition of Different Herbivore-Associated Elicitors in Rice. *Sci. Rep.* **2016**, *6*, 32537, doi:10.1038/srep32537.
 124. Fürstenberg-Hägg, J.; Zagrobelny, M.; Bak, S. Plant Defence against Insect Herbivores. *Int. J. Mol. Sci.* **2013**, *14*, 10242–10297.
 125. Savvides, A.; Ali, S.; Tester, M.; Fotopoulos, V. Chemical Priming of Plants Against Multiple Abiotic Stresses: Mission Possible? *Trends Plant Sci.* **2016**, *21*, 329–340, doi:10.1016/j.tplants.2015.11.003.
 126. Sako, K.; Nguyen, H.M.; Seki, M. Advances in Chemical Priming to Enhance Abiotic Stress Tolerance in Plants. *Plant Cell Physiol.* **2020**, *61*, 1995–2003, doi:10.1093/pcp/pcaa119.
 127. Heimpel, G.E.; Mills, N.J. *Biological Control*; Cambridge University Press, 2017; ISBN 0521845149.
 128. Tripathi, D.; Raikhy, G.; Kumar, D. Chemical Elicitors of Systemic Acquired Resistance—Salicylic Acid and Its Functional Analogs. *Curr. Plant Biol.* **2019**, *17*, 48–59, doi:https://doi.org/10.1016/j.cpb.2019.03.002.
 129. Chanda, B.; Venugopal, S.C.; Kulshrestha, S.; Navarre, D.A.; Downie, B.; Vaillancourt, L.; Kachroo, A.; Kachroo, P. Glycerol-3-Phosphate Levels Are Associated with Basal Resistance to the Hemibiotrophic Fungus *Colletotrichum Higginsianum* in *Arabidopsis*. *Plant Physiol.* **2008**, *147*, 2017–2029, doi:10.1104/pp.108.121335.
 130. Chanda, B.; Xia, Y.; Mandal, M.K.; Yu, K.; Sekine, K.; Gao, Q.; Selote, D.; Hu, Y.; Stromberg, A.; Navarre, D.; et al. Glycerol-3-Phosphate Is a Critical Mobile Inducer of Systemic Immunity in Plants. *Nat. Genet.* **2011**, *43*, 421–427, doi:10.1038/ng.798.
 131. Jung, H.W.; Tschaplinski, T.J.; Wang, L.; Glazebrook, J.; Greenberg, J.T. Priming in Systemic Plant Immunity. *Science (80-.)*. **2009**, *324*, 89–91, doi:10.1126/science.1170025.
 132. Aksakal, O.; Algur, O.F.; Icoglu Aksakal, F.; Aysin, F. Exogenous 5-Aminolevulinic Acid Alleviates the Detrimental Effects of UV-B Stress on Lettuce (*Lactuca Sativa* L) Seedlings. *Acta Physiol. Plant.* **2017**, *39*, 55, doi:10.1007/s11738-017-2347-3.
 133. Zhang, Z.J.; Li, H.Z.; Zhou, W.J.; Takeuchi, Y.; Yoneyama, K. Effect of 5-Aminolevulinic Acid on Development and Salt Tolerance of Potato (*Solanum Tuberosum* L.) Microtubers in Vitro. *Plant Growth Regul.* **2006**, *49*, 27–34, doi:10.1007/s10725-006-0011-9.
 134. Hosseinfard, M.; Stefaniak, S.; Ghorbani Javid, M.; Soltani, E.; Wojtyła, Ł.; Garnczarska, M. Contribution of Exogenous Proline to Abiotic Stresses Tolerance in Plants: A Review. *Int. J. Mol. Sci.* **2022**, *23*.

135. Zulfiqar, F.; Nafees, M.; Chen, J.; Darras, A.; Ferrante, A.; Hancock, J.T.; Ashraf, M.; Zaid, A.; Latif, N.; Corpas, F.J.; et al. Chemical Priming Enhances Plant Tolerance to Salt Stress. *Front. Plant Sci.* **2022**, *13*, 1–22, doi:10.3389/fpls.2022.946922.
136. Freundlich, G.E.; Shields, M.; Frost, C.J. Dispensing a Synthetic Green Leaf Volatile to Two Plant Species in a Common Garden Differentially Alters Physiological Responses and Herbivory. *Agronomy* **2021**, *11*, doi:10.3390/agronomy11050958.
137. Song, G.C.; Ryu, C.-M. Two Volatile Organic Compounds Trigger Plant Self-Defence against a Bacterial Pathogen and a Sucking Insect in Cucumber under Open Field Conditions. *Int. J. Mol. Sci.* **2013**, *14*, 9803–9819.
138. Tahir, H.A.S.; Gu, Q.; Wu, H.; Raza, W.; Safdar, A.; Huang, Z.; Rajer, F.U.; Gao, X. Effect of Volatile Compounds Produced by *Ralstonia Solanacearum* on Plant Growth Promoting and Systemic Resistance Inducing Potential of *Bacillus Volatiles*. *BMC Plant Biol.* **2017**, *17*, 133, doi:10.1186/s12870-017-1083-6.
139. Riahi, C.; González-Rodríguez, J.; Alonso-Valiente, M.; Urbaneja, A.; Pérez-Hedo, M. Eliciting Plant Defences Through Herbivore-Induced Plant Volatiles' Exposure in Sweet Peppers. *Front. Ecol. Evol.* **2022**, *9*, 1–8, doi:10.3389/fevo.2021.776827.
140. Walters, D.R.; Ratsep, J.; Havis, N.D. Controlling Crop Diseases Using Induced Resistance: Challenges for the Future. *J. Exp. Bot.* **2013**, *64*, 1263–1280, doi:10.1093/jxb/ert026.
141. Cofer, T.M.; Engelberth, M.; Engelberth, J. Green Leaf Volatiles Protect Maize (*Zea Mays*) Seedlings against Damage from Cold Stress. *Plant Cell Environ.* **2018**, *41*, 1673–1682, doi:10.1111/pce.13204.
142. Tian, S.; Guo, R.; Zou, X.; Zhang, X.; Yu, X.; Zhan, Y.; Ci, D.; Wang, M.; Wang, Y.; Si, T. Priming with the Green Leaf Volatile (Z)-3-Hexeny-1-Yl Acetate Enhances Salinity Stress Tolerance in Peanut (*Arachis Hypogaea* L.) Seedlings. *Front. Plant Sci.* **2019**, *10*, doi:10.3389/fpls.2019.00785.
143. Park, S.-Y.; Fung, P.; Nishimura, N.; Jensen, D.R.; Fujii, H.; Zhao, Y.; Lumba, S.; Santiago, J.; Rodrigues, A.; Chow, T.F.; et al. Abscisic Acid Inhibits Type 2C Protein Phosphatases via the PYR/PYL Family of START Proteins. *Science (80-.)*. **2009**, *324*, 1068–1071, doi:10.1126/science.1173041.
144. Melcher, K.; Xu, Y.; Ng, L.-M.; Zhou, X.E.; Soon, F.-F.; Chinnusamy, V.; Suino-Powell, K.M.; Kovach, A.; Tham, F.S.; Cutler, S.R.; et al. Identification and Mechanism of ABA Receptor Antagonism. *Nat. Struct. & Mol. Biol.* **2010**, *17*, 1102–1108, doi:10.1038/nsmb.1887.
145. Okamoto, M.; Peterson, F.C.; Defries, A.; Park, S.-Y.; Endo, A.; Nambara, E.; Volkman, B.F.; Cutler, S.R. Activation of Dimeric ABA Receptors Elicits Guard Cell Closure, ABA-Regulated Gene Expression, and Drought Tolerance. *Proc. Natl. Acad. Sci.* **2013**, *110*, 12132–12137, doi:10.1073/pnas.1305919110.
146. Cao, M.; Liu, X.; Zhang, Y.; Xue, X.; Zhou, X.E.; Melcher, K.; Gao, P.; Wang, F.; Zeng, L.; Zhao, Y.; et al. An ABA-Mimicking Ligand That Reduces Water Loss and Promotes Drought Resistance in Plants. *Cell Res.* **2013**, *23*, 1043–1054, doi:10.1038/cr.2013.95.
147. Gonzalez-Guzman, M.; Rodriguez, L.; Lorenzo-Orts, L.; Pons, C.; Sarrion-Perdigones, A.; Fernandez, M.A.; Peirats-Llobet, M.; Forment, J.; Moreno-Alvero, M.; Cutler, S.R.; et al. Tomato PYR/PYL/RCAR Abscisic Acid Receptors Show High Expression in Root, Differential Sensitivity to the Abscisic Acid Agonist Quinabactin, and the Capability to Enhance Plant Drought Resistance. *J. Exp. Bot.* **2014**, *65*, 4451–4464, doi:10.1093/jxb/eru219.
148. Park, S.-Y.; Peterson, F.C.; Mosquna, A.; Yao, J.; Volkman, B.F.; Cutler, S.R. Agrochemical Control of Plant Water Use Using Engineered Abscisic Acid Receptors. *Nature* **2015**, *520*, 545–548, doi:10.1038/nature14123.
149. Wasternack, C. A Plant's Balance of Growth and Defence – Revisited. *New Phytol.* **2017**, *215*, 1291–1294, doi:https://doi.org/10.1111/nph.14720.
150. Huot, B.; Yao, J.; Montgomery, B.L.; He, S.Y. Growth–Defence Tradeoffs in Plants: A Balancing Act to Optimize Fitness. *Mol. Plant* **2014**, *7*, 1267–1287, doi:https://doi.org/10.1093/mp/ssu049.
151. Havko, N.E.; Major, I.T.; Jewell, J.B.; Attaran, E.; Browse, J.; Howe, G.A. Control of Carbon Assimilation and Partitioning by Jasmonate: An Accounting of Growth–Defence Tradeoffs. *Plants* **2016**, *5*, 41–66, doi:10.3390/plants5010007.
152. Zhang, Y.; Turner, J.G. Wound-Induced Endogenous Jasmonates Stunt Plant Growth by Inhibiting Mitosis. *PLoS One* **2008**, *3*, e3699.
153. Gordy, J.W.; Leonard, B.R.; Blouin, D.; Davis, J.A.; Stout, M.J. Comparative Effectiveness of

- Potential Elicitors of Plant Resistance against *Spodoptera Frugiperda* (J. E. Smith) (Lepidoptera: Noctuidae) in Four Crop Plants. *PLoS One* **2015**, *10*, e0136689.
154. FAO *Crops and Climate Change Impact Briefs*; 2022; ISBN 9789251355107.
 155. Fraga, H.; Malheiro, A.C.; Moutinho-Pereira, J.; Santos, J.A. An Overview of Climate Change Impacts on European Viticulture. *Food Energy Secur.* **2012**, *1*, 94–110, doi:10.1002/fes3.14.
 156. Easterling, D.R.; Meehl, G.A.; Parmesan, C.; Changnon, S.A.; Karl, T.R.; Mearns, L.O. Climate Extremes: Observations, Modeling, and Impacts. *Science (80-.)*. **2000**, *289*, 2068–2074, doi:10.1126/science.289.5487.2068.
 157. Karasali, H.; Kasiotis, K.M.; Machera, K.; Ambrus, A. Case Study To Illustrate an Approach for Detecting Contamination and Impurities in Pesticide Formulations. *J. Agric. Food Chem.* **2014**, *62*, 11347–11352, doi:10.1021/jf504729g.
 158. Tudi, M.; Daniel Ruan, H.; Wang, L.; Lyu, J.; Sadler, R.; Connell, D.; Chu, C.; Phung, D.T. Agriculture Development, Pesticide Application and Its Impact on the Environment. *Int. J. Environ. Res. Public Heal.* **2021**, *18*.
 159. Bhandari, G.; Atreya, K.; Yang, X.; Fan, L.; Geissen, V. Factors Affecting Pesticide Safety Behaviour: The Perceptions of Nepalese Farmers and Retailers. *Sci. Total Environ.* **2018**, *631–632*, 1560–1571, doi:https://doi.org/10.1016/j.scitotenv.2018.03.144.
 160. Pham, L. Van; Smith, C. Drivers of Agricultural Sustainability in Developing Countries: A Review. *Environ. Syst. Decis.* **2014**, *34*, 326–341, doi:10.1007/s10669-014-9494-5.
 161. Heeb, L.; Jenner, E.; Cock, M.J.W. Climate-Smart Pest Management: Building Resilience of Farms and Landscapes to Changing Pest Threats. *J. Pest Sci. (2004)*. **2019**, *92*, 951–969, doi:10.1007/s10340-019-01083-y.
 162. Chomel, M.; Guittonny-Larchevêque, M.; Fernandez, C.; Gallet, C.; DesRochers, A.; Paré, D.; Jackson, B.G.; Baldy, V. Plant Secondary Metabolites: A Key Driver of Litter Decomposition and Soil Nutrient Cycling. *J. Ecol.* **2016**, *104*, 1527–1541, doi:https://doi.org/10.1111/1365-2745.12644.
 163. Hartmann, T. Diversity and Variability of Plant Secondary Metabolism: A Mechanistic View BT - Proceedings of the 9th International Symposium on Insect-Plant Relationships. In: Städler, E., Rowell-Rahier, M., Bauer, R., Eds.; Springer Netherlands: Dordrecht, 1996; pp. 177–188 ISBN 978-94-009-1720-0.
 164. Jimenez-Garcia, S.N.; Vazquez-Cruz, M.A.; Guevara-González, R.G.; Torres-Pacheco, I.; Cruz-Hernandez, A.; Feregrino-Perez, A.A. Current Approaches for Enhanced Expression of Secondary Metabolites as Bioactive Compounds in Plants for Agronomic and Human Health Purposes. *Polish J. Food Nutr. Sci.* **2013**, *63*, 67–78, doi:10.2478/v10222-012-0072-6.
 165. Twajj, B.M.; Hasan, M.N. Bioactive Secondary Metabolites from Plant Sources: Types, Synthesis, and Their Therapeutic Uses. *Int. J. Plant Biol.* **2022**, *13*, 4–14.
 166. de Toledo Thomazella, D.P.; Seong, K.; Mackelprang, R.; Dahlbeck, D.; Geng, Y.; Gill, U.S.; Qi, T.; Pham, J.; Giuseppe, P.; Lee, C.Y.; et al. Loss of Function of a DMR6 Ortholog in Tomato Confers Broad-Spectrum Disease Resistance. *Proc. Natl. Acad. Sci. U. S. A.* **2021**, *118*, doi:10.1073/pnas.2026152118.
 167. Brading, P.A.; Hammond-Kosack, K.E.; Parr, A.; Jones, J.D.G. Salicylic Acid Is Not Required for Cf-2- and Cf-9-Dependent Resistance of Tomato to *Cladosporium Fulvum*. *Plant J.* **2000**, *23*, 305–318, doi:https://doi.org/10.1046/j.1365-313x.2000.00778.x.
 168. Oldroyd, G.E.D.; Staskawicz, B.J. Genetically Engineered Broad-Spectrum Disease Resistance in Tomato. *Proc. Natl. Acad. Sci.* **1998**, *95*, 10300–10305, doi:10.1073/pnas.95.17.10300.
 169. Li, X.; Clarke, J.D.; Zhang, Y.; Dong, X. Activation of an EDS1-Mediated R-Gene Pathway in the *Snc1* Mutant Leads to Constitutive, NPR1-Independent Pathogen Resistance. *Mol. Plant-Microbe Interact.* **2001**, *14*, 1131–1139, doi:10.1094/MPMI.2001.14.10.1131.
 170. Bowling, S.A.; Clarke, J.D.; Liu, Y.; Klessig, D.F.; Dong, X. The *Cpr5* Mutant of Arabidopsis Expresses Both NPR1-Dependent and NPR1-Independent Resistance. *Plant Cell* **1997**, *9*, 1573–1584, doi:10.1105/tpc.9.9.1573.
 171. Clarke, J.D.; Liu, Y.; Klessig, D.F.; Dong, X. Uncoupling PR Gene Expression from NPR1 and Bacterial Resistance: Characterization of the Dominant Arabidopsis *Cpr6-1* Mutant. *Plant Cell* **1998**, *10*, 557–569, doi:10.1105/tpc.10.4.557.
 172. Jandaa, M.; Šašek, V.; Ruelland, E. The Arabidopsis *Pi4kIIIβ1β2* Double Mutant Is Salicylic Acid-Overaccumulating: A New Example of Salicylic Acid Influence on Plant Stature. *Plant Signal. Behav.* **2014**, *9*, e977210-1-e977210-3, doi:10.4161/15592324.2014.977210.

173. Ortigosa, A.; Gimenez-Ibanez, S.; Leonhardt, N.; Solano, R. Design of a Bacterial Speck Resistant Tomato by CRISPR/Cas9-Mediated Editing of *SlJAZ2*. *Plant Biotechnol. J.* **2019**, *17*, 665–673, doi:10.1111/pbi.13006.
174. Asai, N.; Nishioka, T.; Takabayashi, J.; Furuichi, T. Plant Volatiles Regulate the Activities of Ca²⁺ - Permeable Channels and Promote Cytoplasmic Calcium Transients in Arabidopsis Leaf Cells. *Plant Signal. Behav.* **2009**, *4*, 294–300, doi:10.4161/psb.4.4.8275.
175. Engelberth, J.; Contreras, C.F.; Dalvi, C.; Li, T.; Engelberth, M. Early Transcriptome Analyses of Z-3-Hexenol-Treated Zea Mays Revealed Distinct Transcriptional Networks and Anti-Herbivore Defence Potential of Green Leaf Volatiles. *PLoS One* **2013**, *8*, e77465.
176. Zebelo, S.A.; Matsui, K.; Ozawa, R.; Maffei, M.E. Plasma Membrane Potential Depolarization and Cytosolic Calcium Flux Are Early Events Involved in Tomato (*Solanum Lycopersicon*) Plant-to-Plant Communication. *Plant Sci.* **2012**, *196*, 93–100, doi:https://doi.org/10.1016/j.plantsci.2012.08.006.
177. Duran-Flores, D.; Heil, M. Sources of Specificity in Plant Damaged-Self Recognition. *Curr. Opin. Plant Biol.* **2016**, *32*, 77–87, doi:https://doi.org/10.1016/j.pbi.2016.06.019.
178. Matsui, K.; Sugimoto, K.; Mano, J.; Ozawa, R.; Takabayashi, J. Differential Metabolisms of Green Leaf Volatiles in Injured and Intact Parts of a Wounded Leaf Meet Distinct Ecophysiological Requirements. *PLoS One* **2012**, *7*, e36433.
179. Heil, M. Herbivore-Induced Plant Volatiles: Targets, Perception and Unanswered Questions. *New Phytol.* **2014**, *204*, 297–306, doi:https://doi.org/10.1111/nph.12977.
180. Quintana-Rodriguez, E.; Duran-Flores, D.; Heil, M.; Camacho-Coronel, X. Damage-Associated Molecular Patterns (DAMPs) as Future Plant Vaccines That Protect Crops from Pests. *Sci. Hortic. (Amsterdam)*. **2018**, *237*, 207–220, doi:10.1016/j.scienta.2018.03.026.
181. Meents, A.K.; Mithöfer, A. Plant–Plant Communication: Is There a Role for Volatile Damage-Associated Molecular Patterns? *Front. Plant Sci.* **2020**, *11*, doi:10.3389/fpls.2020.583275.
182. Jiang, K.; Asami, T. Chemical Regulators of Plant Hormones and Their Applications in Basic Research and Agriculture. *Biosci. Biotechnol. Biochem.* **2018**, *82*, 1265–1300, doi:10.1080/09168451.2018.1462693.
183. Hicks, G.R.; Raikhel, N. V. Plant Chemical Biology: Are We Meeting the Promise? *Front. Plant Sci.* **2014**, *5*, 1–5, doi:10.3389/fpls.2014.00455.
184. Kachroo, P.; Yoshioka, K.; Shah, J.; Dooner, H.K.; Klessig, D.F. Resistance to Turnip Crinkle Virus in Arabidopsis Is Regulated by Two Host Genes and Is Salicylic Acid Dependent but NPR1, Ethylene, and Jasmonate Independent. *Plant Cell* **2000**, *12*, 677–690, doi:10.1105/tpc.12.5.677.
185. Love, A.J.; Yun, B.W.; Laval, V.; Loake, G.J.; Milner, J.J. Cauliflower Mosaic Virus, a Compatible Pathogen of Arabidopsis, Engages Three Distinct Defence-Signalling Pathways and Activates Rapid Systemic Generation of Reactive Oxygen Species. *Plant Physiol.* **2005**, *139*, 935–948, doi:10.1104/pp.105.066803.
186. Corina Vlot, A.; Dempsey, D.A.; Klessig, D.F. Salicylic Acid, a Multifaceted Hormone to Combat Disease. *Annu. Rev. Phytopathol.* **2009**, *47*, 177–206, doi:10.1146/annurev.phyto.050908.135202.
187. Beckers, G.J.M.; Conrath, U. Priming for Stress Resistance: From the Lab to the Field. *Curr. Opin. Plant Biol.* **2007**, *10*, 425–431, doi:https://doi.org/10.1016/j.pbi.2007.06.002.
188. Canet, J. V.; Dobón, A.; Ibáñez, F.; Perales, L.; Tornero, P. Resistance and Biomass in Arabidopsis: A New Model for Salicylic Acid Perception. *Plant Biotechnol. J.* **2010**, *8*, 126–141, doi:https://doi.org/10.1111/j.1467-7652.2009.00468.x.
189. Šašek, V.; Nováková, M.; Dobrev, P.I.; Valentová, O.; Burketová, L. β -Aminobutyric Acid Protects Brassica Napus Plants from Infection by *Leptosphaeria Maculans*. Resistance Induction or a Direct Antifungal Effect? *Eur. J. Plant Pathol.* **2012**, *133*, 279–289, doi:10.1007/s10658-011-9897-9.
190. Harm, A.; Kassemeyer, H.-H.; Seibicke, T.; Regner, F. Evaluation of Chemical and Natural Resistance Inducers against Downy Mildew (Plasmopara Viticola) in Grapevine. *Am. J. Enol. Vitic.* **2011**, *62*, 184 LP – 192, doi:10.5344/ajev.2011.09054.
191. Liljeroth, E.; Bengtsson, T.; Wiik, L.; Andreasson, E. Induced Resistance in Potato to *Phytophthora Infestans*—Effects of BABA in Greenhouse and Field Tests with Different Potato Varieties. *Eur. J. Plant Pathol.* **2010**, *127*, 171–183, doi:10.1007/s10658-010-9582-4.
192. Nakashita, H.; Yoshioka, K.; Takayama, M.; KUGA, R.; Midoh, N.; Usami R.; Horikoshi, K.; Yoneyama, K.; Yamaguchi, I. Characterization of PBZ1, a Probenazole-Inducible Gene, in Suspension-Cultured Rice Cells. *Biosci. Biotechnol. Biochem.* **2001**, *65*, 205–208, doi:10.1271/bbb.65.205.

193. Oostendorp, M.; Kunz, W.; Dietrich, B.; Staub, T. Induced Disease Resistance in Plants by Chemicals. *Eur. J. Plant Pathol.* **2001**, *107*, 19–28, doi:10.1023/A:1008760518772.
194. Brisset M.N. A4 - Faize, M. A4 - Heintz, C. A4 - Cesbron, S. A4 - Chartier, R. A4 - Tharaud, M. A4 - Paulin, J.P., M.N.A.-B. Induced Resistance to *Erwinia Amylovora* in Apple and Pear. *Acta Hort.* **2002**, v., 335-338-2002 v. no.590, doi:10.17660/ActaHortic.2002.590.49.
195. Azami-Sardooui, Z.; Seifi, H.S.; De Vleeschauwer, D.; Höfte, M. Benzothiadiazole (BTH)-Induced Resistance against *Botrytis Cinerea* Is Inversely Correlated with Vegetative and Generative Growth in Bean and Cucumber, but Not in Tomato. *Australas. Plant Pathol.* **2013**, *42*, 485–490, doi:10.1007/s13313-013-0207-1.
196. Zine, H.; Rifai, L.A.; Faize, M.; Smaili, A.; Makroum, K.; Belfaiza, M.; Kabil, E.M.; Koussa, T. Duality of Acibenzolar-S-Methyl in the Inhibition of Pathogen Growth and Induction of Resistance during the Interaction Tomato/*Verticillium Dahliae*. *Eur. J. Plant Pathol.* **2016**, *145*, 61–69, doi:10.1007/s10658-015-0813-6.
197. Faize, M.; Faize, L.; Koike, N.; Ishizaka, M.; Ishii, H. Acibenzolar-S-Methyl-Induced Resistance to Japanese Pear Scab Is Associated with Potentiation of Multiple Defence Responses. *Phytopathology*® **2004**, *94*, 604–612, doi:10.1094/PHYTO.2004.94.6.604.
198. López-Gresa, M.P.; Lisón, P.; Yenush, L.; Conejero, V.; Rodrigo, I.; Bellés, J.M. Salicylic Acid Is Involved in the Basal Resistance of Tomato Plants to Citrus Exocortis Viroid and Tomato Spotted Wilt Virus. *PLoS One* **2016**, *11*, e0166938–e0166938, doi:10.1371/journal.pone.0166938.
199. López-Gresa, M.P.; Payá, C.; Rodrigo, I.; Bellés, J.M.; Barceló, S.; Hae Choi, Y.; Verpoorte, R.; Lisón, P. Effect of Benzothiadiazole on the Metabolome of Tomato Plants Infected by Citrus Exocortis Viroid. *Viruses* **2019**, *11*, 437, doi:10.3390/v11050437.
200. Ameye, M.; Audenaert, K.; De Zutter, N.; Steppe, K.; Van Meulebroek, L.; Vanhaecke, L.; De Vleeschauwer, D.; Haesaert, G.; Smaghe, G. Priming of Wheat with the Green Leaf Volatile Z-3-Hexenyl Acetate Enhances Defence against *Fusarium Graminearum* but Boosts Deoxynivalenol Production. *Plant Physiol.* **2015**, *167*, 1671–1684, doi:10.1104/pp.15.00107.
201. Cofer, T.M.; Engelberth, M.; Engelberth, J. Green Leaf Volatiles Protect Maize (*Zea Mays*) Seedlings against Damage from Cold Stress. *Plant. Cell Environ.* **2018**, *41*, 1673–1682, doi:https://doi.org/10.1111/pce.13204.
202. Quintana-Rodriguez, E.; Rivera-Macias, L.E.; Adame-Alvarez, R.M.; Torres, J.M.; Heil, M. Shared Weapons in Fungus-Fungus and Fungus-Plant Interactions? Volatile Organic Compounds of Plant or Fungal Origin Exert Direct Antifungal Activity in Vitro. *Fungal Ecol.* **2018**, *33*, 115–121, doi:https://doi.org/10.1016/j.funeco.2018.02.005.
203. An, Y.; Liu, L.; Chen, L.; Wang, L. ALA Inhibits ABA-Induced Stomatal Closure via Reducing H₂O₂ and Ca²⁺ Levels in Guard Cells. *Front. Plant Sci.* **2016**, *7*, 1–16, doi:10.3389/fpls.2016.00482.
204. Yang, Q.; Peng, Z.; Ma, W.; Zhang, S.; Hou, S.; Wei, J.; Dong, S.; Yu, X.; Song, Y.; Gao, W.; et al. Melatonin Functions in Priming of Stomatal Immunity in *Panax Notoginseng* and *Arabidopsis Thaliana*. *Plant Physiol.* **2021**, *187*, 2837–2851, doi:10.1093/plphys/kiab419.
205. Baldwin, I.T.; Schultz, J.C. Rapid Changes in Tree Leaf Chemistry Induced by Damage: Evidence for Communication Between Plants. *Science (80-.)*. **1983**, *221*, 277–279, doi:10.1126/science.221.4607.277.
206. Farmer, E.E.; Caldelari, D.; Pearce, G.; Walker-Simmons, M.K.; Ryan, C.A. Diethylthiocarbamic Acid Inhibits the Octadecanoid Signalling Pathway for the Wound Induction of Proteinase Inhibitors in Tomato Leaves. *Plant Physiol.* **1994**, *106*, 337–342, doi:10.1104/pp.106.1.337.
207. Li, Y.; Qiu, L.; Zhang, Q.; Zhuansun, X.; Li, H.; Chen, X.; Krugman, T.; Sun, Q.; Xie, C. Exogenous Sodium Diethylthiocarbamate, a Jasmonic Acid Biosynthesis Inhibitor, Induced Resistance to Powdery Mildew in Wheat. *Plant Direct* **2020**, *4*, e00212, doi:https://doi.org/10.1002/pld3.212.
208. Hu, F.-X.; Zhong, J.-J. Jasmonic Acid Mediates Gene Transcription of Ginsenoside Biosynthesis in Cell Cultures of *Panax Notoginseng* Treated with Chemically Synthesized 2-Hydroxyethyl Jasmonate. *Process Biochem.* **2008**, *43*, 113–118, doi:https://doi.org/10.1016/j.procbio.2007.10.010.
209. Xiang, Y.; Song, M.; Wei, Z.; Tong, J.; Zhang, L.; Xiao, L.; Ma, Z.; Wang, Y. A Jacalin-Related Lectin-like Gene in Wheat Is a Component of the Plant Defence System. *J. Exp. Bot.* **2011**, *62*, 5471–5483, doi:10.1093/jxb/err226.
210. Halitschke, R.; Ziegler, J.; Keinänen, M.; Baldwin, I.T. Silencing of Hydroperoxide Lyase and Allene Oxide Synthase Reveals Substrate and Defence Signalling Crosstalk in *Nicotiana Attenuata*. *Plant*

J. **2004**, *40*, 35–46, doi:<https://doi.org/10.1111/j.1365-313X.2004.02185.x>.

Annex I



A New Role For Green Leaf Volatile Esters in Tomato Stomatal Defense Against *Pseudomonas syringae* pv. *tomato*

María Pilar López-Gresa^{1†}, Celia Payá^{1†}, Miguel Ozáez¹, Ismael Rodrigo¹, Vicente Conejero¹, Harry Klee², José María Bellés¹ and Purificación Lisón^{1*}

¹ Instituto de Biología Molecular y Celular de Plantas, Universitat Politècnica de València-Consejo Superior de Investigaciones Científicas, Valencia, Spain, ² Horticultural Sciences Department, University of Florida, Gainesville, FL, United States

OPEN ACCESS

Edited by:

Laure Weisskopf,
Université de Fribourg, Switzerland

Reviewed by:

Selena Gimenez-Ibanez,
Centro Nacional de Biotecnología
(CNB), Spain
William Underwood,
Agricultural Research Service (USDA),
United States
Ömür Baysal,
Muğla University, Turkey

*Correspondence:

Purificación Lisón
plison@ibmcp.upv.es

[†]These authors have contributed
equally to this work

Specialty section:

This article was submitted to
Plant Microbe Interactions,
a section of the journal
Frontiers in Plant Science

Received: 12 July 2018

Accepted: 30 November 2018

Published: 18 December 2018

Citation:

López-Gresa MP, Payá C, Ozáez M,
Rodrigo I, Conejero V, Klee H,
Bellés JM and Lisón P (2018) A New
Role For Green Leaf Volatile Esters in
Tomato Stomatal Defense Against
Pseudomonas syringae pv. *tomato*.
Front. Plant Sci. 9:1855.
doi: 10.3389/fpls.2018.01855

The volatile esters of (Z)-3-hexenol with acetic, propionic, isobutyric, or butyric acids are synthesized by alcohol acyltransferases (AAT) in plants. These compounds are differentially emitted when tomato plants are efficiently resisting an infection with *Pseudomonas syringae* pv. *tomato*. We have studied the defensive role of these green leaf volatile (GLV) esters in the tomato response to bacterial infection, by analyzing the induction of resistance mediated by these GLVs and the phenotype upon bacterial infection of tomato plants impaired in their biosynthesis. We observed that treatments of plants with (Z)-3-hexenyl propionate (HP) and, to a greater extent with (Z)-3-hexenyl butyrate (HB), resulted in stomatal closure, PR gene induction and enhanced resistance to the bacteria. HB-mediated stomatal closure was also effective in several plant species belonging to *Nicotiana*, *Arabidopsis*, *Medicago*, *Zea* and *Citrus* genus, and both stomatal closure and resistance were induced in HB-treated *NahG* tomato plants, which are deficient in salicylic acid (SA) accumulation. Transgenic antisense *AAT1* tomato plants, which displayed a reduction of ester emissions upon bacterial infection in leaves, exhibited a lower ratio of stomatal closure and were hyper-susceptible to bacterial infection. Our results confirm the role of GLV esters in plant immunity, uncovering a SA-independent effect of HB in stomatal defense. Moreover, we identified HB as a natural stomatal closure compound with potential agricultural applications.

Keywords: AAT1, GLV esters, stomata, defense, tomato, bacteria

INTRODUCTION

Plants synthesize different defensive secondary metabolites in response to biotic stresses. These compounds may exert direct defensive functions by acting on the pathogen, or act indirectly by activating the defensive response of the plant. Some volatile organic compounds (VOCs) belong to this group of defensive molecules. These VOCs are typically lipophilic liquids with high vapor pressures that can freely cross membranes and be emitted (Dudareva et al., 2006).

The defensive role of VOCs has been classically associated with plant defense against herbivores. Emitted volatiles can directly affect herbivores due to their toxic, repelling or deterring properties (Kessler and Baldwin, 2001; Aharoni et al., 2003). They can also attract predators of the attacking

insects, thus displaying tritrophic interactions (Drukker et al., 2000; Kessler and Baldwin, 2001). VOCs can also prime defenses in neighboring plants, constituting mechanisms of interplant communication (Kim and Felton, 2013). Although the roles of VOCs in pathogen defense have received less attention, some volatiles have been implicated in different plant-pathogen interactions (Croft et al., 1993; Huang et al., 2003; Cardoza and Tumlinson, 2006; Niinemets et al., 2013; Hijaz et al., 2016; Ameze et al., 2018).

Recently, a GC-MS metabolomic analysis revealed a number of VOCs that are differentially emitted by tomato cv. Rio Grande plants containing the *Pto* gene, upon infection with virulent or avirulent strains of the bacterium *Pseudomonas syringae* DC3000 pv. *tomato* (*Pst*) (López-Gresa et al., 2017). Infection of this cultivar with avirulent bacteria, carrying both AvrPto and AvrPtoB effectors, elicits establishment of Effector Triggered Immunity (ETI) in the plant, thus preventing development of the infection (Dangl and Jones, 2001; Lin and Martin, 2005). Metabolomic analysis showed that esters of (*Z*)-3-hexenol with acetic (HA), propionic (HP), isobutyric (HiB) or butyric (HB) acids were differentially emitted during ETI (López-Gresa et al., 2017).

These esters belong to the family of green leaf volatiles (GLVs) that are generated through the oxylipin pathway from C18 polyunsaturated fatty acids (PUFAs), such as linolenic or linoleic acids. The first step in their biosynthesis is peroxidation of the PUFAs performed by the action of lipoxygenases (LOXs). These enzymes can act upon PUFAs at either the C9 or C13 position, being classified as 9-LOX and 13-LOX, respectively. GLV esters are known to be synthesized by 13-LOX via 13-hydroperoxides that are later cleaved by 13-hydroperoxide lyases (13-HPL) into (*Z*)-3-hexenal. This aldehyde is reduced by an alcohol dehydrogenase (ADH), and alcohol acyltransferases (AAT) catalyze esterification of an acyl moiety from an acyl-coenzyme A (acyl-CoA) donor onto an alcohol (Scala et al., 2013; Ameze et al., 2018).

Five alcohol acyltransferase genes (*SLAAT1-5*) have been identified in tomato (Goulet et al., 2015). To confirm the function of this protein, tomato plants containing an *AAT1* antisense construct (*as-AAT1*) were generated, resulting in transgenic fruits with reduced acetate ester emissions (Goulet et al., 2015). Consistent with this biochemical activity and the metabolomic data, tomato plants triggering ETI and differentially emitting these GLV esters, significantly induced *AAT1* expression (López-Gresa et al., 2017). These results suggest a possible role of this enzyme and its products in plant defense.

Many foliar pathogens, including bacteria, primarily invade plants through natural surface opening such as wounds or stomata. Plants have developed the ability to restrict entry of pathogens by closing stomata or by inhibition of stomatal opening (Arnaud and Hwang, 2015). Specifically, *Pst* has been observed to activate plant stomatal closure. To evade this innate immune response, *Pst* has evolved specific virulence factors, including coronatine, to effectively cause stomatal reopening. Coronatine is a mimic of the active JA-Ile hormone, and acts as a suppressor of stomata closing by inhibiting SA-induced closing of stomata. Abscisic acid (ABA) and salicylic acid (SA)

have emerged as positive regulators of stomatal defense, while jasmonic acid (JA) is a negative regulator (Melotto et al., 2006, 2008) reviewed in Panchal and Melotto (2017). Although stomata closing is regulated by master ABA and SA signals, it is becoming clear that during biotic interactions, SA is produced upon *Pst* sensing, triggering stomata closing. This SA-induced stomata closing is hijacked by the COR phytotoxin, through the antagonistic the SA-JA crosstalk (Zheng et al., 2012; Gimenez-Ibanez et al., 2017).

To study the possible defensive role of the GLV esters differentially emitted by tomato plants resisting bacterial infection we used a pharmacological approach, assessing the induction of resistance mediated by exogenous treatment with these volatiles. We also examined the mode of action of these compounds and the possible activation of the salicylic acid (SA) pathway caused by VOC treatments. To confirm the defensive role of VOCs, we also used a genetic approach by studying the phenotype of *as-AAT1* tomato plants upon bacterial infection. Our results confirm the role of GLV esters in plant immunity, uncovering a new function of VOCs in stomatal defense. The effect on stomatal aperture of one of these GLV esters was also studied in several plant species, defining a potential use in agriculture.

MATERIALS AND METHODS

Plant Material and GLV Treatments

We used in this study the following tomato plants: *NahG* (Brading et al., 2000) and their corresponding parental MoneyMaker plants; *as-AAT1* (Goulet et al., 2015) and *Flora-Dade* (FD) parental plants; and Rio Grande plants, the only variety containing the *Pto* resistance gene.

The seeds were sterilized with a 1:1 mixture of commercial sodium hypochlorite and distilled H₂O containing a few drops of Tween 20, and then they were sequentially washed with distilled H₂O during 5, 10, and 15 min, respectively. After sterilization treatments, seeds were placed in 12 cm-diameter pots that contained a 1:1 mixture of vermiculite and peat and grown under greenhouse conditions with a relative humidity between 50 and 70% and a 16/8 h (26/30°C) light/dark photoperiod.

Four-week-old tomato plants were treated with (*Z*)-3-hexenyl acetate (HA), (*Z*)-3-hexenyl propionate (HP), (*Z*)-3-hexenyl butyrate (HB), and (*Z*)-3-hexenyl isobutyrate (HiB) into 110 L methacrylate chambers. A concentration of 5 μM of each compound was placed in different hydrophilic cotton buds, and distilled H₂O in the case of the control plants. To avoid VOC mixtures, the treatments were performed individually. Methacrylate chambers were hermetically sealed during the 24 h treatment.

Bacterial Strain, Bacterial Inoculation and CFU Determination

The bacterial strains used in this study were *Pst* DC3000, and *Pst* DC3000 containing deletions in genes *avrPto* and *avrPtoB* (*Pst* DC3000 Δ *avrPto*/ Δ *avrPtoB*) (Lin and Martin, 2005; Ntoukakis et al., 2009). Bacteria were grown during 48 h at 28°C in LB agar medium with different antibiotics: rifampicin (10 mg/mL)

and kanamycin (0.5 mg/mL) for *Pst* DC3000, and rifampicin (10 mg/mL), kanamycin (0.25 mg/mL), and spectinomycin (2.5 mg/mL) for *Pst* DC3000 $\Delta avrPto/\Delta avrPtoB$. When colonies were grown, they were transferred into 3 mL of King's B liquid medium supplemented with rifampicin and were grown overnight at 28°C under continuous stirring. After 24 h, colonies were transferred into 14 mL of King's B liquid medium and were grown under the same conditions than the previous step. Then, bacteria were centrifugated 15 min at 3,000 rpm and resuspended in 10 mM sterile MgCl₂ to an optical density of 0.1 at 600 nm, which corresponds to a final inoculum concentration of 5×10^7 CFU/mL approximately.

Inoculation with bacteria was carried out in 4-week-old tomato plants by immersion or injection methods. For immersion experiments tomato plants were dipped into the bacterial suspension containing 0.05% Silwet L-77. To carry out bacterial injection experiments, each leaflet of the third and fourth leaves was inoculated with a needleless syringe by injecting the bacterial suspension into different sites of the leaflet's abaxial side.

For determining bacterial growth, three leaf disks (1 cm² each) were sampled from the bacterial infected leaves from each plant. A total of five plants were used per treatment or tomato plant variety. Density of bacterial populations was determined by plating serial dilutions of the infected material on King's B medium containing rifampicin and counting colony growth.

Stomatal Aperture Measurement

Tomato leaf impressions were obtained by applying a thin layer of nitrocellulose-based glue (Imedio, Bolton Group, Madrid, Spain) in the abaxial part of the leaves, and then peeling off the glue carefully. In order to observe the stomata, epidermis peels were placed on glass slices and observed under a Leica DC5000 microscope (Leica Microsystems S.L.U.). Pictures of different regions of tomato leaves were taken and at least 50 stomata of each plant and/or each treatment were analyzed using the NIH's *ImageJ* software. Stomatal aperture ratio was calculated as stomata width/stomata length.

RNA Extraction and Quantitative RT-PCR Analysis

Total RNA extraction of tomato leaves was produced using TRIzol reagent (Invitrogen, Carlsbad, CA, United States) following the manufacturer's protocol. Then, RNA was precipitated by adding one volume of 6 M LiCl for 3 h. Thereafter the pellet was washed using 1 volume of 3 M LiCl and resuspended in RNase-free water. So as to remove genomic DNA, 2 U/ μ L RNA of TURBO DNase kit (Ambion, Austin, TX, United States) was utilized.

PrimeScript RT reagent kit (Perfect Real Time, Takara Bio Inc., Otsu, Shiga, Japan) was used to obtain the cDNA from one microgram of total RNA, according to the manufacturer's protocol. Quantitative real-time PCRs were performed as previously described (Campos et al., 2014), in 10 μ L reaction volume on 96-wells plates using SYBR[®] Green PCR Master Mix (Applied Biosystems). Actin gene was used as the endogenous reference gene in all the experiments. Three technical replicates

were performed in all the assays. The PCR primers are listed in Table S1.

HS-SPME Extraction and GC-MS Analysis of Volatile Compounds

For the analysis of the volatile compounds, 100 mg of fully homogenized, frozen tomato leaf tissue were introduced into a 10 mL glass vial, adding subsequently 1 mL of a saturated CaCl₂ solution and 100 μ L of 750 mM EDTA at a pH of 7.5. The vial was air-tight sealed and sonicated for 5 min and volatile compounds extraction was performed by Head Space Solid-Phase Microextraction (HS-SPME) (López-Gresa et al., 2017). The samples were incubated for 10 min at 50°C and the extraction was performed at the same temperature for 20 min with a PDMS/DVB fiber (Supelco, Bellefonte, PA, USA). The desorption of the adhered compounds was carried out for 1 min at 250°C in splitless mode. Solid phase microextraction was performed using a CombiPAL autosampler (CTC Analytics, Zwingen, Switzerland).

VOCs were analyzed using an Agilent 6890N (Santa Clara, CA, USA) gas chromatograph coupled to an Agilent 5975B Inert XL electronic impact (EI) mass detector with an ionization energy of 70 eV and a source temperature of 230°C. Chromatography was carried out on a DB-5-ms fused silica capillary column (60 m long, 0.25 mm i.d., 1 μ m film thickness). The temperature conditions established in the oven were 40°C for 2 min, a ramp from 5°C/min to 250°C and 5 min at a constant temperature of 250°C. The carrier gas was helium at a constant flow of 1.2 mL/min. Data acquisition was performed at 6 scans per second in an *m/z* range of 35–250. Chromatograms and mass spectra were acquired and processed using the Enhanced ChemStation software (Agilent).

Identification of the compounds was performed by using commercial compounds that served as standards. The compounds used as reference or standard were purchased in Sigma-Aldrich (Madrid, Spain) or chemically synthesized by the Metabolomics service of the IBMCP as is the case of (*Z*)-3-hexenol esters (González-Mas et al., 2011). Quantification of HA, HB, HP, and HiB was performed by standard curves using such pure compounds.

HB Treatments in Different Species

Nicotiana benthamiana, *Arabidopsis thaliana*, *Medicago sativa*, *Zea mays*, and *Citrus x jambhiri* plants were treated with (*Z*)-3-hexenyl butyrate (HB). For this purpose, plants were treated by spraying them at a concentration of 2 mM containing 0.05% Silwet L-77. Tomato plants were also sprayed as a positive control. Samples were taken before the treatment, and 24 and 48 h post-treatment in order to determine stomatal aperture ratio (as previously described).

In vitro Antimicrobial Activity Assays

Pseudomonas syringae pv. *tomato* DC3000 $\Delta avrPto$ bacterial strains were grown in LB agar medium during 48 h and then transferred into 15 mL of King's B liquid medium, as previously described. After 24 h, 1 mL of the bacterial culture was mixed with 14 mL of King's B agar and poured into Petri dishes. Once

solidified, 5 mm-diameter Whatman paper disks (GB005 Blotting Paper, Schleicher & Schuell) were placed on top of the agar and then a volume of 10 μ L of each compound [(*Z*)-3-hexenyl acetate (HA), (*Z*)-3-hexenyl propionate (HP), (*Z*)-3-hexenyl butyrate (HB), (*Z*)-3-hexenyl isobutyrate (HiB), (*Z*)-3-hexenal, and (*E*)-2-hexenal] was applied into the disks. Methanol was used as negative control and the antibiotic tetracycline was chosen for the positive one at two different concentrations (50 and 100%).

After incubation during 48 h at 28°C, the inhibition zone was measured using a slide gauge.

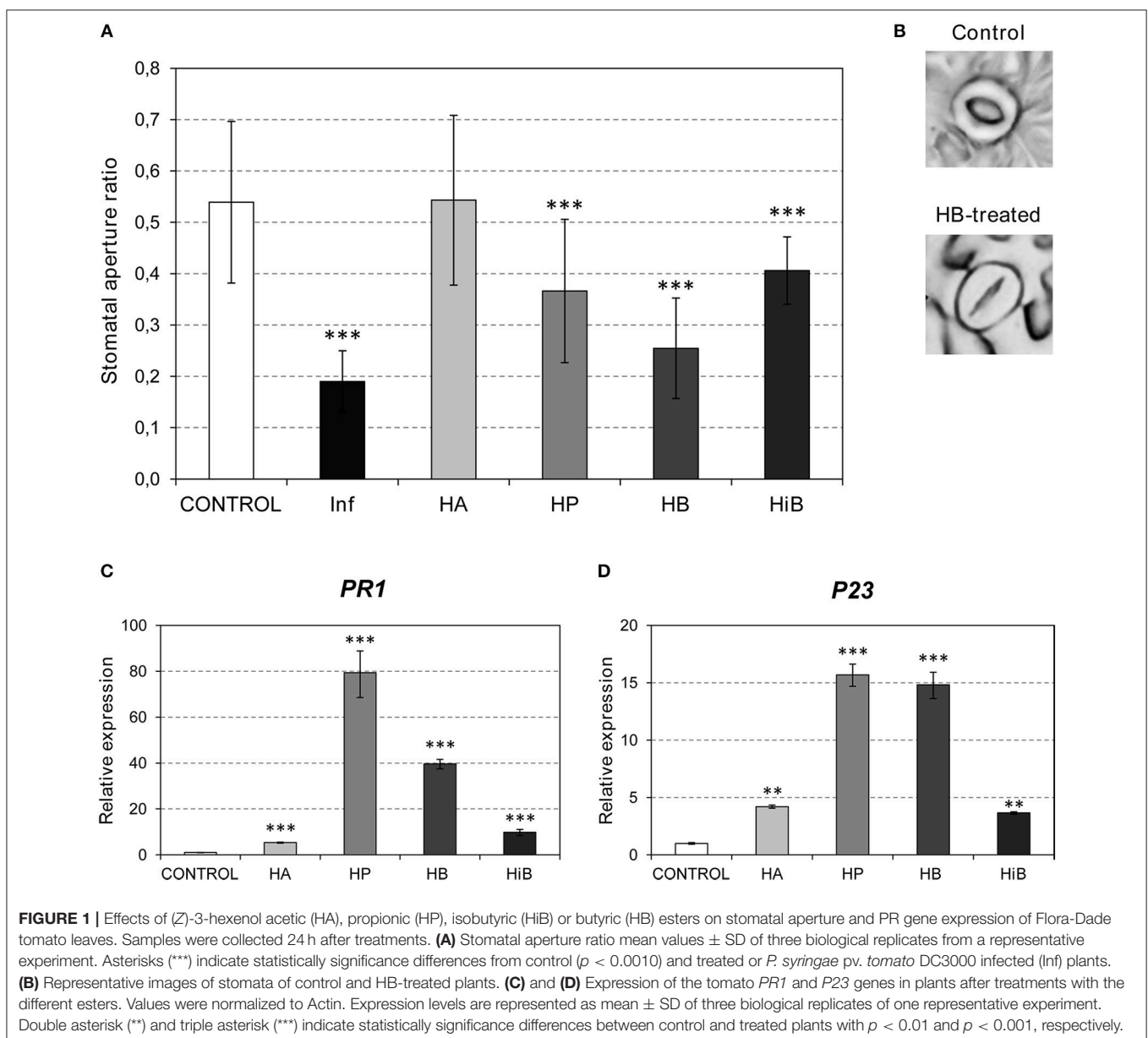
Statistical Analysis

Statistical analyses of two or more variables were performed by using Student's *t*-test or analysis of variance (multifactor ANOVA), respectively (Statgraphics Centurion XVI).

For untargeted analysis of the volatile profile, GC-MS data were processed with the MetAlign software (Wageningen, The Netherlands) for alignment of chromatograms and quantitation of each of the MS features. The resulting dataset was submitted to a Partial Least Square (PLS) study by means of the SIMCA-P software v. 11.0 (Umetrics, Umeå, Sweden) using unit variance (UV) scaling.

Accession Numbers

Sequence data from this article can be found in the GenBank/EMBL and Solgenomics data libraries under accession numbers *PR1* (X68738), *P23* (X70787), *AAT1* (KM975321), *JAZ7* (Solyc11g011030), *JAZ9* (Solyc08g036640), *P5CS* (Solyc06g019170), *RAB18* (Solyc02g084850), and *Actin* (AB695290; Solyc04g011500).



RESULTS

Exogenous Treatments With GLV Esters Close Stomata and Induce PR Gene Expression

Bacterial pathogens and VOCs invade the plant through stomata (Matsui, 2016; Panchal and Melotto, 2017). We decided to test the defensive role of GLV esters by studying the effect of exogenous treatments with these volatiles on stomatal closure. Treatments with HA, HP, HB, and HiB were performed on tomato cv. Flora-Dade plants (see Materials and Methods) and the stomatal aperture ratios were measured 24 h after treatment. As observed in **Figures 1A,B**, treatment with HB produced significant stomatal closure, reaching aperture ratios comparable to those observed in bacterial infected leaves (Lisón et al., 2017). A similar effect was detected when treatments were performed with HP or HiB, although lower effects were observed when compared with those observed for HB. However, HA had no clear effect on stomatal closure, indicating that the effect on stomatal closure is ester-specific. Interestingly, HA was the only ester displaying an antibacterial defensive role, as shown in **Figure S1**.

Several signal molecules have been implicated in plant immunity. SA has been mainly associated with resistance against biotrophic and hemibiotrophic microbes such as *Pst*, while the JA pathway activates resistance against necrotrophs in *Arabidopsis* (Robert-Seilaniantz et al., 2011). To test the VOC-mediated activation of these pathways, we studied the induction of several marker genes. *PR1* and *P23* (Rodrigo et al., 1993; Tornero et al., 1993) were used as markers for the plant response to biotrophic pathogens. To study the involvement of the JA pathway, *JAZ* genes (Ishiga et al., 2013) and *TCI21* (Lisón et al., 2006) were used. Since ABA has been classically associated with stomatal closure, the induction of *RAB18* and *P5CS1* was also analyzed (González-Guzmán et al., 2014). As shown in **Figures 1C,D**, induction of *PR1* and *P23* was observed in the plants treated with any of the VOCs, with HP provoking the highest induction of both PR genes. Interestingly, the markers associated with the ABA pathway were not activated by treatments with any of the GLV esters (**Figure S2**). In contrast, both *JAZ7* and *TCI21* were repressed by HB, but clearly induced in the HiB-treated plants. These results suggest that the stomatal closure caused by HP, HB, and HiB is not accompanied by activation of the ABA pathway, and that the JA pathway is repressed by HB and activated by HiB. Nevertheless, all of the GLV esters appeared to induce the SA pathway (**Figures 1C,D**).

Treatment With (Z)-3-hexenyl-butyrate Induces Resistance to *Pst* in Tomato in a SA-Independent Manner

Based on the observed results, we decided to test whether the observed VOC-mediated PR induction and stomatal closure increases resistance to bacterial infection. To that purpose, tomato plants were pre-treated with VOCs for 24 h and subsequently infected with *Pst*. Only treatments with HP and HB significantly reduced bacterial growth (**Figure 2A**). These results appear to indicate that the stomatal closure accounts very

importantly for the tomato resistance to bacteria (**Figure 1A**). Although HA displayed antibacterial properties (**Figure S1**) and HiB induced PR1 and P23 (**Figures 1C,D**), any of these two VOCs could enhance the tomato resistance to *Pst*. In this sense, the highest resistance observed in the HB-treated plants, with a clear effect also in the observed symptomatology (**Figure 2B**), correlated with the highest efficacy of this VOC on stomatal closure. Our results suggest that HB, and to a lesser extent HP, effectively lead to resistance, confirming an indirect defensive role of both GLV esters.

Beyond its role as a signaling molecule for plant defense responses to bacterial pathogens, SA is a positive regulator of stomatal defense (Panchal and Melotto, 2017). To test if the observed HB-induced stomatal closure is SA-dependent, we studied its effect in *NahG* tomato plants, which are impaired in SA accumulation (Brading et al., 2000).

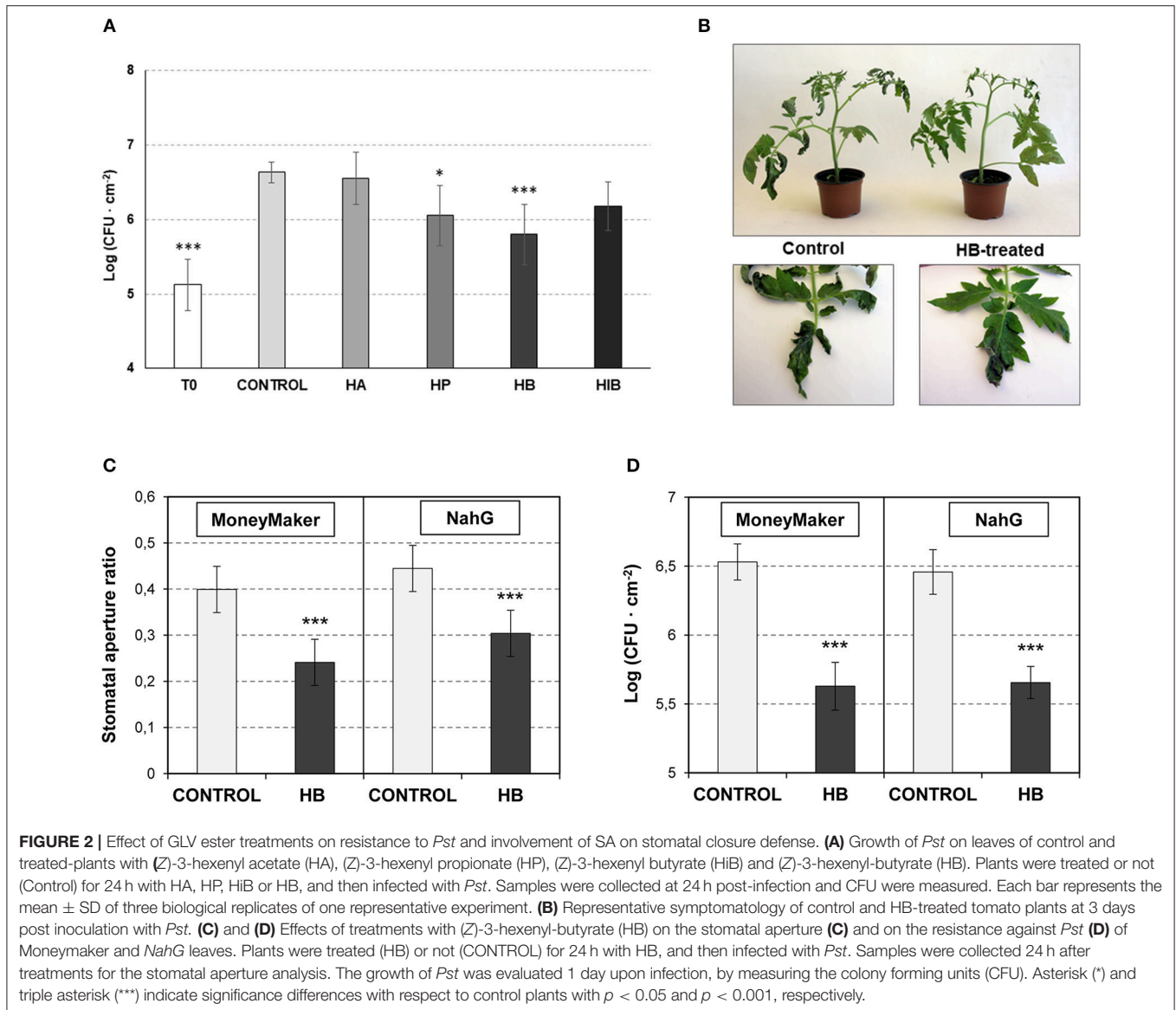
NahG plants and their corresponding Moneymaker parental control were pre-treated with HB for 24 h and subsequently infected with *Pst*. Stomatal aperture ratio and bacterial growth were measured at 24 h post-inoculation. HB treatment resulted in a significant stomatal closure and reduced bacterial growth in *NahG* (**Figures 2C,D**), indicating that the effect of HB is SA-independent.

Antisense *as-AAT1* Plants Are More Susceptible to *Pst* Displaying a Reduction of *AAT1* but No Difference in *PR1* Upon Infection With *Pst*

To better understand the relationship between GLVs and pathogen defense, we examined plants that are impaired in their ability to synthesize GLVs. The last reaction for the biosynthesis of GLVs is carried out by an alcohol acyltransferase (AAT). In tomato, there are five AAT-encoding genes but only one, *SIAAT1*, accounts for almost all of the expression in fruit, and antisense *SIAAT1* fruits produce almost no detectable alcohol esters (Goulet et al., 2015).

To determine whether *SIAAT1* has an active role in plant defense, two independent *as-AAT1* transgenic lines (AAT 3677 and AAT 3936) (Goulet et al., 2015) were infected with *Pst*, and the bacterial populations were measured and compared to the corresponding Flora-Dade control plants. As shown in **Figure 3A**, *as-AAT1* plants had significantly more bacterial growth at 24 hpi than did the control plants. Electrolyte leakage, which is a hallmark of cell death, was also significantly increased in both *as-AAT1* transgenic lines (**Figure 3B**). Our results indicate that reduced expression of *SIAAT1* strongly compromises the defense response against *Pst*.

To characterize the response of *as-AAT1* tomato plants to *Pst* infection, the expression of different genes in *as-AAT1* lines and Flora-Dade plants either mock-inoculated or infected with *Pst* at 24 and 48 hpi was analyzed by qRT-PCR (**Figure S3**). As previously described in cv. Rio Grande tomato plants (López-Gresa et al., 2017), there was an increase in *SIAAT1* transcript in *Pst*-infected Flora-Dade leaves when compared to the mock-inoculated plants, at both 24 and 48 hpi. In contrast, a clear reduction in *SIAAT1* was observed in *as-AAT1*



leaves relative to the Flora-Dade control plants in all conditions (Figure S3A).

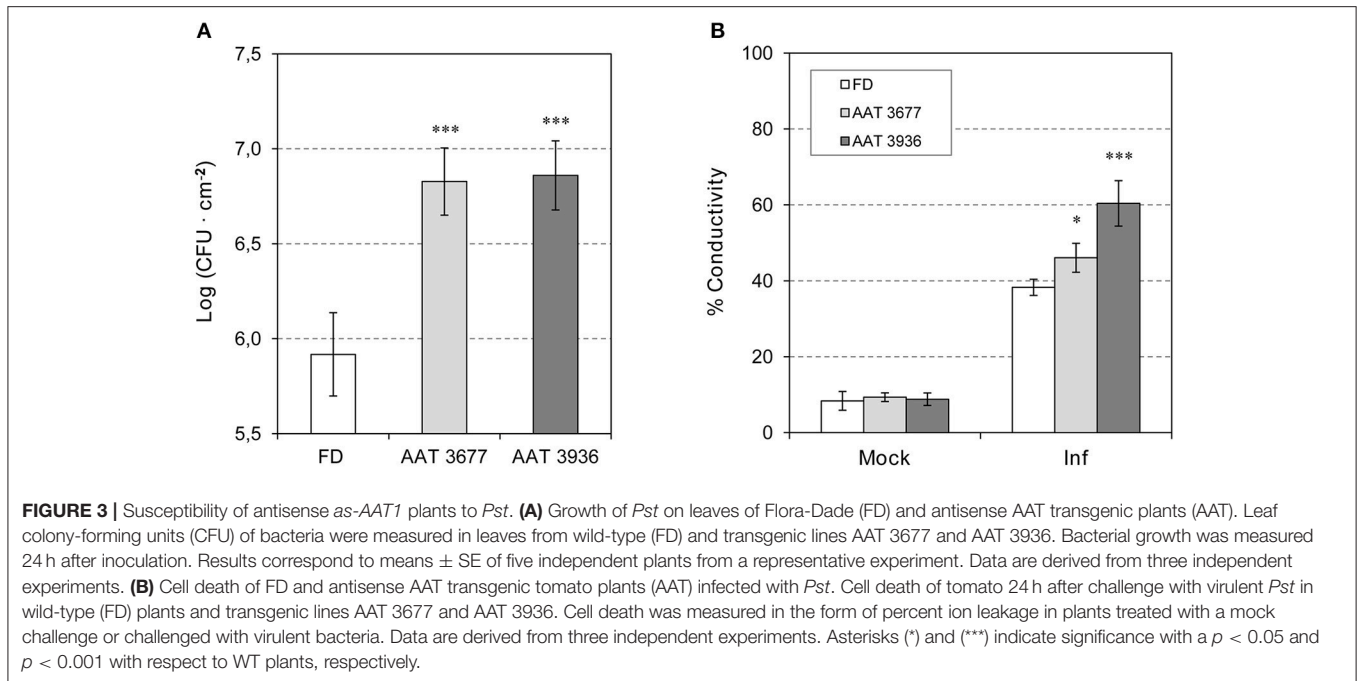
We also studied the induction of *PR1*, observing that activation of this gene only occurs in the presence of the bacteria, being stronger at 48 hpi (Figure S3B). No significant differences in the induction of *PR1* between Flora-Dade and the *as-AAT1* lines were observed after *Pst* infection. These results suggest that the enhanced susceptibility observed in *as-AAT1* transgenic plants correlated with lower expression of *AAT1*, but not with the pathogenesis marker *PR1*.

Antisense *as-AAT1* Plants Emit Less GLV Esters and Display an Impaired Stomatal Closure Upon *Pst* Infection

In order to correlate the observed phenotype with the differential emission of GLV esters, volatiles produced by *as-AAT1* and

Flora-Dade leaves either mock-inoculated or infected with *Pst* at 24 and 48 hpi were analyzed by GC-MS.

To manage the large amount of mass data, a multivariate data analysis was performed. In particular, a partial least square analysis (PLS) was carried out, defining compound abundance as the X variable, and harvest time (24 and 48 hpi) and genotype (FD; AAT 3677 and AAT 3936) as stepwise Y variables. The PLS analysis (Figure S4) showed that the first component (PC1) explained changes in the chemical composition along the time course of the infection (harvest time) while the metabolic alterations due to the genotype were clearly characterized by the second component (PC2). Both *as-AAT1* infected transgenic samples showed an evident variation in their metabolic content compared to FD infected plants. The analysis of loading scatter plot identified the GLV esters as the main compounds contributing to the separation of the samples.



Levels of (*Z*)-3-hexenyl-acetate, -propionate, -isobutyrate, and -butyrate were specifically quantified. As shown in **Figure S5**, these four esters of (*Z*)-3-hexenol were differentially emitted by Flora-Dade plants upon infection with *Pst*, thus extending the previously described emission observed in Rio Grande plants (López-Gresa et al., 2017) to other tomato cultivars. It is worth noting that (*Z*)-3-hexenyl-butyrate displayed the highest levels of emission (around 50 ppm) in Flora-Dade leaves 24 h after the *Pst* inoculation, reaching values even higher than those used for the HB treatments (around 1 ppm). As expected, both *as-AAT1* lines infected with *Pst* differentially emitted less GLV esters when compared with the corresponding Flora-Dade infected plants, displaying levels of emission similar to the mock-inoculated *as-AAT1* leaves. Our results suggest that these GLVs may play a defensive role in tomato plants against bacterial infection.

To study the possible effect of GLV esters on bacterial-mediated stomatal closure, we measured the stomatal aperture ratio in *as-AAT1* and Flora-Dade leaves, both before and 24 h after bacterial infection. As shown in **Figure 4**, before infection, both *as-AAT1* lines had similar ratios of stomatal aperture to Flora-Dade. However, the stomata of Flora-Dade leaves displayed a reduction in the aperture ratio after *Pst* infection. Interestingly, stomatal closure did not occur in *as-AAT1* infected leaves, exhibiting stomatal aperture ratios significantly higher than those observed in the Flora-Dade infected leaves. Our results are consistent with a model in which the increased susceptibility in *as-AAT1* against *Pst* is caused by the reduced ability of these plants to close stomata upon infection due to the lack of the GLV esters emission in these plants. These results uncover a role of GLV esters, and particularly, of HB in stomatal defense.

The GLV Esters Defense Role Is Mainly Due to Their Stomata Closure Effect

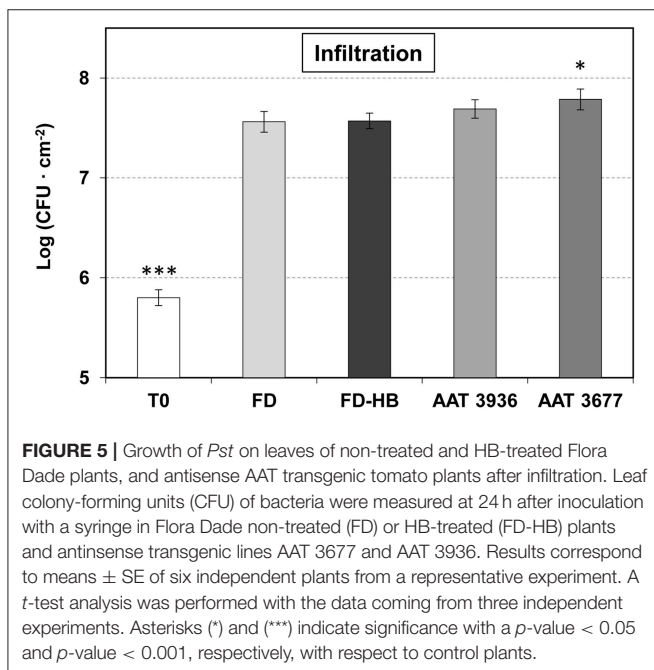
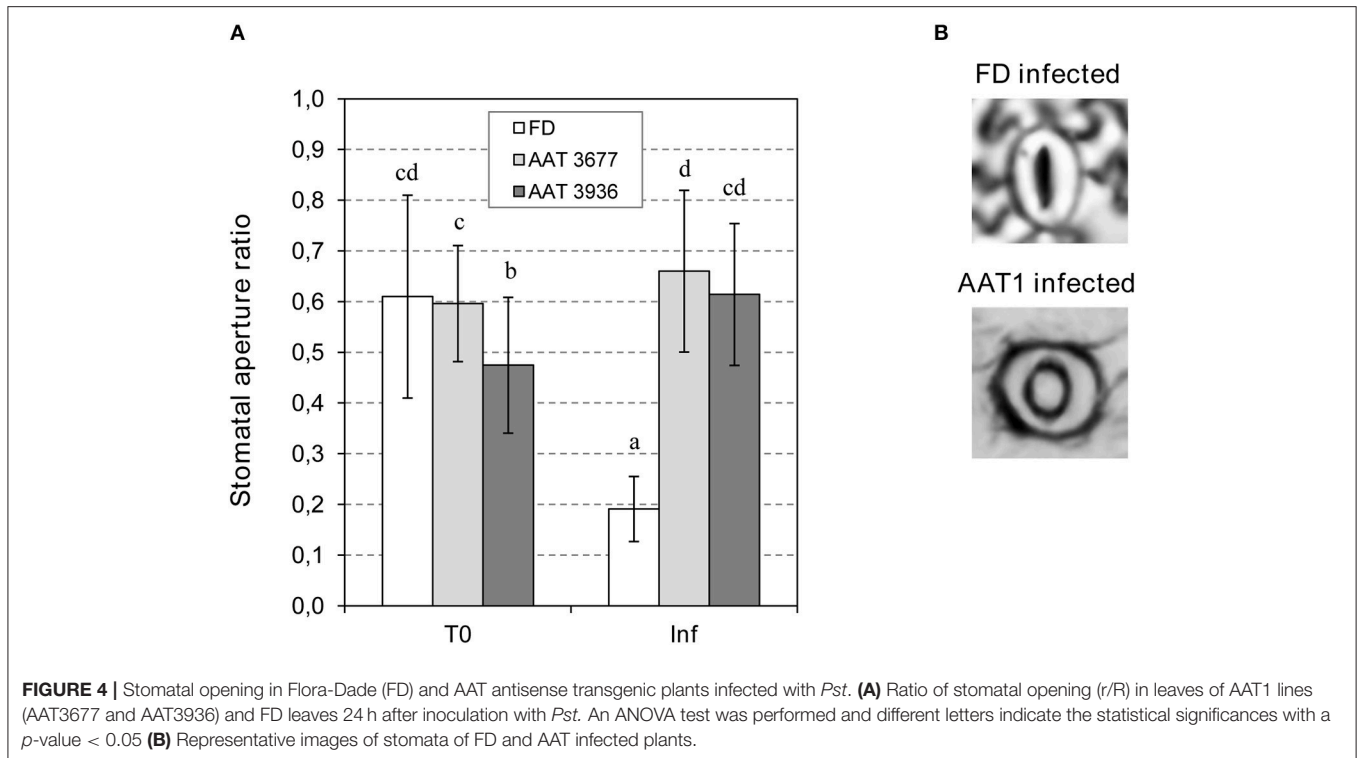
To test if the observed GLV esters defense role was only due to a reduction in stomatal closure, or other factors could be intervening, non-treated and HB-treated tomato Flora-Dade plants were infected by infiltration with a syringe (**Figure 5**). In this case, the bacteria bypass the stomatal defense and directly enter the apoplast. As expected, forced infiltration resulted in higher levels of bacterial growth, when compared to the plants infected by immersion (**Figure 3**). As **Figure 5** shows, no statistical differences in the bacterial content were observed after HB treatments, thus indicating that the HB-induced resistance mainly depends on the stomata closure effect.

To better confirm this idea, *as-AAT1* plants were also infiltrated with *Pst* (**Figure 5**), observing a clear reduction in the hypersusceptibility, that was previously detected by immersion (**Figure 3**). Consistently a similar induction of *PRI* was observed in both Flora-Dade and *as-AAT1* plants infected with the bacteria (**Figure S3B**), thus suggesting that the phenotype is not due to reduced activation of plant defense, but to a reduced ability to close stomata in the *as-AAT1* plants.

All these results confirm the role of Green Leaf Volatile esters in tomato stomatal defense against *Pst*.

Rio Grande Tomato Plants Displaying ETI Exhibit a Slightly Higher Stomatal Closure

Since Rio Grande ETI-displaying tomato plants differentially emit GLV esters at 1 h, 4 h (**Figure S6**), and 24 h post-inoculation (López-Gresa et al., 2017), and treatments with some of them produce stomatal closure (**Figure 1**), we decided to study the stomatal behavior in plants displaying ETI, compared with



those infected with the virulent bacteria. To that purpose, Rio Grande tomato plants carrying the *Pto* gene were infected with an avirulent or a virulent strain of *Pst*, carrying the *AvrPto* gene or a deleted version of it, respectively (see Materials and Methods). The stomatal closure ratios were measured at 1, 4, and 24 h post-inoculation (Figure S7). In correlation with

the differentially emitted levels of GLV esters, tomato plants displaying ETI appeared to exhibit a slightly higher stomatal closure at the early analyzed times.

HB Treatments Produce a Maximum Stomatal Closure at 24 h in Tomato Plants and It Is Also Effective in Several Plant Species

To study the most effective time point for the HB-induced stomata closure, measures of stomata ratios were analyzed in control and HB treated tomato leaves at 6, 10, 24, 48, 72 h post-treatment (hpt), and at 7 and 10 days post-treatment (dpt). As Figure 6A indicates, HB was already effective at 6 hpt, displaying a maximum stomata closure effect at 24 hpt. At this time point, the ratio in HB-treated plants decreased to half of that displayed by the control plants, thus indicating a very pronounced effect of the GLV ester in tomato plants. The resistance of the HB-treated plants was precisely studied after 24 h of treatment (Figure 2A). The durability of the effect remained till 10 dpt, at which the differences between stomata ratios of control and HB-treated plants were not significant.

Once we had demonstrated that HB is a defensive VOC associated with stomatal closure in tomato, with a maximum effect at 24 hpt, we evaluated the effect of this GLV ester in other plant species, including *Nicotiana benthamiana*, *Arabidopsis thaliana*, *Medicago sativa*, *Zea mays*, and *Citrus x jambhiri*. To that end, HB treatments were performed by spraying these species, including tomato plants as a positive control, and measuring stomatal aperture ratios before and 24 or 48 h after

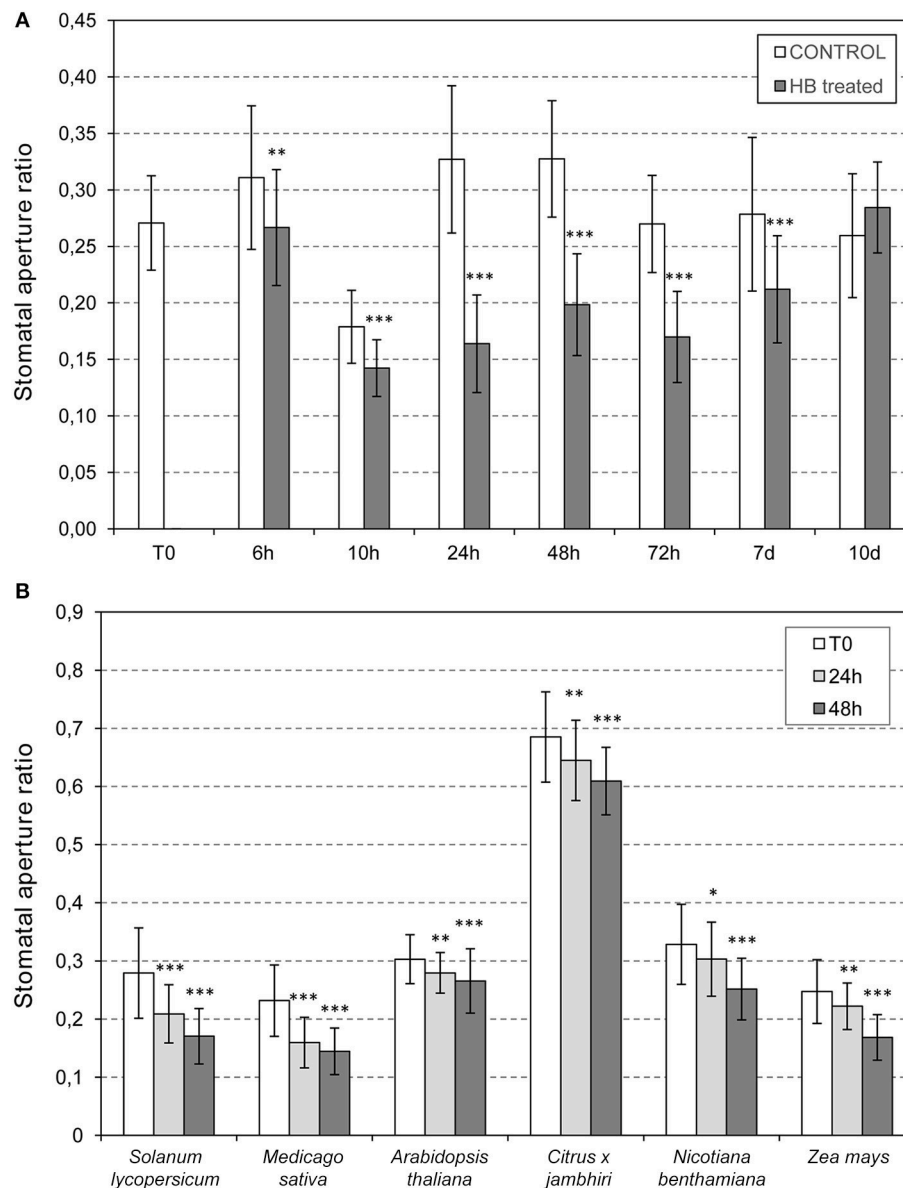


FIGURE 6 | Stomatal opening in plants treated with (Z)-3-hexenyl-butyrate (HB). **(A)** Time course analysis of the (HB) effect on tomato stomata closure. Stomata ratios were analyzed in non-treated (control) and HB-treated (HB) tomato leaves at 0 (T0), 6, 10, 24, 48, 72 h post-treatment (h), and at 7 and 10 days post-treatment (d). **(B)** Effectivity of HB treatments in different species. Samples were collected 24 or 48 h after treatments. Asterisk (*), double asterisks (**) and triple asterisks (***) indicate significant differences between control and HB-treated plants with $p < 0.05$, $p < 0.01$ and $p < 0.001$, respectively.

HB treatment (**Figure 6B**). The treatments produced significant stomatal closure in all the species tested, thus indicating that HB is a universal stomata closer, extending its uses to Solanaceae, Brassicaceae, Fabaceae, Poaceae, and Rutaceae (Lisón et al., 2017). It is worth noting that, despite being significant, the observed effect in *Arabidopsis* was lower than what was observed in the rest of the analyzed species.

Our results support a model in which VOC ester synthesis is stimulated by the presence of *Pst*, triggering stomatal closure that limits entry of *Pst* into leaves and limits subsequent disease symptom development.

DISCUSSION

Green leaf volatiles (GLVs) consist of a family of C6 compounds, including aldehydes, alcohols, and esters, which are abundantly produced across the plant kingdom. Although the defensive role of GLVs has been classically associated with plant-herbivore interaction, it has been recently described that pathogens also provoke a higher emission of these plant volatiles (Ameje et al., 2018). In particular, some GLV esters are differentially emitted by tomato plants during establishment of the ETI triggered by *Pst* (López-Gresa et al., 2017). A direct defensive role of

GLVs against pathogens has been demonstrated, since they display antibacterial activities against both gram-negative and gram-positive bacteria (Nakamura and Hatanaka, 2002). In this sense, GLVs formed during the avirulent infection of beans against *Pseudomonas* were sufficient to be toxic to the pathogenic bacteria (Croft et al., 1993). In the present work, we have also observed antimicrobial properties for HA (Figure S1), although it appears to be insufficient to enhance resistance to *Pst*. Here, we describe an indirect defensive role of GLV esters in stomatal defense of plants against *Pst*.

We observed that tomato plants treated with HP or HB display a higher ratio of stomatal closure, PR gene induction and reduced symptom development following *Pst* inoculation. Moreover, *as-AAT1* tomato plants, which are impaired in the emission of these GLV esters upon bacterial infection, exhibited a lower ratio of stomatal closure and were hyper-susceptible to *Pst*. Similar results have been described with the precursors of these volatiles in *Arabidopsis* (Montillet et al., 2013). These authors demonstrated that treatments with LOX substrates (PUFAs), or with LOX products (fatty acid hydroperoxides; FAHs) trigger stomatal closure, and that the 9-lipoxygenase, *LOX1*, is required to trigger stomatal closure in response to bacteria in *Arabidopsis*. Related to this result, we observed that *Arabidopsis* plants treated with HB have a higher ratio of stomata closure (Figure 6B), consistent with a role for GLV esters affecting stomatal defense in *Arabidopsis* as well. It would be of great interest to study the possible PUFA-mediated emission of GLV esters, or the phenotype against bacteria of *Arabidopsis* mutants in 13-LOX gene, which is responsible for GLV ester biosynthesis.

GLVs have been reported to induce resistance against fungal pathogens. In this context, application of (*E*)-2-hexenal reduced the severity of powdery mildew in tobacco plants (Quaglia et al., 2012). Exogenous treatments with (*E*)-2-hexenal, (*Z*)-3-hexenal, or (*Z*)-3-hexenol induced expression of several defense genes and enhanced resistance against *Botrytis cinerea* in *Arabidopsis* (Kishimoto et al., 2008). Also, transgenic tomato plants overexpressing a tea hydroperoxide lyase (*CsiHPL1*) release more constitutive and wound-induced GLVs, including (*Z*)-3-hexenal and (*Z*)-3-hexen-1-ol, and exhibit enhanced resistance to the necrotrophic fungus *Alternaria alternata* f. sp. *lycopersici* (Xin et al., 2014). Numerous examples of the role of GLVs in plant-fungal interactions have been reviewed (Scala et al., 2013). All these results, together with the work presented here clearly demonstrate the involvement of GLVs in the plant defense response. Furthermore, some species of fungi, such as *Puccinia* are specialized to enter the leaves only through stomata and several fungal metabolites that modulate stomatal behavior have been described (Shafiei et al., 2007; Grimmer et al., 2012; Murata et al., 2015). Therefore, GLVs may also play a role in stomatal defense against fungal pathogens.

Likewise, the regulation of stomatal aperture is known to be part of the plant immune response against bacteria. Two consecutive steps of stomatal movement upon infection with *Pst* in *Arabidopsis* (Melotto et al., 2006) and tomato (Du et al., 2014) have been described. Upon perception of the pathogen-associated molecular patterns (PAMPs), plants close stomata within 1 h in an ABA-dependent manner, thus limiting entry of the pathogen.

In a second phase, bacterial coronatine provokes a JA-dependent reopening of the stomata after 3–4 h. Here we observed that, as a consequence of recognition of the bacterial effectors, a third phase may occur so that the plant recloses the stomata in a SA-independent process. Analogous to the plant immune zig-zag model (Jones and Dangl, 2006), a stomatal defense zig-zag model can be proposed (Figure 7).

Broadening the effect of GLV esters on plants, we observed that HB treatments provoke stomatal closure in several plant species, belonging to Solanaceae, Leguminosae, Brassicaceae, Citrus, and Gramineae (Figure 6B) (Lisón et al., 2017). Stomatal aperture regulates not only the entry of pathogens, but also several important processes including CO₂ uptake for photosynthesis and loss of water by transpiration. It has been widely described that controlling stomatal closure can enhance plant resistance to drought (Cominelli et al., 2010). However, prolonged stomatal closure is not sustainable, since it limits photosynthetic assimilation and growth (Farquhar and Sharkey, 1982). We propose that application of HB may have utility in agriculture for punctuated periods to alleviate both biotic and abiotic stresses. Further studies will be necessary to better establish the HB uses.

Advances in the identification of genes and enzymes responsible for biosynthesis of volatile compounds have made possible the development of metabolic engineering, enabling improvement of different plant characteristics, including reproduction, the quality of the aroma of the fruits and defense against herbivores (Dudareva and Pichersky, 2008). Chemical communication between plants has also received much attention because of the role of the VOCs as possible inducers of defenses in host plants. In this respect,

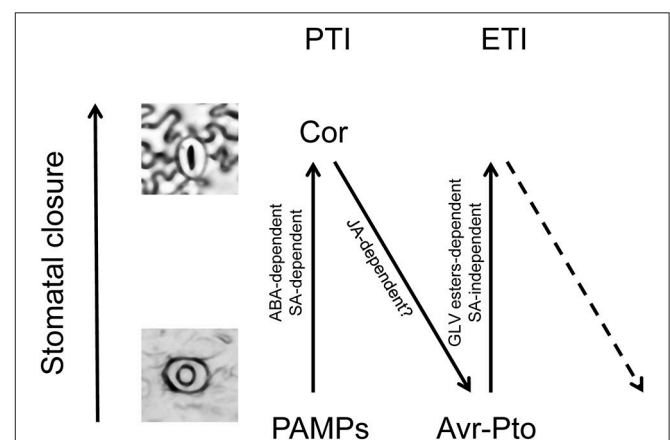


FIGURE 7 | Zig-zag model for stomatal defense. Analogously to the previously proposed zig-zag model for plant immunity (Jones and Dangl, 2006), three different phases are proposed for the stomatal defense. In phase 1, upon perception of the pathogen-associated molecular patterns (PAMPs), plants close stomata in an ABA-dependent manner, contributing to the PAMP-triggered immunity (PTI). In phase 2, bacterial coronatine provokes a JA-dependent reopening of the stomata, interfering with PTI. In phase 3, the bacterial effectors are recognized by NB-LRR proteins activating effector-triggered immunity (ETI), and then the plant recloses the stomata in a GLV-dependent and SA-independent process.

airborne signals from BTH-treated or infected plants can enhance the resistance of lima bean to a bacterial pathogen (Yi et al., 2009). Similarly, overexpressing β -ocimene synthase in tobacco plants results in higher emission of this monoterpene and induces resistance to herbivores in neighboring corn, lima beans and tomato plants (Muroi et al., 2011; Cascone et al., 2015). Moreover, antifungal volatiles released from Chinese chive help control Panama disease in banana (Zhang et al., 2013). Our results could lead to the use of metabolic engineering for improving the defense of plants against pathogens, by modifying GLV ester biosynthetic genes. The volatile nature of GLV esters would permit these transgenic plants to provide protection in non-transgenic neighboring crops.

AUTHOR CONTRIBUTIONS

PL and ML-G conceived and designed the study. ML-G, MO, and CP performed the experiments. CP and IR prepared the figures.

REFERENCES

- Aharoni, A., Giri, A. P., Deurlein, S., Griepink, F., de Kogel, W. J., Verstappen, F. W., et al. (2003). Terpenoid metabolism in wild-type and transgenic Arabidopsis plants. *Plant Cell* 15, 2866–2884. doi: 10.1105/tpc.016253
- Amey, M., Allmann, S., Verwaeren, J., Smagge, G., Haesaert, G., Schuurink, R. C., et al. (2018). Green leaf volatile production by plants: a meta-analysis. *New Phytol.* 220, 666–683. doi: 10.1111/nph.14671
- Arnaud, D., and Hwang, I. (2015). A sophisticated network of signaling pathways regulates stomatal defenses to bacterial pathogens. *Mol. Plant* 8, 566–581. doi: 10.1016/j.molp.2014.10.012
- Brading, P. A., Hammond-Kosack, K. E., Parr, A., and Jones, J. D. (2000). Salicylic acid is not required for Cf-2- and Cf-9-dependent resistance of tomato to *Cladosporium fulvum*. *Plant J.* 23, 305–318. doi: 10.1046/j.1365-3113x.2000.00778.x
- Campos, L., Granell, P., Tarraga, S., Lopez-Gresa, P., Conejero, V., Belles, J. M., et al. (2014). Salicylic acid and genticic acid induce RNA silencing-related genes and plant resistance to RNA pathogens. *Plant Physiol. Biochem.* 77, 35–43. doi: 10.1016/j.plaphy.2014.01.016
- Cardoza, Y. J., and Tumlinson, J. H. (2006). Compatible and incompatible *Xanthomonas* infections differentially affect herbivore-induced volatile emission by pepper plants. *J. Chem. Ecol.* 32, 1755–1768. doi: 10.1007/s10886-006-9107-y
- Cascone, P., Iodice, L., Maffei, M. E., Bossi, S., Arimura, G., and Guerrieri, E. (2015). Tobacco overexpressing beta-ocimene induces direct and indirect responses against aphids in receiver tomato plants. *J. Plant Physiol.* 173, 28–32. doi: 10.1016/j.jplph.2014.08.011
- Cominelli, E., Galbiati, M., and Tonelli, C. (2010). Transcription factors controlling stomatal movements and drought tolerance. *Transcription* 1, 41–45. doi: 10.4161/trns.1.1.12064
- Croft, K. P. C., Juttner, F., and Slusarenko, A. J. (1993). Volatile products of the lipoxygenase pathway evolved from *Phaseolus vulgaris* (L.) leaves inoculated with *Pseudomonas syringae* pv *phaseolicola*. *Plant Physiol.* 101, 13–24.
- Dangl, J. L., and Jones, J. D. G. (2001). Plant pathogens and integrated defence responses to infection. *Nature* 411, 826–833. doi: 10.1038/35081161
- Drukker, B., Bruin, J., Jacobs, G., Kroon, A., and Sabelis, M. W. (2000). How predatory mites learn to cope with variability in volatile plant signals in the environment of their herbivorous prey. *Exp. Appl. Acarol.* 24, 881–895. doi: 10.1023/A:1010645720829
- Du, M., Zhai, Q., Deng, L., Li, S., Li, H., Yan, L., et al. (2014). Closely related NAC transcription factors of tomato differentially regulate stomatal closure and reopening during pathogen attack. *Plant Cell* 26, 3167–3184. doi: 10.1105/tpc.114.128272
- Dudareva, N., Negre, F., Nagegowda, D. A., and Orlova, I. (2006). Plant volatiles: recent advances and future perspectives. *Crit. Rev. Plant Sci.* 25, 417–440. doi: 10.1080/07352680600899973
- Dudareva, N., and Pichersky, E. (2008). Metabolic engineering of plant volatiles. *Curr. Opin. Biotechnol.* 19, 181–189. doi: 10.1016/j.copbio.2008.02.011
- Farquhar, G. D., and Sharkey, T. D. (1982). Stomatal conductance and photosynthesis. *Ann. Rev. Plant Physiol.* 33, 317–345. doi: 10.1146/annurev.pp.33.060182.001533
- Gimenez-Ibanez, S., Boter, M., Ortigosa, A., Garcia-Casado, G., Chini, A., Lewsey, M. G., et al. (2017). JAZ2 controls stomata dynamics during bacterial invasion. *New Phytol.* 213, 1378–1392. doi: 10.1111/nph.14354
- González-Guzmán, M., Rodríguez, L., Lorenzo-Orts, L., Pons, C., Sarrion-Perdigones, A., Fernandez, M. A., et al. (2014). Tomato PYR/PYL/RCAR abscisic acid receptors show high expression in root, differential sensitivity to the abscisic acid agonist quinabactin, and the capability to enhance plant drought resistance. *J. Exp. Bot.* 65, 4451–4464. doi: 10.1093/jxb/eru219
- González-Mas, M. C., Rambla, J. L., Alamar, M. C., Gutierrez, A., and Granell, A. (2011). Comparative analysis of the volatile fraction of fruit juice from different Citrus species. *PLoS ONE* 6:e22016. doi: 10.1371/journal.pone.0022016
- Goulet, C., Kamiyoshihara, Y., Lam, N. B., Richard, T., Taylor, M. G., Tieman, D. M., et al. (2015). Divergence in the enzymatic activities of a tomato and *Solanum pennellii* alcohol acyltransferase impacts fruit volatile ester composition. *Mol. plant* 8, 153–162. doi: 10.1016/j.molp.2014.11.007
- Grimmer, M. K., John Foulkes, M., and Paveley, N. D. (2012). Foliar pathogenesis and plant water relations: a review. *J. Exp. Bot.* 63, 4321–4331. doi: 10.1093/jxb/ers143
- Hijaz, F., Nehela, Y., and Killiny, N. (2016). Possible role of plant volatiles in tolerance against huanglongbing in citrus. *Plant Signal Behav.* 11:e1138193. doi: 10.1080/15592324.2016.1138193
- Huang, J., Cardoza, Y. J., Schmelz, E. A., Raina, R., Engelberth, J., and Tumlinson, J. H. (2003). Differential volatile emissions and salicylic acid levels from tobacco plants in response to different strains of *Pseudomonas syringae*. *Planta* 217, 767–775. doi: 10.1007/s00425-003-1039-y
- Ishiga, Y., Ishiga, T., Uppalapati, S. R., and Mysore, K. S. (2013). Jasmonate ZIM-domain (JAZ) protein regulates host and nonhost pathogen-induced cell death in tomato and *Nicotiana benthamiana*. *PLoS ONE* 8:e75728. doi: 10.1371/journal.pone.0075728
- Jones, J. D., and Dangl, J. L. (2006). The plant immune system. *Nature* 444, 323–329. doi: 10.1038/nature05286

ACKNOWLEDGMENTS

This work was funded by Grant AICO/2017/048 from the Generalitat Valenciana and by Grant INNVAL10/18/005 from the Agència Valenciana de la Innovació (Spain). We would like to thank the Metabolomics Service of the IBMCP (Valencia, Spain), especially to Teresa Caballero for her excellent technical support in the VOCs quantification. We also thank Eduardo Moya for technical assistance.

SUPPLEMENTARY MATERIAL

The Supplementary Material for this article can be found online at: <https://www.frontiersin.org/articles/10.3389/fpls.2018.01855/full#supplementary-material>

- Kessler, A., and Baldwin, I. T. (2001). Defensive function of herbivore-induced plant volatile emissions in nature. *Science* 291, 2141–2144. doi: 10.1126/science.291.5511.2141
- Kim, J., and Felton, G. W. (2013). Priming of antiherbivore defensive responses in plants. *Insect. Sci.* 20, 273–285. doi: 10.1111/j.1744-7917.2012.01584.x
- Kishimoto, K., Matsui, K., Ozawa, R., and Takabayashi, J. (2008). Direct fungicidal activities of C6-aldehydes are important constituents for defense responses in Arabidopsis against *Botrytis cinerea*. *Phytochemistry* 69, 2127–2132. doi: 10.1016/j.phytochem.2008.04.023
- Lin, N. C., and Martin, G. B. (2005). An avrPto/avrPtoB mutant of *Pseudomonas syringae* pv. tomato DC3000 does not elicit Pto-mediated resistance and is less virulent on tomato. *Mol. Plant Microbe Inter.* 18, 43–51. doi: 10.1094/mpmi-18-0043
- Lisón, P., Lopez-Gresa, M. P., Rodrigo, I., and Belles, J. M. (2017). *National Patent. Compuesto Para la Protección de Plantas Mediante Cierre Estomático, Uso, Composición y Método Relacionados*. P201730685. Spain patent application.
- Lisón, P., Rodrigo, I., and Conejero, V. (2006). A novel function for the cathepsin D inhibitor in tomato. *Plant Physiol.* 142, 1329–1339. doi: 10.1104/pp.106.086587
- López-Gresa, M. P., Lison, P., Campos, L., Rodrigo, I., Rambla, J. L., Granell, A., et al. (2017). A Non-targeted metabolomics approach unravels the VOCs associated with the tomato immune response against *Pseudomonas syringae*. *Front. Plant Sci.* 8:1188. doi: 10.3389/fpls.2017.01188
- Matsui, K. (2016). A portion of plant airborne communication is endorsed by uptake and metabolism of volatile organic compounds. *Curr. Opin. Plant Biol.* 32, 24–30. doi: 10.1016/j.pbi.2016.05.005
- Melotto, M., Underwood, W., and He, S. Y. (2008). Role of stomata in plant innate immunity and foliar bacterial diseases. *Annu. Rev. Phytopathol.* 46, 101–122. doi: 10.1146/annurev.phyto.121107.104959
- Melotto, M., Underwood, W., Koczan, J., Nomura, K., and He, S. Y. (2006). Plant stomata function in innate immunity against bacterial invasion. *Cell* 126, 969–980. doi: 10.1016/j.cell.2006.06.054
- Montillet, J. L., Leonhardt, N., Mondy, S., Tranchimand, S., Rumeau, D., Boudsocq, M., et al. (2013). An abscisic acid-independent oxylipin pathway controls stomatal closure and immune defense in Arabidopsis. *PLoS Biol.* 11:e1001513. doi: 10.1371/journal.pbio.1001513
- Murata, Y., Mori, I. C., and Munemasa, S. (2015). Diverse stomatal signaling and the signal integration mechanism. *Annu. Rev. Plant Biol.* 66, 369–392. doi: 10.1146/annurev-arplant-043014-114707
- Muroi, A., Ramadan, A., Nishihara, M., Yamamoto, M., Ozawa, R., Takabayashi, J., et al. (2011). The composite effect of transgenic plant volatiles for acquired immunity to herbivory caused by inter-plant communications. *PLoS ONE* 6:e24594. doi: 10.1371/journal.pone.0024594
- Nakamura, S., and Hatanaka, A. (2002). Green-leaf-derived C6-aroma compounds with potent antibacterial action that act on both Gram-negative and Gram-positive bacteria. *J. Agric. Food Chem.* 50, 7639–7644. doi: 10.1021/jf025808c
- Niinemets, U., Kaennaste, A., and Copolovici, L. (2013). Quantitative patterns between plant volatile emissions induced by biotic stresses and the degree of damage. *Front. Plant Sci.* 4: 262. doi: 10.3389/fpls.2013.00262
- Ntoutkakias, V., Mucyn, T. S., Gimenez-Ibanez, S., Chapman, H. C., Gutierrez, J. R., Balmuth, A. L., et al. (2009). Host inhibition of a bacterial virulence effector triggers immunity to infection. *Science* 324, 784–787. doi: 10.1126/science.1169430
- Panchal, S., and Melotto, M. (2017). Stomate-based defense and environmental cues. *Plant Signal Behav.* 12:e1362517. doi: 10.1080/15592324.2017.1362517
- Quaglia, M., Fabrizi, M., Zizzerini, A., and Zadra, C. (2012). Role of pathogen-induced volatiles in the *Nicotiana tabacum-Golovinomyces cichoracearum* interaction. *Plant Physiol. Biochem.* 52, 9–20. doi: 10.1016/j.plaphy.2011.11.006
- Robert-Seilantantz, A., Grant, M., and Jones, J. D. (2011). Hormone crosstalk in plant disease and defense: more than just jasmonate-salicylate antagonism. *Annu. Rev. Phytopathol.* 49, 317–343. doi: 10.1146/annurev-phyto-073009-114447
- Rodrigo, I., Vera, P., Tornero, P., Hernandez-Yago, J., and Conejero, V. (1993). cDNA cloning of viroid-induced tomato pathogenesis-related protein P23. Characterization as a vacuolar antifungal factor. *Plant Physiol.* 102, 939–945.
- Scala, A., Allmann, S., Mirabella, R., Haring, A. M., and Schuurink, C. R. (2013). Green Leaf Volatiles: a plant's multifunctional weapon against herbivores and pathogens. *Int. J. Mol. Sci.* 14, 17781–17811. doi: 10.3390/ijms140917781
- Shafei, R., Hang, C., Kang, J. G., and Loake, G. J. (2007). Identification of loci controlling non-host disease resistance in Arabidopsis against the leaf rust pathogen *Puccinia triticina*. *Mol. Plant Pathol.* 8, 773–784. doi: 10.1111/j.1364-3703.2007.00431.x
- Tornero, P., Rodrigo, I., Conejero, V., and Vera, P. (1993). Nucleotide sequence of a cDNA encoding a pathogenesis-related protein, P1-p14, from tomato (*Lycopersicon esculentum*). *Plant Physiol.* 102:325.
- Xin, Z., Zhang, L., Zhang, Z., Chen, Z., and Sun, X. (2014). A tea hydroperoxide lyase gene, CsiHPL1, regulates tomato defense response against *Prodenia litura* (Fabricius) and *Alternaria alternata* f. sp. *Lycopersici* by modulating Green Leaf Volatiles (GLVs) release and Jasmonic Acid (JA) gene expression. *Plant Mol. Biol. Rep.* 32, 62–69. doi: 10.1007/s11105-013-0599-7
- Yi, H. S., Heil, M., Adame-Alvarez, R. M., Ballhorn, D. J., and Ryu, C. M. (2009). Airborne induction and priming of plant defenses against a bacterial pathogen. *Plant Physiol.* 151, 2152–2161. doi: 10.1104/pp.109.144782
- Zhang, H., Mallik, A., and Zeng, R. S. (2013). Control of Panama disease of banana by rotating and intercropping with Chinese chive (*Allium tuberosum* Rottler): role of plant volatiles. *J. Chem. Ecol.* 39, 243–252. doi: 10.1007/s10886-013-0243-x
- Zheng, X. Y., Spivey, N. W., Zeng, W., Liu, P. P., Fu, Z. Q., Klessig, D. F., et al. (2012). Coronatine promotes *Pseudomonas syringae* virulence in plants by activating a signaling cascade that inhibits salicylic acid accumulation. *Cell Host Microbe* 11, 587–596. doi: 10.1016/j.chom.2012.04.014



Conflict of Interest Statement: The authors declare that the research was conducted in the absence of any commercial or financial relationships that could be construed as a potential conflict of interest.

Copyright © 2018 López-Gresa, Payá, Ozáez, Rodrigo, Conejero, Klee, Bellés and Lisón. This is an open-access article distributed under the terms of the Creative Commons Attribution License (CC BY). The use, distribution or reproduction in other forums is permitted, provided the original author(s) and the copyright owner(s) are credited and that the original publication in this journal is cited, in accordance with accepted academic practice. No use, distribution or reproduction is permitted which does not comply with these terms.

Annex II

Article

Effect of Benzothiadiazole on the Metabolome of Tomato Plants Infected by Citrus Exocortis Viroid

María Pilar López-Gresa ^{1,*}, Celia Payá ¹, Ismael Rodrigo ¹, José María Bellés ¹,
Susana Barceló ², Young Hae Choi ^{3,4}, Robert Verpoorte ³ and Purificación Lisón ¹

¹ Instituto de Biología Molecular y Celular de Plantas, Universitat Politècnica de València (UPV)-Consejo Superior de Investigaciones Científicas (CSIC), Ciudad Politécnica de la Innovación (CPI), Ingeniero Fausto Elio s/n, 46022 Valencia, Spain; cepamon@etsiamn.upv.es (C.P.); irodrigo@ibmcp.upv.es (I.R.); jmbelles@btc.upv.es (J.M.B.); plison@ibmcp.upv.es (P.L.)

² Department of Applied Statistics and Operational Research, and Quality. Universitat Politècnica de València (UPV), 46022 Valencia, Spain; sbarcelo@eio.upv.es

³ Natural Products Laboratory, Institute of Biology, Leiden University, 2333 BE Leiden, The Netherlands; y.h.choi@biology.leidenuniv.nl (Y.H.C.); verpoort@chem.leidenuniv.nl (R.V.)

⁴ College of Pharmacy, Kyung Hee University, Seoul 02447, Korea

* Correspondence: mplopez@ceqa.upv.es; Tel.: +34-963877862

Received: 28 March 2019; Accepted: 10 May 2019; Published: 14 May 2019



Abstract: Benzothiadiazole (BTH) is a functional analogue of the phytohormone salicylic acid (SA) involved in the plant immune response. NahG tomato plants are unable to accumulate SA, which makes them hypersusceptible to several pathogens. Treatments with BTH increase the resistance to bacterial, fungal, viroid, or viral infections. In this study, metabolic alterations in BTH-treated Money Maker and NahG tomato plants infected by citrus exocortis viroid (CEVd) were investigated by nuclear magnetic resonance spectroscopy. Using multivariate data analysis, we have identified defence metabolites induced after viroid infection and BTH-treatment. Glycosylated phenolic compounds include gentisic and ferulic acid accumulated in CEVd-infected tomato plants, as well as phenylalanine, tyrosine, aspartate, glutamate, and asparagine. Besides, an increase of γ -aminobutyric acid (GABA), glutamine, adenosine, and trigonelline, contributed to a clear discrimination between the metabolome of BTH-treated tomato leaves and their corresponding controls. Among them, GABA was the only metabolite significantly accumulated in both genotypes after the chemical treatment. In view of these results, the addition of GABA was performed on tomato plants infected by CEVd, and a reversion of the NahG hypersusceptibility to CEVd was observed, indicating that GABA could regulate the resistance to CEVd induced by BTH.

Keywords: NMR; metabolomics; tomato; viroid; BTH; defence; NahG plants; GABA

1. Introduction

Plants respond to biotic stress using both innate and acquired immune systems. When challenged, the resistance proteins (R) of the plants recognize the specific avirulence factors (Avr) derived from the pathogen, triggering a hypersensitivity response (HR) in the infected tissues. Following the local pathogen exposure, the distal defensive plant response, known as systemic acquired resistance (SAR), is activated via salicylic acid (SA), inducing the pathogenesis-related (PR) proteins and/or phytoalexins in the uninfected tissues [1]. In contrast, when the acquired immunity is not established, the 5-hydroxylation of SA yields gentisic acid (GA), being the accumulation characteristic of the compatible plant-pathogen interactions [2].

Tomato plants (*Solanum lycopersicum*) inoculated with the citrus exocortis viroid (CEVd) accumulate high levels of both SA and GA, constituting an excellent plant-pathogen system to study the signaling

function of these phenolic compounds [3]. In addition, studies carried out with the SA-deficient NahG transgenic tomato plants [4] highlight the possible defensive role of these signaling molecules in the viroid infection [5].

Benzo (1,2,3) thiadiazole-7-carbothioic acid-S-methyl ester (BTH; Figure 1A), a functional analogue of the plant endogenous hormone SA, is an SAR activator which acts downstream of the SA signaling, providing protection in many crops [6]. Previous work had demonstrated that BTH was a potent inducer of pathogenesis-related genes, thus priming the plants for potential pathogenic attacks [7,8]. Specifically, foliar BTH spray applications of tomato plants conferred resistance against fungal and bacterial infections [9,10]. Moreover, the addition of BTH improves the resistance of the hyper susceptible NahG tomato plants to CEVd and tomato spotted wilt virus (TSWV) infections [5]. BTH applications also produce physiological, biochemical and proteomic changes. In this sense, proteins involved in stress response, energy metabolism, primary and secondary metabolism, signal transduction, and transporters were induced by BTH treatments on muskmelon fruits [11]. However, few reports have been published on how BTH affects the plant metabolome [12]. The activation of key genes involved in secondary metabolic pathways such as phenylalanine ammonia-lyase (PAL), a pivotal gene related to phenylpropanoid metabolism involved in biotic and abiotic stress [13], has been found in cultured parsley cells after the application of both elicitor and BTH [14]. An increase in the levels of stilbenes and anthocyanins in grapevine following BTH treatments has been reported, improving resistance to *Botrytis cinerea* infections [15]. In contrast, the phenolic content was significantly reduced in BTH-treated *Arabidopsis* plants [12].

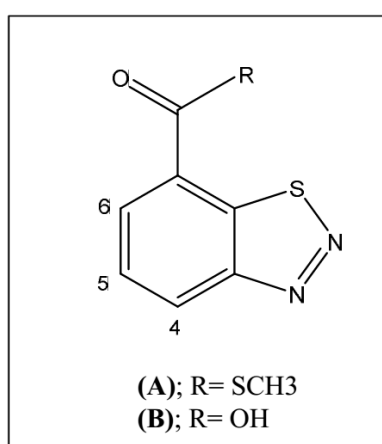


Figure 1. Chemical structures of BTH (A) and hydrolyzed BTH (B).

The employment of the metabolomics platform has provided a new dimension in various study of life sciences, particularly plant-pathogen interactions. This analytical approach enables the monitoring of metabolic alterations produced by different biotic agents. Nuclear magnetic resonance (NMR) is one of the most universally used tools as an analytical platform of metabolomics because it can show the major biomarkers involved in the plant defence response. ¹H-NMR spectroscopy detects simultaneously the most abundant compounds, offering a macroscopic view of the biochemical situation in the cell at a given point in time [16]. Particularly, studies of *Solanum lycopersicum* infected by different pathogens as viroids, bacteria [17], or viruses [18] showed a large number of primary metabolites differentially accumulated, including amino acids, carbohydrates and organic acids, and some secondary compounds such as phenylpropanoids and flavonoids.

Using these technologies, we study the metabolomic changes in NahG tomato plants, which are not able to accumulate SA, and their corresponding parental Money Maker upon infection with CEVd and BTH treatments. In this work, NMR spectroscopy and partial least square analysis (PLS) were applied to distinguish the induced compounds. The obtained results not only provide information about the metabolic plant adaptation to this chemical, but also about its mechanism of action. Among all the

metabolites induced by BTH in tomato plants, we reasoned that GABA, a non-protein, free amino acid involved in multiple signaling processes of abiotic [19] and biotic stresses [20–22], could play an important role in the plant defence response of tomato plants to CEVd. To test this hypothesis, the effect of exogenous addition of GABA on tomato defence response and its resistance to CEVd was investigated.

2. Materials and Methods

2.1. Tomato Plants and Growth Conditions

Tomato plants (*Solanum lycopersicum* cv. Money Maker) and its transformant 35S::NahG expressing the bacterial salicylate hydroxylase [4,23] (kindly provided by Professor J.D.G. Jones, John Innes Centre, Norwich, UK), were used in this study. The tomato seeds were sterilized with a 1:1 mixture of commercial sodium hypochlorite and distilled H₂O containing a few drops of Tween 20. After the sterilization treatment, they were subsequently sequentially washed with distilled H₂O during 5, 10, and 15 min. Then, the seeds were transferred to 14 cm diameter Petri dishes with a filter paper soaked with distilled water and were kept in darkness at 24 °C for 48 h, followed by another 48 h in the presence of light. Seeds were placed in 12 cm-diameter pots containing a 1:1 mixture of vermiculite and peat, and were grown under greenhouse conditions with a day/night photoperiod of 16/8 h (30/26 °C), supplemented with artificial light and a relative humidity between 50–70%. The growth conditions were described in detail in a previous work [5].

2.2. CEVd Infection Procedure

To study the metabolic changes produced by BTH, a total of twelve Money Maker and twelve NahG plants were used for the experiment. To confirm the protective effect of GABA treatments, eighteen tomato plants of each genotype were used. Half of the plants were infected with CEVd (GenBank accession number S67446) obtained from CEVd-infected Rutgers tomato plants bearing strong symptoms. Inoculation was carried out by rubbing with carborundum, both the first leaf and a cotyledon of 2 week-old plantlets in the presence of 50 ng of the pathogen, as described in López-Gresa et al. [5]. The remaining tomato plants were mock-inoculated by applying 50 µL of sterile demineralized water instead of viroid inoculum. After inoculation, plants were grown under the greenhouse conditions described above. Disease severity was recorded at different time points by measuring all the dwarfing, rugosity, rigidity, and epinasty grade. The tip tissues from mock and CEV-inoculated plants were sampled for the analytical measurements at 2.5- and 3-weeks post infection (wpi), frozen in liquid nitrogen, homogenized in cold conditions, and stored at –80 °C until used.

2.3. Treatments with BTH and GABA

Exogenous treatments of GABA and BTH were carried out following the procedure described in López Gresa et al. [5]. A 1 mM solution supplemented with 0.05% (*v/v*) Tween 20, was sprayed at 3 and 6 days after viroid inoculation. BTH (Acibenzolar-S-methyl) was supplied as Bion 50WG (50%, *w/w*) (Syngenta España, Madrid, Spain), and GABA (γ -aminobutyric acid) was purchased from Sigma-Aldrich (Madrid, Spain).

To perform the NMR metabolomics study after CEVd infection, one half of the Money Maker and NahG plants were sprayed with 1 mM BTH, and the other half was treated with 0.05% (*v/v*) Tween 20 in demineralized water at the same time points.

To analyze the primary metabolite content after BTH treatments, two groups of six Money Maker and six NahG 4-week-old tomato plants were used. Three control plants of each group were sprayed with 0.05% (*v/v*) Tween 20 in demineralized water and the others were sprayed with 1 mM BTH. Fifth and sixth tomato leaves were harvested at 48 h post-treatment (hpt) and immediately frozen in liquid nitrogen and stored at –80 °C until processed for GC-MS analysis.

To study the protective effect of GABA, two groups of eighteen Money Maker and eighteen NahG plants were prepared. One group of six tomato plants in each variety was treated with 0.05% (*v/v*)

Tween 20 in demineralized water, and the second and third groups were sprayed with 1 mM BTH or 1 mM GABA solutions, respectively.

2.4. Extraction of Metabolites and NMR Spectra Measurements

For the analysis of polar and semi-polar metabolites, 25 mg of freeze-dried plant material (3 wpi) were extracted in 2 mL-Eppendorf tubes with 1 mL of a 1:1 mixture of KH_2PO_4 buffer (pH 6) in D_2O containing 0.05% trimethylsilane propionic acid sodium salt (TMSP) and tetradeuteromethanol ($\text{CH}_3\text{OH-d}_4$). The mixture was vortexed at room temperature for 1 min, sonicated for 20 min, and centrifuged at 13,000 rpm at room temperature for 10 min. A volume of 700 μL of the supernatant was transferred to a 5 mm-NMR tube for the spectral analysis. $^1\text{H-NMR}$, 2D-J resolved, and $^1\text{H-}^1\text{H}$ correlated spectroscopy (COSY) were recorded at 25 °C on a 600 MHz Bruker AV 600 spectrometer equipped with cryoprobe operating at a proton NMR frequency of 600.13 MHz. As internal lock, methyl signals of $\text{CH}_3\text{OH-d}_4$ were used. Each $^1\text{H-NMR}$ spectrum consisted of 128 scans requiring a 10 min acquisition time with the following parameters: 0.25 Hz/point, pulse width of 30° (10.8 μs), and relaxation delay of 1.5 s. To suppress the residual H_2O signal, a pre-saturation sequence was used at the H_2O frequency during the recycle delay. Free induction decays were Fourier transformed with line broadening (0.3 Hz) and the spectra were zero-filled to 32 K points. The resulting spectra were manually phased, baseline-corrected, and calibrated to TMSP at 0.0 ppm, using Topspin version 2.1, (Bruker, Billerica, MA, USA).

2.5. RNA Extraction and Preparation

Total RNA of tomato leaf tissue of 2.5 wpi plants was isolated using TRIzol reagent (Invitrogen, Carlsbad, CA, USA) according to the manufacturer's protocol. RNA was further precipitated by adding one volume of LiCl 6 M, and then the pellet was washed with LiCl 3 M and dissolved in RNase-free water. To remove contaminating genomic DNA, TURBO DNase (Ambion, Carlsbad, CA, USA) were added (2 units/10 μg of RNA).

2.6. Quantitative Real-Time Polymerase Chain Reaction (PCR) Assay

To obtain the corresponding cDNA target sequences, one μg of total RNA was retrotranscribed using an oligo (dT)₁₈ primer and the Prime Script RT reagent kit (Perfect Real Time, Takara, Kusatsu, Shiga, Japan). PCR was performed in the presence of the double-stranded DNA-specific dye Power SYBR Green PCR Master Mix (Applied Biosystems, Carlsbad, CA, USA). Amplification was monitored in real time with the 7500 FAST Real-Time PCR System (Life Technologies, Carlsbad, CA, USA). The PCR primers used for RT-PCRs are listed in Table S1.

2.7. GC-MS Analysis for Primary Metabolite

Primary metabolite analysis was performed at the Metabolomics Platform of the Instituto de Biología Molecular y Celular de Plantas (UPV-CSIC, Valencia, Spain) using a method modified from that described by Roessner [24]. One hundred mg of frozen tomato leaves per sample were homogenized with liquid nitrogen and extracted in 1400 μL 100% methanol containing 60 μL of internal standard (0.2 mg/mL ribitol). The mixture was kept for 15 min at 70 °C; subsequently, the extract was centrifuged for 10 min at 14,000 rpm. Supernatant was transferred to a glass vial where 750 μL of CHCl_3 and 1500 μL of water were added. The mixture was vortexed for 15 s and centrifuged for 15 min at 14,000 rpm. 150 μL aliquots of the methanol/water supernatant were dried in a vacuum for 6–16 h.

For derivatisation, dry residues were re-dissolved in 40 μL of 20 mg/mL methoxyamine hydrochloride prepared in pyridine and incubated for 90 min at 37 °C, followed by the addition of 70 μL MSTFA (*N*-methyl-*N*-[trimethylsilyl]trifluoroacetamide) and 6 μL of a retention time standard mixture (3.7% [*w/v*] mix of fatty acid methyl esters ranging from C8 to C24) and further incubation for 30 min at 37 °C.

Sample volumes of 2 μL were injected in split and spitless mode to increase metabolite detection range in a 6890N gas chromatograph (Agilent Technologies, Santa Clara, CA, USA) coupled to a Pegasus 4D TOF LECO mass spectrometer. Gas chromatography was performed on a BPX35 (30 m \times 0.32 mm \times 0.25 μm) column with helium as carrier gas at a constant flow of 2 mL/min. The liner was set at 230 $^{\circ}\text{C}$. Oven program was 85 $^{\circ}\text{C}$ for 2 min, 8 $^{\circ}\text{C}/\text{min}$ ramp until 360 $^{\circ}\text{C}$. Mass spectra were collected at 6.25 spectra- s^{-1} in the m/z range 35–900 and ionization energy of 70 eV. Chromatograms and mass spectra were evaluated using the ChromaTOF software (LECO Corporation, Saint Joseph, MI, USA). The unequivocal compound identification of the 65 primary metabolites was carried out by comparing both mass spectra and retention times with those of pure standards. All the commercial standards were purchased from Sigma–Aldrich (Madrid, Spain).

2.8. Statistical Analysis

For the untargeted NMR-metabolomics analysis, the ^1H -NMR spectra were automatically reduced by AMIX (v. 3.7, Bruker Biospin, Billerica, MA, USA) to ASCII files. Spectral intensities were scaled to total intensity TMSF and reduced to integrated regions of equal width (0.04 ppm) corresponding to the region of δ 0.4–10.00. The regions of δ 4.70–4.90 and δ 3.28–3.34 were excluded from the analysis because of the residual signals of water and methanol, respectively. Partial least square (PLS) and orthogonal projection to latent structures-discriminant analysis (OPLS-DA) were performed with the SIMCA-P software (v. 13.0.3, Umetrics, Umeå, Sweden) using the Pareto scaling method. For the targeted GC-MS-metabolomics analysis, the area of each primary metabolite relative to ribitol area was used as the X variable in the Principal Component Analysis (PCA) using unit variance (UV) scaling method.

To compare the symptoms between non-treated and chemical treated CEVd-infected NahG tomato plants, the symptom severity was monitored and scored at every time point and statistically analyzed by a Kruskal-Wallis test (non-parametric test equivalent to the one-way ANOVA). Different letters indicate significant differences ($p < 0.05$) between non-treated and chemical treated CEVd-infected NahG tomato plants.

For the qRT-PCR analysis, a t -test analysis was performed. Comparisons between multiple groups were made by analysis of variance (ANOVA) for each time point. A p value < 0.05 was considered significant.

The IBM SPSS v.19 package was used throughout the statistical analysis.

3. Results

3.1. Partial Least Square of ^1H -NMR Spectra of Control and BTH-treated Money Maker and NahG Tomato Plants Infected by CEVd and Mock-Inoculated

Based on previous knowledge about tomato leaf tissue, a new ^1H -NMR study was performed to identify the metabolic changes after BTH treatments on NahG and Money Maker plants after CEVd inoculation. The analysis of the one- and two-dimensional spectra of the plant extracts, along with our in-house database of standards and published data in our previous studies, allowed for the identification of several compounds described in tomato leaves.

After the chemical analysis of the spectra, a comparison of all the samples involved in the metabolomic study was performed through multivariate data analysis (MVDA). Specifically, a PLS analysis was applied, defining as the X variable the area of binned ^1H -NMR signals of plant extracts at 3 wpi, and as the step-wise Y variables the genotype (Money Maker and NahG), the treatment (BTH and H_2O), and the infection (CEVd and mock inoculation). A clear separation was observed in the score plot of PLS (Figure 2A) between the healthy control and CEVd infected plants by component 1, and BTH or H_2O treatments by component 2. However, no separation was observed in the PLS score plot among Money Maker and NahG plants, indicating that the metabolic content of both cultivars did not differ as much as after the infection and treatments. In fact, both CEVd-inoculated genotypes were

in the positive part of PLS-component 1, and both BTH-treated genotypes were in the positive part of PLS-component 2 independently of the chemical treatment or the infection, respectively.

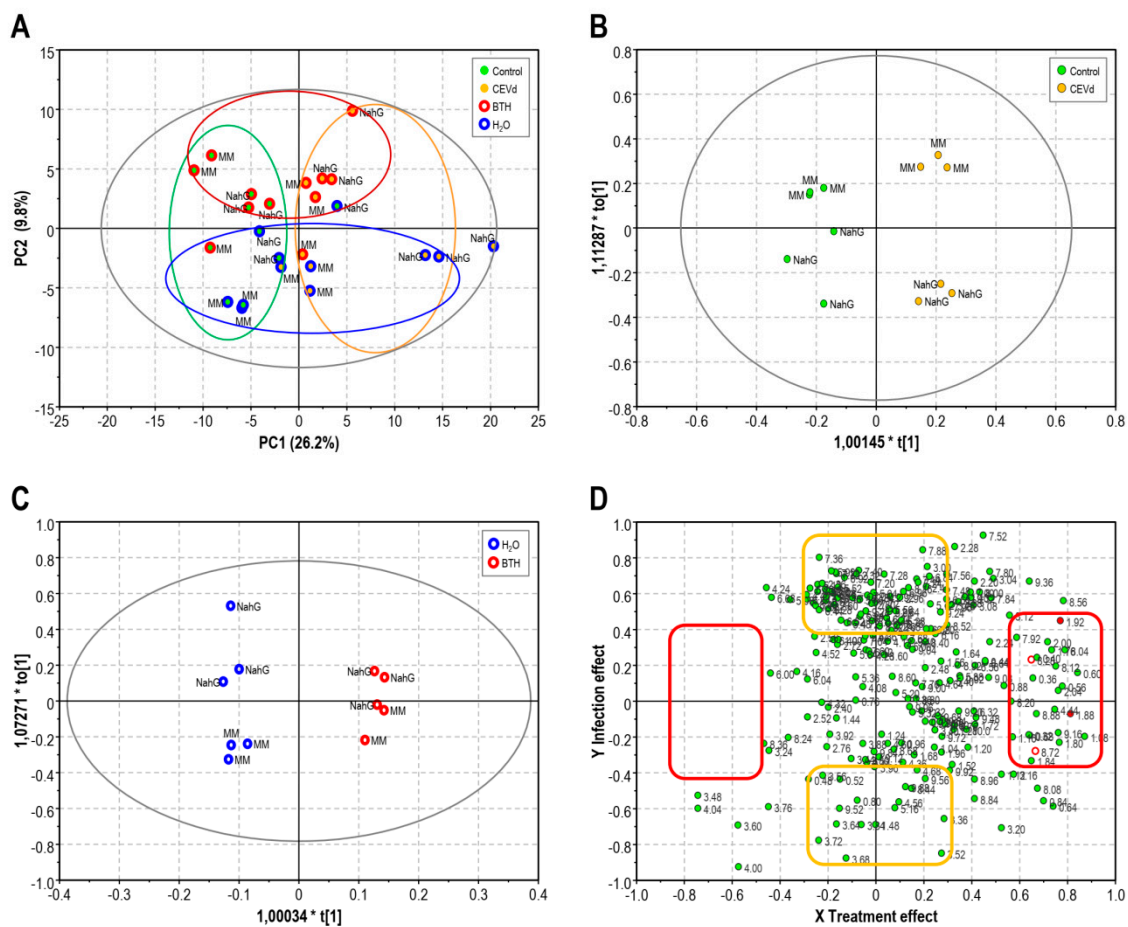


Figure 2. Multivariable data analysis based on the $^1\text{H-NMR}$ signals, in the range of 0.3–10.0 ppm, of the Money Maker (MM) and NahG tomato plants after viroid inoculation and BTH treatments at 3 weeks post infection (green; mock tomato leaves, yellow; tomato leaves infected by CEVd, red; leaves after BTH treatments blue; leaves after H_2O treatments). (A) Score plot of partial least square (PLS) (B) Score plot of orthogonal projection to latent structures-discriminant analysis (OPLS-DA) of the infection ($R^2 = 0.95$, $Q^2 = 0.82$). (C) Score plot of OPLS-DA of chemical treatment ($R^2 = 0.99$, $Q^2 = 0.93$). (D) Shared-and-unique-structures (SUS) plot correlating the two OPLS-DA models with the Y axis as CEVd infection and X axis as BTH treatment ($^1\text{H-NMR}$ signals of GABA in red full circles and $^1\text{H-NMR}$ signals of hydrolyzed BTH in red open circles).

Due to the large number of variables, the PLS could not clearly reveal the metabolites accumulated after the BTH treatment. Therefore, two orthogonal projections to latent structures-discriminant analyses (OPLS-DA) were applied separately to specifically examine the metabolic changes produced by the infection (healthy-CEVd infected; Figure 2B) or the chemical action (H_2O -BTH; Figure 2C). In the score plot of both OPLS-DA models, the samples inoculated by CEVd or sprayed with BTH were clearly separated from their respective controls. These two OPLS-DA models (infection and chemical treatment) were integrated by a shared-and-unique-structures (SUS)-plot (Figure 2D) with the X-axis corresponding to BTH-treatment and the Y-axis to CEVd infection. In this analysis, the diagonally-aligned metabolites were of equal importance and shared by the two models, and the metabolites located along the axis were specifically altered in CEVd-infected (yellow boxes) or BTH-treated tomato plants (red boxes), respectively.

When comparing the metabolome of the control and infected leaves (positive side of *y*-axis SUS-plot yellow boxed, Figure 2D), it was observed that glycosylated phenolic compounds such as gentisic and ferulic acids, as well as the amino acids phenylalanine, tyrosine, aspartate, glutamate, and asparagine were induced in the viroid infection.

The inducing effect of BTH was characterized by the positive side of the *x*-axis (right side of *x*-axis SUS-plot red boxed, Figure 2D) in which GABA, glutamic acid, adenosine, trigonelline, in addition to BTH and its catabolized forms, were found to be the major contributing metabolites induced by the chemical treatment. In fact, the signals observed in the ¹H-NMR spectra at δ 8.72 (H-6, dd, 7.5, 2.3 Hz), δ 8.28 (H-4, d, 7.5 Hz), and δ 7.84 (H-5, t, 7.5 Hz) were discriminant in the SUS-plot model, and were assigned to the residual hydrolyzed BTH (Figure 1B) in accordance with previous results in BTH-treated *Arabidopsis* plants [12].

To better understand the differences between Money Maker and NahG plants, a *t*-test analysis comparing a single variable (BTH) was performed using the ¹H-NMR binned data of each genotype, in both mock-inoculated and CEVd inoculated plants. By doing so, hydrolyzed-BTH and GABA were the compounds that significantly accumulated in mock BTH-treated Money Maker plants, with respect to the corresponding mock non-treated Money Maker plants, whereas GABA and trigonelline displayed higher levels in BTH-treated NahG plants (Table 1).

Table 1. Compounds significantly accumulated (*p*-value ≤ 0.05) after BTH treatments in mock or CEVd-inoculated Money Maker and NahG tomato plants with respect to non-treated corresponding plants.

	BTH Treated vs Non-Treated Plants	
	Money Maker	NahG
Mock-inoculated	GABA hydrolyzed-BTH	GABA ¹ trigonelline
CEVd-inoculated	malic acid aspartic acid trigonelline	caffeic acid ¹ ferulic acid ¹ citric acid ¹ malic acid ¹ aspartic acid threonine alanine α-glucose trigonelline

¹ Compounds differentially overaccumulated in BTH-treated NahG with respect to BTH-treated Money Maker tomato plants.

Moreover, when comparing Money Maker and NahG plants after chemical treatments, the levels of GABA were higher in the transgenic plants, compared to the corresponding non-treated tomato plants. GABA was the most prominent metabolite differentially accumulated in all the comparisons, thus indicating that this molecule could play an important role in the BTH-mediated response. Interestingly, GABA was also significantly accumulated in CEVd-infected and non-treated NahG plants, with respect to the corresponding non-infected plants, no detecting differences caused by the viroid infection in the Money Maker parental plants.

On the other hand, trigonelline, malic, and aspartic acids were induced by BTH in Money Maker infected plants. The same compounds together with α-glucose, citric acid, the amino acids alanine and threonine, and the phenylpropanoids caffeic and ferulic acids were found to accumulate in the infected NahG plants after BTH treatment, with respect to the non-treated transgenic infected plants. Besides, both phenolics together with citric and malic acids also accumulated differentially in BTH treated and infected NahG plants, with respect to the corresponding parental plants. The defensive role of these phenolics could explain their accumulation in the transgenic tomato plants, which recovered from their hyper susceptibility phenotype to viroid infection when treated with BTH [25].

3.2. Study of the Relative Expression Levels of Tomato Genes Involved in GABA Synthesis in Control and BTH-Treated Money Maker and NahG Tomato Plants

To correlate the GABA accumulation after BTH treatments with the transcriptional activation, a qRT-PCR analysis of several genes involved in its biosynthesis (Figure 3) was carried out. Based on the described sequences in several species and using the Blast tool of Solgenomics database, we found the tomato orthologues of the citrate synthase (*mCS*), glutamate dehydrogenase (*GDH*), glutamate decarboxylase (*GAD*), glutamine synthetase (*GS*), aspartate aminotransferase (*AST*), and fumarase (*FH*) genes and designed specific oligonucleotide primers for qRT-PCR analysis (Supplementary Data Table S1).

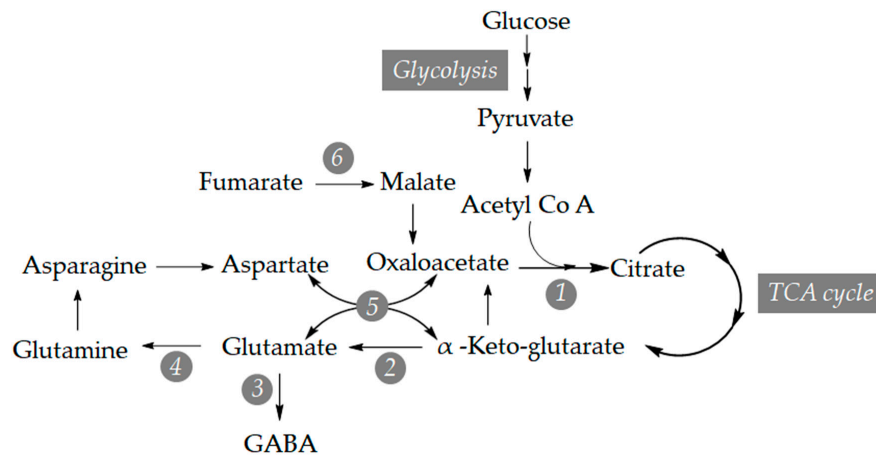


Figure 3. The metabolic inter-relationship between plant metabolism of malate, aspartate, GABA and glucose. 1: Citrate synthase (*mCS*), 2: Glutamate dehydrogenase (*GDH*), 3: Glutamate decarboxylase (*GAD*), 4: Glutamine synthetase (*GS*), 5: Aspartate aminotransferase (*AST*), 6: Fumarase (*FH*).

The results of the induction of these genes in non-treated and BTH-treated Money Maker and NahG mock tomato plants are shown in Figure 4. All the transcripts were induced in Money Maker and NahG plants after the chemical treatments at 2.5 wpi, most of them statistically significant in the transgenic plants. These transcript inductions were well correlated with the relative GABA levels observed in NMR spectra in both genotypes after BTH treatments (Table 1).

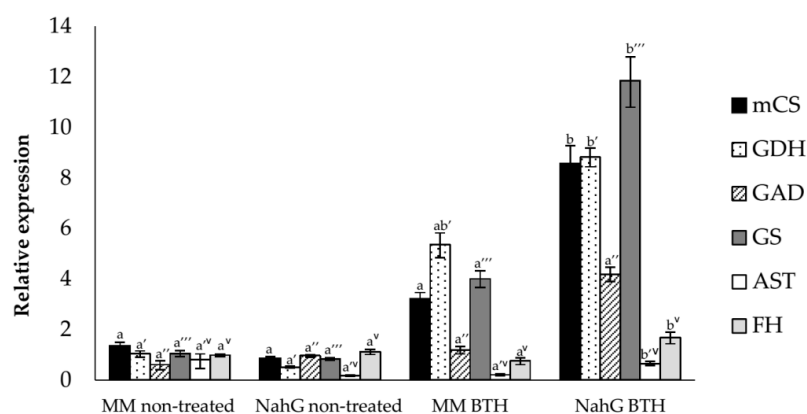


Figure 4. Expression levels of the tomato citrate synthase (*mCS*), glutamate dehydrogenase (*GDH*), glutamate decarboxylase (*GAD*), glutamine synthetase (*GS*), aspartate aminotransferase (*AST*), and fumarase (*FH*) genes in non-treated and BTH-treated (BTH) Money Maker and NahG mock tomato plants at 2.5 wpi, determined by real-time qRT-PCR analysis. Values were first normalized to the actine expression level. Expression levels are represented as mean \pm standard error of three biological repetitions. An ANOVA analysis was performed for each gene, among the four samples (MM-non-treated, MM-BTH, NahG-non-treated and NahG-BTH). Different letters indicate the statistical significance differences among the four samples with p -value < 0.05 .

3.3. Analysis of Primary Metabolites in Money Maker and NahG Tomato Plants after BTH Treatments

To identify other possible changes in primary metabolism underlying the BTH effect, an established gas chromatography-mass spectrometry (GC-MS) method was applied to extracts from Money Maker and NahG tomato leaves after 48 h of 1 mM BTH treatments. A total of 20 amino acids, 22 organic acids, 19 sugars, 2 fatty acids, and 2 nucleotides were analyzed, and only GABA levels were statistically different after chemical treatments in both varieties. These results are in accordance with those obtained by the NMR platform (Table 1), confirming that GABA biosynthesis is induced by BTH in tomato plants.

Following the univariate statistical analysis of mass spectral data, a comparison of all the samples involved in the study was performed through a PCA analysis. An evident separation of BTH-treated NahG plants from all the others was observed by the score scatter plot of PCA, clearly showing that these transgenic plants undergo a greater metabolic change than its parental cultivar after chemical spray (Figure 5). In this case, the discriminant metabolites were GABA and fumarate which remained statistically over-accumulated in NahG tomato leaves after 48 h of BTH treatments. All of these results appear to indicate that GABA could play a role in the BTH-mediated recovery of NahG tomato plants infected with CEVd.

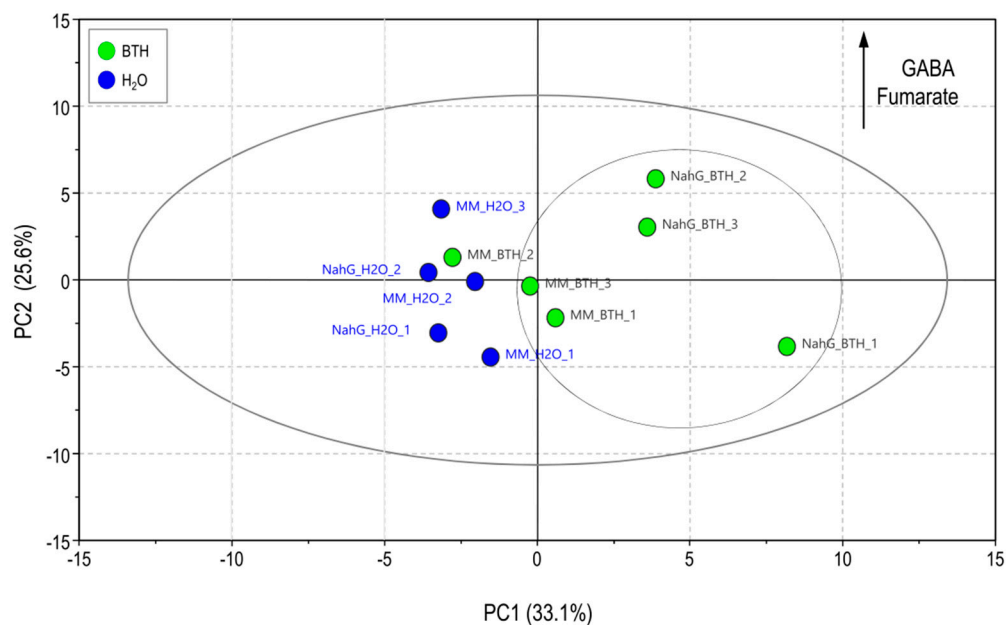


Figure 5. Score plot of principal component analysis (PCA) based on the characteristic ion of the mass spectra from the primary metabolites measured in the m/z range 35–900, of the Money Maker (MM) and NahG tomato plants after at 48 h after BTH treatments (green; leaves after BTH treatments; blue; leaves after H_2O treatments).

3.4. Effect of GABA Treatments in Money Maker and NahG Plants Infected by CEVd

To explore the implication of GABA in the BTH mechanism of action, Money Maker and NahG tomato plants infected by CEVd were pre-treated with 1 mM GABA, and a comparative study of the development of symptoms in CEVd-infected plants was carried out at the indicated time points. The number of tomato plants showing symptoms of the viroid disease was recorded during progression of infection. Applications of GABA in CEVd-inoculated Money Maker plants delayed the initial presence of symptoms as well as BTH (Figure 6, left panel). This effect was more evident in NahG transgenic plants (Figure 6, right panel). In fact, 2 weeks after viroid infection, the GABA protective effect was the same as that observed for BTH in NahG plants. However, a loss in the effectiveness of GABA treatments was observed over the time for both Money Maker and NahG tomato plants. Similar results were observed by analyzing symptom severity in NahG plants (Figure S1).

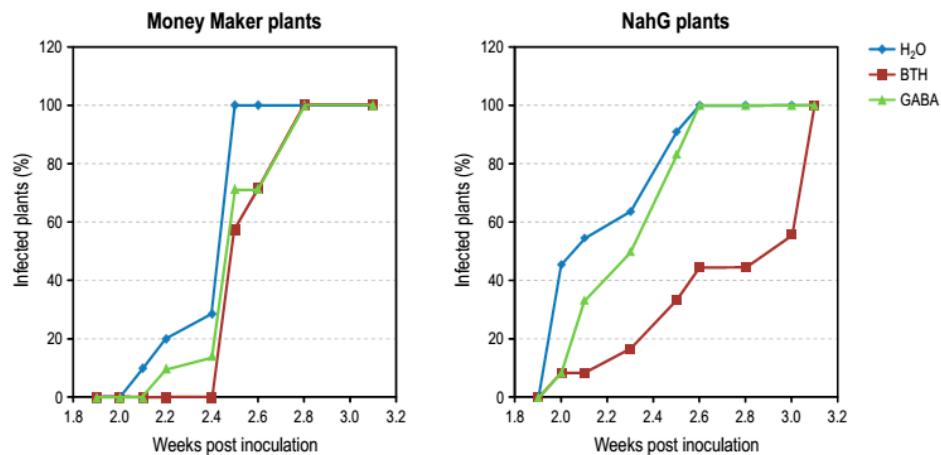


Figure 6. Disease development in Money Maker and NahG plants infected with CEVd and treated with BTH (red), GABA (green) or water (blue). Evolution of tomato plants showing symptoms at the indicated weeks post inoculation. Data correspond to one representative experiment.

GABA treatment visibly reversed the enhanced susceptibility of NahG plants to CEVd during the early times of the infection, but its effectiveness along the entire study was lower as compared to BTH, thus indicating that other compounds added to GABA may be involved in the BTH action mechanism. Figure 7 depicts representative GABA and BTH restored phenotype of CEVd-infected MoneyMaker and NahG plants, respectively, at 3 weeks post inoculation.

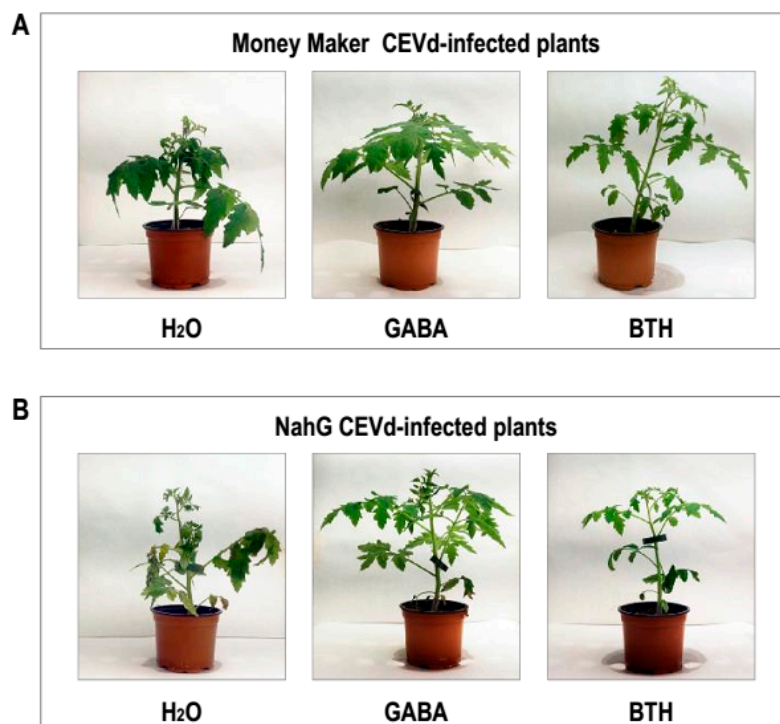


Figure 7. Growth of (A) Money Maker and (B) NahG plants following treatment with GABA or BTH and CEVd inoculation. Representative phenotype observed in infected plants 3 weeks after CEVd inoculation, and in equivalent plants pre-treated with 1 mM GABA or 1 mM BTH.

3.5. Effect of GABA Treatments on the Expression Levels of PAL, PR1, and P23 Genes in Money Maker and NahG Plants

To better characterize the protective role of GABA observed in the first stages of the viroid infection, we explored the relative gene expression of PAL and the pathogenesis-related proteins PR1 and P23 [26] after 48 h of exogenous treatments with GABA. BTH treatments were used as a positive inducer of PR1 and P23 in tomato plants [5]. As Figure 8 shows, BTH clearly induced PR1, P23, and PAL genes in Money Maker plants, while only PR1 induction was statistically significant in the GABA-treated Money Maker plants. The pattern of induction of these genes was maintained in NahG plants, being the induction more evident in the transgenic genotype. In fact, not only PR1, but also P23 and PAL were significantly induced in GABA-treated NahG plants, thus indicating that these transgenic plants could be more sensitive to BTH treatments.

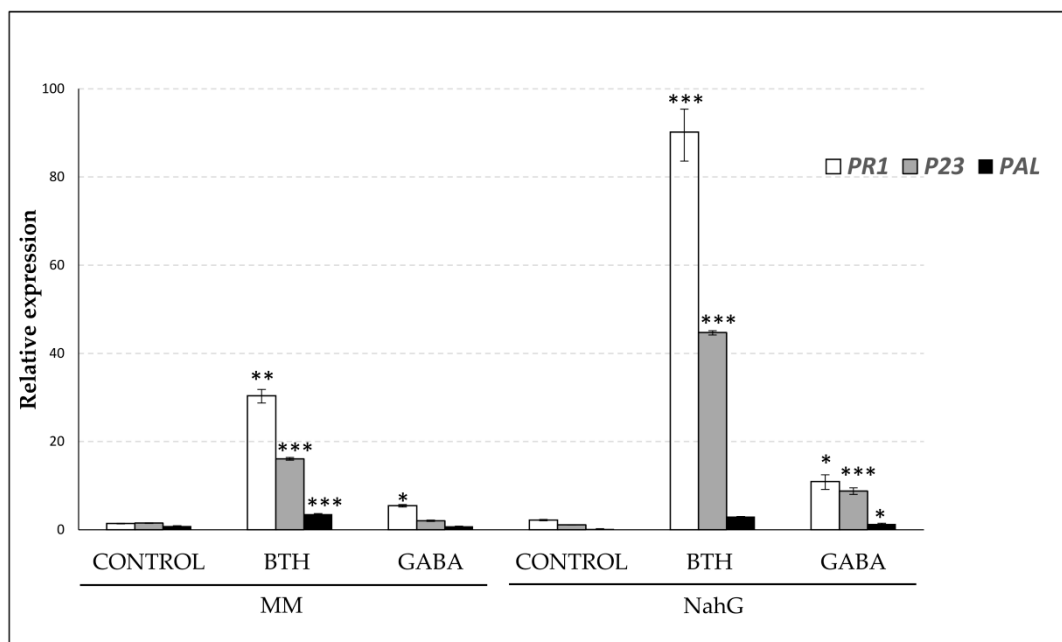


Figure 8. Expression levels of the tomato PAL, PR1 and P23 genes in Money Maker and NahG tomato plants, non-treated (CONTROL) and 48 h after BTH or GABA treatments. Values were first normalized to the actin expression level. Expression levels are represented as mean \pm standard error of three biological repetitions. Asterisk (*), double asterisks (**) and triple asterisks (***) indicate significant differences between chemically-treated and non treated plants with $p < 0.05$, $p < 0.01$ and $p < 0.001$, respectively.

4. Discussion

One of the main responses of plants to pathogen attack is the accumulation of defensive compounds, adapting the metabolome to the infection. Tomato plants effectively respond to different pathogens by synthesizing the appropriate metabolites to slow down the progress of the infection [17]. In this work, using the NMR metabolomics platform, we identified not only the compounds differentially accumulated in Money Maker and NahG tomato plants upon citrus exocortis viroid (CEVd) infection, but the metabolic adaptations induced by BTH treatments. The score plot of PLS based on the $^1\text{H-NMR}$ data revealed evident metabolomic changes in these tomato plants after both viroid infection and BTH treatments (Figure 2A). While PC1 of PLS clearly explained the changes in the chemical composition following the viroid infection, PC2 described the metabolome after the BTH treatments. Moreover, this multivariate data analysis showed that the metabolome of NahG plants infected by CEVd was the most affected, which is in accordance to hyper susceptibility observed in these salicylic acid-deficient transgenic plants upon viroid infection [5]. Interestingly, when these plants were treated

with BTH, both the phenotype and the metabolome were reestablished, placing them closer to their parental in the score plot. The score plots of both OPLS-DA performed upon the infection (Figure 2B) and the chemical treatment (Figure 2C) showed a clear separation indicative of the metabolic changes produced by CEVd and BTH, respectively.

In order to distinguish which metabolites were affected by each factor, an SUS correlation analysis was performed. The analysis of the positive size of the y axis of the SUS correlation showed the compounds accumulated in the viroid infection (Figure 2D). The defensive role of phenylpropanoids is well known, and the specific secondary response mediated by GA signaling is characteristic of the CEVd-tomato compatible interactions [17]. The induction of GA during systemic non-necrotizing infections, as those caused by CEVd, ToMV, and TSWV in tomato plants has been described in previous works [3,5]. In these compatible interactions GA acts as a pathogen-inducible signal of plant defenses and, in contrast with what occurs with SA, GA is predominantly conjugated to xylose [27]. Their precursor amino acids tyrosine and phenylalanine were also found to accumulate in the infected plants to supply the carbon skeleton needed for the biosynthesis of this phenolic compound. Furthermore, the increase in asparagine, aspartate, and glutamate levels have already been described in tomato plants upon ToMV inoculation [18].

To understand the mechanism of action of BTH, an analysis of the positive side of X axis of the SUS correlation was performed (Figure 2D). An increase in the levels of glutamine and BTH as well as its catabolyzed forms had already been found in BTH-treated Arabidopsis [12]. However the enhancement of GABA, adenosine, and trigonelline had not been described yet. Among them, GABA was the only compound that significantly accumulated after the chemical treatments in both Money Maker and NahG healthy tomato plants (Table 1), indicating that BTH could induce the biosynthesis of GABA.

On the other hand, in CEVd-infected tomato plants, BTH spray produced a statistically significant increase of several compounds, being not strictly correlated with the chemical treatment or with the infection process. Interestingly, in CEVd-infected BTH-treated NahG plants, phenylpropanoids accumulated as defence compounds despite the observed hyper susceptibility of these plants to this pathogen (Table 1). We postulate that this increase was not due to the chemical treatment, but to the viroid inoculation, since a reduction of the levels of these phenolic metabolites has been described in BTH-treated Arabidopsis plants [12]. The high levels of malic acid and glucose are needed to supply the substrates for the indispensable tricarboxylic acid cycle, while aspartate is required for the synthesis of alanine or threonine, and citric acid is the starting point for glutamine biosynthesis via α -ketoglutarate and glutamate (Figure 3).

Our results point to GABA as the lead compound highlighted by the NMR-metabolomics study in both genotypes of tomato plants after BTH-treatments. Since GABA levels were higher in the NahG plants than in their corresponding parental after both BTH spray (Table 1) or CEVd infection, SA could be impairing the GABA accumulation induced by this chemical. These results are in accordance with both the induction pattern of several genes involved in GABA biosynthesis, such as glutamate dehydrogenase (GDH), glutamate decarboxylase (GAD) or glutamine synthetase (GS) as analyzed by qRT-PCR (Figure 4), and the relative GABA levels measured by GC-MS 48 h post BTH treatments in Money Maker and NahG plants (See Section 3.3). The most effective BTH-treatment observed in NahG plants in terms of both GABA accumulation and transcriptional regulation of GABA biosynthetic genes could explain the remarkable reversion of the hyper susceptibility observed in these infected plants after BTH treatment. In this respect, we have observed that GABA treatments partially reverse the hyper susceptibility of NahG plants to CEVd (Figure 6, Figure 7) and trigger the induction of defense genes (Figure 8). Our results appear to unravel the GABA role in the BTH-mediated recovery of NahG tomato plants infected with CEVd.

GABA is a four-carbon non-protein amino acid, which acts in animals as an inhibitory neurotransmitter in the central nervous system. In plants, GABA concentrations increase rapidly in response to a number of stresses including heat, cold, salinity, drought, hypoxia, mechanical damage, and pathogens [28]. The role that GABA might play in plants ranges from an involvement in C

and N metabolism, regulation of cytosolic pH, protection against oxidative stress, and mediation of interactions between plants and other organisms, including bacterial and fungal pathogens, nematodes and insects [29]. Both BTH and SA treatments result in increased production of reactive oxygen species (ROS) [30,31], and BTH inhibits catalase and ascorbate peroxidase, the two major H₂O₂-scavenging enzymes in plants [32]. Besides, overactivation of the GABA cycle has been described to result in resistance by both tightly controlling the defense-associated HR and slowing down the pathogen-induced senescence [22]. Therefore, the observed accumulation of GABA in BTH treated plants, and to a greater extent in NahG plants, could be related to a protection against ROS induced by BTH. Measures of ROS in BTH-treated NahG plants when compared to the corresponding BTH-treated parental Money Maker plants, could help to better correlate the GABA accumulation with the ROS production.

The protective role of GABA treatments has been described in several species subjected to different stresses. This metabolite has proven to alleviate oxidative damage in barley [33], to delay senescence in blueberry fruit by regulating the ROS response and phenylpropanoid pathway [34], and to induce resistance against *Penicillium expansum* by priming defense responses in pear fruit [20]. It had been demonstrated previously that exogenous treatments of GABA at similar concentrations used in this work, markedly promoted the induction of PAL in different tissue and plant organs [34–36]. This is in accordance with our results, since we have observed that GABA treatments induce PAL and other defensive genes such PR1 and P23 (Figure 8) mainly in NahG plants, producing a delay at the onset of symptom development in CEVd-infected tomato plants.

On the basis of our results, GABA can be considered as an additional signal to SA or GA involved in the induction of pathogenesis defence genes in tomato plants. In this context, it is worthy to state that genetic manipulation of GABA levels has demonstrated that GABA possesses a defensive role against drought and insect herbivory [37]. Additional studies are needed to further explore the effect of BTH on tomato plants related to GABA accumulation, in order to confirm the specific role of this metabolite in the defensive mechanisms triggered by BTH in plants.

5. Conclusions

BTH treatments produce quantitative and qualitative changes in the tomato metabolome, GABA being one of the most outstanding metabolites induced. This metabolic variation was clearly detectable using a NMR metabolomics platform. Interestingly, NahG tomato plants appear to be more sensitive to BTH or GABA treatments, in terms of both changes in metabolome and induction of defence genes. Our results suggest that the effects of GABA induction could be down-regulated by SA, since tomato plants impaired in the accumulation of this phenolic compound display a higher accumulation of GABA upon BTH treatment.

Taken together, our results indicate that GABA plays a role in tomato defense against CEVd, its protective action more effective in SA-defective NahG tomato plants. From the results presented here, it can also be hypothesized that the mechanism of action of BTH could be at least partially mediated by GABA.

Supplementary Materials: Supplementary materials can be found at <http://www.mdpi.com/1999-4915/11/5/437/s1>.

Author Contributions: Conceptualization, J.M.B. and P.L.; Methodology, Y.H.C., R.V. and M.P.L.G.; Software, Y.H.C.; Validation, C.P.; Formal Analysis, M.P.L.-G. and S.B.; Investigation, J.M.B. and I.R.; Resources, P.L.; Data Curation, I.R.; Writing—Original Draft Preparation, M.P.L.-G. and P.L.; Funding Acquisition, J.M.B.

Funding: This research was funded by Dirección General de Programas y Transferencia de Conocimiento, from the Spanish Ministry of Science and Innovation, Grant BIO2012-33419. MP. López-Gresa was the recipient of a postdoctoral fellowship JC2008-00432 Spanish Ministry of Science and Innovation.

Acknowledgments: We thank Syngenta España SA for kindly providing us with Acibenzolar-S-methyl (Bion50 WG).

Conflicts of Interest: The authors declare no conflict of interest.

References

1. Mou, Z.; Fan, W.; Dong, X. Inducers of Plant Systemic Acquired Resistance Regulate NPR1 Function through Redox Changes. *Cell* **2003**, *113*, 935–944. [[CrossRef](#)]
2. Bellés, J.M.; Garro, R.; Pallás, V.; Fayos, J.; Rodrigo, I.; Conejero, V. Accumulation of gentisic acid as associated with systemic infections but not with the hypersensitive response in plant-pathogen interactions. *Planta* **2006**, *223*, 500–511. [[CrossRef](#)] [[PubMed](#)]
3. Bellés, J.M.; Garro, R.; Fayos, J.; Navarro, P.; Primo, J.; Conejero, V. Gentisic acid as a pathogen-inducible signal, additional to salicylic acid for activation of plant defenses in tomato. *Mol. Plant-Microbe Interact.* **1999**, *12*, 227–235. [[CrossRef](#)]
4. Brading, P.A.; Hammond-Kosack, K.E.; Parr, A.; Jones, J.D.G. Salicylic acid is not required for Cf-2- and Cf-9-dependent resistance of tomato to *Cladosporium fulvum*. *Plant J.* **2000**, *23*, 305–318. [[CrossRef](#)]
5. López-Gresa, M.P.; Lisón, P.; Yenush, L.; Conejero, V.; Rodrigo, I.; Bellés, J.M. Salicylic Acid Is Involved in the Basal Resistance of Tomato Plants to Citrus Exocortis Viroid and Tomato Spotted Wilt Virus. *PLoS ONE* **2016**, *11*, e0166938. [[CrossRef](#)] [[PubMed](#)]
6. Friedrich, L.; Lawton, K.; Ruess, W.; Masner, P.; Specker, N.; Rella, M.G.; Meier, B.; Dincher, S.; Staub, T.; Uknes, S.; et al. A benzothiadiazole derivative induces systemic acquired resistance in tobacco. *Plant J.* **1996**, *10*, 61–70. [[CrossRef](#)]
7. Görlach, J.; Volrath, S.; Knauf-Beiter, G.; Hengy, G.; Beckhove, U.; Kogel, K.H.; Oostendorp, M.; Staub, T.; Ward, E.; Kessmann, H.; et al. Benzothiadiazole, a novel class of inducers of systemic acquired resistance, activates gene expression and disease resistance in wheat. *Plant Cell* **1996**, *8*, 629–643. [[CrossRef](#)]
8. Lawton, K.A.; Friedrich, L.; Hunt, M.; Weymann, K.; Delaney, T.; Kessmann, H.; Staub, T.; Ryals, J. Benzothiadiazole induces disease resistance in Arabidopsis by activation of the systemic acquired resistance signal transduction pathway. *Plant J.* **1996**, *10*, 71–82.
9. Benhamou, N.; Belanger, R.R. Benzothiadiazole-mediated induced resistance to *Fusarium oxysporum* f. sp. *radicis-lycopersici* in tomato. *Plant Physiol.* **1998**, *118*, 1203–1212. [[CrossRef](#)]
10. Louws, F.J.; Wilson, M.; Campbell, H.L.; Cuppels, D.A.; Jones, J.B.; Shoemaker, P.B.; Sahin, F.; Miller, S.A. Field Control of Bacterial Spot and Bacterial Speck of Tomato Using a Plant Activator. *Plant Dis.* **2001**, *85*, 481–488. [[CrossRef](#)]
11. Li, X.; Bi, Y.; Wang, J.; Dong, B.; Li, H.; Gong, D.; Zhao, Y.; Tang, Y.; Yu, X.; Shang, Q. BTH treatment caused physiological, biochemical and proteomic changes of muskmelon (*Cucumis melo* L.) fruit during ripening. *J. Proteom.* **2015**, *120*, 179–193. [[CrossRef](#)]
12. Hien Dao, T.T.; Puig, R.C.; Kim, H.K.; Erkelens, C.; Lefeber, A.W.M.; Linthorst, H.J.M.; Choi, Y.H.; Verpoorte, R. Effect of benzothiadiazole on the metabolome of Arabidopsis thaliana. *Plant Physiol. Biochem.* **2009**, *47*, 146–152. [[CrossRef](#)]
13. Vogt, T. Phenylpropanoid biosynthesis. *Mol. Plant* **2010**, *3*, 2–20. [[CrossRef](#)]
14. Katz, V.A.; Thulke, O.U.; Conrath, U. A Benzothiadiazole Primes Parsley Cells for Augmented Elicitation of Defense Responses. *Plant Physiol.* **1998**, *117*, 1333–1339. [[CrossRef](#)]
15. Iriti, M.; Rossoni, M.; Borgo, M.; Faoro, F. Benzothiadiazole Enhances Resveratrol and Anthocyanin Biosynthesis in Grapevine, Meanwhile Improving Resistance to Botrytis cinerea. *J. Agric. Food Chem.* **2004**, *52*, 4406–4413. [[CrossRef](#)]
16. Verpoorte, R.; Choi, Y.; Kim, H. NMR-based metabolomics at work in phytochemistry. *Phytochem. Rev.* **2007**, *6*, 3–14. [[CrossRef](#)]
17. López-Gresa, M.P.; Maltese, F.; Bellés, J.M.; Conejero, V.; Kim, H.K.; Choi, Y.H.; Verpoorte, R. Metabolic response of tomato leaves upon different plant-pathogen interactions. *Phytochem. Anal.* **2010**, *21*, 89–94. [[CrossRef](#)]
18. López-Gresa, M.P.; Lisón, P.; Kim, H.K.; Choi, Y.H.; Verpoorte, R.; Rodrigo, I.; Conejero, V.; Bellés, J.M. Metabolic fingerprinting of Tomato Mosaic Virus infected Solanum lycopersicum. *J. Plant Physiol.* **2012**, *169*, 1586–1596. [[CrossRef](#)]
19. Shelp, B.J.; Bozzo, G.G.; Trobacher, C.P.; Zarei, A.; Deyman, K.L.; Brikis, C.J. Hypothesis/review: Contribution of putrescine to 4-aminobutyrate (GABA) production in response to abiotic stress. *Plant Sci.* **2012**, *193–194*, 130–135. [[CrossRef](#)]

20. Yu, C.; Zeng, L.; Sheng, K.; Chen, F.; Zhou, T.; Zheng, X.; Yu, T. γ -Aminobutyric acid induces resistance against *Penicillium expansum* by priming of defence responses in pear fruit. *Food Chem.* **2014**, *159*, 29–37. [[CrossRef](#)] [[PubMed](#)]
21. Bolton, M.D. Primary metabolism and plant defense—Fuel for the fire. *Mol. Plant Microbe Interact.* **2009**, *22*, 487–497. [[CrossRef](#)]
22. Seifi, H.S.; Curvers, K.; de Vleeschauwer, D.; Delaere, I.; Aziz, A.; Hofte, M. Concurrent overactivation of the cytosolic glutamine synthetase and the GABA shunt in the ABA-deficient sitiens mutant of tomato leads to resistance against *Botrytis cinerea*. *New Phytol.* **2013**, *199*, 490–504. [[CrossRef](#)]
23. Oldroyd, G.E.D.; Staskawicz, B.J. Genetically engineered broad-spectrum disease resistance in tomato. *Proc. Natl. Acad. Sci. USA* **1998**, *95*, 10300–10305. [[CrossRef](#)]
24. Roessner, U.; Wagner, C.; Kopka, J.; Trethewey, R.N.; Willmitzer, L. Technical advance: Simultaneous analysis of metabolites in potato tuber by gas chromatography-mass spectrometry. *Plant J.* **2000**, *23*, 131–142. [[CrossRef](#)]
25. Bellés, J.M.; López-Gresa, M.P.; Fayos, J.; Pallás, V.; Rodrigo, I.; Conejero, V. Induction of cinnamate 4-hydroxylase and phenylpropanoids in virus-infected cucumber and melon plants. *Plant Sci.* **2008**, *174*, 524–533. [[CrossRef](#)]
26. Conejero, V.; Bellés, J.M.; García-Breijo, F.; Garro, R.; Hernández-Yago, J.; Rodrigo, I.; Vera, P. Signaling in Viroid Pathogenesis. In *Recognition and Response in Plant-Virus Interactions*; Fraser, R.S., Ed.; Springer: Berlin/Heidelberg, Germany, 1990; Volume 41, pp. 233–261.
27. Fayos, J.; Bellés, J.M.; López-Gresa, M.P.; Primo, J.; Conejero, V. Induction of gentisic acid 5-O- β -D-xylopyranoside in tomato and cucumber plants infected by different pathogens. *Phytochemistry* **2006**, *67*, 142–148. [[CrossRef](#)]
28. Kinnersley, A.M.; Turano, F.J. Gamma Aminobutyric Acid (GABA) and Plant Responses to Stress. *Crit. Rev. Plant Sci.* **2000**, *19*, 479–509. [[CrossRef](#)]
29. Roberts, M.R. Does GABA Act as a Signal in Plants?: Hints from Molecular Studies. *Plant Signal. Behav.* **2007**, *2*, 408–409. [[CrossRef](#)]
30. Kawano, T.; Sahashi, N.; Takahashi, K.; Uozumi, N.; Muto, S. Salicylic Acid Induces Extracellular Superoxide Generation Followed by an Increase in Cytosolic Calcium Ion in Tobacco Suspension Culture: The Earliest Events in Salicylic Acid Signal Transduction. *Plant Cell Physiol.* **1998**, *39*, 721–730. [[CrossRef](#)]
31. Van der Merwe, J.A.; Dubery, I.A. Benzothiadiazole inhibits mitochondrial NADH: Ubiquinone oxidoreductase in tobacco. *J. Plant Physiol.* **2006**, *163*, 877–882. [[CrossRef](#)]
32. Wendehenne, D.; Durner, J.; Chen, Z.; Klessig, D.F. Benzothiadiazole, an inducer of plant defenses, inhibits catalase and ascorbate peroxidase. *Phytochemistry* **1998**, *47*, 651–657. [[CrossRef](#)]
33. Song, H.; Xu, X.; Wang, H.; Wang, H.; Tao, Y. Exogenous gamma-aminobutyric acid alleviates oxidative damage caused by aluminium and proton stresses on barley seedlings. *J. Sci. Food Agric.* **2010**, *90*, 1410–1416. [[CrossRef](#)] [[PubMed](#)]
34. Ge, Y.; Duan, B.; Li, C.; Tang, Q.; Li, X.; Wei, M.; Chen, Y.; Li, J. γ -Aminobutyric acid delays senescence of blueberry fruit by regulation of reactive oxygen species metabolism and phenylpropanoid pathway. *Sci. Hortic-Amsterdam* **2018**, *240*, 303–309. [[CrossRef](#)]
35. Ma, Y.; Wang, P.; Chen, Z.; Gu, Z.; Yang, R. GABA enhances physio-biochemical metabolism and antioxidant capacity of germinated hullless barley under NaCl stress. *J. Plant Physiol.* **2018**, *231*, 192–201. [[CrossRef](#)]
36. Aghdam, M.S.; Kakavand, F.; Rabiei, V.; Zaare-Nahandi, F.; Razavi, F. γ -Aminobutyric acid and nitric oxide treatments preserve sensory and nutritional quality of cornelian cherry fruits during postharvest cold storage by delaying softening and enhancing phenols accumulation. *Sci. Hortic-Amsterdam* **2019**, *246*, 812–817. [[CrossRef](#)]
37. Bown, A.W.; Shelp, B.J. Plant GABA: Not Just a Metabolite. *Trends Plant Sci.* **2016**, *21*, 811–813. [[CrossRef](#)]



